



ISSN 2686-7575 (Online)

ТОНКИЕ ХИМИЧЕСКИЕ ТЕХНОЛОГИИ

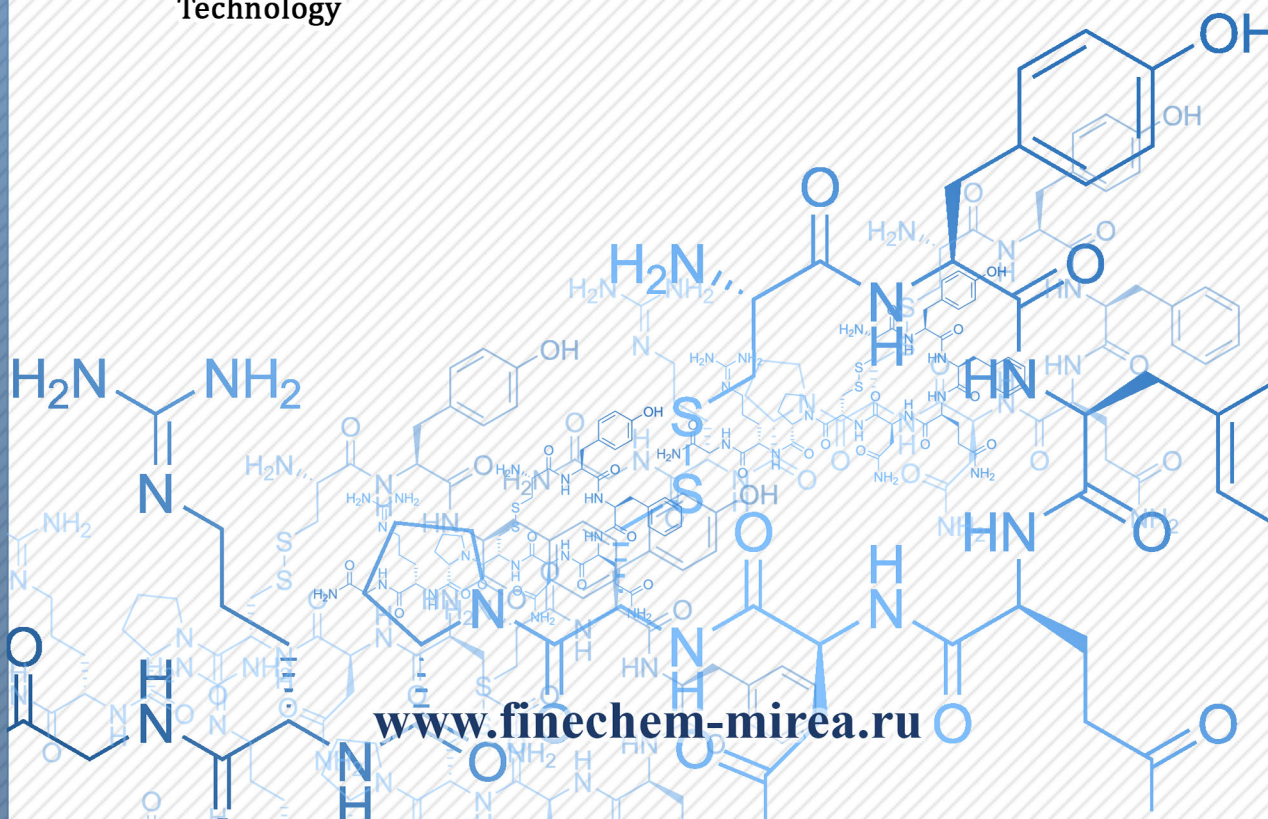
Fine Chemical Technologies

- | Theoretical Bases of Chemical Technology
- | Chemistry and Technology of Organic Substances
- | Chemistry and Technology of Medicinal Compounds and Biologically Active Substances
- | Biochemistry and Biotechnology
- | Synthesis and Processing of Polymers and Polymeric Composites
- | Chemistry and Technology of Inorganic Materials
- | Analytical Methods in Chemistry and Chemical Technology
- | Mathematical Methods and Information Systems in Chemical Technology

19(4)

2024

www.finechem-mirea.ru





ТОНКИЕ ХИМИЧЕСКИЕ ТЕХНОЛОГИИ

Fine Chemical Technologies

- | Theoretical Bases of Chemical Technology
- | Chemistry and Technology of Organic Substances
- | Chemistry and Technology of Medicinal Compounds and Biologically Active Substances
- | Biochemistry and Biotechnology
- | Synthesis and Processing of Polymers and Polymeric Composites
- | Chemistry and Technology of Inorganic Materials
- | Analytical Methods in Chemistry and Chemical Technology
- | Mathematical Methods and Information Systems in Chemical Technology

Tonkie Khimicheskie Tekhnologii =
Fine Chemical Technologies.
Vol. 19, No. 4, 2024

Тонкие химические технологии =
Fine Chemical Technologies.
Том 19, № 4, 2024

<https://doi.org/10.32362/2410-6593-2024-19-4>

www.finechem-mirea.ru

**Tonkie Khimicheskie Tekhnologii =
Fine Chemical Technologies
2024, Vol. 19, No. 4**

The peer-reviewed scientific and technical journal Fine Chemical Technologies highlights the modern achievements of fundamental and applied research in the field of fine chemical technologies, including theoretical bases of chemical technology, chemistry and technology of medicinal compounds and biologically active substances, organic substances and inorganic materials, biochemistry and biotechnology, synthesis and processing of polymers and polymeric composites, analytical and mathematical methods and information systems in chemistry and chemical technology.

Founder and Publisher

Federal State Budget
Educational Institution of Higher Education
“MIREA – Russian Technological University”
78, Vernadskogo pr., Moscow, 119454, Russian Federation.
Publication frequency: bimonthly.
The journal was founded in 2006. The name was Vestnik MITHT until 2015 (ISSN 1819-1487).

The journal is included into the List of peer-reviewed science press of the State Commission for Academic Degrees and Titles of the Russian Federation.

The journal is indexed: SCOPUS, DOAJ, Chemical Abstracts, Science Index, RSCI, Ulrich’s International Periodicals Directory

Editor-in-Chief:

Andrey V. Timoshenko – Dr. Sci. (Eng.), Cand. Sci. (Chem.), Professor, MIREA – Russian Technological University, Moscow, Russian Federation. Scopus Author ID 56576076700, ResearcherID Y-8709-2018, <https://orcid.org/0000-0002-6511-7440>, timoshenko@mirea.ru

Deputy Editor-in-Chief:

Valery V. Fomichev – Dr. Sci. (Chem.), Professor, MIREA – Russian Technological University, Moscow, Russian Federation. Scopus Author ID 57196028937, <http://orcid.org/0000-0003-4840-0655>, fomichev@mirea.ru

Executive Editor:

Sergey A. Durakov – Cand. Sci. (Chem.), Associate Professor, MIREA – Russian Technological University, Moscow, Russian Federation, Scopus Author ID 57194217518, ResearcherID AAS-6578-2020, <http://orcid.org/0000-0003-4842-3283>, durakov@mirea.ru

Editorial staff:

Managing Editor Cand. Sci. (Eng.) Galina D. Seredina
Editor Sofya M. Mazina
Science editors Dr. Sci. (Chem.), Prof. Tatyana M. Buslaeva
Dr. Sci. (Chem.), Prof. Anatolii A. Ischenko
Dr. Sci. (Eng.), Prof. Anatolii V. Markov
Dr. Sci. (Chem.), Prof. Vladimir A. Tverskoy
Desktop publishing Sergey V. Trofimov

86, Vernadskogo pr., Moscow, 119571, Russian Federation.
Phone: +7 (499) 600-80-80 (#31288)
E-mail: seredina@mirea.ru

The registration number ПИ № ФС 77-74580 was issued in December 14, 2018 by the Federal Service for Supervision of Communications, Information Technology, and Mass Media of Russia

The subscription index of *Pressa Rossii*: **36924**

**Тонкие химические технологии =
Fine Chemical Technologies
2024, том 19, № 4**

Научно-технический рецензируемый журнал «Тонкие химические технологии» освещает современные достижения фундаментальных и прикладных исследований в области тонких химических технологий, включая теоретические основы химической технологии, химию и технологию лекарственных препаратов и биологически активных соединений, органических веществ и неорганических материалов, биохимию и биотехнологию, синтез и переработку полимеров и композитов на их основе, аналитические и математические методы и информационные системы в химии и химической технологии.

Учредитель и издатель

федеральное государственное бюджетное образовательное учреждение высшего образования «МИРЭА – Российский технологический университет» 119454, РФ, Москва, пр-т Вернадского, д. 78.
Периодичность: один раз в два месяца.
Журнал основан в 2006 году. До 2015 года издавался под названием «Вестник МИТХТ» (ISSN 1819-1487).

Журнал входит в Перечень ведущих рецензируемых научных журналов ВАК РФ.

Индексируется: SCOPUS, DOAJ, Chemical Abstracts, РИНЦ (Science Index), RSCI, Ulrich’s International Periodicals Directory

Главный редактор:

Тимошенко Андрей Всеволодович – д.т.н., к.х.н., профессор, МИРЭА – Российский технологический университет, Москва, Российская Федерация. Scopus Author ID 56576076700, ResearcherID Y-8709-2018, <https://orcid.org/0000-0002-6511-7440>, timoshenko@mirea.ru

Заместитель главного редактора:

Фомичёв Валерий Вячеславович – д.х.н., профессор, МИРЭА – Российский технологический университет, Москва, Российская Федерация. Scopus Author ID 57196028937, <http://orcid.org/0000-0003-4840-0655>, fomichev@mirea.ru

Выпускающий редактор:

Дураков Сергей Алексеевич – к.х.н., доцент, МИРЭА – Российский технологический университет, Москва, Российская Федерация, Scopus Author ID 57194217518, ResearcherID AAS-6578-2020, <http://orcid.org/0000-0003-4842-3283>, durakov@mirea.ru

Редакция:

Зав. редакцией к.т.н. Г.Д. Середина
Редактор С.М. Мазина
Научные редакторы д.х.н., проф. Т.М. Буслаева
д.х.н., проф. А.А. Ищенко
д.т.н., проф. А.В. Марков
д.х.н., проф. В.А. Тверской
Компьютерная верстка С.В. Трофимов

РФ, 119571, Москва, пр. Вернадского, 86, оф. P-108.
Тел.: +7 (499) 600-80-80 (#31288)
E-mail: seredina@mirea.ru

Регистрационный номер и дата принятия решения о регистрации СМИ: ПИ № ФС 77-74580 от 14.12.2018 г. СМИ зарегистрировано Федеральной службой по надзору в сфере связи, информационных технологий и массовых коммуникаций (Роскомнадзор)

Индекс по Объединенному каталогу «Пресса России»: **36924**

EDITORIAL BOARD

Andrey V. Blokhin – Dr. Sci. (Chem.), Professor, Belarusian State University, Minsk, Belarus.
Scopus Author ID 7101971167,
ResearcherID AAF-8122-2019,
<https://orcid.org/0000-0003-4778-5872>,
blokhin@bsu.by.

Sergey P. Verevkin – Dr. Sci. (Eng.), Professor, University of Rostock, Rostock, Germany.
Scopus Author ID 7006607848, ResearcherID G-3243-2011,
<https://orcid.org/0000-0002-0957-5594>,
Sergey.verevkin@uni-rostock.de.

Konstantin Yu. Zhizhin – Corresponding Member of the Russian Academy of Sciences (RAS), Dr. Sci. (Chem.), Professor, N.S. Kurnakov Institute of General and Inorganic Chemistry of the RAS, Moscow, Russian Federation.
Scopus Author ID 6701495620, ResearcherID C-5681-2013,
<http://orcid.org/0000-0002-4475-124X>,
kyuzhizhin@igic.ras.ru.

Igor V. Ivanov – Dr. Sci. (Chem.), Professor, MIREA – Russian Technological University, Moscow, Russian Federation.
Scopus Author ID 34770109800, ResearcherID I-5606-2016,
<http://orcid.org/0000-0003-0543-2067>,
ivanov_i@mirea.ru.

Carlos A. Cardona – PhD (Eng.), Professor, National University of Columbia, Manizales, Colombia.
Scopus Author ID 7004278560,
<http://orcid.org/0000-0002-0237-2313>,
ccardonaal@unal.edu.co.

Elvira T. Krut'ko – Dr. Sci. (Eng.), Professor, Belarusian State Technological University, Minsk, Belarus.
Scopus Author ID 6602297257,
ela_krutko@mail.ru.

Anatolii I. Miroshnikov – Academician at the RAS, Dr. Sci. (Chem.), Professor, M.M. Shemyakin and Yu.A. Ovchinnikov Institute of Bioorganic Chemistry of the RAS, Member of the Presidium of the RAS, Chairman of the Presidium of the RAS Pushchino Research Center, Moscow, Russian Federation.
Scopus Author ID 7006592304, ResearcherID G-5017-2017,
aiv@ibch.ru.

Aziz M. Muzafarov – Academician at the RAS, Dr. Sci. (Chem.), Professor, A.N. Nesmeyanov Institute of Organoelement Compounds of the RAS, Moscow, Russian Federation.
Scopus Author ID 7004472780, ResearcherID G-1644-2011,
<https://orcid.org/0000-0002-3050-3253>,
aziz@ineos.ac.ru.

РЕДАКЦИОННАЯ КОЛЛЕГИЯ

Блохин Андрей Викторович – д.х.н., профессор Белорусского государственного университета, Минск, Беларусь.
Scopus Author ID 7101971167, ResearcherID AAF-8122-2019,
<https://orcid.org/0000-0003-4778-5872>,
blokhin@bsu.by.

Верёвкин Сергей Петрович – д.т.н., профессор Университета г. Росток, Росток, Германия.
Scopus Author ID 7006607848, ResearcherID G-3243-2011,
<https://orcid.org/0000-0002-0957-5594>,
Sergey.verevkin@uni-rostock.de.

Жижин Константин Юрьевич – член-корр. Российской академии наук (РАН), д.х.н., профессор, Институт общей и неорганической химии им. Н.С. Курнакова РАН, Москва, Российская Федерация.
Scopus Author ID 6701495620, ResearcherID C-5681-2013,
<http://orcid.org/0000-0002-4475-124X>,
kyuzhizhin@igic.ras.ru.

Иванов Игорь Владимирович – д.х.н., профессор, МИРЭА – Российский технологический университет, Москва, Российская Федерация.
Scopus Author ID 34770109800, ResearcherID I-5606-2016,
<http://orcid.org/0000-0003-0543-2067>,
ivanov_i@mirea.ru.

Кардона Карлос Ариэль – PhD, профессор Национального университета Колумбии, Манизалес, Колумбия.
Scopus Author ID 7004278560,
<http://orcid.org/0000-0002-0237-2313>,
ccardonaal@unal.edu.co.

Крутько Эльвира Тихоновна – д.т.н., профессор Белорусского государственного технологического университета, Минск, Беларусь.
Scopus Author ID 6602297257,
ela_krutko@mail.ru.

Мирошников Анатолий Иванович – академик РАН, д.х.н., профессор, Институт биоорганической химии им. академиков М.М. Шемякина и Ю.А. Овчинникова РАН, член Президиума РАН, председатель Президиума Пушкинского научного центра РАН, Москва, Российская Федерация.
Scopus Author ID 7006592304, ResearcherID G-5017-2017,
aiv@ibch.ru.

Музафаров Азиз Мансурович – академик РАН, д.х.н., профессор, Институт элементоорганических соединений им. А.Н. Несмеянова РАН, Москва, Российская Федерация.
Scopus Author ID 7004472780, ResearcherID G-1644-2011,
<https://orcid.org/0000-0002-3050-3253>,
aziz@ineos.ac.ru.

Ivan A. Novakov – Academician at the RAS, Dr. Sci. (Chem.), Professor, President of the Volgograd State Technical University, Volgograd, Russian Federation.
Scopus Author ID 7003436556, ResearcherID I-4668-2015, <http://orcid.org/0000-0002-0980-6591>, president@vstu.ru.

Alexander N. Ozerin – Corresponding Member of the RAS, Dr. Sci. (Chem.), Professor, Enikolopov Institute of Synthetic Polymeric Materials of the RAS, Moscow, Russian Federation.
Scopus Author ID 7006188944, ResearcherID J-1866-2018, <https://orcid.org/0000-0001-7505-6090>, ozerin@ispm.ru.

Tapani A. Pakkanen – PhD, Professor, Department of Chemistry, University of Eastern Finland, Joensuu, Finland.
Scopus Author ID 7102310323, tapani.pakkanen@uef.fi.

Armando J.L. Pombeiro – Academician at the Academy of Sciences of Lisbon, PhD, Professor, President of the Center for Structural Chemistry of the Higher Technical Institute of the University of Lisbon, Lisbon, Portugal.
Scopus Author ID 7006067269, ResearcherID I-5945-2012, <https://orcid.org/0000-0001-8323-888X>, pombeiro@ist.utl.pt.

Dmitrii V. Pyshnyi – Corresponding Member of the RAS, Dr. Sci. (Chem.), Professor, Institute of Chemical Biology and Fundamental Medicine, Siberian Branch of the RAS, Novosibirsk, Russian Federation.
Scopus Author ID 7006677629, ResearcherID F-4729-2013, <https://orcid.org/0000-0002-2587-3719>, pyshnyi@niboch.nsc.ru.

Alexander S. Sigov – Academician at the RAS, Dr. Sci. (Phys. and Math.), Professor, President of MIREA – Russian Technological University, Moscow, Russian Federation.
Scopus Author ID 35557510600, ResearcherID L-4103-2017, sigov@mirea.ru.

Alexander M. Toikka – Dr. Sci. (Chem.), Professor, Institute of Chemistry, Saint Petersburg State University, St. Petersburg, Russian Federation.
Scopus Author ID 6603464176, ResearcherID A-5698-2010, <http://orcid.org/0000-0002-1863-5528>, a.toikka@spbu.ru.

Andrzej W. Trochimczuk – Dr. Sci. (Chem.), Professor, Faculty of Chemistry, Wrocław University of Science and Technology, Wrocław, Poland.
Scopus Author ID 7003604847, andrzej.trochimczuk@pwr.edu.pl.

Aslan Yu. Tsvadze – Academician at the RAS, Dr. Sci. (Chem.), Professor, A.N. Frumkin Institute of Physical Chemistry and Electrochemistry of the RAS, Moscow, Russian Federation.
Scopus Author ID 7004245066, ResearcherID G-7422-2014, tsiv@phyche.ac.ru.

Новаков Иван Александрович – академик РАН, д.х.н., профессор, президент Волгоградского государственного технического университета, Волгоград, Российская Федерация.
Scopus Author ID 7003436556, ResearcherID I-4668-2015, <http://orcid.org/0000-0002-0980-6591>, president@vstu.ru.

Озерин Александр Никифорович – член-корр. РАН, д.х.н., профессор, Институт синтетических полимерных материалов им. Н.С. Ениколопова РАН, Москва, Российская Федерация.
Scopus Author ID 7006188944, ResearcherID J-1866-2018, <https://orcid.org/0000-0001-7505-6090>, ozerin@ispm.ru.

Пакканен Тапани – PhD, профессор, Департамент химии, Университет Восточной Финляндии, Йоенсуу, Финляндия.
Scopus Author ID 7102310323, tapani.pakkanen@uef.fi.

Помбейро Армандо – академик Академии наук Лиссабона, PhD, профессор, президент Центра структурной химии Высшего технического института Университета Лиссабона, Португалия.
Scopus Author ID 7006067269, ResearcherID I-5945-2012, <https://orcid.org/0000-0001-8323-888X>, pombeiro@ist.utl.pt.

Пышный Дмитрий Владимирович – член-корр. РАН, д.х.н., профессор, Институт химической биологии и фундаментальной медицины Сибирского отделения РАН, Новосибирск, Российская Федерация.
Scopus Author ID 7006677629, ResearcherID F-4729-2013, <https://orcid.org/0000-0002-2587-3719>, pyshnyi@niboch.nsc.ru.

Сигов Александр Сергеевич – академик РАН, д.ф.-м.н., профессор, президент МИРЭА – Российского технологического университета, Москва, Российская Федерация.
Scopus Author ID 35557510600, ResearcherID L-4103-2017, sigov@mirea.ru.

Тойкка Александр Матвеевич – д.х.н., профессор, Институт химии, Санкт-Петербургский государственный университет, Санкт-Петербург, Российская Федерация.
Scopus Author ID 6603464176, ResearcherID A-5698-2010, <http://orcid.org/0000-0002-1863-5528>, a.toikka@spbu.ru.

Трохимчук Анджей – д.х.н., профессор, Химический факультет Вроцлавского политехнического университета, Вроцлав, Польша.
Scopus Author ID 7003604847, andrzej.trochimczuk@pwr.edu.pl.

Цивадзе Аслан Юсупович – академик РАН, д.х.н., профессор, Институт физической химии и электрохимии им. А.Н. Фрумкина РАН, Москва, Российская Федерация.
Scopus Author ID 7004245066, ResearcherID G-7422-2014, tsiv@phyche.ac.ru.

Contents

THEORETICAL BASES OF CHEMICAL TECHNOLOGY

273

Marat R. Agliullin, Al'fira N. Khazipova, Arslan F. Akhmetov, Oleg A. Baulin

Hydroisomerization of *n*-hexadecane on Pt-containing silicone aluminum phosphate molecular sieves SAPO-11 with different silicon content

279

Dmitriy A. Ryzhkin, Valentina M. Raeva

Comparison of methods for calculating the enthalpy of vaporization of binary azeotropic mixtures

CHEMISTRY AND TECHNOLOGY OF ORGANIC SUBSTANCES

293

Alexey D. Kirilin, Liya O. Belova, Nataliya A. Golub, Mariya V. Pletneva, Nadezhda I. Kirilina, Denis E. Mironov

Using nitrogen-containing organosilicon compounds in the creation of heat- and fire-resistant filling compositions to seal high-voltage and high-frequency equipment

CHEMISTRY AND TECHNOLOGY OF MEDICINAL COMPOUNDS AND BIOLOGICALLY ACTIVE SUBSTANCES

310

Nikita S. Kirin, Petr V. Ostroverkhov, Maxim N. Usachev, Kirill P. Birin, Mikhail A. Grin

Platinum(II) complexes based on derivatives of natural chlorins with pyridine-containing chelate groups as prototypes of drugs for combination therapy in oncology

327

Larisa A. Shcherbakova, Alsu I. Saitgareeva, Mariia G. Gordienko, Ruslan R. Safarov

Study of inhalation micropowders obtained by spray drying

CHEMISTRY AND TECHNOLOGY OF INORGANIC MATERIALS

337

Anastasia A. Kholodkova, Maksim V. Korniyushin, Andrey V. Smirnov, Levko A. Arbanas, Arseniy N. Khrustalev, Viktoria E. Bazarova, Aleksey V. Shumyantsev, Stepan Yu. Kupreenko, Yurii D. Ivakin

Cold sintering of α - and γ -modifications of aluminum oxohydroxides: A low-temperature route to porous corundum ceramics

SYNTHESIS AND PROCESSING OF POLYMERS AND POLYMERIC COMPOSITES

350

Alexander A. Nikolaev, Alexander P. Kondratov

Application of interlayer perforation and installation of transparent elements in the technology of duplicated decorative polymer films

360

Dmitry A. Nilidin, Marat A. Vaniev, Andrey A. Vernigora, Andrey V. Davidenko, Nikita A. Salykin, Thuy Dang Minh, Sergey G. Gubin, Ivan A. Novakov

N-[(1*RS*)-Camphan-2-ylidene]-4-ethoxyaniline and its reduction product as stabilizers of nitrile butadiene rubbers

ANALYTICAL METHODS IN CHEMISTRY AND CHEMICAL TECHNOLOGY

372

Alexander V. Nikulin, Leonid Yu. Martynov, Ramnat S. Gabaeva, Mikhail A. Lazov

Development of a new inversion-voltammetric technique in determining inorganic iodine in *Laminariae thalli* L. for the quality control of raw materials in factory laboratories

ERRATUM

384

D.S. Polyansky, E.I. Ryabova, A.A. Derkaev, N.S. Starkov, I.S. Kashapova, D.V. Shcheblyakov, A.P. Karpov, I.B. Esmagambetov

Erratum to the article "Development of technology for culturing a cell line producing a single-domain antibody fused with the Fc fragment of human IgG1"

СОДЕРЖАНИЕ

ТЕОРЕТИЧЕСКИЕ ОСНОВЫ ХИМИЧЕСКОЙ ТЕХНОЛОГИИ

273 *М.Р. Аглиуллин, А.Н. Хазипова, А.Ф. Ахметов, О.А. Баулин*
Гидроизомеризация *n*-гексадекана на Pt-содержащих силикоалюмофосфатных молекулярных ситах SAPO-11 с различным содержанием кремния

279 *Д.А. Рыжкин, В.М. Раева*
Сравнение методов расчета энтальпии парообразования бинарных азеотропных смесей

ХИМИЯ И ТЕХНОЛОГИЯ ОРГАНИЧЕСКИХ ВЕЩЕСТВ

293 *А.Д. Кирилин, Л.О. Белова, Н.А. Голуб, М.В. Плетнева, Н.И. Кирилина, Д.Е. Миронов*
Использование азотсодержащих кремнийорганических соединений при создании термо- и огнестойких заливочных композиций для герметизации высоковольтной и высокочастотной аппаратуры

ХИМИЯ И ТЕХНОЛОГИЯ ЛЕКАРСТВЕННЫХ ПРЕПАРАТОВ И БИОЛОГИЧЕСКИ АКТИВНЫХ СОЕДИНЕНИЙ

310 *Н.С. Кирилин, П.В. Островерхов, М.Н. Усачев, К.П. Бирин, М.А. Грин*
Комплексы платины(II) на основе производных природных хлоринов с пиридинсодержащими хелатными группами: прототипы лекарств для комбинированной терапии в онкологии

327 *Л.А. Щербакова, А.И. Саитгареева, М.Г. Гордиенко, Р.Р. Сафаров*
Исследование ингаляционных микропорошков, полученных методом распылительной сушки

ХИМИЯ И ТЕХНОЛОГИЯ НЕОРГАНИЧЕСКИХ ВЕЩЕСТВ

337 *А.А. Холодкова, М.В. Корнюшин, А.В. Смирнов, Л.А. Арбанас, А.Н. Хрусталева, В.Е. Базарова, А.В. Шумянцева, С.Ю. Купреенко, Ю.Д. Ивакин*
Холодное спекание α - и γ -модификаций оксигидроксида алюминия: низкотемпературный способ получения пористой корундовой керамики

СИНТЕЗ И ПЕРЕРАБОТКА ПОЛИМЕРОВ И КОМПОЗИТОВ НА ИХ ОСНОВЕ

350 *А.А. Николаев, А.П. Кондратов*
Применение межслойной перфорации и закладки прозрачных элементов в технологии дублированных декоративных полимерных пленок

360 *Д.А. Нилидин, М.А. Ваниев, А.А. Вернигора, А.В. Давиденко, Н.А. Салыкин, Данг Минь Тхуи, С.Г. Губин, И.А. Новаков*
N-[(1*RS*)-камфан-2-илиден]-4-этоксанилин и продукт его восстановления как стабилизаторы бутадиен-нитрильных резин

АНАЛИТИЧЕСКИЕ МЕТОДЫ В ХИМИИ И ХИМИЧЕСКОЙ ТЕХНОЛОГИИ

372 *А.В. Никулин, Л.Ю. Мартынов, Р.С. Габаева, М.А. Лазов*
Разработка новой инверсионно-вольтамперометрической методики определения неорганического йода в слоевищах ламинарии (*Laminariae thalli* L.) для контроля качества сырья в условиях заводских лабораторий

ИСПРАВЛЕНИЯ

384 *Д.С. Полянский, Е.И. Рябова, А.А. Деркаев, Н.С. Старков, И.С. Кашанова, Д.В. Щебляков, А.П. Карпов, И.Б. Есмагамбетов*
Исправления к статье «Разработка технологии культивирования клеточной линии, продуцирующей однодоменное антитело, слитое с Fc-фрагментом IgG1 человека»

Theoretical bases of chemical technology
Теоретические основы химической технологии

UDC 547.464.7

<https://doi.org/10.32362/2410-6593-2024-19-4-273-278>

EDN SPGLZH



RESEARCH ARTICLE

Hydroisomerization of *n*-hexadecane on Pt-containing silicone aluminum phosphate molecular sieves SAPO-11 with different silicon content

Marat R. Agliullin¹, Al'fira N. Khazipova¹, Arslan F. Akhmetov², Oleg A. Baulin²

¹ Institute of Petrochemistry and Catalysis, Ufa, 450075 Russia

² Ufa State Petroleum Technological University, Ufa, 450064 Russia

✉ Corresponding author; e-mail: maratradikovich@mail.ru

Abstract

Objectives. To obtain silicone aluminum phosphate molecular sieves SAPO-11 with different silicon content, to determine their pore space and acidic properties, to apply 0.5 wt % to their surface Pt, and to evaluate the effectiveness of the use of *n*-hexadecane in the hydroisomerization reaction.

Methods. The chemical composition of the SAPO-11 molecular sieves obtained was determined by means of X-ray fluorescence spectroscopy using a Shimadzu EDX-7000P device. The radiographs of non-calcined SAPO-11 were recorded on a Shimadzu XRD-7000 diffractometer in CuK α radiation.

Results. Silicone aluminum phosphate molecular sieves SAPO-11 containing 0.5 wt % Pt on the surface were obtained from gels. As the SiO₂/Al₂O₃ ratio increases, the number of acid centers increases. This then leads to an increase in the conversion of *n*-hexadecane. The selectivity of the formation of hydrocarbons of the structure decreases at the same time.

Conclusions. Silicone aluminum phosphate molecular sieves Pt-SAPO-11 were obtained. It was also found that the samples undergo *n*-hexadecane conversion.

Keywords

molecular sieves, silicone aluminum phosphate SAPO-11, catalysts for hydroisomerization of *n*-hexadecane

Submitted: 15.03.2024

Revised: 08.04.2024

Accepted: 01.07.2024

For citation

Agliullin M.R., Chazipova A.N., Achmetov A.F., Baulin O.A. Hydroisomerization of *n*-hexadecane on Pt-containing silicone aluminum phosphate molecular sieves SAPO-11 with different silicon content. *Tonk. Khim. Tekhnol. = Fine Chem. Technol.* 2024;19(4):273–278. <https://doi.org/10.32362/2410-6593-2024-19-4-273-278>

НАУЧНАЯ СТАТЬЯ

Гидроизомеризация *n*-гексадекана на Pt-содержащих силикоалюмофосфатных молекулярных ситах SAPO-11 с различным содержанием кремния

М.Р. Аглиуллин¹✉, А.Н. Хазипова¹, А.Ф. Ахметов², О.А. Баулин²

¹ Институт нефтехимии и катализа, Уфа, 450075 Россия

² Уфимский государственный нефтяной технический университет, Уфа, 450064 Россия

✉ Автор для переписки, e-mail: maratradikovich@mail.ru

Аннотация

Цель. Получить силикоалюмофосфатные молекулярные сита SAPO-11 с различным содержанием кремния, изучить свойства их пористой структуры и кислотные свойства; приготовить на их основе бифункциональные Pt-содержащие катализаторы (0.5 мас. % Pt) и оценить их каталитические свойства в реакции гидроизомеризации *n*-гексадекана.

Методы. Анализ химического состава синтезированных силикоалюмофосфатов SAPO-11 проводили на приборе Shimadzu EDX-7000P методом рентгенофлуоресцентной спектроскопии. Фазовый состав образцов SAPO-11 анализировали методом рентгеновской порошковой дифракции на дифрактометре Shimadzu XRD-7000 в Cu-K α излучении.

Результаты. Синтезированы из реакционных гелей силикоалюмофосфатные молекулярные сита SAPO-11 с различным содержанием Si и приготовлены на их основе бифункциональные Pt-содержащие катализаторы гидроизомеризации высших *n*-парафинов. С ростом соотношения SiO₂/Al₂O₃ увеличивается число кислотных центров, что приводит к возрастанию конверсии *n*-гексадекана. Селективность образования углеводородов *изо*-строения при этом снижается.

Выводы. Установлено, что соотношение SiO₂/Al₂O₃ в исходных реакционных гелях оказывает влияние как на концентрацию кислотных центров, так и на свойства пористой структуры силикоалюмофосфатов SAPO-11. Показано, что соотношение SiO₂/Al₂O₃ оказывает существенное влияние на каталитические свойства SAPO-11 в гидроизомеризации *n*-гексадекана.

Ключевые слова

молекулярные сита, силикоалюмофосфат SAPO-11, катализаторы гидроизомеризации *n*-гексадекана

Поступила: 15.03.2024

Доработана: 08.04.2024

Принята в печать: 01.07.2024

Для цитирования

Аглиуллин М.Р., Хазипова А.Н., Ахметов А.Ф., Баулин О.А. Гидроизомеризация *n*-гексадекана на Pt-содержащих силикоалюмофосфатных молекулярных ситах SAPO-11 с различным содержанием кремния. *Тонкие химические технологии*. 2024;19(4):273–278. <https://doi.org/10.32362/2410-6593-2024-19-4-273-278>

INTRODUCTION

Zeolite catalysts are widely used in modern oil refining and petrochemistry [1–2]. Silicoaluminophosphate molecular sieves (SAPO-*n*) are used [3–10] in particular, for the hydroisomerization of *n*-paraffins C₁₄–C₁₈. Their efficiency is determined by acidity, pore size and the nature of adsorbed metal. The catalytic properties of SAPO-*n* zeolites are largely determined by the silicon content and the preparation technology, on which the pore size and acidity depend [3, 11–19].

We have previously described the preparation of SAPO-11 molecular sieves (structured type AEL) with a one-dimensional channel system and a pore size of 4.0–6.5 Å and SiO₂/Al₂O₃ ratio of 0.1 and 0.5 (SAPO-11-0.1 and SAPO-11-0.5), used in the oligomerization process

of α -methylstyrene [20]. Continuing this research, we deposited 0.5 wt % metallic platinum on these zeolites. After extruding and grinding, particles of 20–40 μ m size were used as catalysts for the hydroisomerization of *n*-hexadecane.

MATERIALS AND METHODS

SAPO-11 Synthesis

SAPO-11 silicoaluminophosphate molecular sieves were synthesized according to the method described in [21] from reaction gels with the following compositions: 1.0Al₂O₃ : 1.0P₂O₅ : (0; 0.2; 0.5) SiO₂ : 1.0(Templat) : 45H₂O. Phosphoric acid (H₃PO₄, 85%, *Reakhim*, Russia), pseudobemite (AlO(OH), 72% Al₂O₃, *Ishimbay Specialized Chemical Catalyst Plant*, Russia), white soot (*SIGMA*, USA), di-*n*-propylamine (99%,

Table 1. Chemical and phase composition of reaction gels and their crystallization products (SAPO-11 and AIPO-11 molecular sieves)

Sample	Chemical composition of the initial reaction mass	Chemical composition of SAPO-11	Crystallinity, %
AIPO-11-0	$\text{Al}_{1.00}\text{P}_{0.98}\text{Si}_{0.00}$	$\text{Al}_{1.00}\text{P}_{0.98}\text{Si}_{0.00}$ (AIPO-11)	~93
SAPO-11-0.1	$\text{Al}_{1.00}\text{P}_{0.98}\text{Si}_{0.05}$	$\text{Al}_{1.00}\text{P}_{0.90}\text{Si}_{0.03}$ (SAPO-11)	~92
SAPO-11-0.5	$\text{Al}_{1.00}\text{P}_{0.98}\text{Si}_{0.25}$	$\text{Al}_{1.00}\text{P}_{0.91}\text{Si}_{0.18}$ (SAPO-11)	~95

Acros Organics, Belgium) and distilled water were used in the preparation of reaction gels. After the addition of all components, the reaction mixture was stirred at room temperature (25°C) for 1 h. The resulting thick gel was then incubated in an air thermostat for 24 h at 90°C. It had previously been found that preliminary aging of the gel at 90°C allows silicoaluminophosphate SAPO-11 of high phase purity and degree of crystallinity to be selectively obtained during its further crystallization [21]. After the aging step, the gels were loaded into Teflon-coated autoclaves (*TEFIC*, China) and crystallized at 200°C for 24 h. After crystallization, the reaction mass was centrifuged, washed with distilled water and dried at 100°C for 24 h. The SAPO-11 samples obtained from gels with $\text{SiO}_2/\text{Al}_2\text{O}_3$ ratios of 0.1 and 0.5 are designated as SAPO-11-0.1 and SAPO-11-0.5. Furthermore, a sample from a silicon-free gel was synthesized and designated as AIPO-11.

Preparation of catalytic systems

Bifunctional catalysts containing platinum (Pt/SAPO-11) were prepared in the following way: SAPO-11 samples with different silicon contents calcined at 600°C for 6 h in air were impregnated with an aqueous solution of $\text{H}_2\text{PtCl}_6 \cdot 6\text{H}_2\text{O}$ at the rate of 0.5 wt % Pt per weight of catalyst, then dried at room temperature at 25°C for 48 h and at 100°C for 24 h. The samples containing platinum compounds were then calcined in a muffle furnace at 600°C for 6 h in air. Next, the samples containing platinum compounds were subjected to calcination in a muffle furnace (*LIOP*, China) at 550°C for 5 h. After calcination, the samples were extruded, pulverized and sieved, in order to obtain a particle size fraction of 20–40 μm. The samples containing Pt SAPO-11-0.1 and SAPO-11-0.5 are hereinafter designated as Pt/SAPO-11-0.1 and Pt/SAPO-11-0.5, respectively. The silicon-free catalyst sample is designated as Pt/AIPO-11.

Methods of material analysis

The chemical composition of the synthesized SAPO-11 silicoaluminophosphates was analyzed using an EDX-7000P (*Shimadzu*, Japan) instrument by means of X-ray fluorescence spectroscopy.

The phase composition of SAPO-11 samples was analyzed by means of X-ray powder diffraction on an XRD-7000 diffractometer (*Shimadzu*, Japan) in Cu-K α radiation. Scanning was carried out in the region of 2 θ angles from 5° to 40° with a step of 1 deg/min. The processing of X-ray images and phase analysis were performed using the Shimadzu XRD program. The crystallinity was evaluated by the content of amorphous halo in the region from 20° to 30° of 2 θ angles using the Shimadzu XRD program.

More detailed properties of the synthesized silicoaluminophosphate molecular sieves SAPO-11 are described in the dissertation of O.S. Travkina¹.

Hydroisomerization of *n*-hexadecane

The hydroisomerization reaction of *n*-hexadecane ($n\text{-C}_{16}\text{H}_{34}$, 99%, *ReaKhim*, Russia) was carried out in an integral flow reactor under a pressure of 3.0 MPa at 280–350°C with a molar ratio of $\text{H}_2/n\text{-C}_{16}\text{H}_{34} = 12$ mol/mol and a mass feed rate of 2 h⁻¹. The reaction products were analyzed by means of gas–liquid chromatography on HRGC 5300 Mega Series Carlo Erba chromatograph (*Carlo Erba*, Italy) using a flame ionization detector (glass capillary column 50 m, SE-30). The products were identified by means of chromatography-mass spectrometry on a chromatography-mass spectrometer GCMS-TQ8050 (*Shimadzu*, Japan) using the WILEY mass-spectrum library. The physicochemical characteristics of the products obtained corresponded to the data available in literature [9].

¹ Travkina O.S. *Granular zeolites A, X, Y, mordenite and ZSM-5 of a high degree of crystallinity with a hierarchical porous structure: synthesis, properties and application in adsorption and catalysis*. Diss. Dr. Sci. (Chem.). Ufa; 2023. 332 p. (in Russ.).

RESULTS AND DISCUSSION

The hydroisomerization of *n*-hexadecane $n\text{-C}_{16}\text{H}_{34}$ upon the Pt/SAPO-11-0.1, Pt/SAPO-11-0.5, and Pt/AlPO-11 samples in the temperature range 280–340°C was studied (Fig. 1). It was found that the reaction products mainly contain methyl pentadecanes. Among them the corresponding 2-, 3-, and 4-monomethyl derivatives are the main isomers.

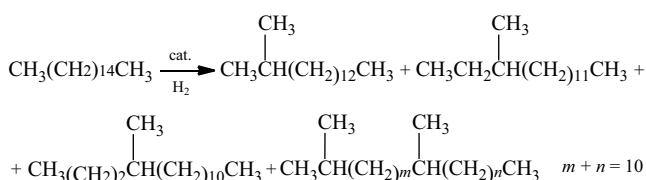
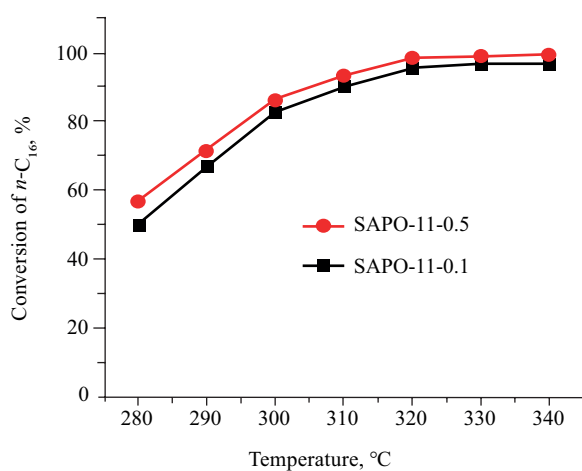


Fig. 1. Hydroisomerization of *n*-hexadecane $n\text{-C}_{16}\text{H}_{34}$

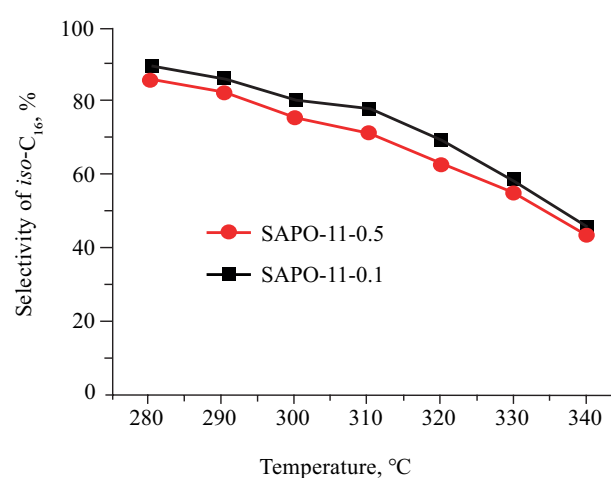
It follows from [22] that the predominant formation of such products (Table 2) is associated with the structure of the microporous structure of silicoaluminophosphates Pt/SAPO-11. In parallel, low hydrocarbons $\text{C}_6\text{--C}_8$ (cracking products) are formed in small amounts.

When the loading ratio of $\text{SiO}_2/\text{Al}_2\text{O}_3$ is increased to 0.5, the selectivity of their formation increases up to 30% (310°C). As temperature increases from 310 to 340°C, the selectivity of isomerization sharply decreases, and the main priority is cracking (Fig. 2).

It follows from the data obtained (Table 2) that the catalyst Pt/SAPO-11-0.1 is more effective for isomerization processes, providing a higher total yield of isomers. We assume that this is due to the number of acid centers in the sample Pt/SAPO-11-0.5, which are 5 times greater, including on the outer surface of the crystals, relative to the sample Pt/SAPO-11-0.1.



(a)



(b)

Fig. 2. Hydroisomerization of *n*-hexadecane over Pt/SAPO-11 catalysts: (a) conversion of *n*-C₁₆; (b) selectivity of *iso*-C₁₆ formation

Table 2. Results of hydroisomerization of *n*-hexadecane at 310°C on Pt-containing samples of silicoaluminophosphate molecular sieves

Name	Pt/SAPO-11-0.1	Pt/SAPO-11-0.5
Conversion of <i>n</i> -C ₁₆ , %	90	94
Selectivity of $\Sigma i\text{-C}_{16}$, %	78	71
Composition of reaction products, %		
2-MeC ₁₅ , %	21	20
3-MeC ₁₅ , %	18	16
4-MeC ₁₅ , %	13	11
5-MeC ₁₅ , %	5	3
6-MeC ₁₅ , %	9	6
(CH ₃) ₂ -C ₁₄ , %	12	15
$\Sigma \text{C}_6\text{--C}_8$, %	22	29

Symbols: selectivity of $\Sigma i\text{-C}_{16}$ is the total selectivity for C₁₆ isomers; (CH₃)₂-C₁₄ is di- and trimethylisomers of C₁₆; $\Sigma \text{C}_6\text{--C}_8$ are cracking products.

It should be noted that in the silicon-free aluminophosphate Pt/AlPO-11, the hydroisomerization of $n\text{-C}_{16}\text{H}_{34}$ under these conditions is not observed. We attribute this to the fact that the acid centers in silicoaluminophosphates, responsible for the course of skeletal isomerization, are formed only when silicon oxide is introduced into the material. This was shown in a previous study [23].

CONCLUSIONS

This study examined the effect of different silicon content on the degree of crystallinity, morphology and size of SAPO-11 silicoaluminophosphates. Samples SAPO-11-0.1 and SAPO-11-0.5 with 0.5 wt % Pt deposited were investigated as catalysts for the hydroisomerization of *n*-hexadecane. It was shown that the samples of bifunctional catalysts at 300°C, 3 MPa, 2.0 h⁻¹ and H₂/C₁₆ = 12 mol/mol enable *iso*-hexadecane yields of at least 70% to be obtained, with *n*-hexadecane conversion of more than 90%.

REFERENCES

1. Vermeiren W., Gilson J.P. Impact of zeolites on the petroleum and petrochemical industry. *Top. Catal.* 2009;52(9): 1131–1161. <http://doi.org/10.1007/s11244-009-9271-8>
2. Lin C.C.H., Dambrowitz K.A., Kuznicki S.M. Evolving applications of zeolite molecular sieves. *Canadian J. Chem. Eng.* 2012;90(2):207–216. <https://doi.org/10.7939/R3862BJ6C>
3. Blasco T., Chica A., Corma A., Murphy W.J., Agundez-Rodriguez J., Perez-Pariente J. Changing the Si distribution in SAPO-11 by synthesis with surfactants improves the hydroisomerization/dewaxing properties. *J. Catal.* 2006;242:153–161. <https://doi.org/10.1016/j.jcat.2006.05.027>
4. Song Ch.-M., Yang H., Wang Y., Feng Y., Shi X., Duan H. Dry-gel conversion synthesis of SAPO-11 molecular sieves and their use in hydroisodewaxing of hydrocracking recycle oil. *Asia-Pac. J. Chem. Eng.* 2016;11(6):846–854. <https://doi.org/10.1002/apj.2018>
5. Wei X., Kikhtyanin O.V., Parmon V.N., Wu W., Bai X., Zhang J., Xiao L., Su X., Zhang Y. Synergetic effect between the metal and acid sites of Pd/SAPO-41 bifunctional catalysts in *n*-hexadecane hydroisomerization. *J. Por. Mater.* 2018;25: 235–247. <https://doi.org/10.1007/s10934-017-0437-7>
6. Miller S.J. New molecular sieve process for lube dewaxing by wax isomerization. *Micropor. Mater.* 1994;2(5):439–449. [https://doi.org/10.1016/0927-6513\(94\)00016-6](https://doi.org/10.1016/0927-6513(94)00016-6)
7. Zhang Sh., Chen Sh.-L., Dong P., Yuan G., Xu K. Characterization and hydroisomerization performance of SAPO-11 molecular sieves synthesized in different media. *Appl. Catal. A: Gen.* 2007;332(1):46–55. <http://doi.org/10.1016/j.apcata.2007.07.047>
8. Zhang Sh., Chen Sh.-L., Dong P., Ji Zh., Zhao J., Xu K. Synthesis, characterization and hydroisomerization catalytic performance of nanosize SAPO-11 molecular sieves. *Catal. Lett.* 2007;118(1–2):109–117. <https://doi.org/10.1007/s10562-007-9138-1>
9. Du Y., Feng B., Jiang Y., Yuan L., Huang K., Li J. Solvent-Free Synthesis and *n*-Hexadecane Hydroisomerization Performance of SAPO-11 Catalyst. *Eur. J. Inorg. Chem.* 2018;2018(22):2599–2606. <https://doi.org/10.1002/ejic.201800134>
10. Gerasimov D.N., Kashin E.V., Pigoleva I.V., Maslov I.A., Fadeev V.V., Zaglyadova S.V. Effect of Zeolite Properties on Dewaxing by Isomerization of Different Hydrocarbon Feedstocks. *Energ. Fuel.* 2019;33(4):3492–3503. <https://doi.org/10.1021/acs.energyfuels.9b00289>
11. Yang Zh., Li J., Liu Y., Liu Ch. Effect of silicon precursor on silicon incorporation in SAPO-11 and their catalytic performance for hydroisomerization of *n*-octane on Pt-based catalysts. *J. Energy Chem.* 2017;26(4):688–694. <https://doi.org/10.1016/j.jechem.2017.02.002>
12. Araujo A.S., Fernandes V.J., Diniz J.C., Silva A.O.S., Silva C.C., Santos R.H.A. Hydrothermal synthesis and crystallographic properties of silicoaluminophosphate with different content of silicon. *Mater. Res. Bull.* 1999;34(9):1369–1373. [https://doi.org/10.1016/S0025-5408\(99\)00135-X](https://doi.org/10.1016/S0025-5408(99)00135-X)
13. Wang X., Zhang W., Guo Sh., Zhao L., Xiang H. Optimization of the Synthesis of SAPO-11 for the Methylation of Naphthalene with Methanol by Varying Templates and Template Content. *J. Braz. Chem. Soc.* 2013;24(7):1180–1187. <https://doi.org/10.5935/0103-5053.20130152>
14. Yang L., Wang W., Song X., Bai X., Feng Zh., Liu T., Wu W. The hydroisomerization of *n*-decane over Pd/SAPO-11 bifunctional catalysts: The effects of templates on characteristics and catalytic performances. *Fuel Proc. Tech.* 2019;190:13–20. <https://doi.org/10.1016/j.fuproc.2019.02.027>
15. Liu P., Ren J., Sun Y. Synthesis, characterization and catalytic properties of SAPO-11 with high silicon dispersion. *Catal. Commun.* 2008;9(9):1804–1809. <https://doi.org/10.1016/j.catcom.2008.01.030>
16. Liu P., Ren J., Sun Y. Influence of template on Si distribution of SAPO-11 and their performance for *n*-paraffin isomerization. *Micropor. Mesopor. Mater.* 2008;114(1–3):365–372. <https://doi.org/10.1016/j.micromeso.2008.01.022>
17. Singh P.S., Bandyopadhyay R., Rao B.S. Characterization of SAPO-11 synthesized conventionally and in the presence of fluoride ions. *J. Chem. Soc. Faraday Trans.* 1996;92(11): 2017–2026. <https://doi.org/10.1039/FT9969202017>
18. Sinha A.K., Seelan S. Characterization of SAPO-11 and SAPO-31 synthesized from aqueous and non-aqueous media. *Appl. Catal. A: Gen.* 2004;270(1–2):245–252. <https://doi.org/10.1016/j.apcata.2004.05.013>
19. Wang Zh., Tian Zh., Teng F., Wen G., Xu Y., Xu Zh., Lin L. Hydroisomerization of Long-Chain Alkane Over Pt/SAPO-11 Catalysts Synthesized from Nonaqueous Media. *Catal. Lett.* 2005; 103(1–2):109–116. <https://doi.org/10.1007/s10562-005-6510-x>
20. Agliullin M.R., Cherepanova S.V., Fayzullina Z.R., Serebrennikov D.V., Khalilov L.M., Prosochkina T.R., Kutepov B.I. Crystallization of SAPO-11 Molecular Sieves Prepared from Silicoaluminophosphate Gels Using Boehmites with Different Properties. *Gels.* 2023;9(2):123. <https://doi.org/10.3390/gels9020123>

Acknowledgments

The research was financially supported by of the Priority 2030 program.

Authors' contributions

M.R. Agliullin—conducting research, collecting and processing material, and writing the text of the article.

A.N. Khazipova—review of publications on the topic of the article.

A.F. Akhmetov—planning consultations.

O.A. Baulin—conceptualization of the research paper, critical revision with the introduction of valuable intellectual content.

The authors declare no conflicts of interest.

21. Agliullin M.R., Arzumanov S.S., Gerasimov E.Y., Grigorieva N.G., Bikbaeva V.R., Serebrennikov D.V., Khalilov L.M., Kutepov B.I. Crystal engineering of SAPO-11 sieves by forming intermediate phases. *CrystEngComm*. 2023;25(20):3096–3107. <https://doi.org/10.1039/d3ce00278k>
22. Lok B.M., Messina C.A., Patton R.L., Gajek R.T., Cannan T.R., Flanigen E.M. *Crystalline Silicoaluminophosphates*: USA Pat. 44440871. Publ. 03.04.1984.
23. Flanigen E.M., Patton R.L., Wilson S.T. Structural, synthetic and physicochemical concepts in aluminophosphate-based molecular sieves. *Studies in Surface Science and Catalysis*. 1988;37:13–27. [http://doi.org/10.1016/S0167-2991\(09\)60578-4](http://doi.org/10.1016/S0167-2991(09)60578-4)

About the authors

Marat R. Agliullin, Cand. Sci. (Chem.), Senior Researcher, Institute of Petrochemistry and Catalysis, Ufa Federal Research Center, Russian Academy of Sciences (141, Oktyabrya pr., Ufa, 450075, Russia). E-mail: maratradikovich@mail.ru. Scopus Author ID 56480769400, ResearcherID M-6486-2016, <https://orcid.org/0000-0002-2210-9520>

Alfira N. Khazipova, Cand. Sci. (Chem.), Senior Researcher, Institute of Petrochemistry and Catalysis, Ufa Federal Research Center, Russian Academy of Sciences (141, Oktyabrya pr., Ufa, 450075, Russia). E-mail: khazipova@gmail.com. Scopus Author ID 6506529764, ResearcherID AAC-3049-2022, RSCI SPIN-code 1558-3478, <https://orcid.org/0000-0002-2643-8233>

Arslan F. Akhmetov, Dr. Sci. (Eng.), Professor, Head of the Department of Oil and Gas Technology, Ufa State Petroleum Technological University (1, Kosmonavtov ul., Ufa, 450064, Russia). E-mail: tngrusoil@mail.ru. Scopus Author ID 7004645636, ResearcherID L-4129-2017, RSCI SPIN-code 3282-5937, <https://orcid.org/0000-0003-0478-5928>

Oleg A. Baulin, Cand. Sci. (Eng.), Associate Professor, Rector, Ufa State Petroleum Technological University (1, Kosmonavtov ul., Ufa, 450064, Russia). E-mail: rector@rusoil.net. Scopus Author ID 57189619506, RSCI SPIN-code 3207-2586, <https://orcid.org/0000-0002-6744-7451>

Об авторах

Аглиуллин Марат Радикович, к.х.н., старший научный сотрудник, Институт нефтехимии и катализа – обособленное структурное подразделение, ФГБНУ Уфимский федеральный исследовательский центр Российской академии науки (450075, Россия, г. Уфа, пр. Октября, 141). E-mail: maratradikovich@mail.ru. Scopus Author ID 56480769400, ResearcherID M-6486-2016, <https://orcid.org/0000-0002-2210-9520>

Хазипова Альфира Наилевна, к.х.н., старший научный сотрудник, Институт нефтехимии и катализа – обособленное структурное подразделение, ФГБНУ Уфимский федеральный исследовательский центр Российской академии науки (450075, Россия, г. Уфа, пр. Октября, 141). E-mail: khazipova@gmail.com. Scopus Author ID 6506529764, ResearcherID AAC-3049-2022, SPIN-код РИНЦ 1558-3478, <https://orcid.org/0000-0002-2643-8233>

Ахметов Арслан Фаритович, д.т.н., профессор, заведующий кафедрой «Технология нефти и газа», ФГБОУ ВО «Уфимский государственный нефтяной технический университет» (450064, Россия, г. Уфа, ул. Космонавтов, д. 1). E-mail: tngrusoil@mail.ru. Scopus Author ID 7004645636, ResearcherID L-4129-2017, SPIN-код РИНЦ 3282-5937, <https://orcid.org/0000-0003-0478-5928>

Баулин Олег Александрович, к.т.н., доцент, ректор, ФГБОУ ВО «Уфимский государственный нефтяной технический университет» (450064, Россия, г. Уфа, ул. Космонавтов, д. 1). E-mail: rector@rusoil.net. Scopus Author ID 57189619506, SPIN-код РИНЦ 3207-2586, <https://orcid.org/0000-0002-6744-7451>

Translated from Russian into English by H. Moshkov

Edited for English language and spelling by Dr. David Mossop

Theoretical bases of chemical technology
Теоретические основы химической технологии

UDC 544.012+544.3.032.3

<https://doi.org/10.32362/2410-6593-2024-19-4-279-292>

EDN WXQZSM



RESEARCH ARTICLE

Comparison of methods for calculating the enthalpy of vaporization of binary azeotropic mixtures

Dmitriy A. Ryzhkin, Valentina M. Raeva✉

MIREA — Russian Technological University (M.V. Lomonosov Institute of Fine Chemical Technologies), Moscow, 119571 Russia

✉ Corresponding author; e-mail: raevalentina1@gmail.com

Abstract

Objectives. To calculate the molar enthalpy of vaporization of binary homogeneous mixtures based on isothermal and isobaric vapor–liquid equilibrium data, and to compare the results of calculation of molar enthalpy of vaporization by different methods with experimental data.

Methods. Simulation of the vapor–liquid equilibrium of binary systems according to the Non-Random Two Liquid “local compositions” equation and thermodynamic calculations of molar vaporization enthalpies of binary mixtures at different conditions of vapor–liquid equilibrium were used.

Results. Arrays of calculated data were obtained with regard to molar enthalpies of vaporization for 25 compositions of binary azeotropes (isothermal, isobaric conditions of phase equilibrium), and the full range of compositions of the benzene–ethanol system at atmospheric pressure.

Conclusions. The accuracy of thermodynamic methods for calculating the vaporization enthalpy of binary azeotropic mixtures according to vapor–liquid equilibrium data is higher in 85% of cases for isothermal, and in 75% of cases for isobaric conditions. By taking into account the influence of temperature on the activity coefficients of components in the liquid phase, the values of excess molar enthalpy both for azeotrope compositions and for the full concentration range of the benzene–ethanol system under isobaric conditions of liquid–vapor phase equilibrium can be accurately reproduced.

Keywords

molar enthalpy of vaporization, binary azeotropes, vapor–liquid equilibrium

Submitted: 22.08.2023

Revised: 12.12.2023

Accepted: 01.07.2024

For citation

Ryzhkin D.A., Raeva V.M. Comparison of methods for calculating the enthalpy of vaporization of binary azeotropic mixtures. *Tonk. Khim. Tekhnol. = Fine Chem. Technol.* 2024;19(4):279–292. <https://doi.org/10.32362/2410-6593-2024-19-4-279-292>

НАУЧНАЯ СТАТЬЯ

Сравнение методов расчета энтальпии парообразования бинарных азеотропных смесей

Д.А. Рыжкин, В.М. Раева✉

МИРЭА — Российский технологический университет (Институт тонких химических технологий им. М.В. Ломоносова), Москва, 119571 Россия

✉ Автор для переписки, e-mail: raevalentina1@gmail.com

Аннотация

Цели. Расчет молярных энтальпий парообразования бинарных гомогенных смесей по изотермическим и изобарическим данным парожидкостного равновесия; сравнение результатов расчета молярных энтальпий парообразования по разным методам с экспериментальными данными.

Методы. Моделирование парожидкостного равновесия бинарных систем по уравнению «локальных составов» NRTL (Non-Random Two Liquid); термодинамические расчеты молярных энтальпий парообразования смесей в разных условиях парожидкостного равновесия.

Результаты. Получены массивы расчетных данных по молярным энтальпиям парообразования для 25 составов бинарных азеотропов (изотермические, изобарические условия фазового равновесия) и полного диапазона составов системы бензол–этанол при атмосферном давлении.

Выводы. Точность термодинамических методов расчета энтальпий парообразования бинарных азеотропных смесей по данным парожидкостного равновесия выше в 85% случаев для изотермических и в 75% случаев для изобарических условий. Учет влияния температуры на коэффициенты активности компонентов в жидкой фазе позволяет качественно верно воспроизводить значения избыточной молярной энтальпии как для составов азеотропов, так и для полного концентрационного диапазона системы бензол–этанол в изобарических условиях фазового равновесия жидкость–пар.

Ключевые слова

молярная энтальпия парообразования, бинарные азеотропы, парожидкостное равновесие

Поступила: 22.08.2023

Доработана: 12.12.2023

Принята в печать: 01.07.2024

Для цитирования

Рыжкин Д.А., Раева В.М. Сравнение методов расчета энтальпии парообразования бинарных азеотропных смесей. *Тонкие химические технологии*. 2024;19(4):279–292. <https://doi.org/10.32362/2410-6593-2024-19-4-279-292>

INTRODUCTION

The enthalpy of vaporization is the most important thermophysical property of substances and mixtures [1–4]. The accurate estimation of the enthalpy of vaporization and its dependence on temperature is a requirement for the study of phase transitions [5–7]. In order to calculate the thermal balances of distillation columns, reliable data on molar enthalpies of vaporization of substances H_V^0 and mixtures H_V (designations: V—vaporization, 0—pure substance) in different conditions of phase equilibrium are necessary [8–10].

Direct calorimetric measurements of vaporization enthalpies are difficult and time-consuming [5, 11–15]. Experimentally measured H_V values of mixtures are given in [16–20] for individual compositions. There are few experimental data for the full range of compositions of binary systems $H_V(x)$ [9, 14, 21–23]. $H_V(x)$

binary mixtures can be calculated using different arrays of experimental data: excess enthalpies (heat of mixing) of liquid solution $H^E(x)$ (index E stands for Excess); and enthalpies of vaporization of pure substances at a particular temperature [9, 23, 24]. Thermal calculations of distillation columns require data $H_V(x, T)$ on the isobaric conditions of vapor–liquid equilibrium (VLE).

Data on the enthalpies of vaporization of multicomponent mixtures is much less common. The calorimetric measurements are usually carried out for specific compositions of hydrocarbon fractions [25–27] and fuel mixtures [28–30].

Due to the limited amount of experimental data, including those under different VLE conditions, reliable methods need to be developed to calculate the enthalpies of vaporization of mixtures [9, 15, 20]. Currently, methods for calculating and/or predicting the enthalpies

of vaporization of individual substances belonging to certain classes of organic compounds using a limited amount of experimental data have predominantly been developed. The possibilities of calculations using various models and equations of state are considered in [32–35].

Thermodynamic methods for calculations of molar enthalpies of vaporization can be successfully applied to hydrocarbons and their binary mixtures [36–38]. For substances and mixtures, the components of which form hydrogen bonds, special methods for calculating enthalpies of vaporization have been developed [35, 39–41].

CALCULATIONS

A simplified method for calculating the molar enthalpies of vaporization H_V of multicomponent systems from $P(T)$ data for the vapor phase under different VLE conditions is presented in [15]. Let us assume that the vapor phase state of a multicomponent system is determined by the equation of state (1) [42, 43]:

$$PV = ZRT, \quad (1)$$

where P —pressure; V —volume of vapor phase; Z —compressibility coefficient; R —universal gas constant; T —temperature, K. According to the Clausius–Clapeyron equation, the H_V values are defined as:

$$H_V = -RZ \left[\frac{d \ln P}{d(1/T)} \right]_x. \quad (2)$$

If by correlating the experimental P – T data, the following dependence coefficients can be obtained:

$$\ln P = a + \frac{b}{T}, \quad (3)$$

then we can calculate the values of molar enthalpies of vaporization by using the following formula [15]:

$$H_V = -RZb, \quad (4)$$

where a and b are correlation coefficients. Instead of correlation of experimental data, the following ratio can also be applied:

$$H_V = -\frac{RZ \Delta \ln P}{\Delta \left(\frac{1}{T} \right)}. \quad (5)$$

At phase equilibrium, the pressure P over the liquid phase of composition x_i is defined as:

$$P = \sum_{i=1}^N x_i \gamma_i P_i^0, \quad (6)$$

where i —component; γ_i —activity coefficient of the component; P_i^0 —saturated vapor pressure of the component. In order to calculate phase equilibria, phase equilibrium models can be used which take into account the dependence of activity coefficients on the mixture composition and model parameters in various ways [43, 44]. For example, for calculations of VLE and molar enthalpies of vaporization from $P(T)$ data of N -component systems, we used the dependence of the activity coefficients of the components on the mixture composition and parameters of the following VLE model: UNIFAC (UNIversal Functional Activity Coefficient) [15] and NRTL (Non-Random Two Liquid) [45].

Tamir [15] obtained a thermodynamic expression which establishes the relationship between the pressure and temperature of the N -component system under VLE conditions:

$$\frac{d \ln P}{dT} = \sum_{i=1}^N x_i \left[\left(\frac{x_i \gamma_i P_i^0}{P} \right) \left(\frac{d \ln P_i^0}{dT} \right) \right] + \sum_{i=1}^N x_i \left[\left(\frac{x_i P_i^0}{P} \right) \left(\frac{d \gamma_i}{dT} \right) \right]. \quad (7)$$

For azeotropes (Az), $P_i^0 \gamma_i / P = 1$. After introducing the assumption that the activity coefficients of the components are independent of temperature ($d \gamma_i / dT = 0$), which is strictly true only for athermal solutions, Eq. (7) can be transformed to the following form:

$$H_V^{Az} = RT^2 Z \sum_{i=1}^N x_i \left[\frac{d \ln P_i^0}{dT} \right]. \quad (8)$$

Tamir [15] used Antoine's Eq. (9), in order to calculate the dependence of the saturated vapor pressure of the components on temperature, i.e., Eq. (10) is valid for pure substances:

$$\lg P_i^0 = A_i - \frac{B_i}{(T + C_i)}, \quad (9)$$

$$\frac{d P_i^0}{dT} = P_i^0 \frac{B_i}{(T + C_i)^2}, \quad (10)$$

where A , B , and C are equation coefficients (9).

In order to calculate the enthalpies of vaporization of mixtures of azeotropic composition H_V^{Az} , a simplified expression is proposed [39]:

$$H_V^{Az} = 2.3026 RT^2 Z \sum_{i=1}^N \frac{x_i B_i}{(t + C_i)^2},$$

where t is a temperature, °C.

Tamir [15] calculated H_V^{Az} for the ideal vapor phase ($Z = 1$):

$$H_V^{Az} = 2.3026RT^2 \sum_{i=1}^N \frac{x_i B_i}{(t + C_i)^2}. \quad (11)$$

In fact, the enthalpy of vaporization of a mixture of azeotropic composition is determined in Eq. (11) by the data $P_i^0(T)$ for individual components.

Earlier we proposed a procedure for calculating the enthalpy of vaporization H_V of binary and three-component systems under the assumption of ideal vapor phase behavior, while taking into account the temperature dependence of the activity coefficients of the components for any (zeotropic, azeotropic) compositions [45, 46]:

$$P = \sum_{i=1}^N P_i^0(T) x_i \gamma_i(x, T). \quad (12)$$

For binary systems we formulate dP/dT as follows:

$$\begin{aligned} \frac{dP}{dT} &= \sum_{i=1,2} \left(\frac{dP_i^0(T)}{dT} x_i \gamma_i(x, T) + P_i^0(T) x_i \frac{d\gamma_i(x, T)}{dT} \right) = \\ &= \sum_{i=1,2} x_i \left(\frac{dP_i^0(T)}{dT} \gamma_i(x, T) + P_i^0(T) \frac{d\gamma_i(x, T)}{dT} \right). \end{aligned} \quad (13)$$

The values of dP/dT and enthalpy of vaporization of mixtures (14) were determined on the basis of the calculated data of VLE.

$$H_V = \frac{dP}{dT} \frac{RT^2}{P}. \quad (14)$$

A comparison of experimental data arrays $H_V(x)$ with calculated values was previously carried out for the full range of compositions of the benzene–cyclohexane system under isobaric VLE conditions [45], the behavior of the vapor phase of which can be considered ideal [47]. The maximum relative errors for arrays of calculated values of the benzene–cyclohexane system at 50.662, 75.992, and 101.320 kPa do not exceed 5, 5.1, and 6 relative % (rel. %), respectively [45]. A comparison of the results of calculations of molar enthalpies of vaporization, must not only be based on the quantitative indices. The qualitative correspondence of signs of excess values determined from experimental and calculated data was shown to be fundamental.

Molar enthalpies of vaporization can be represented through partial values of

$$H_V = (H_{V1}^0 + \bar{H}_{V1}^E) x_1 + (H_{V2}^0 + \bar{H}_{V2}^E) x_2. \quad (15)$$

Here \bar{H}_{V1}^E and \bar{H}_{V2}^E are partial excess enthalpies of the components, x_i is the composition of the azeotrope

($i = 1; 2$). The partial excess enthalpies for the vapor and liquid phases have opposite signs. The excess value H_V^E can be determined from experimental or calculated data H_V [23, 24, 45]:

$$H_V^E = H_V + H_V^{\text{add}}, \quad (16)$$

where H_V^{add} is an additive value:

$$H_V^{\text{add}} = H_{V1}^0 x_1 + H_{V2}^0 x_2. \quad (17)$$

A comparison of experimental and calculated values $H_V^E(x)$ for the benzene–cyclohexane system shows that the use of Eq. (14) provides a qualitatively correct reproduction of the sign of the excess thermodynamic quantity [45].

The purpose of the present study is to compare experimental and calculated data of molar enthalpies of vaporization for binary homogeneous azeotrope compositions under different VLE conditions.

RESULTS

Binary mixtures of azeotropic compositions H_V^{exp} for which viable modeling of VLE using the NRTL model is possible, were selected from the array of experimental data [15] (Tables 1 and 2). The parameters of the NRTL equation were taken from the database of the Aspen Plus V.10.0 software package. The azeotropic data description errors do not exceed 5 rel. % for compositions and 0.4 rel. % for temperature. Table 2 additionally summarizes the calculated pressure values P^{calc} (kPa) obtained from the NRTL model.

The molar enthalpies of vaporization of binary mixtures of azeotropic compositions were calculated in different ways according to VLE data.

Method I. VLE and H_V were calculated independently using the Aspen Plus V.10.0 platform. Saturated vapor pressures of components P_i^0 in the software package were determined by the following expression:

$$\ln P_i^0 = C_{1i} + \frac{C_{2i}}{T + C_{3i}} + C_{4i} T + C_{5i} \ln T + C_{6i} T^{C_{7i}}. \quad (18)$$

$C_{1i}-C_{7i}$ coefficients are given in the Aspen Plus V.10.0 database.

Molar enthalpies of vaporization of substances H_{Vi}^0 were calculated by means of the Watson equation in the following form:

$$H_{Vi}^0(T) = H_{Vi}^*(T_1) \left(\frac{1 - \frac{T}{T_{ci}}}{1 - \frac{T_1}{T_{ci}}} \right)^{a_i + b_i \left(1 - \frac{T}{T_{ci}} \right)}, \quad (19)$$

where T_{ci} is the critical temperature of component i (index c stands for critical); T_1 is the temperature for which the experimental value of enthalpy of vaporization H_V^* is known; and T is the temperature for which the calculation of H_{Vi}^0 is performed. Parameters a_p , b_p , and critical temperature T_{ci} values are from the NIST database¹.

The enthalpy of vaporization of the mixture H_V was determined as follows:

$$H_V = H^V - H^L, \quad (20)$$

where H^V and H^L are molar enthalpies of vapor (V) and liquid (L) of a mixture of a particular composition.

Method II. The calculations of mixtures H_V were carried out using the VLE data (Eqs. (13) and (14)). The procedure for calculating dP/dT is described in detail in [45]. The molar enthalpies of vaporization of individual substances H_{Vi}^0 (18) were determined using the coefficients of the Antoine equation in the form presented in a previous study [46]:

$$H_{Vi}^0 = \frac{dP_i^0}{dT} \frac{RT^2}{P_i^0}. \quad (21)$$

In all tables, molar enthalpies of vaporization of mixtures H_V are given in kJ/mol, compositions of mixtures—in molar fractions of the component indicated in the name of the mixture first.

Tables 3 and 4 show the data sets for comparison of experimental values H_V^{exp} with the results of calculations H_V^{calc} by methods I and II. Relative errors ΔH_V were determined in the standard way:

$$\Delta H_V = \frac{H_V^{\text{exp}} - H_V^{\text{calc}}}{H_V^{\text{exp}}} \times 100\%. \quad (22)$$

For Eqs. (4) and (11) in [15] only errors (22) are given, by which we determined the calculated values of H_V (Tables 3 and 4).

Table 1. Experimental values of molar vaporization enthalpies for binary mixtures (azeotropic compositions) at atmospheric pressure [15]

No.*	Mixture 1–2	T , K	x_1 , mol. fr.	H_V^{exp} , kJ/mol
1	<i>p</i> -Xylene–hexanol-1	411.49	0.870	42.0
2	Toluene–2-methylpropanol-1	372.64	0.550	39.9
3	Toluene–butanol-1	378.20	0.680	34.2
4	Benzene–methanol	330.62	0.609	33.6

*Experimental point number.

Table 2. Experimental values of molar vaporization enthalpies for binary mixtures (azeotropic compositions) at isothermal VLE [15]

No.	Mixture 1–2	T , K	x_1 , mol. fr.	H_V^{exp} , kJ/mol	P^{calc} , kPa
5	Chloroform–ethanol	320	0.859	31.7	65
6	Acetone–chloroform	320	0.384	33.6	54
7	Propanol-1–ethyl acetate	330	0.218	34.6	52
8	Ethanol–1,4-dioxane	330	0.871	39.7	42
9	Water–1,4-dioxane	330	0.447	39.7	30

¹ Standard Reference Database of National Institute of Standards and Technology. *NIST Chemistry WebBook*. Number 69 (SRD 69). 2022. <https://doi.org/10.18434/T4D303>

Table 2. Continued

No.	Mixture 1–2	T , K	x_1 , mol. fr.	H_V^{exp} , kJ/mol	P^{calc} , kPa
10	Carbon tetrachloride–propanol-1	320	0.876	33.0	39
11	Methanol–benzene	350	0.649	33.2	198
12	Cyclohexane–propanol-2	330	0.647	34.9	64
13	Water–2-chloroethanol	350	0.852	42.8	45
14	Benzene–ethanol	350	0.522	34.9	139
15	Tetrahydrofuran–water	300	0.903	31.0	24
16		320	0.855	32.1	55
17	Water–formic acid	320	0.582	42.4	9
18		360	0.490	41.1	50
19	Water–pyridine	310	0.718	44.7	8
20		350	0.758	41.5	53
21	Ethanol–ethyl acetate	293.8	0.296	36.4	11
22		314.2	0.341	36.0	30
23		320	0.384	35.8	38
24		334	0.417	35.5	67
25		363.2	0.543	34.8	189

Note: Experimental point numbers are given for each temperature condition.

Table 3. Calculated values of molar vaporization enthalpies and relative errors at 101.32 kPa

No.	Eq. (4)		Eq. (11)		Method I		Method II	
	H_V^{calc} , kJ/mol	ΔH_V , %	H_V^{calc} , kJ/mol	ΔH_V , %	H_V^{calc} , kJ/mol	ΔH_V , %	H_V^{calc} , kJ/mol	ΔH_V , %
1	45.2	7.6	43.8	4.4	37.2	–11.5	39.0	–7.1
2	40.7	1.9	46.2	15.7	35.6	–10.8	37.3	–6.5
3	30.5	–10.8	29.8	–12.9	34.7	1.5	36.4	6.3
4	32.6	–3.0	32.7	–2.6	32.3	–3.9	33.9	0.9

Note: the mixture number corresponds to the same number in Table 1.

Table 4. Calculated values of molar vaporization enthalpies and relative errors at isothermal VLE

No.	Eq. (11)		Method I		Method II	
	H_V^{calc} , kJ/mol	ΔH_V , %	H_V^{calc} , kJ/mol	ΔH_V , %	H_V^{calc} , kJ/mol	ΔH_V , %
5	31.5	-0.6	31.4	-1.0	31.8	0.3
6	36.4	8.3	32.0	-4.9	32.8	-2.3
7	32.7	-5.5	34.3	-0.7	34.6	0.1
8	38.7	-2.5	39.7	-0.1	40.4	1.7
9	40.4	1.8	39.2	-1.2	39.7	0.1
10	32.4	-1.8	32.5	-1.5	33.1	0.4
11	31.5	-5.1	31.7	-4.6	33.8	1.8
12	33.6	-3.7	34.5	-1.1	35.1	0.6
13	43.3	1.2	42.4	-1.0	42.7	-0.3
14	35.2	-3.7	33.8	-3.2	35.1	0.7
15	28.5	-8.1	32.9	6.0	33.2	7.1
16	30.9	-3.7	32.4	0.8	32.9	2.5
17	44.5	5.0	36.4	-14.1	40.8	-3.9
18	44.1	7.3	33.7	-17.9	38.8	-5.5
19	33.6	4.5	43.3	-3.1	43.6	-2.5
20	46.7	1.0	41.5	0	41.8	0.7
21	41.9	4.5	36.8	1.1	36.7	0.8
22	38.0	4.3	35.7	-0.8	35.9	-0.4
23	37.5	-4.5	35.5	-0.7	35.8	-0.1
24	34.2	4.6	34.8	-2.0	35.4	-0.3
25	37.1	5.7	33.4	-3.9	35.2	1.3

Note: the mixture number corresponds to the same number in Table 2.

Method II provides a higher level of calculation accuracy when compared to Eqs. (4) and (11), and method I for atmospheric pressure in 75% of cases (Table 3). For isothermal VLE conditions, method II provides a more accurate calculation compared to the results of (11) for 85% of azeotropic compositions (18 out of 21) (Table 4). The accuracy of calculations using method II is lower than by method I only in the

systems ethanol–1,4-dioxane, tetrahydrofuran–water, and pyridine–water (Nos. 8, 15, 16, 20, Table 4).

For the benzene–ethanol system, experimental data $H_V^{\text{exp}}(x)$ is also available for the full range of compositions at atmospheric pressure, but no temperature values are given [22]. The calculated values obtained by the NRTL model are presented in Table 5.

The calculation of VLE using the NRTL model was performed with the binary interaction parameters (τ_{ij} , τ_{ji} , G_{ij} , G_{ji} , α) in the following form:

$$\tau_{ij} = a_{ij} + \frac{b_{ij}}{T}, \quad G_{ij} = \exp(-\alpha\tau_{ij}),$$

where i and j are component indices; τ , α , and G are parameters of the NRTL equation. The parameter α determines the ordering of the molecule distribution in the solution and is related to the coordination number of the liquid, τ is the reduced energy parameter, and G is a variable characterizing the interaction energy. The values $i = 1; 2, j = 1; 2$. The parameters were estimated on the basis of experimental data of the VLE of the benzene (1)–ethanol (2) system [48, 49]. Where $a_{12}=0.7596, b_{12}=309.183, a_{21}=-5.8653, b_{21}=2314.74$, and $\alpha = 0.604$. The average relative errors of the array descriptions do not exceed 1.01 (maximum 3.55) rel. % for vapor phase compositions and 0.02 (maximum 0.08) rel. % for temperature.

The arrays of calculated data for the benzene (1)–ethanol (2) system at atmospheric pressure are summarized in Table 5. The average relative errors of

calculation of molar enthalpies of vaporization of binary mixtures do not exceed 3 rel. %.

The concentration dependencies $H_V(x)$ are presented in Fig. 1. Quantitative differences are caused, as in the case of the benzene (1)–cyclohexane (2) system [45], by the values of molar enthalpies of vaporization of pure substances calculated differently by Eqs. (16) and (18).

Method II provides a qualitative coincidence of concentration dependence types for experimental and calculated data, namely in the whole range of compositions $H_V < H_V^{\text{add}}$ (Fig. 1b). Method I provides qualitatively incorrect results for benzene-enriched mixtures: $H_V > H_V^{\text{add}}$, which does not correspond to the experimental data (Fig. 1a).

The excess values H_V^E were calculated using Eqs. (16) and (17). Quantitative agreement of the values of H_V^E , determined on the basis of experimental and calculated values under isobaric VLE conditions was not achieved. However, method II also qualitatively correctly reproduces the sign of the excess component of the molar enthalpy: $H_V^E < 0$ for all compositions of binary mixtures (Fig. 2b).

Table 5. Experimental and calculated values of the enthalpy of vaporization and relative errors for the benzene (1)–ethanol (2) system at 101.32 kPa

x_1 , mol. fr.	Experiment [22]		Method I			Method II		
	H_V^{exp} , kJ/mol	H_V^E , kJ/mol	H_V^{calc} , kJ/mol	ΔH_V , %	H_V^E , kJ/mol	H_V^{calc} , kJ/mol	ΔH_V , %	H_V^E , kJ/mol
1	30.6	0	30.7	-0.36	0	32.0	-4.35	0
0.929	31.2	-0.02	31.9	-2.18	0.53	30.9	0.81	-1.64
0.852	31.6	-0.23	32.2	-1.80	0.19	31.6	-0.04	-1.63
0.770	32.3	-0.20	32.3	-0.13	-0.34	32.6	-0.99	-1.35
0.672	32.5	-0.77	32.5	-0.01	-0.98	33.6	-3.17	-1.27
0.540	32.9	-1.45	33.0	-0.36	-1.58	34.4	-4.40	-1.61
0.410	33.6	-1.82	33.9	-0.97	-1.78	34.9	-3.78	-2.24
0.310	35.2	-1.01	34.8	1.19	-1.74	35.2	0.11	-2.79
0.208	36.5	-0.57	35.9	1.61	-1.50	35.5	2.65	-3.34
0.086	37.8	-0.25	37.7	0.47	-0.80	36.4	3.71	-3.53
0	38.8	0	39.2	-1.05	0	40.7	-4.98	0

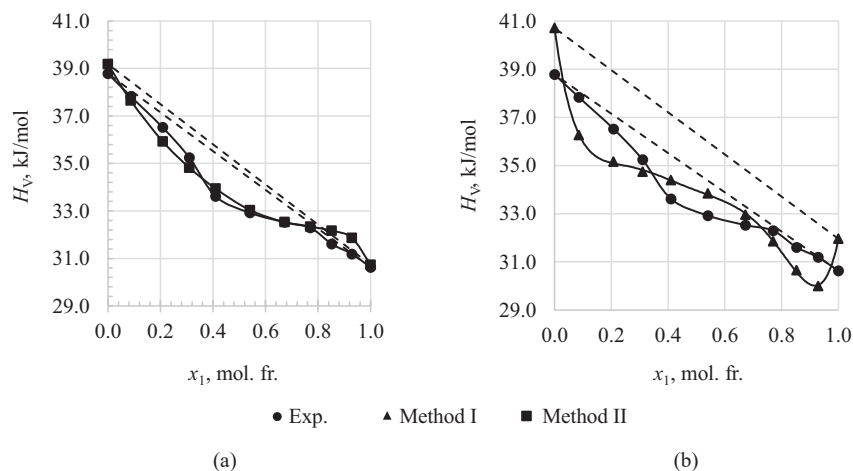


Fig. 1. Dependences of molar vaporization enthalpy for benzene (1)–ethanol (2) system on the composition: (a) method I, (b) method II

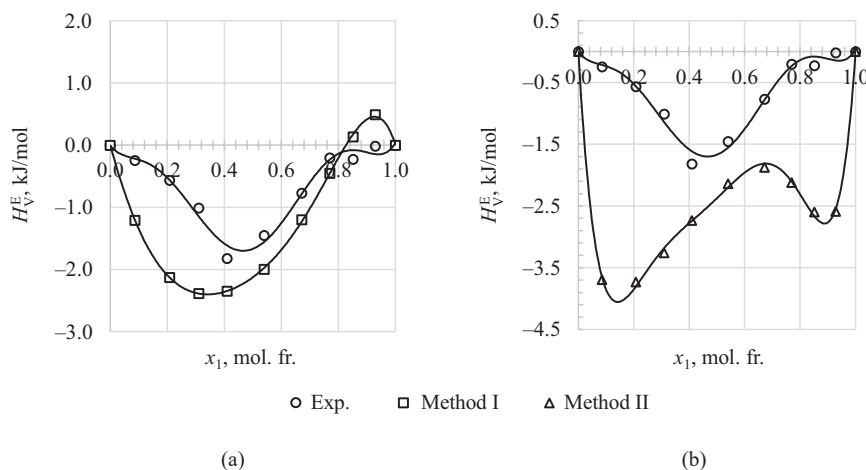


Fig. 2. Comparison of experimental and calculated values of the excess molar vaporization enthalpy for benzene (1)–ethanol (2) system at 101.32 kPa: (a) method I, (b) method II

The results obtained are similar to the conclusions for the benzene–cyclohexane system at 50.663, 75.992, and 101.320 kPa (Table 6). Method II allows qualitatively correct types of concentration dependencies $H_V^E(x) < 0$ to be obtained, while method I familiar-variable ones to be obtained, when in one region of compositions H_V^E are negative and in the other—positive [45].

Thus, the calculation of molar enthalpies of vaporization of binary systems from dP/dT data under VLE conditions is more correct for isobaric conditions.

The properties of binary systems formed by non-associated liquids are usually linear functions of composition or exhibit insignificant deviations from additive values. However, the enthalpies of vaporization

of mixtures H_V are an exception [9]. Therefore, for systems containing substances which form complexes of molecules, the association constants of molecules in the vapor phase must be taken into account [40]. Analysis of experimental calorimetric data for binary systems containing lower carboxylic acids allowed the authors [40] to conclude that simplified methods for estimating enthalpies of vaporization in mixtures with associated components are acceptable, if the excess molar enthalpy (heat of mixing) of the liquid solution does not exceed 5% of the enthalpy of vaporization.

It was established that calculated values H_V^{calc} , obtained from dP/dT data at VLE are less accurate than calculations based on independent arrays of experimental data in systems formed by components capable of

Table 6. Excess values for benzene (1)–cyclohexane (2) system at isobaric vapor–liquid

x_1 , mol. fr.	p^{calc} , kPa								
	101.320			75.992			50.662		
	H_V^{exp} , kJ/mol	Method I	Method II	H_V^{exp} , kJ/mol	Method I	Method II	H_V^{exp} , kJ/mol	Method I	Method II
		H_V^{calc} , kJ/mol			H_V^{calc} , kJ/mol			H_V^{calc} , kJ/mol	
0.143	−0.34	0.03	−0.05	−0.35	0.01	−0.05	−0.41	0.01	−0.04
0.250	−0.42	0.01	−0.08	−0.47	0.00	−0.07	−0.72	−0.01	−0.07
0.397	−0.57	−0.03	−0.11	−0.54	−0.03	−0.10	−0.78	−0.04	−0.09
0.443	−0.59	−0.04	−0.12	−0.55	−0.05	−0.11	−0.66	−0.06	−0.11
0.541	−0.55	−0.06	−0.13	−0.60	−0.07	−0.13	−0.73	−0.08	−0.13
0.700	−0.37	−0.05	−0.15	−0.41	−0.06	−0.14	−0.37	−0.07	−0.14
0.842	−0.12	−0.02	−0.12	−0.47	−0.03	−0.14	−0.34	−0.04	−0.14

forming hydrogen bonds in solutions: tetrahydrofuran–water, water–pyridine, ethanol–1,4-dioxane. The application of method II for calculations of molar enthalpies of vaporization of benzene–cyclohexane system provides more accurate reproduction of experimental data H_V^{exp} in comparison with benzene–ethanol mixtures. This can be explained by the use of the assumption of ideal behavior of the vapor phase containing ethanol.

CONCLUSIONS

Molar enthalpies of vaporization of azeotropic mixtures were calculated for 18 binary systems under different conditions of phase VLE and for the full range of compositions of the benzene–ethanol system at atmospheric pressure.

Rigorous thermodynamic methods of calculating the molar enthalpies of vaporization from VLE data of binary systems, even under the assumption of ideal

behavior of the vapor phase, are more accurate than simplified methods of calculation.

The comparison of experimental and calculated data arrays obtained by thermodynamic methods I and II was carried out. The proposed calculation method II provides more accurate results for 85% of the compositions of azeotropic mixtures in isothermal conditions, and for 75% of them in isobaric conditions.

Acknowledgments

The work was financially supported by the grant of the State Assignment No. FSFZ-2023-0003.

Authors' contributions

D.A. Ryzhkin—conducting a calculating research, analysis and presentation of research results, and preparing the work for publication.

V.M. Raeva—formulation of research objectives and aims, analysis of results, preparing the work for publication, and leadership for the research execution.

The authors declare no conflicts of interest.

REFERENCES

- Karapet'yants M.Kh. *Khimicheskaya termodinamika (Chemical Thermodynamics)*. Moscow: Khimiya; 1975. 583 p. (in Russ.)
- Black C. Importance of thermophysical data in process simulation. *Int. J. Thermophys.* 1986;7(4):987–1002. <https://doi.org/10.1007/BF00503853>
- Sandler S.I. Thermophysical properties: What have we learned recently, and what do we still need to know? *Int. J. Thermophys.* 1994;15(6):1013–1035. <https://doi.org/10.1007/BF01458812>
- Oscarson J.L., Rowley R.L., Wilding W.V., Izatt R.M. Industrial need for accurate thermophysical data and for reliable prediction methods. *J. Therm. Anal. Calorim.* 2008;92(2):465–470. <https://doi.org/10.1007/s10973-007-8972-0>
- Solomonov B.N., Varfolomeev M.A., Nagrimanov R.N., Novikov V.B., Zaitsau D.H., Verevkin S.P. Solution calorimetry as a complementary tool for the determination of enthalpies of vaporization and sublimation of low volatile compounds at 298.15 K. *Thermochimica Acta.* 2014;589:164–173. <https://doi.org/10.1016/j.tca.2014.05.033>
- Yu D., Chen Z. A theoretical analysis on enthalpy of vaporization: Temperature dependence and singularity at the critical state. *Fluid Phase Equil.* 2020;516:112611. <https://doi.org/10.1016/j.fluid.2020.112611>
- Solomonov B.N., Yagofarov M.I. Compensation relationship in thermodynamics of solvation and vaporization: Features and applications. II. Hydrogen-bonded systems. *J. Mol. Liq.* 2023;372(2):121205. <https://doi.org/10.1016/j.molliq.2023.121205>
- Tyrer D. CLXXXVI. Latent heats of vaporization of mixed liquids. Part I. *J. Chem. Soc., Trans.* 1911;99:1633–1645. <https://doi.org/10.1039/CT9119901633>
- Shivabasappa K.L., Nirguna Babu P., Jagannadha Rao Y. Enthalpy of mixing and heat of vaporization of ethyl acetate with benzene and toluene at 298.15 K and 308.15 K. *Braz. J. Chem. Eng.* 2008;25(1):167–174. <https://doi.org/10.1590/S0104-66322008000100017>
- Zakharov M.K., Egorov A.V., Podmetenny A.A. Liquid mixtures separation and heat consumption in the process of distillation. *Tonk. Khim. Tekhnol. = Fine Chem. Technol.* 2021;16(1):7–15 (Russ., Eng.). <https://doi.org/10.32362/2410-6593-2021-16-1-7-15>
- Pashchenko L.L., Druzhinina A.I. Enthalpy of vaporization measurements by calorimetric techniques. *J. Therm. Anal. Calorim.* 2018;133(2):1173–1179. <https://doi.org/10.1007/s10973-018-7370-0>
- Vicencio L.A., López-Porfiri P., de la Fuente J.C. Vapour pressure and vaporisation enthalpy for two key apple odorants, ethyl butyrate and ethyl hexanoate, at pressures from (15 to 105) kPa. *J. Chem. Thermodyn.* 2020;142:105982. <https://doi.org/10.1016/j.jct.2019.105982>
- Abdullah R.S., Solomonov B.N.. Sublimation/vaporization and solvation enthalpies of monosubstituted pyridine derivatives. *Chem. Thermodyn. Therm. Anal.* 2022;8(20):100087. <https://doi.org/10.1016/j.ctta.2022.100087>
- Dong J.-Q., Lin R.-S., Yen W.-H. Heats of vaporization and gaseous molar heat capacities of ethanol and the binary mixture of ethanol and benzene. *Can. J. Chem.* 1988;66(4):783–790. <https://doi.org/10.1139/v88-136>
- Tamir A. Prediction of latent heat of vaporization of multicomponent mixtures. *Fluid Phase Equil.* 1982;8(2):131–147. [https://doi.org/10.1016/0378-3812\(82\)80031-9](https://doi.org/10.1016/0378-3812(82)80031-9)
- Ito T., Yamaguchi T., Akasaka R. Heat of vaporization of mixtures. *Heat Transfer Japanese Res.* 1996;25(1):12–24. [https://doi.org/10.1002/\(SICI\)1520-6556\(1996\)25:1%3C12::AID-HTJ2%3E3.0.CO;2-1](https://doi.org/10.1002/(SICI)1520-6556(1996)25:1%3C12::AID-HTJ2%3E3.0.CO;2-1)
- Marchelli G., Ingenmey J., Hollóczy O., Chaumont A., Kirchner B. Hydrogen-bonding and vaporization thermodynamics in hexafluoroisopropanol-acetone and -methanol mixtures. A Jointed cluster analysis and molecular dynamic study. *ChemPhysChem.* 2022;23(1):e202100620. <https://doi.org/10.1002/cphc.202100620>
- Swietoslawski W., Zielenkiewicz A. Vaporization enthalpy of the homologous series of binary azeotropes. *Rocz. Chem.* 1958;32:913–922.
- Tamir A. Compilation and correlation of binary azeotropic data. *Fluid Phase Equil.* 1981;5(3–4):199–206. [https://doi.org/10.1016/0378-3812\(80\)80057-4](https://doi.org/10.1016/0378-3812(80)80057-4)
- Zherin I.I. Halogen fluorides in nuclear fuel technology. Thermodynamics of phase equilibria in systems containing UF₆, BrF₃, IF₅, and HF. *Izvestiya Tomskogo Politekhniceskogo Universiteta = Bulletin of the Tomsk Polytechnic University.* 2003;306(6):8–11 (in Russ.).
- Neilson E.F., White D. The heat of vaporization and solution of a binary mixture of fluorocarbons. *J. Phys. Chem.* 1959;63(9):1363–1365. <https://doi.org/10.1021/j150579a005>
- Pandey J.D., Srivastava T., Chandra P., Prashant R., Dwivedi P.K. Estimation of cohesive forces, energy of vaporization, heat of vaporization, cohesive energy density, solubility parameter and Van der Waals constant of binary liquid mixtures using generalized hole theory. *Indian J. Chem.* 2007;46A:1605–1610.
- Bedretdinov F., Tsvetov N., Raeva V., Chelyuskina T. Research of the properties of binary biazeotropic mixtures. In: *Proc. of the 46th International Conference of the Slovak Society of Chemical Engineering*. Tatranské Matliare, High Tatras, Slovakia May 20–23, 2019. Bratislava; 2019. P. 171.
- Raeva V.M. Vaporization heat of binary mixtures. *Tonk. Khim. Tekhnol. = Fine Chem. Technol.* 2013;8(1):43–50 (in Russ.).
- Lenoir J.M., Hipkin H.G. Measured enthalpies of eight hydrocarbon fractions. *J. Chem. Eng. Data.* 1973;18(2):195–202. <https://doi.org/10.1021/je60057a026>
- Grigoriev B., Alexandrov I., Gerasimov A. Application of multiparameter fundamental equations of state to predict the thermodynamic properties and phase equilibria of technological oil fractions. *Fuel.* 2018;215:80–89. <https://doi.org/10.1016/j.fuel.2017.11.022>
- Tatar A., Barati-Harooni A., Partovi M., Najafi-Marghmaleki A., et al. An accurate model for predictions of vaporization enthalpies of hydrocarbons and petroleum fractions. *J. Mol. Liq.* 2016;220:192–199. <https://doi.org/10.1016/j.molliq.2016.04.069>
- Balabin R.M., Syunyaev R.Z., Karpov S.A.. Molar enthalpy of vaporization of ethanol–gasoline mixtures and their colloid state. *Fuel.* 2007;86(3):323–327. <https://doi.org/10.1016/j.fuel.2006.08.008>
- Gautam A., Kumar A.A.. Determination of important biodiesel properties based on fuel temperature correlations for application in a locomotive engine. *Fuel.* 2015;142:289–302. <https://doi.org/10.1016/j.fuel.2014.10.032>
- Abernathy S.M., Brown K.R. Predicting the enthalpy of vaporization and calculating the entropy of vaporization of 87 octane gasoline using vapor pressure. *Open Access Library Journal (OALib. Journal).* 2016;3(e2954):1–11. <http://doi.org/10.4236/oalib.1102954>
- Akasaka R., Yamaguchi T., Ito T. Practical and direct expressions of the heat of vaporization for mixtures. *Chem. Eng. Science.* 2005;60(16):4369–4376. <https://doi.org/10.1016/j.ces.2005.03.005>

32. Benkouider A.M., Kessas R., Guella S., Yahiaoui A., Bagui F. Estimation of the enthalpy of vaporization of organic components as a function of temperature using a new group contribution method. *J. Mol. Liq.* 2014;194:48–56. <https://doi.org/10.1016/j.molliq.2014.01.006>
33. Bolmatenkov D.N., Yagofarov M.I., Notfullin A.A., Solomonov B.N. Calculation of the vaporization enthalpies of alkylaromatic hydrocarbons as a function of temperature from their molecular structure. *Fluid Phase Equil.* 2022;554:113303. <https://doi.org/10.1016/j.fluid.2021.113303>
34. Bolmatenkov D.N., Yagofarov M.I., Valiakmetov T.F., Rodionov N.O., Solomonov B.N. Vaporization enthalpies of benzanthrene, 1-nitropyrene, and 4-methoxy-1-naphthonitrile: Prediction and experiment. *J. Chem. Thermodyn.* 2022;168:106744. <https://doi.org/10.1016/j.jct.2022.106744>
35. Bolmatenkov D.N., Yagofarov M.I., Sokolov A.A., Solomonov B.N. Vaporization enthalpies of self-associated aromatic compounds at 298.15 K: A review of existing data and the features of heat capacity correction. Part I. Phenols. *Thermochimica Acta.* 2023;721:179455. <https://doi.org/10.1016/j.tca.2023.179455>
36. Arutionov B.A., Elsadig Y.A. Thermodynamic method of calculation of heat of steam formation for binary mixes. *Tonk. Khim. Tekhnol. = Fine Chem. Technol.* 2010;5(5):36–39 (in Russ.).
37. Arutionov B.A., Elsadig Y.A., Ausheva E.V. Temperature dependence of heat of vaporization of pure hydrocarbons and their binary mixtures. *Tonk. Khim. Tekhnol. = Fine Chem. Technol.* 2010;5(5):40–42 (in Russ.).
38. Arutyunov B.A., Rytova E.V., Raeva V.M., et al. Methods for calculating the evaporation heats of hydrocarbons and their mixtures in a wide temperature range. *Theor. Found. Chem. Eng.* 2017;51(5):742–751. <https://doi.org/10.1134/S0040579517050268>
[Original Russian Text: Arutyunov B.A., Rytova E.V., Raeva V.M., Frolkova A.K. Methods for calculating the heat of vaporization of hydrocarbons and their mixtures in a wide temperature range. *Teoreticheskie Osnovy Khimicheskoi Tekhnologii.* 2017;51(5):595–604 (in Russ.). <https://doi.org/10.7868/S0040357117050025>]
39. Tamir A., Dragoescu C., Apelblat A., Wisniak J. Heats of vaporization and vapor–liquid equilibria in associated solutions containing formic acid, acetic acid, propionic acid and carbon tetrachloride. *Fluid Phase Equil.* 1983;10(1):9–42. [https://doi.org/10.1016/0378-3812\(83\)80002-8](https://doi.org/10.1016/0378-3812(83)80002-8)
40. Solomonov B.N., Yagofarov M.I., Nagrimanov R.N. Additivity of vaporization enthalpy: Group and molecular contributions exemplified by alkylaromatic compounds and their derivatives. *J. Mol. Liq.* 2021;342:117472. <https://doi.org/10.1016/j.molliq.2021.117472>
41. Solomonov B.N., Yagofarov M.I. Compensation relationship in thermodynamics of solvation and vaporization: Features and applications. II. Hydrogen-bonded systems. *J. Mol. Liq.* 2023;372:121205. <https://doi.org/10.1016/j.molliq.2023.121205>
42. Morachevskii A.G., Smirnova N.A., Alekseeva M.V., Balashova I.M., Viktorov A.I., Kuranov G.L., Piotrovskaya E.M., Pukinskii I.B. *Termodinamika ravnovesiya zhidkost'–par (Thermodynamics of Liquid–Vapor Equilibrium)*. Leningrad: Khimiya; 1989. 344 p. (in Russ.).
43. Reid R.C., Prausnitz J.M., Sherwood T.K. *Svoistva gazov i zhidkostei (The Properties of Gases and Liquids)*; transl. from Engl. Leningrad: Khimiya; 1982. 592 p. (in Russ.).
[Reid R.C., Prausnitz J.M., Sherwood T.K. *The Properties of Gases and Liquids*. NY: McGraw-Hill; 1977. 710 p.]
44. Walas S.M. *Fazovye ravnovesiya v khimicheskoi tekhnologii (Phase Equilibria in Chemical Engineering)*: in 2 v.; transl. from Engl. Moscow: Mir; 1989. V. 1. 304 p. (in Russ.).
[Walas S.M. *Phase Equilibria in Chemical Engineering*. Oxford: Butterworth-Heinemann Publ., 1985. 671 p.]
45. Raeva V.M., Anisimov A.V., Ryzhkin D.A. Calculation of vaporization enthalpies of a benzene–cyclohexane system. *Russ. Chem. Bull.* 2021;70(4):715–721. <https://doi.org/10.1007/s11172-021-3141-3>
[Original Russian Text: Raeva V.M., Anisimov A.V., Ryzhkin D.A. Calculation of vaporization enthalpies of a benzene–cyclohexane system. *Izvestiya Akademii Nauk. Seriya Khimicheskaya.* 2021;(4):715–721 (in Russ.).]
46. Ryzhkin D.A., Raeva V.M. Calculation of vaporization enthalpies of methanol–tetrahydrofuran–acetonitrile at atmospheric pressure. In: *Proc. of the 23rd International Conference on Chemical Thermodynamics in Russia*. Russia, Kazan, August 22–27, 2022. P. 298.
47. Carrero-Mantilla J., Llano-Restrepo M. Vapor–phase chemical equilibrium for the hydrogenation of benzene to cyclohexane from reaction-ensemble molecular simulation. *Fluid Phase Equil.* 2004;219(2):181–193. <https://doi.org/10.1016/j.fluid.2004.02.009>
48. Wang X., Xu W., Li Y., Wang J., He F. Phase equilibria of three binary systems containing 2,5-dimethylthiophene and 2-ethylthiophene in hydrocarbons. *Fluid Phase Equil.* 2016;409:30–36. <https://doi.org/10.1016/j.fluid.2015.09.030>
49. Chen G., Wang Q., Zhang L.-Z., Bao J., Han S.-J. Study and applications of binary and ternary azeotropes. *Thermochim. Acta.* 1995;253:295–305. [https://doi.org/10.1016/0040-6031\(94\)02078-3](https://doi.org/10.1016/0040-6031(94)02078-3)

СПИСОК ЛИТЕРАТУРЫ

1. Карапетьянц М.Х. Химическая термодинамика. М.: Химия; 1975. 583 с.
2. Black C. Importance of thermophysical data in process simulation. *Int. J. Thermophys.* 1986;7(4):987–1002. <https://doi.org/10.1007/BF00503853>
3. Sandler S.I. Thermophysical properties: What have we learned recently, and what do we still need to know? *Int. J. Thermophys.* 1994;15(6):1013–1035. <https://doi.org/10.1007/BF01458812>
4. Oscarson J.L., Rowley R.L., Wilding W.V., Izatt R.M. Industrial need for accurate thermophysical data and for reliable prediction methods. *J. Therm. Anal. Calorim.* 2008;92(2):465–470. <https://doi.org/10.1007/s10973-007-8972-0>
5. Solomonov B.N., Varfolomeev M.A., Nagrimanov R.N., Novikov V.B., Zaitsau D.H., Verevkin S.P. Solution calorimetry as a complementary tool for the determination of enthalpies of vaporization and sublimation of low volatile compounds at 298.15 K. *Thermochimica Acta.* 2014;589:164–173. <https://doi.org/10.1016/j.tca.2014.05.033>

6. Yu D., Chen Z. A theoretical analysis on enthalpy of vaporization: Temperature dependence and singularity at the critical state. *Fluid Phase Equil.* 2020;516:112611. <https://doi.org/10.1016/j.fluid.2020.112611>
7. Solomonov B.N., Yagofarov M.I. Compensation relationship in thermodynamics of solvation and vaporization: Features and applications. II. Hydrogen-bonded systems. *J. Mol. Liq.* 2023;372(2):121205. <https://doi.org/10.1016/j.molliq.2023.121205>
8. Tyrer D. CLXXXVI. Latent heats of vaporization of mixed liquids. Part I. *J. Chem. Soc., Trans.* 1911;99:1633–1645. <https://doi.org/10.1039/CT9119901633>
9. Shivabasappa K.L., Nirguna Babu P., Jagannadha Rao Y. Enthalpy of mixing and heat of vaporization of ethyl acetate with benzene and toluene at 298.15 K and 308.15 K. *Braz. J. Chem. Eng.* 2008;25(1):167–174. <https://doi.org/10.1590/S0104-66322008000100017>
10. Захаров М.К., Егоров А.В., Подметенный А.А. Разделение жидких смесей и затраты теплоты при ректификации. *Тонкие химические технологии.* 2021;16(1):7–15. <https://doi.org/10.32362/2410-6593-2021-16-1-7-15>
11. Pashchenko L.L., Druzhinina A.I. Enthalpy of vaporization measurements by calorimetric techniques. *J. Therm. Anal. Calorim.* 2018;133(2):1173–1179. <https://doi.org/10.1007/s10973-018-7370-0>
12. Vicencio L.A., López-Porfiri P., de la Fuente J.C. Vapour pressure and vaporisation enthalpy for two key apple odorants, ethyl butyrate and ethyl hexanoate, at pressures from (15 to 105) kPa. *J. Chem. Thermodyn.* 2020;142:105982. <https://doi.org/10.1016/j.jct.2019.105982>
13. Abdullah R.S., Solomonov B.N.. Sublimation/vaporization and solvation enthalpies of monosubstituted pyridine derivatives. *Chem. Thermodyn. Therm. Anal.* 2022;8(20):100087. <https://doi.org/10.1016/j.cta.2022.100087>
14. Dong J.-Q., Lin R.-S., Yen W.-H. Heats of vaporization and gaseous molar heat capacities of ethanol and the binary mixture of ethanol and benzene. *Can. J. Chem.* 1988;66(4):783–790. <https://doi.org/10.1139/v88-136>
15. Tamir A. Prediction of latent heat of vaporization of multicomponent mixtures. *Fluid Phase Equil.* 1982;8(2):131–147. [https://doi.org/10.1016/0378-3812\(82\)80031-9](https://doi.org/10.1016/0378-3812(82)80031-9)
16. Ito T., Yamaguchi T., Akasaka R. Heat of vaporization of mixtures. *Heat Transfer Japanese Res.* 1996;25(1):12–24. [https://doi.org/10.1002/\(SICI\)1520-6556\(1996\)25:1%3C12::AID-HTJ2%3E3.0.CO;2-1](https://doi.org/10.1002/(SICI)1520-6556(1996)25:1%3C12::AID-HTJ2%3E3.0.CO;2-1)
17. Marchelli G., Ingenmey J., Hollóczki O., Chaumont A., Kirchner B. Hydrogen-bonding and vaporization thermodynamics in hexafluoroisopropanol-acetone and -methanol mixtures. A Jointed cluster analysis and molecular dynamic study. *ChemPhysChem.* 2022;23(1):e202100620. <https://doi.org/10.1002/cphc.202100620>
18. Swietoslawski W., Zielenkiewicz A. Vaporization enthalpy of the homologous series of binary azeotropes. *Rocz. Chem.* 1958;32:913–922.
19. Tamir A. Compilation and correlation of binary azeotropic data. *Fluid Phase Equil.* 1981;5(3–4):199–206. [https://doi.org/10.1016/0378-3812\(80\)80057-4](https://doi.org/10.1016/0378-3812(80)80057-4)
20. Жерин И.И. Фториды галогенов в технологии ядерного топлива. Термодинамика фазовых равновесий в системах, содержащих UF₆, BrF₃, IF₅ и HF. *Изв. Томского политехн. ун-та.* 2003;306(6):8–11.
21. Neilson E.F., White D. The heat of vaporization and solution of a binary mixture of fluorocarbons. *J. Phys. Chem.* 1959;63(9):1363–1365. <https://doi.org/10.1021/j150579a005>
22. Pandey J.D., Srivastava T., Chandra P., Prashant R., Dwivedi P.K. Estimation of cohesive forces, energy of vaporization, heat of vaporization, cohesive energy density, solubility parameter and Van der Waals constant of binary liquid mixtures using generalized hole theory. *Indian J. Chem.* 2007;46A:1605–1610.
23. Bedretdinov F., Tsvetov N., Raeva V., Chelyuskina T. Research of the properties of binary biazotropic mixtures. In: *Proc. of the 46th International Conference of the Slovak Society of Chemical Engineering.* Tatranské Matliare, High Tatras, Slovakia May 20–23, 2019. Bratislava; 2019. P. 171.
24. Раева В.М. Теплоты испарения бинарных смесей. *Тонкие химические технологии.* 2013;8(1):43–50.
25. Lenoir J.M., Hipkin H.G. Measured enthalpies of eight hydrocarbon fractions. *J. Chem. Eng. Data.* 1973;18(2):195–202. <https://doi.org/10.1021/je60057a026>
26. Grigoriev B., Alexandrov I., Gerasimov A. Application of multiparameter fundamental equations of state to predict the thermodynamic properties and phase equilibria of technological oil fractions. *Fuel.* 2018;215:80–89. <https://doi.org/10.1016/j.fuel.2017.11.022>
27. Tatar A., Barati-Harooni A., Partovi M., Najafi-Marghmaleki A., et al. An accurate model for predictions of vaporization enthalpies of hydrocarbons and petroleum fractions. *J. Mol. Liq.* 2016;220:192–199. <https://doi.org/10.1016/j.molliq.2016.04.069>
28. Balabin R.M., Syunyaev R.Z., Karpov S.A.. Molar enthalpy of vaporization of ethanol–gasoline mixtures and their colloid state. *Fuel.* 2007;86(3):323–327. <https://doi.org/10.1016/j.fuel.2006.08.008>
29. Gautam A., Kumar A.A.. Determination of important biodiesel properties based on fuel temperature correlations for application in a locomotive engine. *Fuel.* 2015;142:289–302. <https://doi.org/10.1016/j.fuel.2014.10.032>
30. Abernathy S.M., Brown K.R. Predicting the enthalpy of vaporization and calculating the entropy of vaporization of 87 octane gasoline using vapor pressure. *Open Access Library Journal (OALib. Journal).* 2016;3(e2954):1–11. <http://doi.org/10.4236/oalib.1102954>
31. Akasaka R., Yamaguchi T., Ito T. Practical and direct expressions of the heat of vaporization for mixtures. *Chem. Eng. Science.* 2005;60(16):4369–4376. <https://doi.org/10.1016/j.ces.2005.03.005>
32. Benkouider A.M., Kessas R., Guella S., Yahiaoui A., Bagui F. Estimation of the enthalpy of vaporization of organic components as a function of temperature using a new group contribution method. *J. Mol. Liq.* 2014;194:48–56. <https://doi.org/10.1016/j.molliq.2014.01.006>
33. Bolmatenkov D.N., Yagofarov M.I., Notfullin A.A., Solomonov B.N. Calculation of the vaporization enthalpies of alkylaromatic hydrocarbons as a function of temperature from their molecular structure. *Fluid Phase Equil.* 2022;554:113303. <https://doi.org/10.1016/j.fluid.2021.113303>
34. Bolmatenkov D.N., Yagofarov M.I., Valiakhmetov T.F., Rodionov N.O., Solomonov B.N. Vaporization enthalpies of benzanthrene, 1-nitropyrene, and 4-methoxy-1-naphthonitrile: Prediction and experiment. *J. Chem. Thermodyn.* 2022;168:106744. <https://doi.org/10.1016/j.jct.2022.106744>
35. Bolmatenkov D.N., Yagofarov M.I., Sokolov A.A., Solomonov B.N. Vaporization enthalpies of self-associated aromatic compounds at 298.15 K: A review of existing data and the features of heat capacity correction. Part I. Phenols. *Thermochimica Acta.* 2023;721:179455. <https://doi.org/10.1016/j.tca.2023.179455>

36. Арутюнов Б.А., Мохаммед Ю.А. Термодинамический метод расчета теплоты парообразования бинарных смесей. *Тонкие химические технологии*. 2010;5(5): 36–39.
37. Арутюнов Б.А., Мохаммед Ю.А., Аушева Е.В. Температурная зависимость теплоты парообразования чистых углеводородов и их бинарных смесей. *Тонкие химические технологии*. 2010;5(5):40–42.
38. Арутюнов Б.А., Рытова Е.В., Раева В.М., Фролкова А.К. Методы расчета теплот парообразования углеводородов и их смесей в широком диапазоне температур. *Теор. основы хим. технологии*. 2017;51(5):595–604. <https://doi.org/10.7868/S0040357117050025>
39. Tamir A., Dragoescu C., Apelblat A., Wisniak J. Heats of vaporization and vapor–liquid equilibria in associated solutions containing formic acid, acetic acid, propionic acid and carbon tetrachloride. *Fluid Phase Equil.* 1983;10(1):9–42. [https://doi.org/10.1016/0378-3812\(83\)80002-8](https://doi.org/10.1016/0378-3812(83)80002-8)
40. Solomonov B.N., Yagofarov M.I., Nagrimanov R.N. Additivity of vaporization enthalpy: Group and molecular contributions exemplified by alkylaromatic compounds and their derivatives. *J. Mol. Liq.* 2021;342:117472. <https://doi.org/10.1016/j.molliq.2021.117472>
41. Solomonov B.N., Yagofarov M.I. Compensation relationship in thermodynamics of solvation and vaporization: Features and applications. II. Hydrogen-bonded systems. *J. Mol. Liq.* 2023;372:121205. <https://doi.org/10.1016/j.molliq.2023.121205>
42. Морачевский А.Г., Смирнова Н.А., Алексеева М.В., Балашова И.М., Викторов А.И., Куранов Г.Л., Пиотровская Е.М., Пукинский И.Б. *Термодинамика равновесия жидкость-пар*. Л.: Химия; 1989. 344 с.
43. Рид Р., Праунсниц Дж., Шервуд Т. *Свойства газов и жидкостей*; пер. с англ. Л.: Химия; 1982. 592 с.
44. Уэйлес С. *Фазовые равновесия в химической технологии*: в 2-х ч.; пер. с англ. М.: Мир; 1989. Ч. 1. 304 с.
45. Раева В.М., Анисимов А.В., Рыжкин Д.А.. Расчет энтальпий парообразования системы бензол–циклогексан. *Изв. АН. Сер. хим.* 2021;(4):715–721. <https://doi.org/10.1007/s11172-021-3141-3>
46. Ryzhkin D.A., Raeva V.M. Calculation of vaporization enthalpies of methanol–tetrahydrofuran–acetonitrile at atmospheric pressure. In: *Proc. of the 23rd International Conference on Chemical Thermodynamics in Russia*. Russia, Kazan, August 22–27, 2022. P. 298.
47. Carrero-Mantilla J., Llano-Restrepo M. Vapor–phase chemical equilibrium for the hydrogenation of benzene to cyclohexane from reaction-ensemble molecular simulation. *Fluid Phase Equil.* 2004;219(2):181–193. <https://doi.org/10.1016/j.fluid.2004.02.009>
48. Wang X., Xu W., Li Y., Wang J., He F. Phase equilibria of three binary systems containing 2,5-dimethylthiophene and 2-ethylthiophene in hydrocarbons. *Fluid Phase Equil.* 2016;409:30–36. <https://doi.org/10.1016/j.fluid.2015.09.030>
49. Chen G., Wang Q., Zhang L.-Z., Bao J., Han S.-J. Study and applications of binary and ternary azeotropes. *Thermochim. Acta.* 1995;253:295–305. [https://doi.org/10.1016/0040-6031\(94\)02078-3](https://doi.org/10.1016/0040-6031(94)02078-3)

About the authors

Dmitry A. Ryzhkin, Postgraduate Student, Department of Chemistry and Technology of Basic Organic Synthesis, M.V. Lomonosov Institute of Fine Chemical Technologies, MIREA — Russian Technological University (86, Vernadskogo pr., Moscow, 119571, Russia). E-mail: dima-ryzhkin@mail.ru. Scopus Author ID 57223230408, ResearcherID AAU-6583-2021, RSCI SPIN-code 7429-1472, <https://orcid.org/0000-0001-6415-8059>

Valentina M. Raeva, Cand. Sci. (Eng.), Associate Professor, Department of Chemistry and Technology of Basic Organic Synthesis, M.V. Lomonosov Institute of Fine Chemical Technologies, MIREA — Russian Technological University (86, Vernadskogo pr., Moscow, 119571, Russia). E-mail: raevaValentina1@gmail.com. Scopus Author ID 6602836975, ResearcherID C-8812-2014, RSCI SPIN-code 5147-0319, <https://orcid.org/0000-0002-5664-4409>

Об авторах

Рыжкин Дмитрий Антонович, аспирант кафедры химии и технологии основного органического синтеза, Институт тонких химических технологий им. М.В. Ломоносова, ФГБОУ ВО «МИРЭА — Российский технологический университет» (119571, Россия, Москва, пр-т Вернадского, д. 86). E-mail: dima-ryzhkin@mail.ru. Scopus Author ID 57223230408, ResearcherID AAU-6583-2021, RSCI SPIN-code 7429-1472, <https://orcid.org/0000-0001-6415-8059>

Раева Валентина Михайловна, к.т.н., доцент кафедры химии и технологии основного органического синтеза, Институт тонких химических технологий им. М.В. Ломоносова, ФГБОУ ВО «МИРЭА — Российский технологический университет» (119571, Россия, Москва, пр-т Вернадского, д. 86). E-mail: raevaValentina1@gmail.com. Scopus Author ID 6602836975, ResearcherID C-8812-2014, RSCI SPIN-code 5147-0319, <https://orcid.org/0000-0002-5664-4409>

Translated from Russian into English by H. Moshkov

Edited for English language and spelling by Dr. David Mossop

UDC 547.245; 678.4

<https://doi.org/10.32362/2410-6593-2024-19-4-293-309>

EDN ZVSAGK



RESEARCH ARTICLE

Using nitrogen-containing organosilicon compounds in the creation of heat- and fire-resistant filling compositions to seal high-voltage and high-frequency equipment

Alexey D. Kirilin¹, Liya O. Belova¹, Nataliya A. Golub¹, Mariya V. Pletneva¹✉, Nadezhda I. Kirilina², Denis E. Mironov¹

¹ MIREA — Russian Technological University (M.V. Lomonosov Institute of Fine Chemical Technology), Moscow, 119571 Russia

² State Research Institute of Chemistry and Technology of Organoelement Compounds, Moscow, 105118 Russia

✉ Corresponding author; e-mail: pletneva@mirea.ru

Abstract

Objectives. To study the possibility of using nitrogen-containing organosilicon compounds in the creation of heat-resistant and fire-resistant casting compositions to seal high-voltage high-frequency equipment.

Methods. Nitrogen-containing organosilicon compounds were obtained using the *N*-siloxycarbonylation, formylation, and silylation methods. The methods used in the work were infrared spectroscopy, elemental analysis, viscometry, and differential scanning calorimetry. The mechanical and dielectric properties of the samples were determined.

Results. Previously unknown substances and compounds containing nitrogen-containing organosilicon products as components of the curing composition were obtained. Their physicochemical and operational properties were examined, including the possibility of using them as filling heat-resistant and fire-resistant compositions for sealing high-voltage and high-frequency equipment.

Conclusions. It was shown that nitrogen-containing organosilicon compounds—3-(diethylamino)-2-[(triethoxysilyloxy)propyl]-2-methacrylate and triethoxysilyl ester of γ -triethoxysilylpropyl-carbamic acid—can be used as part of a curing system together with bromine-containing fillers, in order to obtain compounds used for filling high-voltage high-frequency transformers, throttle valves, and other electronic equipment elements with non-combustible properties and increased heat resistance.

Keywords

nitrogen-containing organosilicon compounds, filling compositions, heat-resistant and fire-resistant filling compositions, sealing high-voltage and high-frequency equipment

Submitted: 17.04.2023

Revised: 06.07.2023

Accepted: 24.06.2024

For citation

Kirilina A.D., Belova L.O., Golub N.A., Pletneva M.V., Kirilina N.I., Mironov D.E. Using nitrogen-containing organosilicon compounds in the creation of heat- and fire-resistant filling compositions to seal high-voltage and high-frequency equipment. *Tonk. Khim. Tekhnol. = Fine Chem. Technol.* 2024;19(4):293–309. <https://doi.org/10.32362/2410-6593-2024-19-4-293-309>

НАУЧНАЯ СТАТЬЯ

Использование азотсодержащих кремнийорганических соединений при создании термо- и огнестойких заливочных композиций для герметизации высоковольтной и высокочастотной аппаратуры

А.Д. Кирилин¹, Л.О. Белова¹, Н.А. Голуб¹, М.В. Плетнева^{1,✉}, Н.И. Кирилина², Д.Е. Миронов¹

¹ МИРЭА — Российский технологический университет (Институт тонких химических технологий им. М.В. Ломоносова), Москва, 119571 Россия

² Государственный научно-исследовательский институт химии и технологии элементоорганических соединений, Москва, 105118 Россия

✉ Автор для переписки, e-mail: pletneva@mirea.ru

Аннотация

Цели. Изучение возможности использования азотсодержащих кремнийорганических соединений при создании термо- и огнестойких заливочных композиций для герметизации высоковольтной и высокочастотной аппаратуры.

Методы. С помощью методов N-силоксикарбонилирования, формилирования и силилирования получены азотсодержащие кремнийорганические соединения. В работе использованы инфракрасная спектроскопия, элементный анализ, вискозиметрия, дифференциальная сканирующая калориметрия. Определены механические и диэлектрические свойства образцов.

Результаты. Получены ранее неизвестные соединения и компаунды, содержащие в составе отверждающей композиции азотсодержащие кремнийорганические продукты, изучены их физико-механические, эксплуатационные свойства, в том числе возможность использования в качестве заливочных термо- и огнестойких композиций для герметизации высоковольтной и высокочастотной аппаратуры.

Выводы. Показано, что впервые синтезированные азотсодержащие кремнийорганические соединения — 3-(диэтиламино)-2-[(триэтоксисилил)окси]пропил-2-метакрилат и триэтоксисилиловый эфир γ -триэтоксисилилпропилкарбаминовой кислоты — можно использовать в составе отверждающей системы совместно с бромсодержащими наполнителями для получения компаундов, применяемых для заливки высоковольтных и высокочастотных трансформаторов, дросселей и других элементов радиоэлектронной аппаратуры, обладающих негорючими свойствами и повышенной теплостойкостью.

Ключевые слова

азотсодержащие кремнийорганические соединения, заливочные композиции, термо- и огнестойкие заливочные композиции, герметизация высоковольтной и высокочастотной аппаратуры

Поступила: 17.04.2023

Доработана: 06.07.2023

Принята в печать: 24.06.2024

Для цитирования

Кирилин А.Д., Белова Л.О., Голуб Н.А., Плетнева М.В., Кирилина Н.И., Миронов Д.Е. Использование азотсодержащих кремнийорганических соединений при создании термо- и огнестойких заливочных композиций для герметизации высоковольтной и высокочастотной аппаратуры. *Тонкие химические технологии*. 2024;19(4):293–309. <https://doi.org/10.32362/2410-6593-2024-19-4-293-309>

INTRODUCTION

Organosilicon sealants and compounds based on low-molecular silicone rubbers curable at room temperature in contact with air moisture began to be actively developed in the second half of the last century. These products are currently finding increased practical application in various fields of science and technology. They are used in construction, the chemical and aviation industries, in modern electronic and radio products and household chemicals [1–3].

Cold-curable sealant compositions consist of rubber, filler, vulcanizing agent, and curing catalyst. The catalyst can be present in the mixture (one-component compositions) or introduced into it immediately before vulcanization (two-component compositions). Depending on the purpose, these compositions are produced in different consistencies: paste-like, thixotropic or viscous-flowing [4, 5].

The most common cold-curable compositions are based on linear low-molecular polyorganosiloxane

rubbers with a molecular weight from 25000 to 100000, containing terminal silanol groups (Scheme 1) [6, 7]. Of greatest practical interest are: polydimethylsiloxanes **1**, polydimethylmethylphenylsiloxanes **2**, graft copolymers of α,ω -polydimethylsiloxanediol containing 1–3% of methylvinylsiloxane units and styrene in a ratio of 1 : 150–200, **3**, as well as polydimethylmethyltrifluoropropylsiloxanes **4**.

Silicon dioxide (pyrogenic or precipitated), carbon black, quartz sand, or pigment titanium dioxide are usually used as fillers [8, 9]. Organic peroxides, diphenylguanidine, tetraethoxysilane, silicon or organometallic compounds consisting of at least three functional groups are used as vulcanizing agents [10]. Salts of metals (Sn, Pb, Ti, Cr, Zn, etc.) and carboxylic acids, most often diethyl dicaprylate, dibutyl dicaprylate and dibutyl tin dilaurate are usually used as curing catalysts [11–13]. In this case, the performance of organosiloxanes in air is determined by temperatures in the range of 250–300°C [14–16]. In order to increase this temperature range, polysiloxanes containing phenyl and trifluoropropyl radicals or, more often, so-called superstructural polymers—block copolymers with a ladder structure—are usually used [16, 17]. However, since polymer materials are flammable, in order to increase the heat resistance and fire safety of silicone compositions, mineral fillers such as oxides, hydroxides, halides, oxyhalides, and carbonates of metals—Ni, Co, Al, Sn, Fe, Cr, Ti—are used as a rule. Zirconium and calcium silicates, aluminosilicates, etc., or

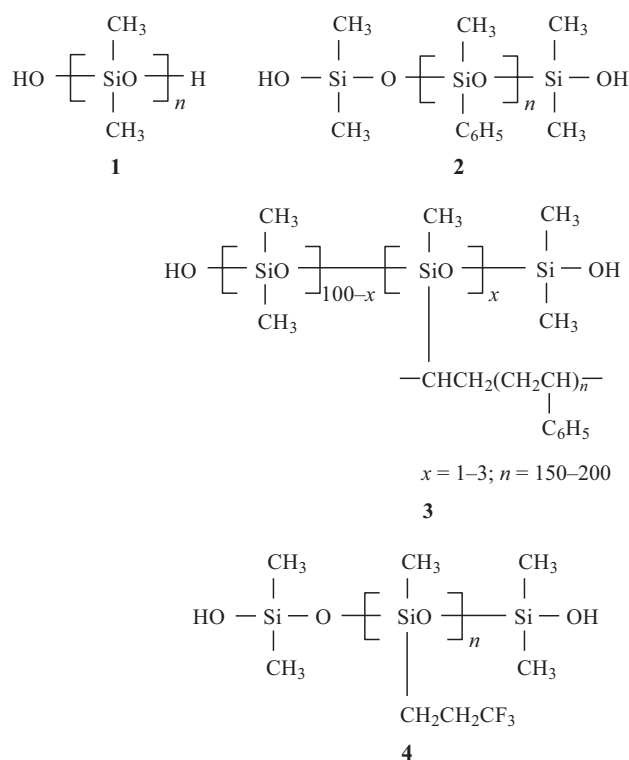
organic fillers, such as nitrogen-, boron-, phosphorus- and halogen-containing organic compounds, for example, melamine, phosphorus-containing diols and polyols can also be used [17, 18].

The use of azo compounds in addition to metal oxides is known to increase the thermal stability of silicone materials [19, 20]. However, the use of nitrogen-containing organosilicon compounds for these purposes is unknown. There is only a report on the use of γ -aminopropyltriethoxysilane as a modifier to increase the adhesion of silicone and natural rubbers to glass and plastics upon low-temperature vulcanization of rubber [21].

The simultaneous combination of heat-resistant and fire-resistant properties in one material is an important objective, so it seemed viable to study the possibility of using nitrogen-containing organosilicon compounds, in order to create heat- and fire-resistant filling compositions to seal high-voltage and high-frequency equipment.

EXPERIMENTAL

The basis for creating the compound was a linear low-molecular polyorganosiloxane rubber—styrosil—a graft copolymer of α,ω -polydimethylsiloxanediol **3** containing methylvinylsiloxane units, and styrene with a viscosity of 8–12 Pa·s. A mixture of ethyl silicate or tetraethoxysilane with dibutyltin oxide or with tin diethyl dicaprylate with the addition of a nitrogen-containing organosilicon compound was used as a vulcanizing agent (Table 1).



Scheme 1. Some linear low molecular weight organopolysiloxane rubbers with molecular weight from 25000 to 100000 containing end silanol groups

Table 1. Used nitrogen-containing organosilicon compounds

Substance	Manufacturer, country of origin	Reference to production procedure
Styrosil (low molecular weight polymer styrosil)	<i>NIISK</i> ¹ , St. Petersburg, Russia	–
Ethyl silicate (ethyl silicate-40, grade A, premium grade) (ethyl silicate-32)	<i>EKOTEK Chemical Components Plant</i> ² , Russia	–
Tetraethoxysilane (tetraethoxysilane, grade A, 98.5%)	<i>EKOTEK Chemical Components Plant</i> , Russia	–
Dibutyltin oxide (dibutyltin oxide, 98%)	<i>Acros Organics</i> ³ , Belgium	–
Tin diethyl dicaprylate (catalyst 230-15—solution of tin diethyl dicaprylate in ethyl silicate-32)	<i>EKOTEK Chemical Components Plant</i> , Russia	–
γ -Aminopropyltriethoxysilane (3-aminopropyltriethoxysilane, 99%)	<i>Acros Organics</i> , Belgium	–
Diethylcarbamic acid trimethylsilyl ester	–	[22]
Glycidyl methacrylate (glycidyl methacrylate, 97%, stable)	<i>Acros Organics</i> , Belgium	–
Triethoxysilane (triethoxysilane, 95%)	<i>Acros Organics</i> , Belgium	–
Diethylcarbamic acid triethoxysilyl ester	–	Diss. Dr. Sci. (Chem.) of L.O. Belova ⁴
Methyl formate (methyl formate, 97%)	<i>Acros Organics</i> , Belgium	–

Infrared (IR) spectra were recorded on a Nicolet 7600 spectrometer (*Thermo Fisher Scientific*, USA) in petroleum jelly or in a thin layer. Elemental analysis was carried out using a FLASH EA 1112 instrument (Italy). Differential scanning calorimetry was carried out on a differential scanning calorimeter DSC-822e (*Mettler Toledo*, Switzerland) at a heating rate of 10 deg/min. The dielectric properties were measured using a Novocontrol Alpha-A impedance analyzer (*Novocontrol Technologies*, Germany) and a ZGS Alpha Active Sample Cell (*Novocontrol Technologies*, Germany) with gold disk electrodes with a diameter of 20 mm. The measurements were performed in the frequency range of 10^{-1} – 10^6 Hz. The mechanical properties of the samples

were determined using a universal testing machine AGS-10kNG (*Shimadzu Corporation*, Japan). The samples used to determine the tensile strength and elongation at break were strips with a working part size of 3×20 mm. The stretching speed was 10 mm/min. The dynamic viscosity was determined using a Haake Viscotester C rotational viscometer (*Thermo Electron Corporation*, USA).

All starting compounds were thoroughly dried and purified by distillation before use. Synthetic operations, isolation and sampling for the analysis of compounds were carried out in a dry nitrogen atmosphere. Table 2 shows chemical formulas, names, and codes for used nitrogen-containing organosilicon compounds.

¹ <https://fgupniisk.ru/>. Accessed April 03, 2024.

² <https://www.eko-tec.ru/>. Accessed April 03, 2024.

³ <https://www.thermofisher.com/ru/ru/home/chemicals/acros-organics.html>. Accessed April 03, 2024.

⁴ Belova L.O. *New approaches to the synthesis and application of diazot-containing organosilicon compounds*: Diss. Dr. Sci. (Chem.). Moscow: 2011. 283 p. (in Russ.).

Table 2. Used nitrogen-containing organosilicon compounds

Chemical formula	Name	Code
$(\text{EtO})_2\text{Si}(\text{CH}_2)_3\text{NHC}(\text{O})\text{O}$	2,2-Diethoxy-1,6,2-oxaazasilepan-7-one	Product 111-269
$(\text{EtO})_3\text{Si}(\text{CH}_2)_3\text{NHC}(\text{O})\text{H}$	γ -(Triethoxysilylpropyl)-formamide	Product 111-300
$(\text{EtO})_3\text{SiOCH}_2\text{CH}(\text{NEt}_2)\text{CH}_2\text{OC}(\text{O})\text{C}(\text{Me})=\text{CH}_2$	2-(Diethylamino)-3-[(triethoxysilyl)oxy]propyl-2-methacrylate	ESAM
$(\text{EtO})_3\text{Si}(\text{CH}_2)_3\text{NHC}(\text{O})\text{OSi}(\text{OEt})_3$	Triethoxysilyl ester of γ -triethoxysilylpropyl-carbamic acid	OSU

2,2-Diethoxy-1,6,2-oxaazasilepan-7-one (product 111-269). A mixture of 15 g (0.07 mol) of γ -aminopropyltriethoxysilane and 12.83 g (0.07 mol) of diethylcarbamic acid trimethylsilyl ester was heated using a total refluxing head until the release of diethylamine and ethoxytrimethylsilane ceased. Product 111-269, 14.9 g (97%) was isolated by means of vacuuming in the form of a viscous oily substance, refractive index n_D^{20} 1.4459. IR spectrum (ν , cm^{-1}): 1690 (C=O); 3310 (N–H). Found, %: C 43.81; H 7.82; N 6.39. $\text{C}_8\text{H}_{17}\text{O}_4\text{NSi}$. Calculated C 47.96; H 9.77; N 7.99. In the dissertation of O. V. Belova (Footnote 4): n_D^{20} 1.4459. IR spectrum (ν , cm^{-1}): 1680 (C=O); 3310 (N–H).

3-(Diethylamino)-2-[(triethoxysilyl)oxy]propyl-2-methacrylate (ESAM). Diethylcarbamic acid triethoxysilyl ester, 15.9 g (0.057 mol) was slowly added to 8.1 g (0.057 mol) of glycidyl methacrylate. The reaction mixture was stirred at 55°C for 6 h. ESAM, 17.22 g (80%) was isolated by means of vacuuming at 1 mm Hg within 1 h in the form of a non-distillable liquid, n_D^{20} 1.4255. IR spectrum (ν , cm^{-1}): 1690 (C=O); 1640 (C=C). Found, %: C 54.15; H 9.45; N 3.91. $\text{C}_{17}\text{H}_{35}\text{O}_6\text{NSi}$. Calculated C 54.08; H 9.34; N 3.70.

Triethoxysilyl ester of γ -triethoxysilylpropyl-carbamic acid (OSU). A mixture of 141.6 g (0.64 mol) of γ -aminopropyltriethoxysilane and 105 g (0.64 mol) of triethoxysilane was heated to 45°C, and carbon dioxide was introduced with stirring for a period of 12 h. OSU, 245.5 g (96%) was obtained by evacuation at 1 mm Hg within 1 h in the form of a non-distillable liquid, n_D^{20} 1.4244. IR spectrum (ν , cm^{-1}): 1690 (C=O); 3340 (N–H). Found, %: C 44.85; H 8.85; N 3.31. $\text{C}_{16}\text{H}_{37}\text{O}_8\text{NSi}_2$. Calculated C 44.94; H 8.7; N 3.27.

γ -(Triethoxysilylpropyl) formamide (product 111-300). 23.4 g (0.11 mol) of γ -aminopropyltriethoxysilane and 6.6 g (0.11 mol) of methyl formate were placed in

a flask equipped with a thermometer and a distillation column head. The reaction mixture was heated. After separating the released methyl alcohol, distillation of the still bottom gave 23.84 g (86.9%) of product 111-300, boiling point 146–147°C (2 mm Hg), n_D^{20} 1.4390. IR spectrum (ν , cm^{-1}): 1680 (C=O); 3310 (N–H). Found, %: C 48.07; N 9.30; N 5.40. $\text{C}_{10}\text{H}_{23}\text{O}_4\text{NSi}$. Calculated C 48.16; H 9.31; N 5.61.

RESULTS AND DISCUSSION

We had previously conducted research on the possibility of using nitrogen-containing organosilicon compounds as catalysts for the curing of silicone rubbers [24, 25]. The resulting coatings possessed frost resistance, high dielectric properties, increased mechanical and electrical strength, and adhesion. However, they turned out to be flammable which did not always make it possible for them to be used, especially in the electrical insulation of power and radio equipment.

Continuing these studies, first of all product 111-269 (2,2-diethoxy-1,6,2-oxaazasilepan-7-one) and ethyl silicate-40, which had worked well previously, were used as a hardener. Then a number of other first synthesized nitrogen-containing organosilicon compounds were used (Table 1). ESAM was synthesized using diethylcarbamic acid triethoxysilyl ester (Scheme 2). OSU was obtained by *N*-silyloxycarbonylation (Scheme 3), and product 111-300 was obtained by formylation (Scheme 4).

Two compositions were used as fillers: a mixture containing Aerosil (filler based on hexabromobenzene (GB filler), see composition in Table 3) and a mixture without Aerosil (filler based on hexabromobenzene (DB filler), see composition in Table 4). The results of testing the compositions using a range of vulcanizing agents and fillers are presented in Tables 5–11.

Table 5. Influence of the type of filler and the degree of its filling on the viscosity of rubber, the physical and mechanical properties of the vulcanizate, and the ability to self-extinguish. Hardener, weight parts (wt.p.): ethyl silicate-40, 2.6; dibutyltin oxide, 0.025

Parameter	Value								
Stirosil (9.0 Pa·s), wt.p.	100	100	100	100	100	100	100	100	100
DB filler, wt.p.	–	30	–	40	–	50	–	60	–
GB filler, wt.p.	–	–	30	–	40	–	50	–	60
Dynamic viscosity, Pa·s	9.0	13.5	16.6	18.3	21.5	28.3	33.0	35.0	38.0
Viability at 20°C, min	>120	40	40	40	40	40	40	30	30
Tensile strength, MPa	2.45	2.55	1.86	2.45	2.06	1.18	0.98	2.45	2.06
Relative elongation, %	120	110	100	85	120	85	110	105	80
Compression module at 20°C, MPa	2.94	–	–	2.45	–	2.84	–	3.14	–
Crystallization temperature, °C	–60	–	–	–60	–	–60	–	–60	–
Dielectric constant at 10 ³ Hz, 20°C	3.2	–	–	3.2	–	3.4	–	3.5	–
tg δ* at 10 ³ Hz, 20°C	0.002	–	–	0.0051	–	0.0087	–	0.0073	–
Self-extinguishing, s	–	2	2	1.6	1.5	1.5	1.5	1.5	2
Electrical strength, kV/mm	35	–	–	40	–	38	–	33	–

*tg δ (dielectric loss tangent) is defined as the ratio of the active component of the leakage current through the insulation to its reactive component.

Table 6. Influence of the curing system on the technological and physicochemical properties of the compound. Hardener (2 wt.p. — 100%): tetraethoxysilane — 80%; product 111-269 — 20%; tin diethyldicaprylate — 0.02%

Parameter	Value
Stirosil (3.3–9.0 Pa·s), wt.p.	100
DB filler, wt.p.	–
GB filler, wt.p.	–
Dynamic viscosity, Pa·s	8–9
Viability at 20°C, min	120
Tensile strength, MPa	1–2.7
Relative elongation, %	70–210
Compression module at 20°C, MPa	1.96–2.94
Curing time at 20°C, day	1–2
Crystallization temperature, °C	–60

Table 6. Continued

Parameter	Value
Dielectric constant at 10^3 Hz, 20°C	3.6
tg δ at 10^3 Hz, 20°C	0.002
Self-extinguishing, s	–
Electrical strength, kV/mm	24–30
Heat resistance, °C	150

Table 7. Influence of the curing system on the technological and physicochemical properties of the compound. Hardener, 2 wt.p.: tetraethoxysilane — 80%; ESAM — 20%; tin diethyldicaprylate — 0.02%

Parameter	Value				
	100	100	100	100	100
Stirosil (3.3–9.0 Pa·s), wt.p.	100	100	100	100	100
DB filler, wt.p.	–	–	40	50	60
GB filler, wt.p.	–	30	–	–	–
Dynamic viscosity, Pa·s	9.0	16.6	18.3	28.3	35.0
Viability at 20°C, min	120	120	120	90	90
Tensile strength, MPa	2.16	1.96	2.26	2.35	2.06
Relative elongation, %	113	100	120	90	90
Compression module at 20°C, MPa	2.75	3.14	2.75	2.65	3.04
Curing time at 20°C, day	1	1	1	1	1
Crystallization temperature, °C	–60	–60	–60	–60	–60
Dielectric constant at 10^3 Hz, 20°C	3.2	3.2	3.3	3.4	3.5
tg δ at 10^3 Hz, 20°	0.0018	0.0039	0.0047	0.0104	0.0072
Self-extinguishing, s	–	2	2	1	1.6
Electrical strength, kV/mm	27	30	30	–	40
Heat resistance, °C	150	–	–	–	–

Table 8. Influence of the curing system on the technological and physicomechanical properties of the compound. Hardener, 2 wt.p.: ESAM — 20%; tin diethyldicaprylate — 0.03%

Parameter	Value				
Stirosil (3.3–9.0 Pa·s), wt.p.	100	100	100	100	100
DB filler, wt.p.	–	–	40	50	60
GB filler, wt.p.	–	30	–	–	–
Dynamic viscosity, Pa·s	9.0	16.6	18.3	28.3	35.0
Viability at 20°C, min	120	90	90	90	60
Tensile strength, MPa	1.27	1.37	1.47	1.47	1.47
Relative elongation, %	250	150	180	170	130
Compression module at 20°C, MPa	2.16	2.16	2.45	2.75	2.84
Curing time at 20°C, day	1–2	1	1	1	1
Crystallization temperature, °C	–60	–60	–60	–60	–60
Dielectric constant at 10 ³ Hz, 20°C	–	3.2	3.3	3.4	3.4
tg δ at 10 ³ Hz, 20°C	–	0.0052	0.0053	0.0074	0.0083
Self-extinguishing, s	–	–	2	–	–
Electrical strength, kV/mm	–	–	36	–	–

Table 9. Influence of the curing system on the technological and physicomechanical properties of the compound. Hardener, 2–3 wt.p.: product 111-300 — 100%; tin diethyldicaprylate — 0.02%

Parameter	Value		
Stirosil (3.3–9.0 Pa·s), wt.p.	100	100	100
DB filler, wt.p.	40	50	60
Dynamic viscosity, Pa·s	18.3	28.3	35.0
Viability at 20°C, min	40	40	30
Tensile strength, MPa	2.55	–	2.35
Relative elongation, %	90	–	80

Table 9. Continued

Parameter	Value		
Compression module at 20°C, MPa	2.45–3.43	2.45–2.94	2.55–2.84
Curing time at 20°C, day	1	1	1
Crystallization temperature, °C	–60	–60	–60
Dielectric constant at 10 ³ Hz, 20°C	3.4	–	3.5
tg δ at 10 ³ Hz, 20°C	0.0050	–	0.0184
Self-extinguishing, s	1	2	2
Electrical strength, kV/mm	36	–	–
Heat resistance, °C	180	–	–

Table 10. Influence of the curing system on the technological and physicomechanical properties of the compound. Hardener, 2 wt.p: tetraethoxysilane — 80%; ESAM — 20%; tin diethyldicaprylate — 0.02%

Parameter	Value		
Stirosil (3.3–9.0 Pa·s), wt.p.	100	100	100*
DB filler, wt.p.	–	40	40
GB filler, wt.p.	30	–	–
Dynamic viscosity, Pa·s	16.6	18.3	18.3
Viability at 20°C, min	120	120	0.5
Tensile strength, MPa	2.35	2.35	–
Relative elongation, %	100	120	–
Compression module at 20°C, MPa	2.84	3.24	2.55–2.84
Curing time at 20°C, day	1	1	1
Crystallization temperature, °C	–60	–60	–60
Dielectric at 10 ³ Hz, 20°C	–	3.2	–

Table 10. Continued

Parameter	Value		
tg δ at 10^3 Hz, 20°C	–	0.006	–
Self-extinguishing, s	2	1–2	–
Electrical strength, kV/mm	–	32	–
Heat resistance, $^\circ\text{C}$	170	176	130

*3–4 wt.p. — 100%: tetraethoxysilane — 80%; ESAM — 20%; tin diethyldiacrylate — 0.02%.

Table 11. Influence of the curing system on the technological and physicochemical properties of the compound. Hardener, 2–3 wt.p.: OSU — 100%; tin diethyldiacrylate — 0.02%

Parameter	Value		
Stirosil (3.3–9.0 Pa·s), wt.p.	100	100	100
DB filler, wt.p.	–	40	40
GB filler, wt.p.	30	–	–
Dynamic viscosity, Pa·s	17.5	18.3	18.3
Viability at 20°C , min	90	90	90
Tensile strength, MPa	2.45	2.75	2.75
Relative elongation, %	170	210	210
Compression module at 20°C , MPa	3.63	3.92	3.92
Curing time at 20°C , day	1	1	1
Crystallization temperature, $^\circ\text{C}$	–60	–60	–60
Dielectric constant at 10^3 Hz, 20°C	3.2	3.2	3.2
tg δ at 10^3 Hz, 20°C	0.0006	0.0007	0.0007
Self-extinguishing, s	0.7	0.5	0.5
Electrical strength, kV/mm	31	35	35
Heat resistance, $^\circ\text{C}$	180	190	190

Table 12. Effect of the curing system [ESAM + tin diethyldiacrylate] on the properties of rubber vulcanizates

Parameter	Value						
ESAM	3 wt.p.						
Tin diethyldiacrylate, wt.p.	0.164	0.02	0.016	0.005	0.004	0.003	0.002
Stirosil (9.0 Pa·s), wt.p.	60	60	60	60	60	60	60
DB filler, wt.p.	40	40	40	40	40	40	40
Viability at 20°C, min	No	<10	30	60	90	90	120
Curing time at 20°C, day	0.33	0.5	1	<24	<24	24	24

Table 13. Influence of the curing system [ESAM + tin diethyldiacrylate on the properties of rubber vulcanizates]

Parameter	Value			
Tin diethyldiacrylate, wt.p.	0.003			
ESAM, wt.p.	2	3	5	8
Stirosil (9.0 Pa·s), wt.p.	60	60	60	60
DB filler, wt.p.	40	40	40	40
Viability at 20°C, min	120	90	90	60
Tensile strength, MPa	1.67	1.47	1.47	–
Relative elongation, %	160	185	180	–
Curing time at 20°C, day	48	24	24	48

The results presented (Tables 5–11) clearly indicate that self-extinguishing, i.e., decay time after removal from the flame, *s*, of the filled compositions, regardless of the amount of filler used (30–60 wt.p.), attained value 1–2 s, while their heat resistance increased at the same time from 150 to 180°C.

The data obtained (Tables 5–11) on tensile strength, relative elongation and compression modulus shows

that the introduction of filler has virtually no effect on the mechanical properties of the polymer, as well as on the crystallization temperature of the compositions. In addition, it is clearly shown that GB filler, compared to DB filler, increases the polymer system viscosity to a greater extent (apparently due to the presence of aerosil), while the degree of filling significantly affects the increase in viscosity. For example, with a viscosity

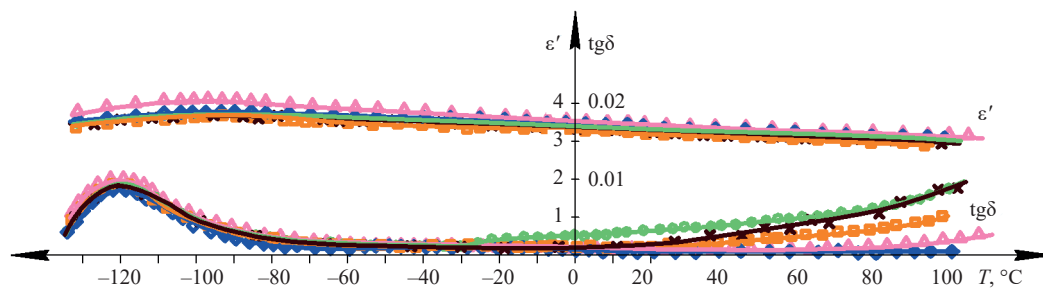


Fig. 1. Temperature dependence of $\text{tg}\delta$ and ϵ' on the type of hardener at a frequency of 1000 Hz. Hardener: ●●● ethyl silicate 40 + dibutyltin oxide; xxx product 111-300; ▲▲▲ tetraethoxysilane + ESAM; ○○○ OSU; *** ESAM

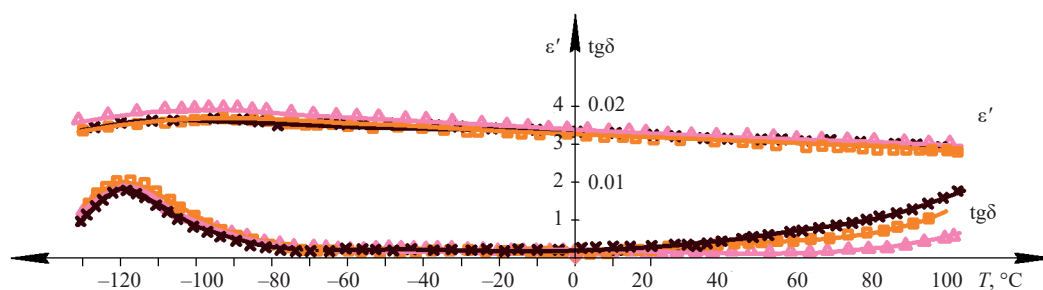


Fig. 2. Temperature dependence of $\text{tg}\delta$ and ϵ' on the amount of hardener ESAM at a frequency of 1000 Hz: ●●● 2; xxx 3; and ▲▲▲ 5 wt.p. hardener per 100 wt.p. polymer

of the original rubber of 9.0 Pa·s, the introduction of 40 wt.p. of a filler increases its value approximately by a factor of 2, while using 60 wt.p. of a filler, viscosity becomes equal to 35.0 Pa·s. The constant value of the compositions crystallization temperature can be explained by the inertness of the fillers with respect to styrosil.

When studying the dielectric properties of the resulting compositions, which characterize the behavior of the material in an electric field, the dielectric constant (ϵ'), dielectric losses ($\text{tg}\delta$) and electrical strength (E_s) were considered in detail. They depend on the compound operating conditions and are closely related to the macrochain chemical composition and structure. From the results obtained it is clear that a wide asymmetric maximum of dipole-segmental losses can be observed in the temperature range from -90 to -130°C (at a frequency of 1000 Hz) (Fig. 1). The asymmetry of the $\text{tg}\delta$ maximum appears to be due to the influence of the supramolecular organization on the polymer electrical properties. As a rule, this effect is especially pronounced for crystallizing polymers: something which we observed for this composition. In contrast, in the temperature

range from -90 to $+100^\circ\text{C}$, the value of the dielectric loss tangent remains practically unchanged and is about 0.005, which allows us to recommend its use at high frequencies in this temperature range.

The influence of the brand and amount of hardener on the value of the dielectric loss tangent (Fig. 2) is manifested both in the region of positive temperatures (as the amount of hardener increases, losses increase slightly, since the polar component amount increases) and in the region of subzero temperatures (fluctuations in $\text{tg}\delta_{\text{max}}$ values and relaxation time spectrum are observed, apparently due to the influence of functional groups on molecular mobility).

However, the differences observed in the dependence of the dielectric loss tangent $\text{tg}\delta$ on temperature are so small that they can be neglected for the practical use of the compound. At the same time, the dielectric properties of the filled compositions change somewhat with an increase in the $\text{tg}\delta$ value. For compositions containing up to 40 wt.p. of filler, the $\text{tg}\delta$ value does not exceed 0.005, and at a higher degree of filling, it increases to 0.01, exceeding the permissible value for a high-voltage, high-frequency dielectric.

Thus, after the introduction of fillers, a compound using nitrogen-containing organosilicon compounds as part of the curing system retains high dielectric properties, increased electrical and mechanical strength and frost resistance. This is characteristic of high-voltage and high-frequency compounds. At the same time, the compound acquires non-flammable properties with a simultaneous increase in heat resistance.

CONCLUSIONS

The study shows that the use of synthetically available nitrogen-containing organosilicon compounds—3-(diethylamino)-2-[(triethoxysilyloxy)propyl]-2-methacrylate and triethoxysilyl ester of γ -triethoxysilylpropylcarbamic acid—as part of a curing system together with bromine-containing fillers makes it possible for compounds to be obtained to fill high-voltage and high-frequency transformers, throttles and other elements of radio-electronic equipment with non-flammable

properties, while simultaneously increasing heat resistance.

The physicochemical and dielectric properties of a self-extinguishing organosilicon compound were studied, showing that it is manufacturable, has a high fire resistance (no more than 10 s) and increased heat resistance (up to 180°C). The compound retains high dielectric properties ($\tan\delta$ no more than 0.005) and electrical strength (not less than 25 kV/mm), good mechanical properties (tensile strength not less than 1.5 MPa) with high elasticity (relative elongation not less than 140%).

Authors' contributions

A.D. Kirilin—idea of the study and general management.

L.O. Belova, N.I. Kirilina—the analysis of the obtained results and writing the text of the article.

N.A. Golub, M.V. Pletneva—conducting the experiments, scientific editing.

D.E. Mironov—conducting the experiments.

The authors declare that there is no conflict of interest.

REFERENCES

1. Andrianov K.A., Khananashvili L.M. *Tekhnologiya elementoorganicheskikh monomerov i polimerov (Technology of Organoelement Monomers and Polymers)*. Moscow: Khimiya; 1973. 400 p. (in Russ.).
2. Sobolevskii M.V., Muzovskaya O.A., Popeleva G.S. *Svoistva i oblasti primeneniya kremniorganicheskikh produktov (Properties and Applications of Organosilicon Products)*. Moscow: Khimiya; 1975. 296 p. (in Russ.).
3. Gerasimov D.M., Iluhina M.A., Glazov P.A. Low-molecular organosilicone rubbers in sealant compositions. *Trudy VIAM = Proceedings of VIAM*. 2020;90(8):35–45 (in Russ.). <https://doi.org/10.18577/2307-6046-2020-0-8-35-45>
4. Smyslova R.A., Kotlyarova S.V. *Spravochnoe posobie po germetiziruyushchim materialam na osnove kauchukov (A Guide to Rubber Based Sealing Materials)*. Moscow: Khimiya; 1976. 72 p. (in Russ.).
5. Severnyi V.V., Minasyan R.M., Makarenko I.A., Biryuzova N.M. The mechanism of “cold-curing” low molecular weight polyorganosiloxane rubbers. *Polym. Sci. U.S.S.R.* 1976;18(6):1464–1471. [https://doi.org/10.1016/0032-3950\(76\)90342-7](https://doi.org/10.1016/0032-3950(76)90342-7) [Original Russian Text: Severnyi V.V., Minasyan R.M., Makarenko I.A., Biryuzova N.M. The mechanism of “cold-curing” low molecular weight polyorganosiloxane rubbers. *Vysokomolekulyarnye soedineniya. Ser. A*. 1976;18(6):1276–1281 (in Russ.).]
6. Karlin A.V., Reikhsfeld V.O., Kagan E.G. *Khimiya i tekhnologiya kremniorganicheskikh elastomerov (Chemistry and Technology of Organosilicon Elastomers)*. Leningrad: Khimiya; 1973. 176 p. (in Russ.).
7. Meals R.N., Lewis F.M. *Silikony (Silicones)*: transl. from Engl. Moscow: Khimiya; 1964. 256 p. (in Russ.). [Meals R.N., Lewis F.M. *Silicones*. NY.: Reinhold Publ. Corp.; 1959. 296 p.]
8. Degussa-Silicas for HTV-Silicone Rubber. *Technical Bulletin Pigments No. 12*. Degussa AG. 2008.
9. Dolgov O.N., Voronkov M.G., Grinblat M.P. *Kremniorganicheskie zhidkie kauchuki i materialy na ikh osnove (Organosilicon Liquid Rubbers and Materials Based on them)*. Leningrad: Khimiya; 1975. 112 p. (in Russ.).
10. Severnyi V.V., Minasyan R.M., Minasyan O.I. Effect of organofunctional organosilicon crosslinking agents on the rate of cure of α,ω -hydroxypolydimethylsiloxanes. *Polym. Sci. U.S.S.R.* 1977;19(7):1775–1783. [https://doi.org/10.1016/0032-3950\(77\)90191-5](https://doi.org/10.1016/0032-3950(77)90191-5) [Original Russian Text: Severnyi V.V., Minasyan R.M., Minasyan O.I. Effect of organofunctional organosilicon crosslinking agents on the rate of cure of α,ω -hydroxypolydimethylsiloxanes. *Vysokomolekulyarnye soedineniya. Ser. A*. 1977;19(7):1549–1555 (in Russ.).]

- Pocius A.V. *Klei, adgeziya, tekhnologiya sklevaniya (Adhesives, Adhesion, Bonding Technology)*: transl. from Engl.; Komarov G.V. (Ed.). St. Petersburg: Professiya; 2016. 384 p. (in Russ.). [Pocius A.V. *Adhesion and Adhesives Technology: An Introduction*. München; Cincinnati, OH: Carl Hanser Gardener Verlag GmbH & Co; 2012. 386 p.]
- Schatz M. *Silikonovyi kauchuk (Silicone Rubber)*: transl. from Czech. Leningrad: Khimiya; 1975. 192 p. (in Russ.). [Schatz M. *Silikonový Kaučuk*. Praha: SNTL-Nakladatelství Technické Literatury; 1971 (in Czech.)]
- Sakamoto T., Arai M., Miyoshi K. *Vulcanizable Organopolysiloxane Composition*: USA Pat. 5371116. Publ. 06.12.1994.
- Kodolov V.I. *Zamedliteli goreniya polimernykh materialov (Flame Retardants of Polymeric Materials)*. Moscow: Khimiya; 1980. 269 p. (in Russ.).
- Mikhailin Yu.A. *Konstruksionnye polimernye kompozitsionnye materialy (Structural Polymeric Composite Materials)*. St. Petersburg: Nauchnye osnovy i tekhnologii; 2010. 820 p. (in Russ.). ISBN 978-5-91703-003-6
- Chaykun A.M., Venediktova M.A., Bryk Ya.A. Development of the compounding of rubber extremely high heat resistance with temperature range of exploitation from the -60 to +500°C. *Trudy VIAM = Proceedings of VIAM*. 2019;73(1):21–30 (in Russ.). <https://doi.org/10.18577/2307-6046-2019-0-1-21-30>
- Semenova S.N., Chaykun A.M. Highly heat-resistant silicone rubber compositions (review). *Trudy VIAM = Proceedings of VIAM*. 2020;93(11):31–36 (in Russ.). <https://doi.org/10.18577/2307-6046-2020-0-11-31-37>
- Goldin G.S., Fedorov S.G., Kravtsova S.F. *Antipireny i ogranichenno goryuchie materialy na osnove oligo- i polifosfazenov (Flame Retardants and Limited Combustible Materials Based on Oligo- and Polyphosphazenes)*. Moscow: NIITEKhIM; 1988. 35 p. (in Russ.).
- Ninomiya K., Kamiya M. *Heat-Resistant Silicone Rubber Composition and its Molded Product*: Japan Pat. JP2001348481A. Publ. 18.12.2001.
- Ninomiya K., Kamiya M. *Heat-Resistant Silicone Rubber Composition and Molded Article Obtained by Curing the Composition*: Japan Pat. JP2002220532A. Publ. 09.08.2002.
- Chernyshev E.A., Belyakova Z.V., Knyazeva L.K. *Aminopropiltrietskisilan (poluchenie, svoistva, oblasti primeneniya) (Aminopropyltriethoxysilane (Obtaining, Properties, Applications))*. Overview Information. Series “Organoelement Compounds and Their Applications.” Moscow: NIITEKhIM; 1985. 32 p. (in Russ.).
- Varlamova N.V., Sunekants T.I., Kotrikadze E.L., Kirilin A.D., Severnyi V.V., Khananashvili L.M., Sheludyakov V.D. Organo(diethylcarbaminooxy)silanes – hardeners for polyorganosiloxane resins. *Soobshcheniya Akademii nauk Gruzinskoi SSR = Bulletin of the Georgian Academy of Sciences of the SSR*. 1981;104:5356 (in Russ.).

СПИСОК ЛИТЕРАТУРЫ

- Андрианов К.А., Хананашвили Л.М. *Технология элементо-органических мономеров и полимеров*. М.: Химия; 1973. 400 с.
- Соболевский М.В., Музовская О.А., Попелева Г.С. *Свойства и области применения кремнийорганических продуктов*. М.: Химия; 1975. 296 с.
- Герасимов Д.М., Илюхина М.А., Глазов П.А. Низкомолекулярные кремнийорганические каучуки в составе герметизирующих композиций. *Труды ВИАМ*. 2020;90(8): 35–45. <https://doi.org/10.18577/2307-6046-2020-0-8-35-45>
- Смыслова Р.А., Котлярова С.В. *Справочное пособие по герметизирующим материалам на основе каучуков*. М.: Химия; 1976. 72 с.
- Северный В.В., Минасян Р.М., Макаренко И.А., Бирюзова Н.М. Механизм «холодной» вулканизации низкомолекулярных полиорганосилоксановых каучуков. *Высокомолекулярные соединения. Сер. А*. 1976;18(6): 1276–1281.
- Карлин А.В., Рейхсфельд В.О., Каган Е.Г. *Химия и технология кремнийорганических эластомеров*. Л.: Химия; 1973. 176 с.
- Милс Р.Н., Льюис Ф.М. *Силиконы*: пер. с англ. М.: Химия; 1964. 256 с.
- Degussa-Silicas for HTV-Silicone Rubber. *Technical Bulletin Pigments No. 12*. Degussa AG. 2008.
- Долгов О.Н., Воронков М.Г., Гринблат М.П. *Кремний-органические жидкие каучуки и материалы на их основе*. Л.: Химия. 1975. 112 с.
- Северный В.В., Минасян Р.М., Минасян О.И. Влияние органофункциональных кремнийорганических сшивающих агентов на скорость вулканизации α, ω -гидроксиполидиметилсилоксанов. *Высокомолекулярные соединения. Сер. А*. 1977;19(7):1549–1555.
- Поциус А. *Клеи, адгезия, технология склеивания*: пер. с англ.; под ред. Г.В. Комарова. СПб: Профессия; 2016. 384 с.
- Шетц М. *Силиконовый каучук*: пер. с чешского. Л.: Химия; 1975. 192 с.
- Sakamoto T., Arai M., Miyoshi K. *Vulcanizable Organopolysiloxane Composition*: USA Pat. 5371116. Publ. 06.12.1994.
- Кодолов В.И. *Замедлители горения полимерных материалов*. М.: Химия; 1980. 269 с.
- Михайлин Ю.А. *Конструкционные полимерные композиционные материалы*. СПб: Научные основы и технологии; 2010. 820 с. ISBN 978-5-91703-003-6
- Чайкун А.М., Вenediktova M.A., Bryk Ya.A. Разработка рецептуры резины экстремально высокой теплостойкости с температурным диапазоном эксплуатации от -60 до +500°C. *Труды ВИАМ*. 2019;73(1):21–30. <https://doi.org/10.18577/2307-6046-2019-0-1-21-30>

17. Семенова С.Н., Чайкун А.М. Силиконовые резиновые композиции с повышенной термостойкостью. *Труды ВИАМ*. 2020;93(11):31–37. <https://doi.org/10.18577/2307-6046-2020-0-11-31-37>
18. Гольдин Г.С., Федоров С.Г., Кравцова С.Ф. *Антипирены и ограниченно горючие материалы на основе олиго- и полифосфазенов*. М.: НИИТЭХИМ; 1988. 35 с.
19. Ninomiya K., Kamiya M. *Heat-Resistant Silicone Rubber Composition and its Molded Product*: Japan Pat. JP2001348481A. Publ. 18.12.2001.
20. Ninomiya K., Kamiya M. *Heat-Resistant Silicone Rubber Composition and Molded Article Obtained by Curing the Composition*: Japan Pat. JP2002220532A. Publ. 09.08.2002.
21. Чернышев Е.А., Белякова З.В., Князева Л.К. *Аминопропилтриэтоксисилан (получение, свойства, области применения)*. Обзорная информация. Серия «Элементоорганические соединения и их применение». М.: НИИТЭХИМ; 1985. 32 с.
22. Варламова Н.В., Сунеканц Т.И., Котрикадзе Э.Л., Кирилин А.Д., Северный В.В., Хананашвили Л.М., Шелудяков В.Д. Органо(диэтилкарбаминоокси)силаны – отвердители полиорганосилоксановых смол. *Сообщения АН Грузинской ССР*. 1981;104:53–56.

About the authors

Alexey D. Kirilin, Dr. Sci. (Chem.), Professor, Head of the K.A. Andrianov Department of Chemistry and Technology of Organoelement Compounds, M.V. Lomonosov Institute of Fine Chemical Technologies, MIREA – Russian Technological University (86, Vernadskogo pr., Moscow, 119571, Russia). E-mail: kirilinada@rambler.ru. Scopus Author ID 6603604447, ResearcherID O-9744-215, RSCI SPIN-code 5500-5030, <https://orcid.org/0000-0001-9225-9551>

Liya O. Belova, Dr. Sci. (Chem.), Professor, K.A. Andrianov Department of Chemistry and Technology of Organoelement Compounds, M.V. Lomonosov Institute of Fine Chemical Technologies, MIREA – Russian Technological University (86, Vernadskogo pr., Moscow, 119571, Russia). E-mail: belova@mirea.ru. Scopus Author ID 7102282244, RSCI SPIN-code 3499-7697, <https://orcid.org/0000-0002-3920-2908>

Nataliya A. Golub, Cand. Sci. (Chem.) Associate Professor, K.A. Andrianov Department of Chemistry and Technology of Organoelement Compounds, M.V. Lomonosov Institute of Fine Chemical Technologies, MIREA – Russian Technological University (86, Vernadskogo pr., Moscow, 119571, Russia). E-mail: golub@mirea.ru. Scopus Author ID 56084643600, RSCI SPIN-code 4240-3509, <https://orcid.org/0000-0001-9932-7588>

Mariya V. Pletneva, Cand. Sci. (Chem.) Associate Professor, K.A. Andrianov Department of Chemistry and Technology of Organoelement Compounds, M.V. Lomonosov Institute of Fine Chemical Technologies, MIREA – Russian Technological University (86, Vernadskogo pr., Moscow, 119571, Russia). E-mail: pletneva@mirea.ru. Scopus Author ID 37104888400, RSCI SPIN-code 9399-0150, <https://orcid.org/0000-0002-4940-292X>

Nadezhda I. Kirilina, Cand. Sci. (Chem.), Leading Engineer, State Scientific Research Institute of Chemistry and Technology of Organoelement Compounds (38, Entuziastov shosse, Moscow, 111123, Russia). E-mail: ous@eos.su. Scopus Author ID 57193056863, RSCI SPIN-code 4549-8907, <https://orcid.org/0000-0001-9932-7588>

Denis E. Mironov, Postgraduate Student, K.A. Andrianov Department of Chemistry and Technology of Organoelement Compounds, M.V. Lomonosov Institute of Fine Chemical Technologies, MIREA – Russian Technological University (86, Vernadskogo pr., Moscow, 119571, Russia). E-mail: mironov_d@mirea.ru. RSCI SPIN-code 3780-5095, <https://orcid.org/0009-0006-0659-1886>

Об авторах

Кирилин Алексей Дмитриевич, д.х.н., профессор, заведующий кафедрой химии и технологии элементоорганических соединений им. К.А. Андрианова, Институт тонких химических технологий им. М.В. Ломоносова, ФГБОУ ВО «МИРЭА – Российский технологический университет» (119571, Россия, Москва, пр-т Вернадского, д. 86). E-mail: kirilinada@rambler.ru. Scopus Author ID 6603604447, ResearcherID O-9744-215, SPIN-код РИНЦ 5500-5030, <https://orcid.org/0000-0001-9225-9551>

Белова Лия Олеговна, д.х.н., профессор кафедры химии и технологии элементоорганических соединений им. К.А. Андрианова, Институт тонких химических технологий им. М.В. Ломоносова, ФГБОУ ВО «МИРЭА – Российский технологический университет» (119571, Россия, Москва, пр-т Вернадского, д. 86). E-mail: belova@mirea.ru. Scopus Author ID 7102282244, SPIN-код РИНЦ 3499-7697, <https://orcid.org/0000-0002-3920-2908>

Голуб Наталия Александровна, к.х.н., доцент кафедры химии и технологии элементоорганических соединений им. К.А. Андрианова, Институт тонких химических технологий им. М.В. Ломоносова, ФГБОУ ВО «МИРЭА – Российский технологический университет» (119571, Россия, Москва, пр-т Вернадского, д. 86). E-mail: golub@mirea.ru. Scopus Author ID 56084643600, SPIN-код РИНЦ 4240-3509, <https://orcid.org/0000-0001-9932-7588>

Плетнева Мария Владимировна, к.х.н., доцент кафедры химии и технологии элементоорганических соединений им. К.А. Андрианова, Институт тонких химических технологий им. М.В. Ломоносова, ФГБОУ ВО «МИРЭА – Российский технологический университет» (119571, Россия, Москва, пр-т Вернадского, д. 86). E-mail: pletneva@mirea.ru. Scopus Author ID 37104888400, SPIN-код РИНЦ 9399-0150, <https://orcid.org/0000-0002-4940-292X>

Кирилина Надежда Ивановна, к.х.н., ведущий инженер, ГНЦ РФ АО «Государственный научно-исследовательский институт химии и технологии элементоорганических соединений» (111123, Россия, Москва, шоссе Энтузиастов, д. 38). E-mail: ous@eos.su. Scopus Author ID 57193056863, SPIN-код РИНЦ 4549-8907, <https://orcid.org/0000-0001-9932-7588>

Миронов Денис Евгеньевич, аспирант кафедры химии и технологии элементоорганических соединений им. К.А. Андрианова, Институт тонких химических технологий им. М.В. Ломоносова, ФГБОУ ВО «МИРЭА – Российский технологический университет» (119571, Россия, Москва, пр-т Вернадского, д. 86). E-mail: mironov_d@mirea.ru. SPIN-код РИНЦ 3780-5095, <https://orcid.org/0009-0006-0659-1886>

Translated from Russian into English by M. Povorin

Edited for English language and spelling by Dr. David Mossop

UDC 551.464.797.9

<https://doi.org/10.32362/2410-6593-2024-19-4-310-326>

EDN OOWRYZ



RESEARCH ARTICLE

Platinum(II) complexes based on derivatives of natural chlorins with pyridine-containing chelate groups as prototypes of drugs for combination therapy in oncology

Nikita S. Kirin¹✉, Petr V. Ostroverkhov¹, Maxim N. Usachev¹, Kirill P. Birin^{1,2}, Mikhail A. Grin¹

¹ MIREA – Russian Technological University (M.V. Lomonosov Institute of Fine Chemical Technologies), Moscow, 119571 Russia

² Frumkin Institute of Physical Chemistry and Electrochemistry, Russian Academy of Sciences, Moscow, 119071 Russia

✉ Corresponding author, e-mail: n-kirin97@mail.ru

Abstract

Objectives. To synthesize Pt-containing derivatives of natural chlorins as potential agents for the combination therapy in oncology. Platinum compounds are known to occupy an important place as chemotherapeutic agents in the treatment of oncological diseases. However, Pt(II) complexes are highly toxic to the body and are not selectively accumulated in tumor cells. If photodynamic and chemotherapy methods are combined in a single drug, the pigments are responsible for the selectivity of conjugate accumulation in the tumor, while a chemotherapeutic agent based on Pt(II) complexes is responsible for the cytotoxic effect on tumor cells. This will not affect healthy cells and thereby minimize the systemic toxicity of the drug to the body.

Methods. Methods for the synthesis of pyridine-containing derivatives of natural chlorins and their metal complexes for use as potential binary agents in oncology were applied. As part of the study, the structures of the compounds obtained were confirmed by mass spectrometry, nuclear magnetic resonance spectroscopy, ultraviolet spectroscopy, and high-resolution chromatography-mass spectrometry. Preparative methods, including thin-layer and column chromatography, centrifugation and recrystallization, were used to isolate and purify the compounds obtained.

Results. Platinum(II) complexes of pyridine-containing derivatives of natural chlorins were obtained for application in combination therapy in oncology. The schemes for synthesizing the target photosensitizers were optimized, in order to increase the yields and for subsequent transfer to industrial sites.

Conclusions. It was found that pyridine-containing derivatives of natural chlorins could be obtained in high yields, that they possess chelating properties for platinum, and can be considered as binary agents in cancer therapy after successful preclinical trials.

Keywords

photodynamic therapy, chlorins, bacteriochlorins, platinum complexes, photosensitizer, combination therapy, pyridines

Submitted: 19.06.2024

Revised: 02.07.2024

Accepted: 08.07.2024

For citation

Kirin N.S., Ostroverkhov P.V., Usachev M.N., Birin K.P., Grin M.A. Platinum(II) complexes based on derivatives of natural chlorins with pyridine-containing chelate groups as prototypes of drugs for combination therapy in oncology. *Tonk. Khim. Tekhnol. = Fine Chem. Technol.* 2024;19(4):310–326. <https://doi.org/10.32362/2410-6593-2024-19-4-310-326>

НАУЧНАЯ СТАТЬЯ

Комплексы платины(II) на основе производных природных хлоринов с пиридинсодержащими хелатными группами: прототипы лекарств для комбинированной терапии в онкологии

Н.С. Кирин¹, П.В. Островерхов¹, М.Н. Усачев¹, К.П. Бирин^{1,2}, М.А. Грин¹

¹ МИРЭА – Российский технологический университет (Институт тонких химических технологий им. М.В. Ломоносова), Москва, 119571 Россия

² Институт физической химии и электрохимии им. А.Н. Фрумкина, Российская академия наук, Москва, 119071 Россия

✉ Автор для переписки, e-mail: n-kirin97@mail.ru

Аннотация

Цели. Целью настоящей работы является синтез Pt-содержащих производных природных хлоринов как потенциальных агентов для комбинированной терапии в онкологии. Известно, что соединения платины в качестве химиотерапевтических агентов занимают важное место в лечении онкологических заболеваний. Однако комплексы Pt(II) высокотоксичны для организма и не обладают селективностью накопления в опухолевых клетках. При комбинировании методов фотодинамической и химиотерапии в составе одного препарата пигменты будут отвечать за селективность накопления конъюгата в опухоли, а химиотерапевтический агент на основе комплексов Pt(II) — за цитотоксический эффект в отношении опухолевых клеток, не затрагивая здоровые клетки и, тем самым, минимизируя системную токсичность препарата на организм.

Методы. В работе реализованы методы синтеза пиридинсодержащих производных природных хлоринов и их металлокомплексов для применения их в качестве потенциальных бинарных агентов в онкологии. В ходе выполнения работы структуры полученных соединений были подтверждены методами масс-спектрометрии, спектроскопии ядерного магнитного резонанса, ультрафиолетовой спектроскопии, а также хромато-масс-спектрометрии высокого разрешения. При выделении и очистке полученных соединений применялись препаративные методы, включая тонкослойную и колоночную хроматографию, центрифугирование и перекристаллизацию.

Результаты. Получены комплексы платины(II) пиридинсодержащих производных природных хлоринов с целью их применения в комбинированной терапии в онкологии, а также оптимизированы схемы синтеза целевых фотосенсибилизаторов для увеличения их выходов и последующего трансфера на промышленные площадки.

Выводы. Установлено, что пиридинсодержащие производные природных хлоринов обладают хелатирующими свойствами в отношении платины, могут быть получены с высокими выходами и после успешных доклинических испытаний могут рассматриваться как бинарные агенты в терапии рака.

Ключевые слова

фотодинамическая терапия, хлорины, бактериохлорины, комплексы платины, фотосенсибилизатор, комбинированная терапия, пиридины

Поступила: 19.06.2024

Доработана: 02.07.2024

Принята в печать: 08.07.2024

Для цитирования

Кирин Н.С., Островерхов П.В., Усачев М.Н., Бирин К.П., Грин М.А. Комплексы платины(II) на основе производных природных хлоринов с пиридинсодержащими хелатными группами: прототипы лекарств для комбинированной терапии в онкологии. *Тонкие химические технологии*. 2024;19(4):310–326. <https://doi.org/10.32362/2410-6593-2024-19-4-310-326>

INTRODUCTION

Chemotherapy is one of the primary and most efficient methods of cancer treatment [1]. Its main advantage is the direct cytotoxic effect of chemotherapeutic drugs on tumor cells. However, these drugs feature many of

side effects due to their effect on normal cells [2, 3]¹. Platinum-based antitumor drugs occupy an important place in cancer chemotherapy, both in monotherapy, and as part of combination therapy. However, they cause serious side effects and are not always efficient due to the drug resistance of tumor cells. Therefore,

¹ Ostroverkhov P.V. *Theranostics based on natural chlorins for non-invasive diagnostic methods and therapy in oncology*: Diss. Cand. Sci. (Chem.). Moscow: 2022, 115 p.

significant efforts on the part of drug developers are aimed at creating platinum-containing drugs with higher selectivity of action.

Over past decades, platinum-based mixed-ligand complexes have been produced and their biological activity has been studied (Fig. 1). Since the discovery of the cytotoxic effect of platinum by Rosenberg in 1964 [4] about 30 drugs have undergone clinical trials. Of the drugs studied, in addition to Cisplatin, only Carboplatin and Oxaliplatin are used in clinical practice. Other drugs are used locally. For example, nedaplatin has been approved in Japan for the treatment of various types of cancer; Lobaplatin is used in China for the treatment of metastatic breast cancer, chronic myeloid leukemia, and small cell lung cancer; and Heptaplatin is used in Korea to treat stomach cancer [5].

The mechanism of the action of platinum-group drugs involves internalization into the cell where they

undergo hydrolysis before binding to purine bases in DNA, formation of cross-links between DNA branches, and initiation of the cell apoptosis process. The formation of cross-linked adducts leads to disruption of DNA expression (Fig. 2).

The use of photodynamic therapy in combination with chemotherapy has shown a high degree of efficiency both in *in vitro* and *in vivo* studies, and in clinical practice. Analysis of publications distinguishes two approaches. The first involves the use of photodynamic therapy (PDT) and chemotherapy with various variants of their combination, while in the second approach, new combination drugs have been developed [6].

In the monotherapy regimen, PDT and chemotherapy have their own drawbacks and limitations. In clinical practice, combination therapy is currently being widely used, in order to enhance the efficiency of antitumor treatment by using two different methods of affecting the

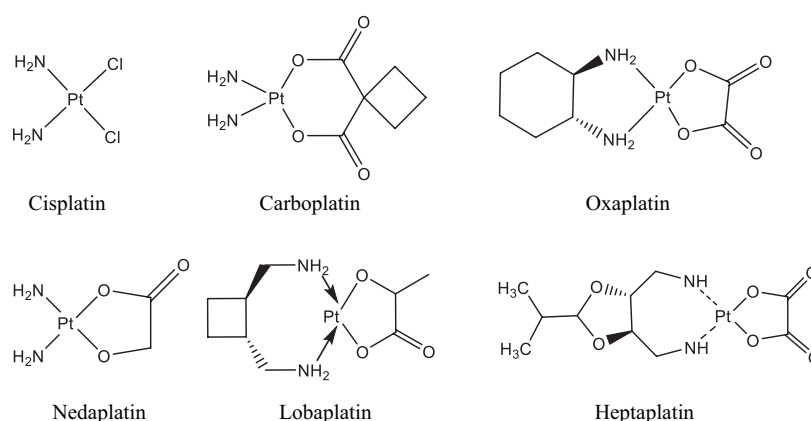


Fig. 1. Structure of platinum complexes

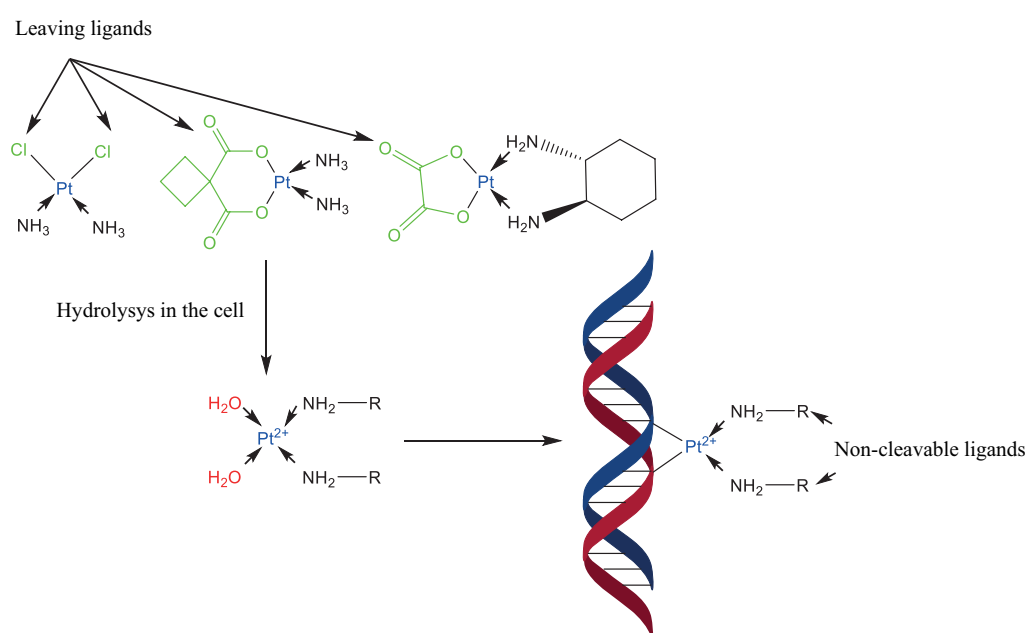


Fig. 2. Simplified mechanism of action of platinum preparations in the cell

tumor. This multimodal approach allows for synergistic effects and better healing results.

Tae-Gyu *et al.* estimated the combined effects of Cisplatin chemotherapy and PDT on EMT6 breast carcinoma in *in vivo* experiments using Nude mice [7].

Kaplan *et al.* presented data on the efficiency of the combined treatment of rats with M-1 sarcoma using Photolon and Cisplatin as photodynamic and cytotoxic agents [8]. The authors used various treatment regimens and drug doses. The treatment effect was assessed by the absolute rate of tumor growth, inhibition of tumor growth, and complete tumor regression. The most efficient treatment regimen was found to involve photodynamic therapy with irradiation 2 h after photosensitizer administration followed by Cisplatin 1 and 4 days after PDT with a total chemotherapeutic agent dose of 2.5 mg/kg. By the end of the study, complete regression of the tumor was observed in 88.9% of the animals, and inhibition of tumor growth was observed in the vast majority of tumor-bearing animals. The results of the study allowed the authors to conclude that the combination of photodynamic therapy with Cisplatin therapy is more efficient than monotherapy since it leads to a synergistic effect and helps reduce the dose of Cisplatin.

One of the first examples of the preparation of conjugates of platinum and a photosensitizer was reported by Brunner *et al.* in 1994. They assumed that the selectivity of tumor treatment with Cisplatin could be enhanced by combining it with a protoporphyrin IX derivative, since the latter has some affinity for low-density lipoprotein receptors. The resulting carboxylate complex of platinum and the protoporphyrin derivative exhibited a pronounced synergistic effect both in the dark and upon irradiation on MDA-MB-231 human breast cancer cells [9].

In later studies, Brunner showed that the nature of the non-cleavable ligands bound to platinum strongly affected the anticancer activity of the entire conjugate [10–12].

In addition to protoporphyrins, synthetic porphyrins with pegylated substituents are also used for conjugation with platinum [13]. It is interesting to note that replacement of protoporphyrin with synthetic derivatives did not lead to significant changes in the antiproliferative properties of the conjugates on incubation with MDA-MB-231 cells.

Mao obtained new platinum-phthalocyanine conjugates based on silicon phthalocyanines with axial pyridine ligands for binding to Cisplatin [14]. The steric hindrance which can arise between axial ligands after complexation with Cisplatin prevents the aggregation

of phthalocyanines, ensuring the preservation of photophysical characteristics and photodynamic activity.

In 2014, Springler *et al.* suggested tetrakis-(4-pyridyl)porphyrin containing four pyridyl moieties as a substance for complexation with platinum [15]. A number of porphyrin derivatives with various *cis*- and *trans*-platinum complexes showed significant toxicity to several tumor cell lines under irradiation. Among these, the conjugate with transplatin was found to be the most active. It showed a low level of dark cytotoxicity, while the photoinduced toxicity was in the nanomolar concentration range.

Later, Alberto *et al.* studied the effect of replacing the porphyrin ligand with a chlorin or bacteriochlorin ligand [16]. It was shown that, along with enhanced absorption in the long-wavelength region, the reduction of the porphyrin ligand decreased the hydrolysis rate of the conjugated platinum complex. This, in turn, can lead to a decrease in undesirable side toxicity which is related, among other things, to the rate of formation of platinum aqua complexes [17].

In 2021, Springler's research team obtained a synthetic bacteriochlorin with an absorption maximum in the region of 750 nm containing pyridine moieties for complexation with platinum, as well as fluoro- and chloro-substituted phenyl and sulfonamide groups for increasing resistance of the macrocycle to oxidation [18, 19]. *In vitro* studies of the activity of the resulting bacteriochlorins with platinum on various cell lines showed an increase in cytotoxicity by an order of magnitude, when compared to the metal-free bacteriochlorins.

MATERIALS AND METHODS

The solvents were purified and prepared according to the standard procedures². The following reagents were used in the study: potassium hydroxide (*Sigma-Aldrich*, USA), hydrochloric acid (reagent grade) (*Merck*, Germany), *N*-methyl-*N*-nitrosourea (*Sigma-Aldrich*, USA), sodium periodate (*Acros Organics*, Belgium), osmium tetroxide (*Tokyo Chemical Industry*, Japan), ammonium acetate (*Sigma-Aldrich*, USA), sodium hydrosulfite (*Sigma-Aldrich*, USA), acetic acid (reagent grade) (*ALDOSA*, Russia), potassium carbonate (*Merck*, Germany), hydrazine hydrate (*Sigma-Aldrich*, USA), hydroxylamine hydrochloride (*Sigma-Aldrich*, USA), Cisplatin (*Clearsynth*, India), silver nitrate (*Merck*, Germany), diazabicycloundecene (*Sigma-Aldrich*, USA), isoniazid (*Sigma-Aldrich*, USA), trifluoroacetic acid (*ALDOSA*, Russia), and phenanthroline dione (*Sigma-Aldrich*, USA). Thin layer chromatography (TLC)

² Gordon A.J., Ford R.A. *The Chemist's Companion*. New York: Wiley-Interscience; 1972.

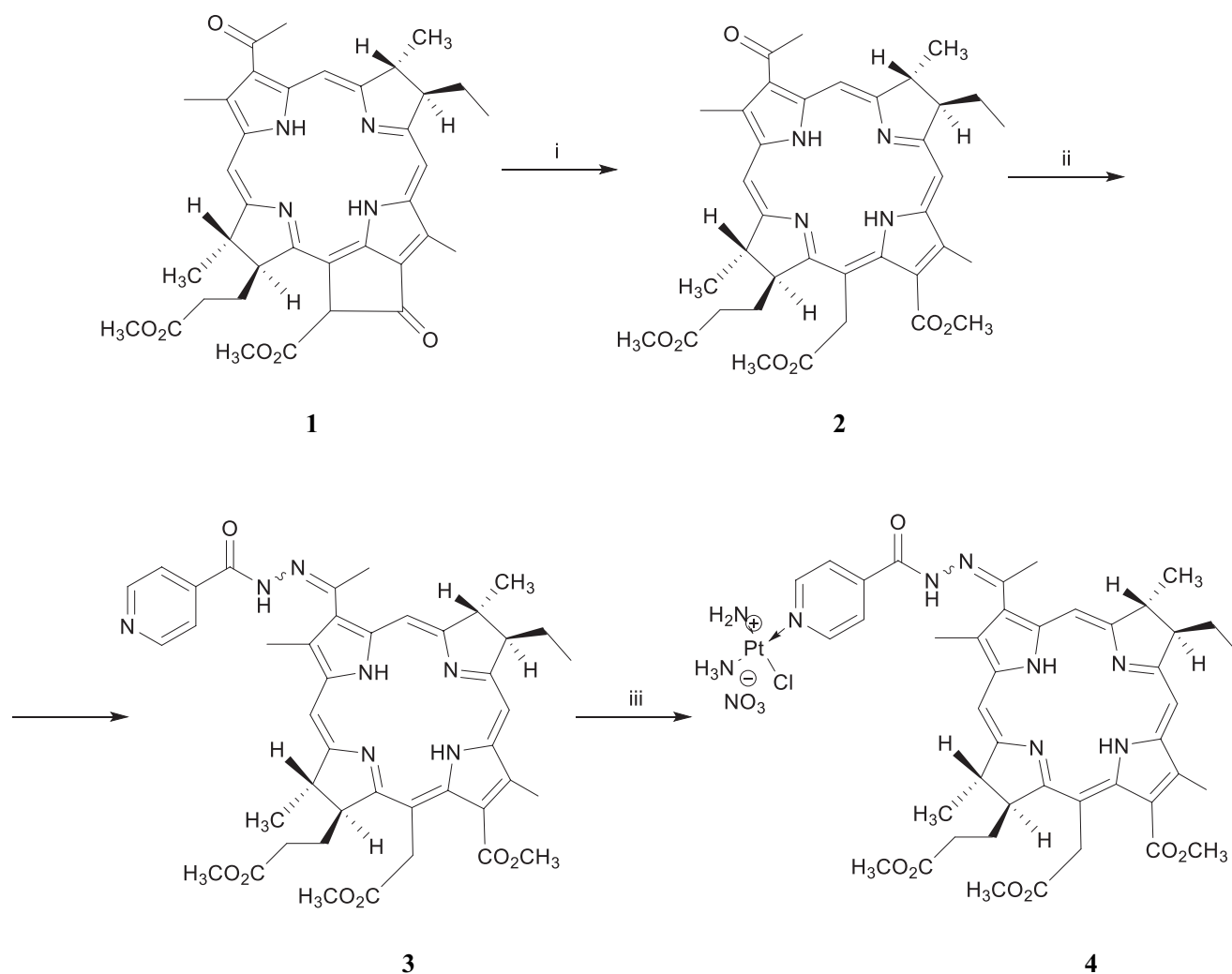
was performed using TLC-Kieselgel 60 F₂₅₄ and TLC Aluminiumoxide 60 F₂₅₄ neutral plates (Merck, Germany). Column chromatography was performed on Silica gel 60 (Merck, Germany). For preparative TLC, Aluminum oxide 60 G neutral (type E) and Silica gel 60 G (Merck, Germany) were used. Chromatography was carried out in the dichloromethane–methanol system in various ratios. Nuclear magnetic resonance (NMR) spectra were recorded in deuteriochloroform on a DPX-300 spectrometer (Bruker, Germany) with an operating frequency of 300 MHz. High-resolution mass spectra were recorded on an Orbitrap Elite mass spectrometer (Thermo Scientific, USA) and on a micrOTOF II instrument (Bruker, Germany) using electrospray ionization (ESI). Electronic absorption spectra were obtained on an Ultrospec 2100 Pro spectrophotometer (GE HealthCare, USA), in 10 mm thick quartz cells. All the spectral studies were performed at 25°C. Sedimentation was carried out on a Hermle Z 206 A centrifuge (Hermle, Germany).

RESULTS AND DISCUSSION

In continuation of the studies described above performed by various research teams, this work obtained pyridine-containing complexes of natural chlorins and their complexes with Pt(II) as prototypes of drugs for combined photodynamic and chemotherapy.

Bacteriopheophorbide (1) obtained from bacteriochlorophyll, which in turn was isolated by the standard method from *Rhodobacter spheroids* bacteria [20], was chosen as the initial compound. It was then converted into bacteriochlorin *e*₆ by nucleophilic opening of the cyclopentanone ring by treatment with a solution of NaOH in acetone at 50°C for 1.5 h.

Bacteriochlorin *e*₆ was converted to its trimethyl ester (2) by treatment with diazomethane (Scheme 1). The chromatographic mobility of the product increased significantly, enabling its chromatographic purification to be performed efficiently. Next, Schiff base (3) was prepared by treatment of compound (2) with isonicotinic



Scheme 1. Preparation of bacteriochlorin *e* derivative with isoniazid and its complex with Pt(II). i: (1) NaOH, H₂O/Acetone; (2) HCl, H₂O/Acetone; (3) CH₂N₂, Et₂O/CH₂Cl₂, 1 h; ii: isonicotinic acid hydrazide, TosOH, *N,N*-dimethylformamide (DMF), Ar, 24 h; iii: Pt(NH₃)₂(H₂O)Cl, DMF, 24 h

acid hydrazide. The reaction was carried out in *N,N*-dimethylformamide (DMF) in an inert environment for 96 h using *p*-toluenesulfonic acid as the catalyst. Chromatography of the product (**3**) showed the presence of two compounds with similar retention coefficients R_f and identical molar masses, suggesting the formation of that *syn*- and *anti*-isomers.

Incorporation of an isonicotinic acid moiety leads to a hypsochromic shift of the main absorption band by 15 nm (Fig. 3).

Next, a platinum complex of isonicotinyl-containing bacteriochlorin (**4**) was obtained by the reaction of compound (**3**) with Cisplatin in 5 : 1 ratio using an equimolar ratio (1 : 1) of silver nitrate to compound (**3**).

Excess of Cisplatin was required, in order to increase the overall yield of the reaction, since platinum can be reduced during activation with silver nitrate. As a result of the reaction, silver chloride precipitated and was separated by centrifugation. The reaction was performed in an argon atmosphere for 48 h.

Analysis of the electronic absorption spectra showed that platinum is coordinated at the periphery of the macrocycle rather than the internal cavity of the latter (Fig. 4).

The structure of the resulting compound was confirmed by mass spectrometry (Fig. 5) where splitting of the molecular ion $[M+H]^+$ 1118.3 Da matching the isotopic composition of platinum atoms was observed.

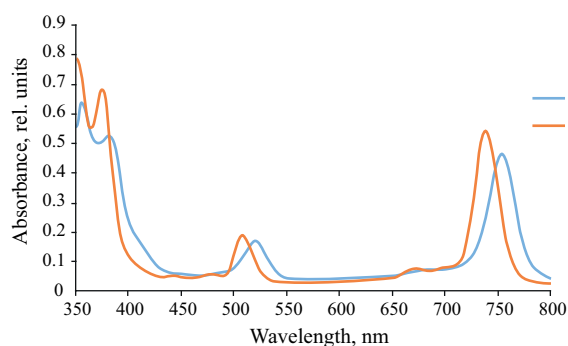


Fig. 3. Absorption spectra of compounds (2) and (3)

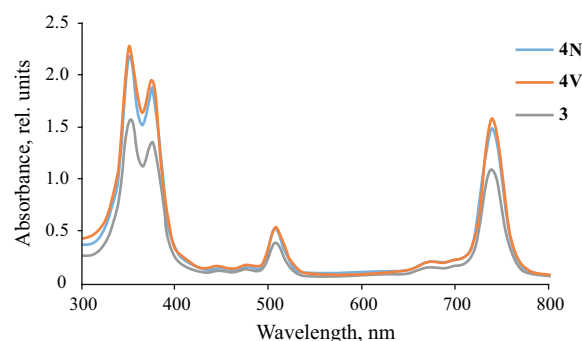


Fig. 4. Absorption spectra of compounds (3) and (4)

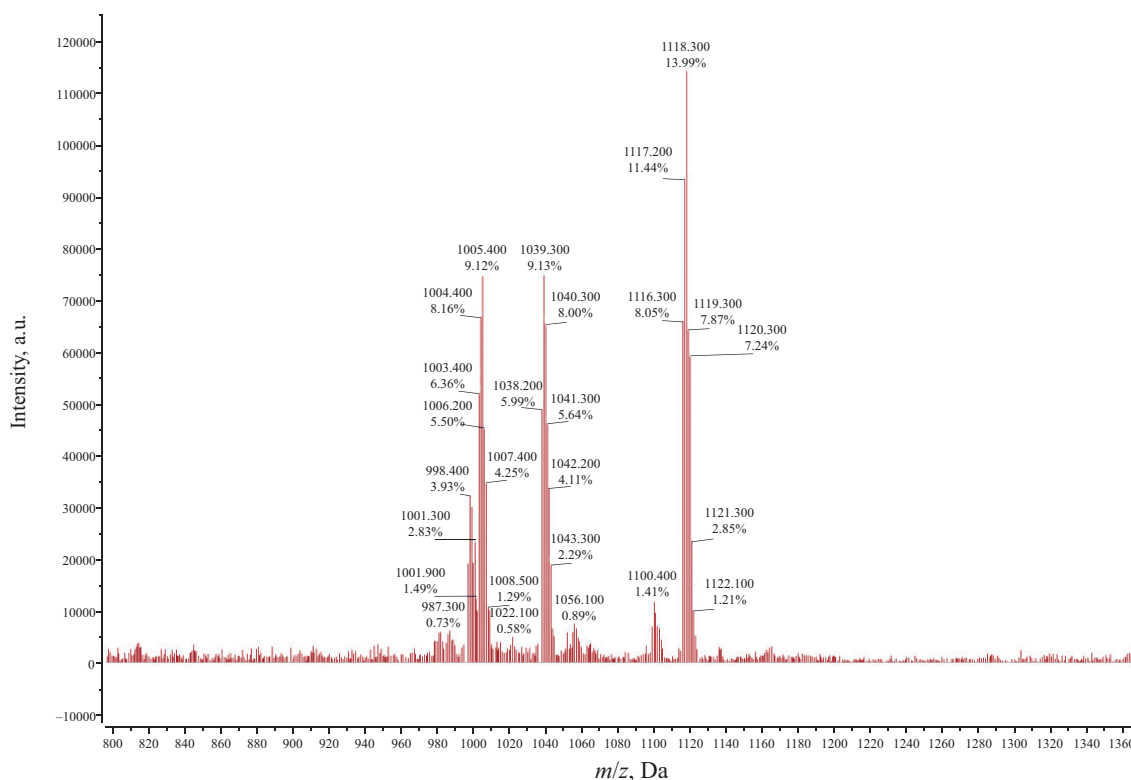
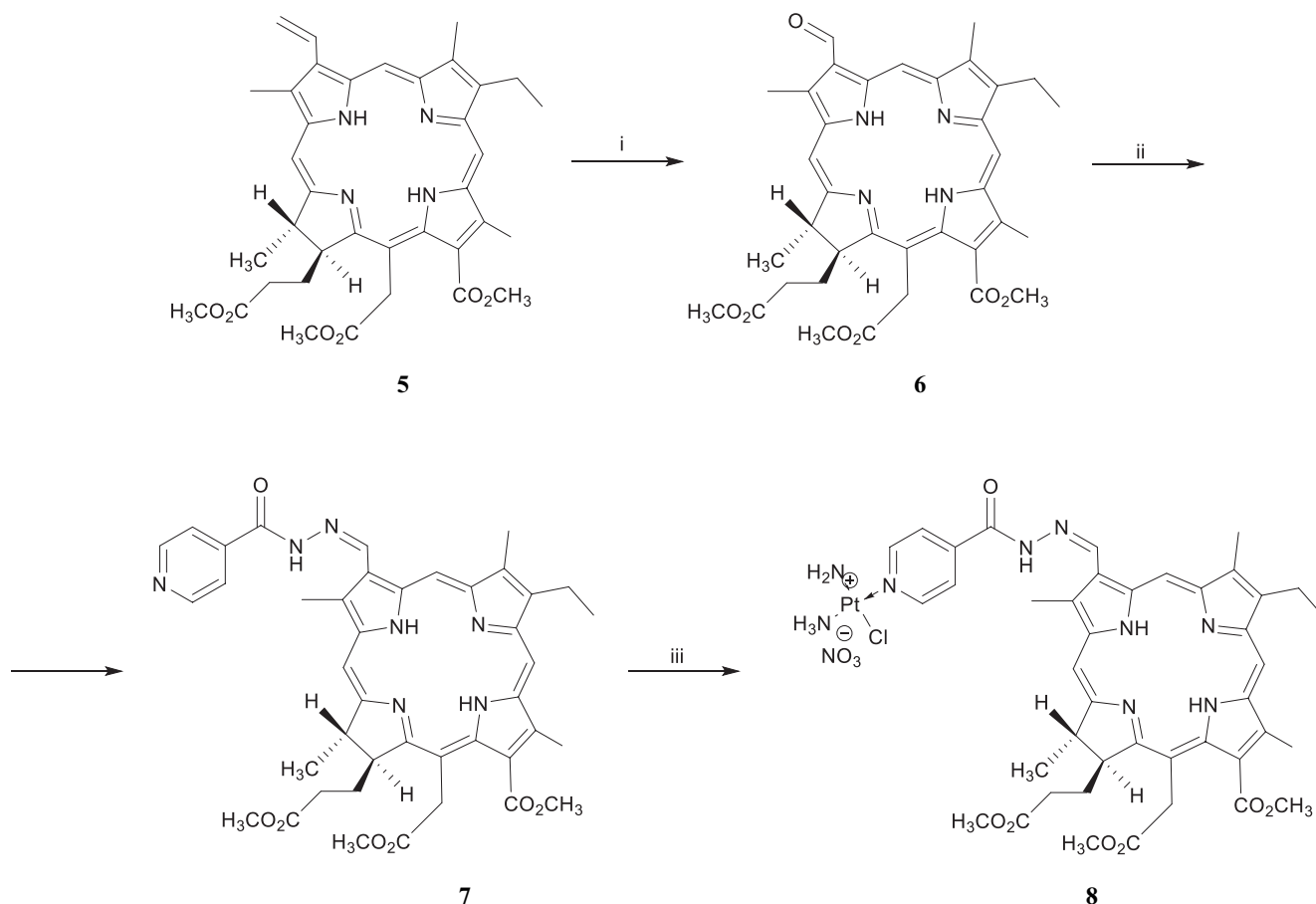


Fig. 5. Mass spectrum of compound (4)

In a similar way, we obtained a monopyridyl platinum complex of natural chlorin (Scheme 2). The starting compound was formylchlorin e_6 (**6**) obtained by the Lemieux–Johnson reaction from trimethyl ester of chlorin e_6 (**5**) using OsO_4 and NaIO_4 [21]. This method was used due to the presence of a vinyl group in pyrrole A, and mild oxidation reaction conditions

which do not affect the chlorin macrocycle. The platinum complex of the monopyridyl derivative of chlorin e_6 was prepared according to a scheme involving the preparation of enimine (**7**) followed by metalation with dichlorodiaminoplatinum.

The resulting metal complex (**8**) was characterized using chromatography-mass spectrometry (Fig. 6). Here



Scheme 2. Preparation of a chlorin e_6 derivative with isoniazide and its complex with Pt(II). i: NaIO_4 , OsO_4 , tetrahydrofuran (THF), 1 h; ii: isonicotinic acid hydrazide, TosOH, DMF, Ar, 24 h; iii: $\text{Pt}(\text{NH}_3)_2(\text{H}_2\text{O})\text{Cl}$, DMF, 24 h

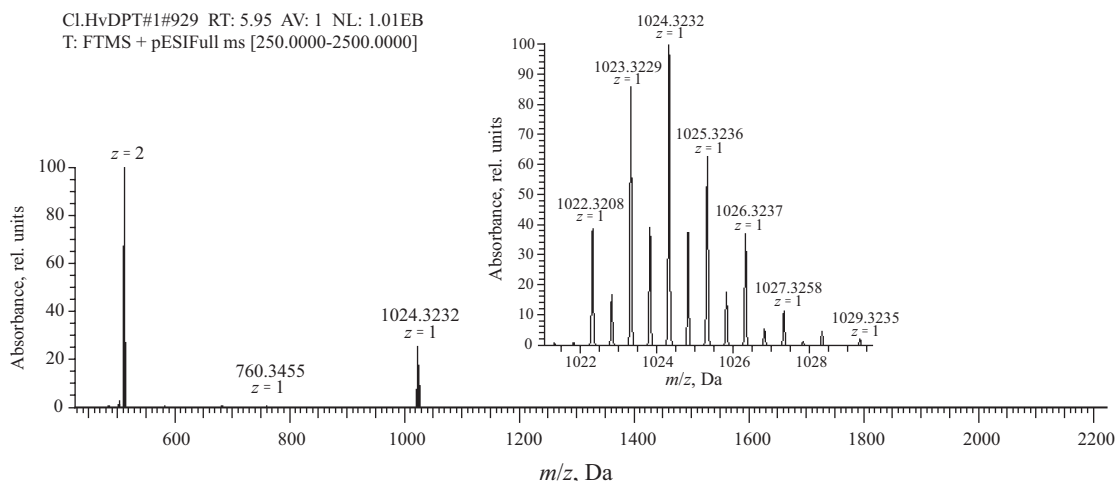


Fig. 6. Chromato-mass spectrum of compound (**8**)

a molecular ion peak $M^+ = 1024.3232$ Da with isotopic splitting characteristic of platinum compounds was observed.

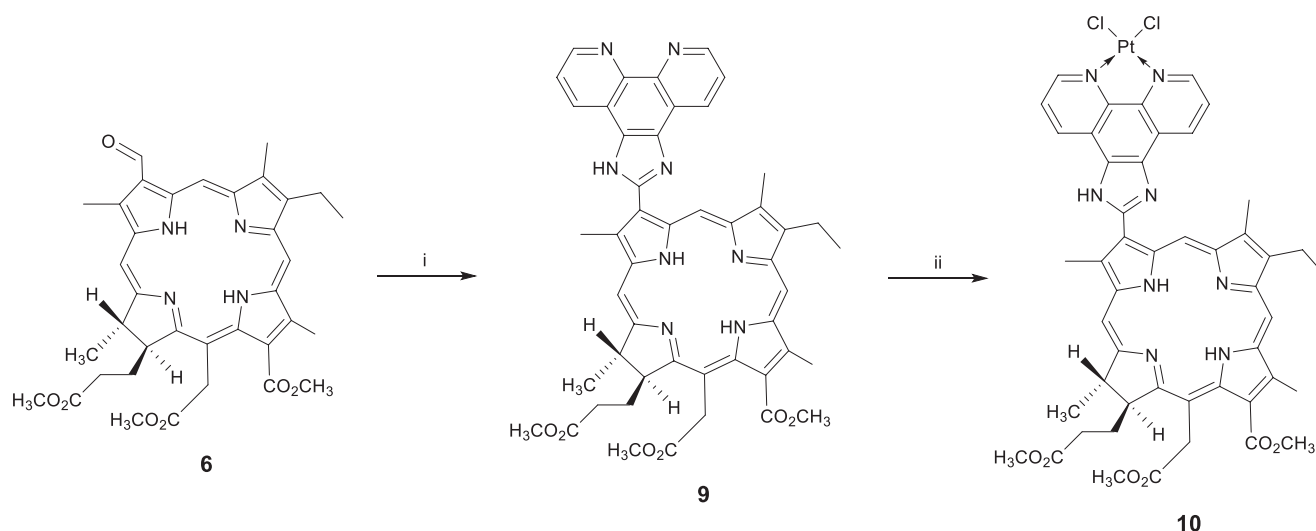
In the next experiment, a phenanthroline residue was introduced into the chlorin macrocycle as a chelating moiety. The Debus–Radziszewski condensation of formylchlorin e_6 (**6**) with phenanthroline was used to this end, resulting in the phenanthroline imidazole derivative of chlorin (**9**) [22–25]. The reaction was carried out in the presence of ammonium acetate in a chloroform-acetic acid mixture under reflux for 24 h (Scheme 3).

Incorporation of an electron-acceptor substituent into pyrrole A leads to a bathochromic shift of the long-wave absorption band of chlorin by 21 nm relative to the

methyl ester of pheophorbide a and by 24 nm relative to the trimethyl ester of chlorin e_6 (**5**) (Fig. 7).

Logical continuation for modifying the conjugate of chlorin with a phenanthroline-imidazole moiety is to incorporate a Pt atom on the periphery of the macrocycle by the reaction of the pigment with potassium tetrachloroplatinate refluxing in DMF for 18 h. The resulting metal complex (**10**) can be considered as a prototype of an antitumor drug with combined photodynamic and chemotherapeutic effects.

The binding of nitrogen atoms in the phenanthroline ring to the platinum cation caused a hypsochromic shift in the long-wavelength absorption band of the pigment (Fig. 8).



Scheme 3. Preparation of a chlorin e_6 derivative with phenanthroline and its complex with Pt(II). i: phenanthroline, $CHCl_3/AcOH$, NH_4OAc , reflux, 12 h; ii: $K_2[PtCl_4]$, DMF/H_2O , Ar, 18 h

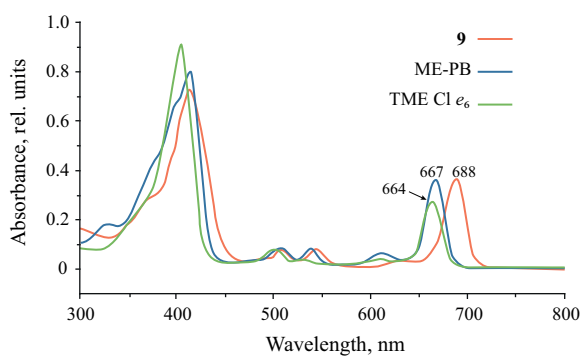


Fig. 7. Electronic absorption spectrum of compound (**9**). ME-PB—methyl ester of pheophorbide a , TME CL—trimethyl ester of chlorin e_6

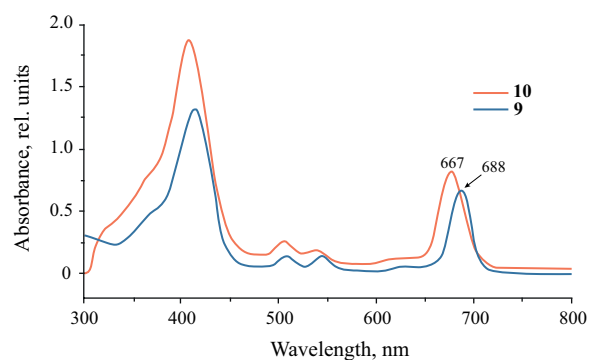


Fig. 8. Electronic absorption spectra of compounds (**9**) and (**10**)

The mass spectrum of compound **(10)** exhibited a molecular ion peak $[M+H]^+ = 1097.260$ Da and an accompanying isotope splitting characteristic of platinum compounds (Fig. 9).

Terpyridine was the next pyridine-containing chelating moiety used for complexation with platinum. Bacteriochlorin *N*-aminocycloimide methyl ester (**11**) [26] was the starting compound. It was reacted with bromotolyl terpyridine in tetrahydrofuran in the presence of diisopropylethylamine (Scheme 4). The

substitution reaction occurs at the exocyclic primary amino group of the pigment, enabling the formation of mono- and disubstituted amines. In order to obtain the monosubstituted product (**12**), a molar ratio of reagents of 1 : 1 and dilution of the reaction mixture were used. A 2–3-fold excess of the alkylating agent was used [27] in order to obtain the disubstituted product.

Product (**12**) was purified using preparative TLC on neutral alumina since due to high polarity, the target pigments are “stretched” on the silica gel plate.

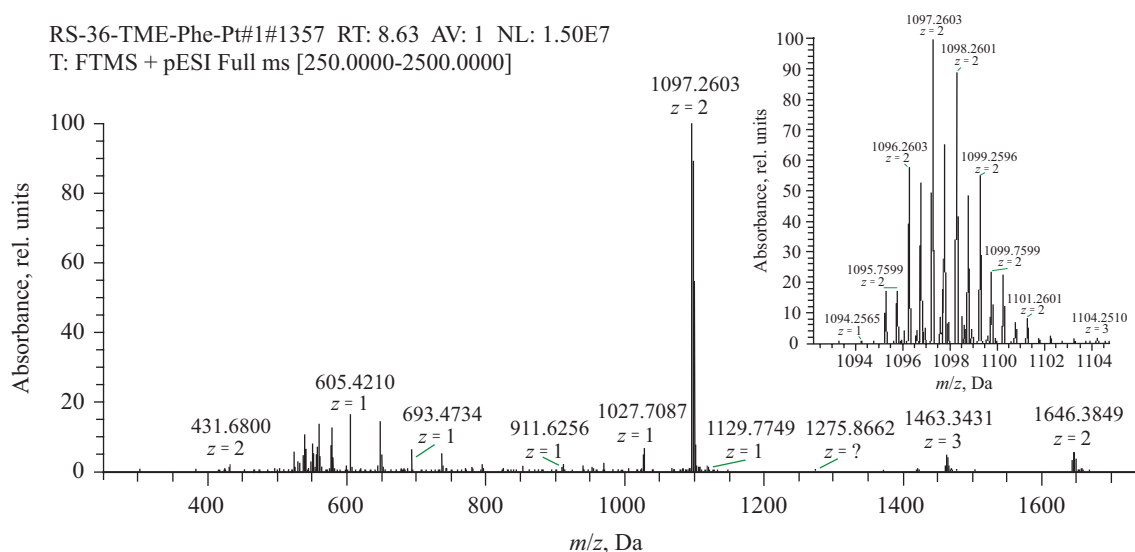
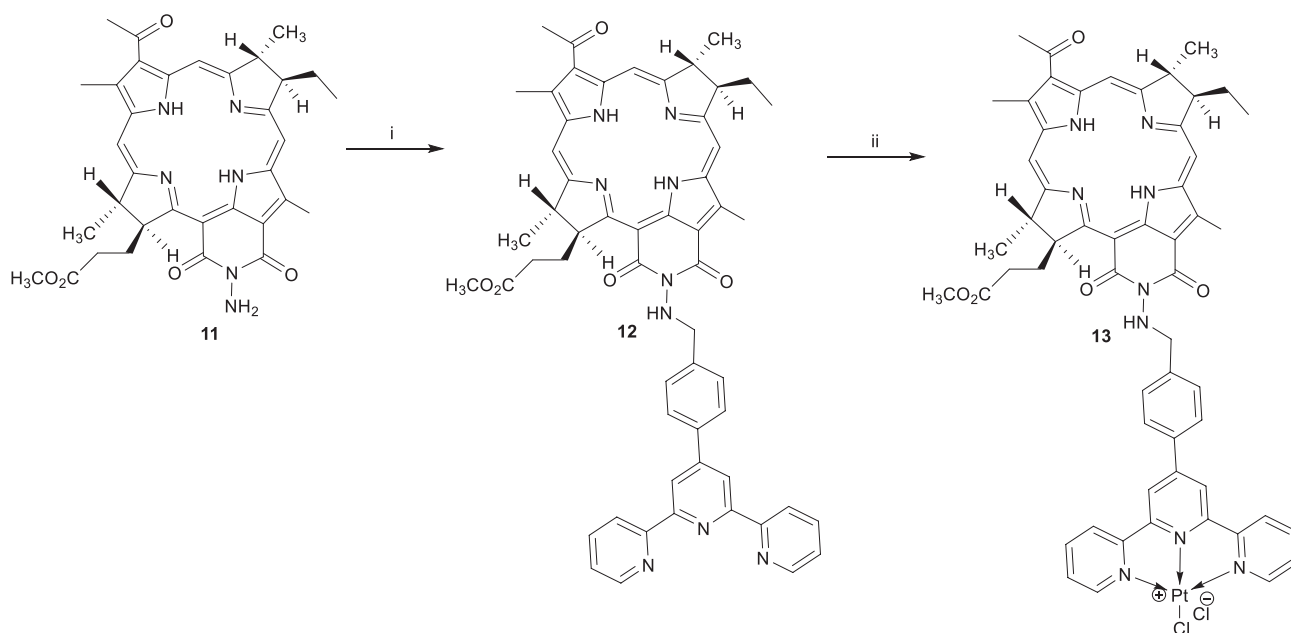


Fig. 9. Electrospray ionization Fourier transform mass spectrum of compound **(10)**



Scheme 4. Preparation of the *N*- NH_2 -bacteriopurpurinimide derivative with terpyridine and its complex with Pt(II).
i: 4-(4-bromomethylphenyl)-2,2':6',2''-terpyridine, THF, reflux, 8 h; ii: $K_2[PtCl_4]$, DMF/ H_2O , Ar, 75°C, 4 h

In the case of monosubstituted bacteriochlorin, a hypsochromic shift is observed in the electronic absorption spectrum from 834 to 828 nm with respect to the parent compound (**11**). The ^1H NMR spectra of both compounds contain characteristic signals of the protons in the pyridine rings of the tolyl terpyridine moiety in the region of 8 ppm.

The metallation of terpyridine-containing bacteriochlorin was carried out using potassium tetrachloroplatinate in DMF in the presence of a small amount of water. The progress of the reaction was monitored using analytical TLC on alumina, since the chromatographic mobility of the resulting metal complex decreases abruptly.

The electrospray ionization + high-resolution mass spectrometry (ESI-HRMS) showed a molecular ion peak with isotopic splitting characteristic of platinum compounds (Fig. 10).

Another way of incorporating a terpyridine moiety into a bacteriochlorin molecule involves the use of *N*-hydroxybacteriopurpurinimide oxime (**14**) synthesized previously in the Preobrazhensky laboratory of the Department of Chemistry and Technology of Biologically Active Compounds at the Lomonosov Institute of Fine Chemical Technologies (Scheme 5) [28]. The presence of two reaction centers in the molecule of the latter results in an ambiguous reaction. Due to enhanced acidity, the substitution reaction at the OH group of the exocycle occurs more readily (**15**), while replacement of the OH

group of the oxime requires refluxing for 15 h to give the disubstituted reaction product (**16**) in 38% yield. The structure of the resulting compounds was reliably confirmed by a combination of physicochemical analytical methods.

Since the formation of the metal complex of compound (**16**) is difficult due to the steric properties of the molecule, mono-Pt-containing photosensitizer (**17**) was obtained by the method reported for the synthesis of compound (**13**) involving the use of potassium tetrachloroplatinate in DMF and heating.

The resulting complex (**17**) was characterized by electrospray ionization mass spectrometry (ESI-MS) where a molecular ion peak with isotopic splitting characteristic of platinum compounds was observed.

Thus, as a result of the work described above, pyridine-containing chelator groups such as residues of isonicotinic acid, phenanthroline, and terpyridine, which show affinity to the platinum atom and form stable complexes with it, were incorporated into the structure of natural chlorins. On the one hand, the resulting metal complexes can exhibit photodynamic activity on irradiation into the absorption band of the chlorin used. On the other hand, platinum complexes have a cytotoxic effect, alkylating DNA and exerting an antiproliferative effect. After conducting biological tests and confirming the synergistic effect, the metal complexes obtained can be considered as binary photosensitizers for photodynamic and chemotherapy in oncology.

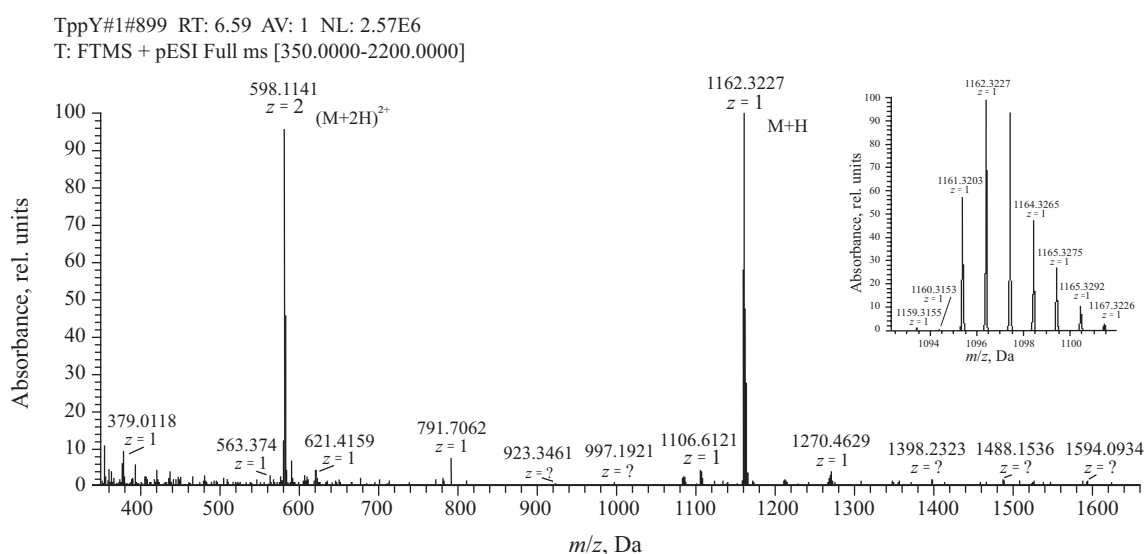
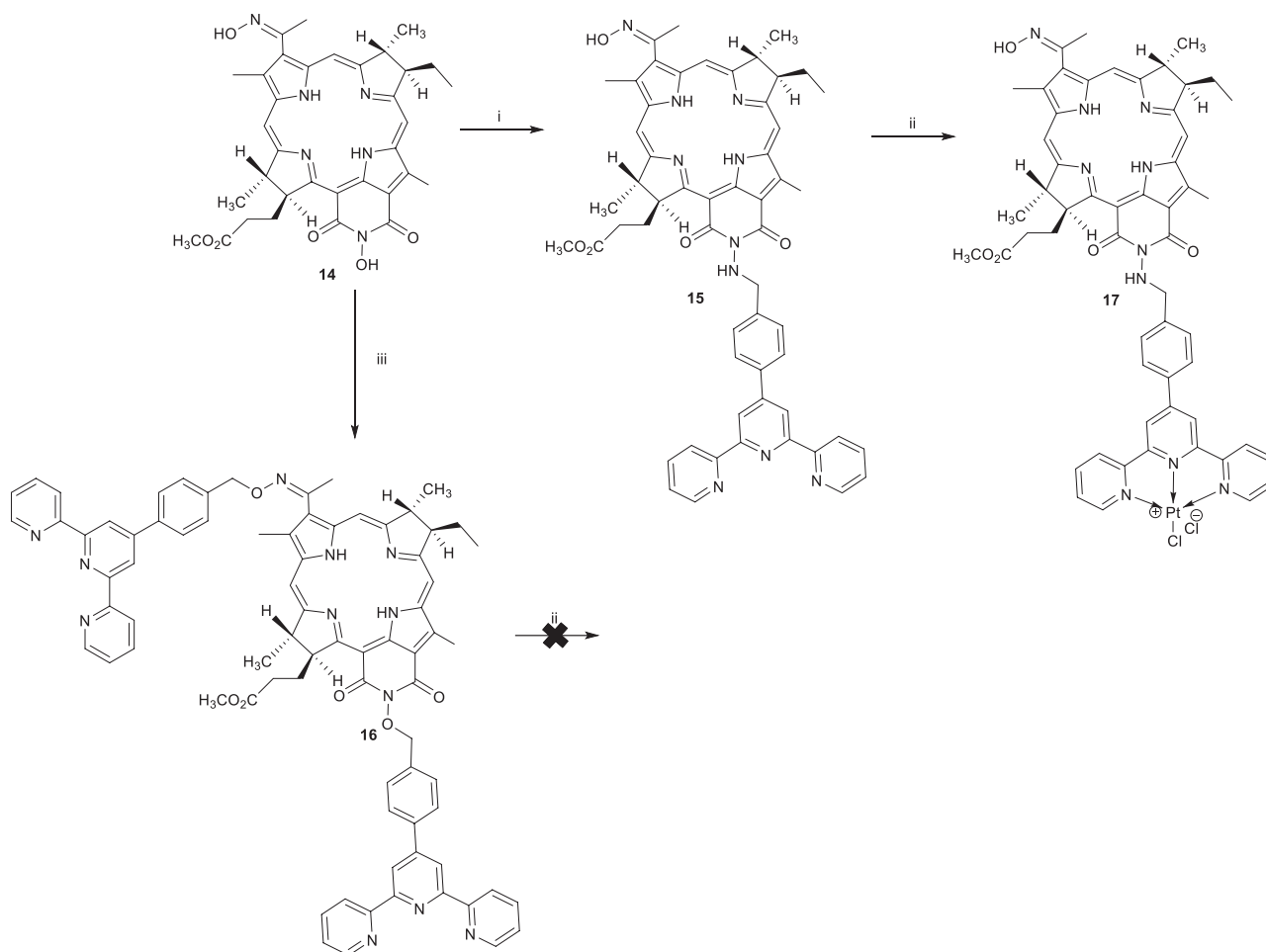


Fig. 10. ESI-HRMS spectrum of compound (**13**)



Scheme 5. Preparation of *N*-OH-bacteriopheophorbtyl derivatives with terpyridine and its complex with Pt(II).

i: 4'-(4-bromomethylphenyl)-2,2':6',2''-terpyridine, diazabicycloundecene (DBU), CHCl_3 , 1 h; ii: $\text{K}_2[\text{PtCl}_4]$, DMF/ H_2O , Ar, 75°C , 4 h; iii: 4'-(4-bromomethylphenyl)-2,2':6',2''-terpyridine (2eq), DBU, CHCl_3 , 15 h

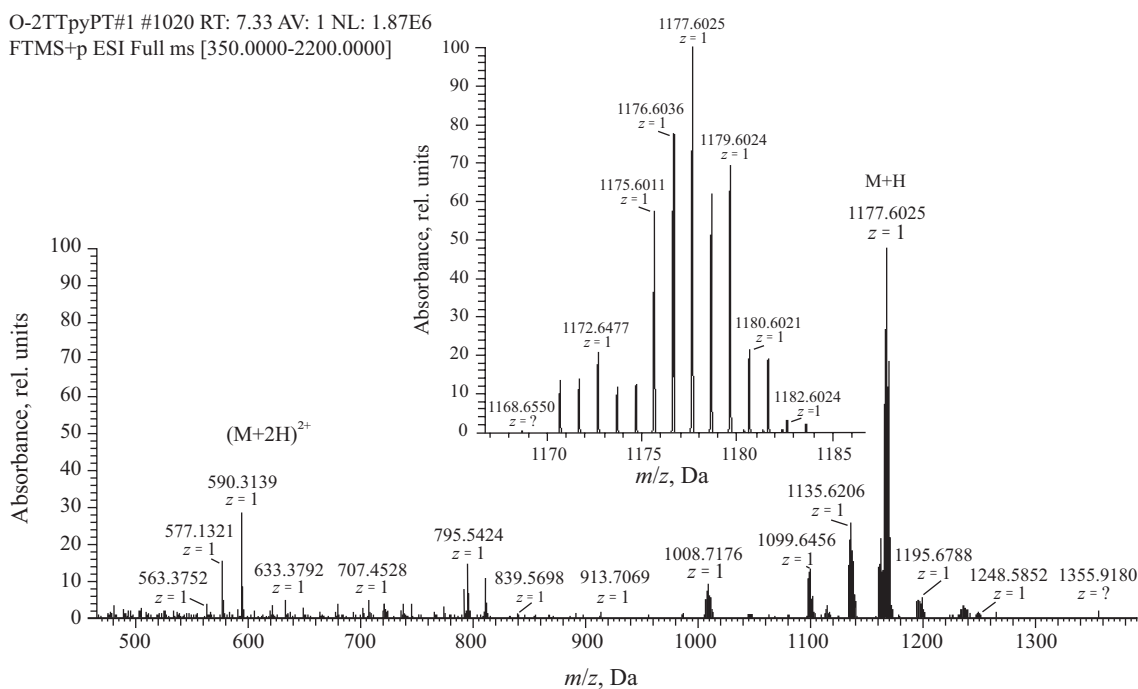


Fig. 11. ESI-MS spectrum of compound (17)

EXPERIMENTAL

Bacteriochlorin trimethyl ester e_6 (2).

Bacteriopheophorbide *a* (1) (250 mg, 0.409 mmol) was dissolved in 28 mL of degassed acetone. The reaction mixture was degassed for 10 min in an ultrasonic bath, then argon was bubbled through it for 5 min with stirring. A degassed aqueous solution (28 mL) of potassium hydroxide (3.64 g, 0.065 mol) was added to the reaction mixture. Then the reaction mixture was heated in a water bath for 1.5 h at 51°C. The reaction progress was monitored by TLC on silica gel in the CH_2Cl_2 :MeOH (5 : 1) solvent system. Next, the reaction mixture was diluted with water and adjusted to pH 4.5 with hydrochloric acid. The precipitate formed was separated, an aqueous solution of hydrochloric acid with pH 4.6 was added, and the suspension was then centrifuged for 10 min (6000 rpm). The supernatant was removed and the procedure was repeated two more times. Then, 15 mL of a solution of freshly prepared diazomethane in diethyl ether was added. The reaction mixture was stirred for 1 h at room temperature (25°C). The reaction progress was monitored by TLC in the dichloromethane/methanol (50 : 1) system to give 160 mg (80%) of compound 2.

$^1\text{H NMR}$ (CDCl_3 , δ , ppm): 9.29 (s, 5-H), 8.69 (s, 10-H), 8.63 (s, 20-H), 5.20 (s, 15- CH_2^a), 5.16 (s, 15- CH_2^b), 4.38–4.15 (m, 7-H, 18-H, 17-H, 13- COOCH_3), 3.76 (m, 15- COOCH_3), 3.67 (m, 8-H), 3.65 (s, 17- COOCH_3), 3.61 (s, 2-Me), 3.37 (s, 12-Me), 3.21 (s, 3²-Me), 2.38–1.92 (m, 17¹- CH_2 , 8²- CH_2 , 17²- CH_2), 1.86 (d, $J = 7.2$ Hz, 7-Me), 1.67 (d, $J = 7.1$ Hz, 18-Me), 1.10 (t, $J = 7.3$ Hz, 8³-Me), –1.12 (s, NH), –1.20 (s, NH).

Mass spectrum, m/z : $[\text{M}+\text{H}]^+$; calculated for $\text{C}_{37}\text{H}_{44}\text{N}_4\text{O}_7 + \text{H}$: 656.32; obtained: 657.3.

Conjugate of bacteriochlorin with isonicotinic acid (3).

Bacteriochlorin e_6 trimethyl ester (2) (62.4 mg, 0.095 mmol), isonicotinic acid hydrazide (65.15 mg, 0.475 mmol), and $\text{TosOH}\cdot\text{H}_2\text{O}$ (18.07 mg, 0.095 mmol) were dissolved in 2 mL of DMF, after which argon was bubbled through the solution for 15 min. The reaction mixture was stirred for 24 h at room temperature. The reaction progress was monitored by TLC on silica gel in the CH_2Cl_2 :MeOH (100 : 1) solvent system. The product was purified using preparative TLC on neutral alumina in the dichloromethane/methanol solvent system (80 : 1) to give 49.6 mg (79.5%) of compound 3.

$^1\text{H NMR}$ (CDCl_3 , δ , ppm): 9.43 (s, 5-H), 8.77–8.66 (m, N-CH-Nic), 8.37 (d, 20-H), 8.23 (m, CH-Nic), 8.01 (s, NH-Nic), 5.40–5.05 (m, 15¹- CH_2), 4.40–4.27 (m, 7-H, 17-H, 18-H), 4.24 (s, 13- COOCH_3), 3.78 (s, 15- COOCH_3), 3.71–3.67 (m, 8-H), 3.66 (s, 17- COOCH_3), 3.40 (s, 2-Me), 3.36 (s, 12-Me), 3.00 (s, 3²-Me), 2.46–1.97 (m, 8²- CH_2 , 17¹- CH_2 , 17²- CH_2), 1.84 (d, 18-Me), 1.71 (d, 7-Me), 1.06 (t, 8³-Me), (–1.61)–(–1.31) (m, NH).

Mass spectrum, m/z : $[\text{M}+\text{H}]^+$ calculated for $\text{C}_{43}\text{H}_{49}\text{N}_7\text{O}_7 + \text{H}$: 775.37; obtained: 776.3.

Bacteriochlorin platinum complex (4). Silver nitrate (2.82 mg, 0.017 mmol) and Cisplatin (5 mg, 0.011 mol) were suspended in 1.5 mL of DMF in an inert environment without access of light, after which the mixture was stirred for 12 h at room temperature. The suspension was then centrifuged for 5 min (10000 rpm), after which the supernatant was added to compound 7 (5 mg, 0.007 mmol). The solution was stirred for 12 h at room temperature in an argon atmosphere without access of light. The reaction progress was monitored by TLC in the dichloromethane/methanol solvent system (10 : 1). After reaction completion, the reaction mixture was concentrated in the vacuum of an oil pump to give 4.98 mg (99.6%) of compound 4.

Mass spectrum, m/z : $[\text{M}+\text{H}]^+$ calculated for $\text{C}_{43}\text{H}_{49}\text{N}_7\text{O}_7\text{PtClNO}_3(\text{NH}_2)_2 + \text{H}$: 1118.292; obtained: 1118.3.

3-Formylchlorin e_6 trimethyl ester (6). Chlorin e_6 trimethyl ester (5) (498 mg, 0.780 mmol) was dissolved in 20 mL of THF, then a solution of NaIO_4 (670 mg, 3.133 mmol) in 5 mL of H_2O and 300 μL of OsO_4 solution (2.75 g, 0.039 mmol) in 90 mL of dichloromethane were added. The reaction was carried out using stirring in an argon atmosphere and cooling to 0°C for 3 h. The progress of the reaction was monitored by TLC in a hexane/ethyl acetate (1 : 1) system. A saturated solution of NaHSO_3 in 10 mL of methanol was then added to the reaction mixture that was stirred for another 15 min. The reaction mixture was extracted with dichloromethane (1 \times 30 mL). The resulting extract was washed with water (3 \times 100 mL), dried with anhydrous Na_2SO_4 and concentrated under reduced pressure. The product was isolated using column chromatography in a hexane/ethyl acetate system (2 : 1) and crystallized from dichloromethane on a watch glass to give 206 mg (41.0%) of compound 6 as purple crystals.

$^1\text{H NMR}$ (CDCl_3 , δ , ppm): 1.66–1.79 (m, 6H, 8²- CH_3 , 18³- CH_3), 2.12–2.30 (m, 2H, 17²- CH_2), 2.50–2.66 (m, 1H, 17¹- CH_2), 3.33 (s, 3H, 7¹- CH_3), 3.57 (s, 3H, 2¹- CH_3), 3.59 (q, $J = 7.2$ Hz, 2H, 8¹- CH_2), 3.64 (s, 3H, 12¹- CH_3), 3.80 (s, 3H, 15³- CH_3), 3.83 (s, 3H, 17⁴- CH_3), 4.27 (s, 3H, 13²- CH_3), 4.39–4.52 (m, 2H, 17-H, 18-H), 5.25 (d, $J = 18.8$ Hz, 1H, 15¹- CH_2), 5.38 (d, $J = 18.8$ Hz, 1H, 15¹- CH_2), 8.94 (s, 1H, 20-H), 9.67 (s, 1H, 5-H), 10.27 (s, 1H, 10-H), 11.55 (s, 1H, 3¹-CH).

Mass spectrum, m/z : $[\text{M}]^+$ calculated for $\text{C}_{36}\text{H}_{40}\text{N}_4\text{O}_7^+$: 640.290, obtained: 640.909 $[\text{M}]^+$.

Ultraviolet and visible (UV/VIS) radiation (CH_2Cl_2), maximum wavelengths λ_{max} , nm ($\log \epsilon$): 416 (4.24), 512 (3.28), 547 (3.36), 634 (3.06), 691 (3.98).

Chlorin conjugate with isonicotinic acid (7). Formyl derivative of chlorin e_6 (**6**) (62.4 mg, 0.095 mmol), isonicotinic acid hydrazide (65.15 mg, 0.475 mmol), and diazabicycloundecene (18.07 mg, 0.095 mmol) were dissolved in 3 mL of DMF, after which argon was bubbled for 10 min through the solution. The reaction mixture was stirred for 36 h at room temperature. The reaction progress was monitored by TLC on silica gel in the dichloromethane/methanol (100 : 1) solvent system. The product was isolated using preparative TLC on neutral alumina in the CH_2Cl_2 : MeOH (80 : 1) solvent system to give 52.7 mg (81.3%) of compound **7**.

^1H NMR (CDCl_3 , δ , ppm): 9.43 (s, 5-H), 8.77–8.66 (m, N-CH-Nic), 8.37 (d, 20-H), 8.23 (m, CH-Nic), 8.01 (s, NH-Nic), 5.40–5.05 (m, 15^1-CH_2), 4.40–4.27 (m, 7-H, 17-H, 18-H), 4.24 (s, 13-COOCH₃), 3.78 (s, 15-COOCH₃), 3.71–3.67 (m, 8-H), 3.66 (s, 17-COOCH₃), 3.40 (s, 2-Me), 3.36 (s, 12-Me), 3.00 (s, 3²-Me), 2.46–1.97 (m, 8^2-CH_2 , 17^1-CH_2 , 17^2-CH_2), 1.84 (d, 18-Me), 1.71 (d, 7-Me), 1.06 (t, 8^3-Me), (–1.61)–(–1.31) (m, NH).

Mass spectrum, m/z : $[\text{M}+\text{H}]^+$ calculated for $\text{C}_{42}\text{H}_{44}\text{N}_7\text{O}_7 + \text{H}$: 759.421; obtained: 760.5.

Platinum complex of monopyridyl chlorin derivative (8). Silver nitrate (2.82 mg, 0.017 mmol) and Cisplatin (5 mg, 0.011 mol) were suspended in 1 mL of DMF in an inert environment without access of light, after which the mixture was stirred for 12 h at room temperature. The suspension was then centrifuged for 5 min (10000 rpm), after which the supernatant was added to compound **7** (5 mg, 0.007 mmol). The solution was stirred in an argon atmosphere for 12 h at room temperature without access of light. The reaction progress was monitored by TLC in the dichloromethane/methanol (10 : 1) solvent system. After completion of the reaction, the reaction mixture was concentrated in the vacuum of an oil pump to give 5.54 mg (99.7%) of compound **8**.

Mass spectrum, m/z : $[\text{M}+\text{H}]^+$ calculated for $\text{C}_{42}\text{H}_{44}\text{N}_7\text{O}_7\text{PtClNO}_3(\text{NH}_2)_2 + \text{H}$: 1204.3243; obtained: 1204.3232.

3-(Phenanthrolineimidazol-2-yl) chlorin e_6 trimethyl ester (9). To a solution of compound **6** (25 mg, 0.039 mmol) in a mixture of $\text{CHCl}_3/\text{AcOH}$ (5%), phenanthroline (16.4 mg, 0.078 mmol) and NH_4OAc (60.2 mg, 0.781 mmol) were added in two portions with an interval of 7 h under reflux conditions. The progress of the reaction was monitored by TLC in the hexane/ethyl acetate system (1 : 1). At the end of the reaction, the mixture was washed with saturated NaCl solution, dried with anhydrous Na_2SO_4 , and concentrated under reduced pressure. The product was isolated using preparative TLC in the dichloromethane/methanol (50 : 1) system and

crystallized from dichloromethane on a watch glass to give 24.8 mg (77%) of compound **9**.

^1H NMR spectrum (CDCl_3 , δ , ppm): 2.18 (s, 1H, NH), 1.39 (t, $J = 7.6$ Hz, 3H, 8^2-CH_3), 1.94 (d, $J = 7.2$ Hz, 3H, 18^3-CH_3), 2.72–3.02 (m, 4H, 17^1-CH_2 , 17^2-CH_2), 3.22 (s, 3H, 7^1-CH_3), 3.44 (s, 3H, 2^1-CH_3), 3.76 (s, 2H, 17^1-CH_3), 3.95 (s, 3H, 12^1-CH_3), 4.38 (s, 3H, 13^2-CH_3), 4.53 (d, $J = 10.1$ Hz, 1H, 17-H), 4.62 (d, $J = 7.3$ Hz, 1H, 18-H), 5.54–5.31 (m, 2H, 15^1-CH_2), 6.83 (s, 1H, NH), 7.47 (s, 2H, Ph- H^2), 8.09 (s, 2H, Ph- H^1), 8.76 (s, 2H, Ph- H^3), 8.85 (s, 1H, 20-H), 9.09 (s, 1H, 5-H), 10.50 (s, 1H, 10-H).

Mass spectrum, m/z : $[\text{M}]^+$: calculated for $\text{C}_{48}\text{H}_{46}\text{N}_8\text{O}_6^+$: 832.361; obtained: 832.300.

UV/VIS (CH_2Cl_2), λ_{max} , nm ($\epsilon \times 10^{-3}$, $\text{M}^{-1}\cdot\text{cm}^{-1}$): 413 (5.49), 508 (4.50), 543 (4.55), 631 (4.14), 688 (5.19).

High performance liquid chromatography – mass spectrometry (HPLC-MS) (CH_3CN), retention time t_{R} , min (m/z): 10.95 (832.3445).

Platinum complex of 3-(phenanthrolineimidazol-2-yl)chlorin trimethyl ester e_6 (10). To compound **9** (32 mg, 0.039 mmol) dissolved in 4 mL of DMF, a solution of $\text{K}_2[\text{PtCl}_4]$ (24 mg, 0.058 mmol) in 1 mL of H_2O was added. The reaction was carried out with stirring for 18 h. The progress of the reaction was monitored by TLC in the dichloromethane/methanol (20 : 1) system. The reaction mixture was extracted with dichloromethane. The resulting extract was washed three times with saturated NaCl solution, dried with anhydrous Na_2SO_4 , and concentrated under reduced pressure. Next, the product was isolated using preparative TLC in the dichloromethane/methanol (20 : 1) system and crystallized from dichloromethane on a watch glass to give 6.4 mg (15%) of compound **10**.

Mass spectrum, m/z : $[\text{M}]^+$: calculated for $\text{C}_{48}\text{H}_{46}\text{N}_8\text{O}_6\text{Cl}_3\text{Pt}^+$: 1097.256; obtained: 1097.260.

HPLC-MS (CH_3CN), t_{R} , min (m/z): 8.63 (1097.2603).

Bacteriochlorin 13,15-(*N*-(4-((2,2':6',2''-terpyridin)-4'-yl)benzyl)amino)cycloimide methyl ester (12). Bacteriochlorin 13,15-(*N*-amino)cycloimide methyl ester (15 mg, 0.025 mmol), *N,N*-diisopropylethylamine (9.6 μL , 0.055 mmol) and 4'-(4-bromomethylphenyl)-2,2':6',2''-terpyridine (11.1 mg, 0.028 mmol) were dissolved in 15 mL of THF and refluxed for 8 h in a stream of argon. The reaction mixture was diluted with 10 mL of chloroform and washed with 50 mL of water. The organic layer was dried with anhydrous Na_2SO_4 and concentrated on a rotary evaporator. The residue was purified using preparative TLC on neutral alumina in a dichloromethane/methanol system (200 : 1) to give 14.4 mg (63%) of compound **12**.

^1H NMR spectrum (CDCl_3 , δ , ppm), terpyridine moiety (TTPy): 9.19 (1H, s, 10-H), 8.79 (1H, s, 5-H), 8.75–8.55 (9H, m, 20-H and TTPy-H), 7.94–7.79 (4H,

TTpy-H), 7.36–7.31 (2H, m, TTpy-H), 5.22 (1H, m, 17-H), 4.56 (2H, s, TTpy-CH₂), 4.27 (1H, m, 18-H), 4.08 (1H, m, 7-H), 3.88 (1H, m, 8-H), 3.71 (3H, s, 12-CH₃), 3.57 (3H, s, 17⁵-CH₃), 3.53 (3H, s, 2-CH₃), 3.17 (3H, s, 3²-CH₃), 2.61 (2H, m, 8¹-CH₂), 2.39 (2H, m, 17²-CH₂), 2.04 (2H, m, 17¹-CH₂), 1.81 (3H, d, *J* = 7 Hz, 7-CH₃), 1.69 (3H, d, *J* = 7.8 Hz, 18-CH₃), 1.11 (3H, t, *J* = 7.4 Hz, 8²-CH₃), –0.34 (1H, br.s, s, NH), –0.56 (1H, br.s, s, NH).

ESI-HRMS, *m/z*: [M+H]⁺: calculated for C₅₆H₅₃N₉O₅ + H: 932.42; obtained: 932.42.

UV/VIS (CH₂Cl₂), λ_{max}, nm (ε × 10^{–3}, M^{–1}·cm^{–1}): 365 (49.2), 417 (42.7), 551(33.4), 828(40.5).

Platinum complex of compound 12 (13).

Compound 12 (3.5 mg, 0.0037 mmol) was dissolved in 2 mL of DMF. K₂[PtCl₄] (1.7 mg, 0.0041 mmol) was dissolved in 0.5 mL of water and added to the DMF solution. The reaction mixture was stirred for 6 h at 75°C. The reaction mixture was diluted with 10 mL of chloroform and washed with 50 mL of water. The organic layer was dried with anhydrous Na₂SO₄ and concentrated on a rotary evaporator to give 0.9 mg (21%) of compound 13.

UV/VIS (CH₂Cl₂), λ_{max}, nm (ε × 10^{–3}, M^{–1}·cm^{–1}): 349 (46.2), 368 (83.7), 418 (42.7), 541(33.4), 799 (40.5).

ESI-HRMS, *m/z*: [M+H]⁺: calculated for C₅₆H₅₃Cl₂N₉O₅Pt + H: 1162.4170; obtained: 1162.4248.

Bacteriochlorin 13,15-(N-(4-((2,2':6',2''-terpyridin]-4'-yl)benzyl)oxy)cycloimide oxime methyl ester (15). Bacteriochlorin 13,15-(N-hydroxy)cycloimide methyl ester 14 [28] (28.9 mg, 0.046 mmol), diazabicycloundecene (13.8 μL, 0.092 mmol), and 4'-(4-bromomethylphenyl)-2,2':6',2''-terpyridine (20.4 mg, 0.042 mmol) were dissolved in 3 mL of chloroform and stirred for 1 h. The reaction mixture was washed with 30 mL of water. The organic layer was dried with anhydrous Na₂SO₄ and concentrated on a rotary evaporator. The residue was purified using preparative TLC on neutral alumina in a dichloromethane/methanol system (200 : 1) to give 29.8 mg (66%) of compound 15.

¹H NMR spectrum (CDCl₃, δ, ppm): 8.80 (1H, s, 5-H), 8.75–8.36 (10H, m, 10-H, 20-H and TTpy-H), 7.99–7.71 (4H, m, *J* = 8 Hz, TTpy-H), 7.43–7.35 (2H, m, TTpy-H), 5.18 (1H, m, 17-H), 4.27–4.22 (2H, m, TTpy-CH₂), 4.19–4.10 (2H, m, 7-H, 18-H), 4.05 (1H, m, 8-H), 3.58 (3H, s, 12-CH₃), 3.50 (3H, s, 17⁵-CH₃), 3.22 (3H, s, 2-CH₃), 2.78 (3H, s, 3²-CH₃), 2.32 (2H, m, 17²-CH₂), 2.22 (2H, m, 8¹-CH₂), 2.02 (2H, m, 17¹-CH₂), 1.95 (3H, d, *J* = 7.3 Hz, 7-CH₃), 1.75 (3H, d, *J* = 7 Hz, 18-CH₃), 1.09 (3H, t, *J* = 7.3 Hz, 8²-CH₃), 0.03 (1H, br.s, s, NH), –0.23 (1H, br.s, s, NH).

UV/VIS (CH₂Cl₂), λ_{max}, nm (ε × 10^{–3}, M^{–1}·cm^{–1}): 349 (46.2), 368 (83.7), 418 (42.7), 541(33.4), 799 (40.5).

ESI-HRMS, *m/z*: [M+H]⁺: calculated for C₅₆H₅₃N₉O₆ + H: 948.41; obtained: 948.40.

Methyl ester of 13,15-(N-(4-((2,2':6',2''-terpyridin]-4'-yl)benzyl)oxy)cycloimide 3-devinyl-3-(((4-((2,2':6',2''-terpyridin]-4'-yl)benzyl)oxy)imino) bacteriochlorin (16). 13,15-(N-Hydroxy)cycloimide bacteriochlorin methyl ester 14 (30 mg, 0.048 mmol), diazabicycloundecene (28.6 μL, 0.191 mmol), and 4'-(4-bromomethylphenyl)-2,2':6',2''-terpyridine (38.6 mg, 0.096 mmol) were dissolved in 3 mL of chloroform and stirred for 15 h under reflux. The reaction mixture was washed with 30 mL of water. The organic layer was dried with anhydrous Na₂SO₄ and concentrated on a rotary evaporator. The residue was purified using preparative TLC on neutral alumina in a dichloromethane/methanol system (200 : 1) to give 23.1 mg (38%) of compound 16.

¹H NMR spectrum (CDCl₃, δ, ppm): 9.15 (1H, s, 10-H), 8.70 (1H, s, 5-H), 8.69–7.53 (27H, m, 20-H and TTpy-H), 5.30 (1H, m, 17-H), 4.92 (2H, m, TTpy-CH₂), 4.23 (2H, m, 7-H, 18-H), 4.10 (1H, m, 8-H), 3.89 (2H, m, TTpy-CH₂'), 3.73 (3H, s, 12-CH₃), 3.65 (3H, s, 17⁵-CH₃), 3.55 (3H, s, 2-CH₃), 3.24 (3H, s, 3²-CH₃), 3.27–2.12 (4H, m, 8¹-CH₂, 17²-CH₂), 1.98 (2H, m, 17¹-CH₂), 1.75 (3H, d, *J* = 7.3 Hz, 7-CH₃), 1.72 (3H, d, *J* = 7.2 Hz, 18-CH₃), 1.08 (3H, t, *J* = 7.4 Hz, 8²-CH₃), –0.26 (1H, br.s, s, NH), –0.64 (1H, br.s, s, NH).

ESI-HRMS, *m/z*: [M+H]⁺: calculated for C₅₆H₅₃N₉O₆ + H: 1268.91; obtained: 1268.92.

Platinum complex compound 15 (17). Compound 15 (15 mg, 0.016 mmol) was dissolved in 2 mL of DMF. K₂[PtCl₄] (9.86 mg, 0.024 mmol) was dissolved in 0.5 mL water and added to the DMF solution. The reaction mixture was stirred for 6 h at 75°C. The reaction mixture was then diluted with 10 mL of chloroform and washed with 50 mL of water. The organic layer was dried with anhydrous Na₂SO₄ and concentrated on a rotary evaporator to give 3.5 mg (18%) of compound 17.

UV/VIS (CH₂Cl₂), λ_{max}, nm (ε × 10^{–3}, M^{–1}·cm^{–1}): 349 (46.2), 368 (83.7), 418 (42.7), 541(33.4), 799 (40.5).

ESI-HRMS, *m/z*: [M+H]⁺: calculated for C₅₆H₅₃Cl₂N₉O₆Pt + H: 1177.63; obtained: 1177.60.

CONCLUSIONS

In this study, a series of platinum complexes of pyridine-containing derivatives of natural chlorins and bacteriochlorins were obtained for potential use in combination therapy in oncology. The structure of all the compounds obtained was reliably confirmed by a combination of physicochemical methods of analysis. The study demonstrated the high chelating ability of pyridine-containing derivatives of natural chlorins. Biological tests of photoinduced and dark cytotoxicity of the leader compounds have been scheduled along with an assessment of the antitumor activity at the organism level.

Acknowledgments

This research work was conducted within the “Radiopharmaceuticals 2024” project implemented under the “Priority 2030” Strategic Academic Leadership Program of the RTU MIREA.

Authors' contributions

N.S. Kirin—data collecting and processing on terpyridine derivatives of natural bacteriochlorins and their metal complexes, phenanthroline-containing natural chlorin and its metal complex, and writing the text of the article.

P.V. Ostroverkhov—data collecting and processing on isonicotinyl-containing derivatives of natural chlorins and bacteriochlorins and their metal complexes.

M.N. Usachev—selection of optimal conditions and chromatographic purification of the compounds obtained.

K.P. Birin—scientific consulting at all stages of the work.

M.A. Grin—concept, idea, and design of research, data collecting and processing.

The authors declare no conflicts of interest.

REFERENCES

- Schirmacher V. From chemotherapy to biological therapy: A review of novel concepts to reduce the side effects of systemic cancer treatment (Rewier). *Int. J. Oncol.* 2019;54(2):407–419. <https://doi.org/10.3892/ijo.2018.4661>
- Sun J., Wei Q., Zhou Y., Wang J., Liu Q., Xu H. A systematic analysis of FDA-approved anticancer drugs. *BMC Syst. Biol.* 2017;11(s5):87. <https://doi.org/10.1186/s12918-017-0464-7>
- Zheng W., Zhao Y., Luo Q., Zhang Y., Wu K., Wang F. Multi-targeted anticancer agents. *Curr. Top. Med. Chem.* 2017;17:3084–3098. <https://doi.org/10.2174/1568026617666170707124126>
- Rosenberg B., Van Camp L., Krigas T. Inhibition of cell division in *Escherichia coli* by electrolysis products from a platinum electrode. *Nature.* 1965;205(4972):698–699. <https://doi.org/10.1038/205698a0>
- Zeng Q., Li X., Xie S., Xing D., Zhang T. Specific disruption of glutathione-defense system with activatable single molecule-assembled nanoprodug for boosted photodynamic/chemotherapy eradication of drug-resistant tumors. *Biomaterials.* 2022;290:121867. <https://doi.org/10.1016/j.biomaterials.2022.121867>
- Tanaka M., Sasaki M., Suzuki T., Nishie H., Kataoka H. Combination of talaporfin photodynamic therapy and Poly (ADP-Ribose) polymerase (PARP) inhibitor in gastric cancer. *Biochem. Biophys. Res. Commun.* 2021;539:1–7. <https://doi.org/10.1016/j.bbrc.2020.12.073>
- Ahn T.G., Jung J.M., Lee E.J., Choi J.H. Effects of cisplatin on photosensitizer-mediated photodynamic therapy in breast tumor-bearing nude mice. *Obstet. Gynecol. Sci.* 2019;62(2):112–119. <https://doi.org/10.5468/ogs.2019.62.2.112>
- Kaplan M.A., Galkin V.N., Romanenko Yu.S., Drozhzhina V.V., Arkhipov L.M. Combination photodynamic therapy sarcomas M-1 in combination with chemotherapy. *Radiation and Risk.* 2016;25(4):90–99. <https://doi.org/10.21870/0131-3878-2016-25-4-90-99>
- Brunner H., Maiterth F., Treitinger B. Synthese und Antitumoraktivität neuer Porphyrin-Platin(II)-Komplexe mit an den Porphyrin-Seitenketten gebundenem cytotostatischen Platin-Rest. *Chemische Berichte.* 1994;127(11):2141–2149. <https://doi.org/10.1002/cber.1491271109>
- Brunner H., Obermeier H., Szeimies R.M. Platin(II)-Komplexe mit Porphyrinliganden: Synthese und Synergismen bei der photodynamischen Tumorthherapie. *Chemische Berichte.* 1995;128(2):173–181. <https://doi.org/10.1002/cber.19951280215>
- Lottner C., Bart K.C., Bernhardt G., Brunner H. Hematoporphyrin-derived soluble porphyrin-platinum conjugates with combined cytotoxic and phototoxic antitumor activity. *J. Med. Chem.* 2002;45(10):2064–2078. <https://doi.org/10.1021/jm0110688>
- Brunner H., Schellerer K.M. New porphyrin platinum conjugates for the cytostatic and photodynamic tumor therapy. *Inorg. Chim. Acta.* 2003;350:39–48. [https://doi.org/10.1016/S0020-1693\(02\)01490-1](https://doi.org/10.1016/S0020-1693(02)01490-1)
- Lottner C., Bart K.C., Bernhardt G., Brunner H. Soluble tetraarylporphyrin-platinum conjugates as cytotoxic and phototoxic antitumor agents. *J. Med. Chem.* 2002;45(10):2079–2089. <https://doi.org/10.1021/jm0110690>
- Mao J., Zhang Y., Zhu J., Zhang C., Guo Z. Molecular combo of photodynamic therapeutic agent silicon(IV) phthalocyanine and anticancer drug cisplatin. *Chem. Commun.* 2009;(8):908–910. <https://doi.org/10.1039/B817968A>
- Naik A., Rubbiani R., Gasser G., Spingler B. Visible-light-induced annihilation of tumor cells with platinum-porphyrin conjugates. *Angew. Chem.* 2014;126(27):7058–7061. <https://doi.org/10.1002/ange.201400533>
- Alberto M.E., Adamo C. Synergistic Effects in Pt^{II}-Porphyrinoid Dyes as Candidates for a Dual-Action Anticancer Therapy: A Theoretical Exploration. *Chemistry. Eur. J.* 2017;23(60):15124–15132. <https://doi.org/10.1002/chem.201702876>
- Abu-Surrah A.S., Kettunen M. Platinum group antitumor chemistry: design and development of new anticancer drugs complementary to cisplatin. *Curr. Med. Chem.* 2006;13(11):1337–1357. <https://doi.org/10.2174/092986706776872970>
- Le N.A., Babu V., Kalt M., *et al.* Photostable platinated bacteriochlorins as potent photodynamic agents. *J. Med. Chem.* 2021;64(10):6792–6801. <https://doi.org/10.1021/acs.jmedchem.1c00052>
- Arnaut L.G., Pereira M.M., Dabrowski M., *et al.* Photodynamic therapy efficacy enhanced by dynamics: the role of charge transfer and photostability in the selection of photosensitizers. *Chemistry. Eur. J.* 2014;20(18):5346–5357. <https://doi.org/10.1002/chem.201304202>
- Grin M., Mironov A., Shtil A. Bacteriochlorophyll *a* and its derivatives: chemistry and perspectives for cancer therapy. *Anti-Cancer Agents Med. Chem.* 2012;8(6):683–697. <http://doi.org/10.2174/187152008785133128>
- Psotka M., Martinkova M., Gonda J. A Lemieux–Johnson oxidation of shikimic acid derivatives: facile entry to small library of protected (2*S*,3*S*,4*R*)-2,3,4,7-tetrahydroxy-6-oxoheptanals. *Chem. Pap.* 2017;71(4):709–719. <https://doi.org/10.1007/s11696-016-0004-8>
- Crossley M.J., McDonald J.A. Fused porphyrin-imidazole systems: new building blocks for synthesis of porphyrin arrays. *J. Chem. Soc. Perkin Trans. 1.* 1999;(17):2429–2431. <https://doi.org/10.1039/A905507J>

23. Hayashi H., Touchy A.S., Kinjo Y., *et al.* Triarylamine-Substituted Imidazole- and Quinoxaline-Fused Push-Pull Porphyrins for Dye-Sensitized Solar Cells. *ChemSusChem*. 2013;6(3):508–517. <https://doi.org/10.1002/cssc.201200869>
24. Lee S.-H., Larsen A.G., Ohkubo K., *et al.* Long-lived long-distance photochemically induced spin-polarized charge separation in β,β' -pyrrolic fused ferrocene-porphyrin-fullerene systems. *Chem. Sci.* 2012;3(1):257–269. <https://doi.org/10.1039/C1SC00614B>
25. Sokhraneva V.A., Yusupova D.A., Boriskin V.S., Groza N.V. Obtaining substituted phenol derivatives with potential antimicrobial activity. *Tonk. Khim. Tekhnol. = Fine Chem. Technol.* 2022;17(3):210–230. <https://doi.org/10.32362/2410-6593-2022-17-3-210-230>
26. Mironov A.F., Grin M.A., Pantushenko I.V., *et al.* Synthesis and Investigation of photophysical and biological properties of novel S-containing bacteriopurpurinimides. *J. Med. Chem.* 2017;60(24):10220–10230. <https://doi.org/10.1021/acs.jmedchem.7b00577>
27. Grin M., Ostroverkhov P., Suvorov N., *et al.* Potential agents for combined photodynamic and chemotherapy in oncology based on Pt(II) complexes and pyridine-containing natural chlorins. *J. Porphyrins Phthalocyanines*. 2023;27(01n04):728–740. <https://doi.org/10.1142/S1088424623500761>
28. Grin M.A., Reshetnikov R.I., Yakubovskaya R.I., *et al.* Novel bacteriochlorophyll-based photosensitizers and their photodynamic activity. *J. Porphyrins Phthalocyanines*. 2014;18(01n02):129–138. <https://doi.org/10.1142/S1088424613501265>

About the authors

Nikita S. Kirin, Postgraduate Student, Senior Lecturer, N.A. Preobrazhensky Department of Chemistry and Technology of Biologically Active Compounds, Medical and Organic Chemistry, M.V. Lomonosov Institute of Fine Chemical Technologies, MIREA – Russian Technological University (86, Vernadskogo pr., Moscow, 119571, Russia). E-mail: n-kirin97@mail.ru. Scopus Author ID 57219094144, ResearcherID AAA-7238-2020, <https://orcid.org/0000-0001-9591-403X>

Petr V. Ostroverkhov, Cand. Sci. (Chem.), Lecturer, N.A. Preobrazhensky Department of Chemistry and Technology of Biologically Active Compounds, Medical and Organic Chemistry, M.V. Lomonosov Institute of Fine Chemical Technologies, MIREA – Russian Technological University (86, Vernadskogo pr., Moscow, 119571, Russia). E-mail: mrp_ost@mail.ru. Scopus Author ID 57194061159, <https://orcid.org/0000-0001-5778-4510>

Maxim N. Usachev, Cand. Sci. (Chem.), Associate Professor, N.A. Preobrazhensky Department of Chemistry and Technology of Biologically Active Compounds, Medical and Organic Chemistry, M.V. Lomonosov Institute of Fine Chemical Technologies, MIREA – Russian Technological University (86, Vernadskogo pr., Moscow, 119571, Russia). E-mail: maximus021989@mail.ru. Scopus Author ID 57387781000, RSCI SPIN-code 8025-8073, <https://orcid.org/0000-0002-8266-6337>

Kirill P. Birin, Dr. Sci. (Chem.), Associate Professor, N.A. Preobrazhensky Department of Chemistry and Technology of Biologically Active Compounds, Medical and Organic Chemistry, M.V. Lomonosov Institute of Fine Chemical Technologies, MIREA – Russian Technological University (86, Vernadskogo pr., Moscow, 119571, Russia); Leading Researcher, Laboratory of New Physico-Chemical Problems, A.N. Frumkin Institute of Physical Chemistry and Electrochemistry, Russian Academy of Sciences (31-4, Leninskii pr., Moscow, 119071, Russia). E-mail: kirill.birin@gmail.com. Scopus Author ID 6508264517, ResearcherID O-4758-2016, RSCI SPIN-code 3279-9050, <https://orcid.org/0000-0001-6951-2440>

Mikhail A. Grin, Dr. Sci. (Chem.), Professor, Head of the N.A. Preobrazhensky Department of Chemistry and Technology of Biologically Active Compounds, Medical and Organic Chemistry, M.V. Lomonosov Institute of Fine Chemical Technologies, MIREA – Russian Technological University (86, Vernadskogo pr., Moscow, 119571, Russia). E-mail: michael_grin@mail.ru. Scopus Author ID 6603356480, RSCI SPIN-code 2212-1579, <https://orcid.org/0000-0002-4333-4516>

Об авторах

Кирин Никита Сергеевич, аспирант, старший преподаватель кафедры химии и технологии биологически активных соединений, медицинской и органической химии им. Н.А. Преображенского, Институт тонких химических технологий им. М.В. Ломоносова, ФГБОУ ВО «МИРЭА – Российский технологический университет» (119571, Россия, Москва, пр-т Вернадского, д. 86). E-mail: n-kirin97@mail.ru. Scopus Author ID 57219094144, ResearcherID AAA-7238-2020, <https://orcid.org/0000-0001-9591-403X>

Островерхов Петр Васильевич, к.х.н., преподаватель кафедры химии и технологии биологически активных соединений, медицинской и органической химии им. Н.А. Преображенского, Институт тонких химических технологий им. М.В. Ломоносова, ФГБОУ ВО «МИРЭА – Российский технологический университет» (119571, Россия, Москва, пр-т Вернадского, д. 86). E-mail: mpr_ost@mail.ru. Scopus Author ID 57194061159, <https://orcid.org/0000-0001-5778-4510>

Усачев Максим Николаевич, к.х.н., доцент кафедры химии и технологии биологически активных соединений, медицинской и органической химии им. Н.А. Преображенского, Институт тонких химических технологий им. М.В. Ломоносова, ФГБОУ ВО «МИРЭА – Российский технологический университет» (119571, Россия, Москва, пр-т Вернадского, д. 86). E-mail: maximus021989@mail.ru. Scopus Author ID 57387781000, SPIN-код РИНЦ 8025-8073, <https://orcid.org/0000-0002-8266-6337>

Бирин Кирилл Петрович, д.х.н., доцент кафедры химии и технологии биологически активных соединений, медицинской и органической химии им. Н.А. Преображенского, Институт тонких химических технологий им. М.В. Ломоносова, ФГБОУ ВО «МИРЭА – Российский технологический университет» (119571, Россия, Москва, пр-т Вернадского, д. 86); ведущий научный сотрудник лаборатории новых физико-химических проблем, ФГБУН «Институт физической химии и электрохимии им. А.Н. Фрумкина Российской академии наук» (119071, Россия, Москва, Ленинский пр-т, д. 31, корп. 4), E-mail: kirill.birin@gmail.com. Scopus Author ID 6508264517, ResearcherID O-4758-2016, SPIN-код РИНЦ 3279-9050, <https://orcid.org/0000-0001-6951-2440>

Грин Михаил Александрович, д.х.н., профессор, заведующий кафедрой химии и технологии биологически активных соединений, медицинской и органической химии им. Н.А. Преображенского, Институт тонких химических технологий им. М.В. Ломоносова, ФГБОУ ВО «МИРЭА – Российский технологический университет» (119571, Россия, Москва, пр-т Вернадского, д. 86). E-mail: michael_grin@mail.ru. Scopus Author ID 6603356480, SPIN-код РИНЦ 2212-1579, <https://orcid.org/0000-0002-4333-4516>

Translated from Russian into English by the authors

Edited for English language and spelling by Dr. David Mossop

Chemistry and technology of medicinal compounds
and biologically active substances

Химия и технология лекарственных препаратов
и биологически активных соединений

UDC 661.12.01:66.047.596

<https://doi.org/10.32362/2410-6593-2024-19-4-327-336>

EDN PVTYTQ



RESEARCH ARTICLE

Study of inhalation micropowders obtained by spray drying

Larisa A. Shcherbakova✉, Alsu I. Saitgareeva, Mariia G. Gordienko, Ruslan R. Safarov

D.I. Mendeleev University of Chemical Technology of Russia, Moscow, 125047 Russia

✉ *Corresponding author; e-mail: shcherbakova.l.a@muctr.ru*

Abstract

Objectives. To study the influence of the type of matrix-forming material and excipients concentration, spray drying parameters on the characteristics of the powder for inhalation, as well as to investigate the inhalation compositions for stability under stressful conditions.

Methods. Spray drying was used to obtain powder compositions with the required characteristics for inhalation therapy. Microscopic and analytical studies of powders were carried out. Statistical analysis made it possible to estimate the influence of factors on the powder characteristics and rank them by importance. The stability of spray dried powders was studied.

Results. The optimal parameters for obtaining powders for inhalation were found by means of mathematical statistics: air flow rate was 37 m³/h; compressed air flow rate — 601 L/h; inlet air temperature — 150°C; solution flow rate — 45% of the power of the peristaltic pump (16.3 g/min for this composition); L-leucine concentration — 10 wt %; ratio of components of the matrix polyvinylpyrrolidone K-30/D-mannitol = 1 : 3. Under these conditions, as well as by means of 2 experiments additionally selected from the research design, a composition with isoniazid as an active substance was spray dried. The resulting powders were analyzed, in order to confirm the correctness of the recommended parameters.

Conclusions. The selection of compositions and spray drying conditions involves multiple criteria. The characteristics of the powder for inhalation may deteriorate significantly during long-term storage. The optimal parameters were determined using statistical analysis and confirmed by experimental data.

Keywords

spray drying, active pharmaceutical ingredient, micropowders, inhalation, experiment planning methods, optimization

Submitted: 30.11.2023

Revised: 16.02.2024

Accepted: 27.06.2024

For citation

Shcherbakova L.A., Saitgareeva A.I., Gordienko M.G., Safarov R.R. Study of inhalation micropowders obtained by spray drying. *Tonk. Khim. Tekhnol. = Fine Chem. Technol.* 2024;19(4):327–336. <https://doi.org/10.32362/2410-6593-2024-19-4-327-336>

НАУЧНАЯ СТАТЬЯ

Исследование ингаляционных микропорошков, полученных методом распылительной сушки

Л.А. Щербакова✉, А.И. Саитгареева, М.Г. Гордиенко, Р.Р. Сафаров

Российский химико-технологический университет им. Д.И. Менделеева, Москва, 125047 Россия

✉ Автор для переписки, e-mail: shcherbakova.l.a@muctr.ru

Аннотация

Цели. Исследовать влияние типа материала, формирующего каркас частицы, концентрации вспомогательных веществ и параметров распылительной сушки на характеристики порошка для ингаляций. Проверить ингаляционный состав на стабильность в стрессовых условиях.

Методы. Для получения порошковых композиций с требуемыми характеристиками для ингаляционной терапии использовалась распылительная сушка. Были проведены микроскопические и аналитические исследования частиц сухого порошка. Статистический анализ позволил оценить влияние факторов на характеристики получаемого порошка для ингаляций и проранжировать их по значимости. Было проведено исследование стабильности порошков, полученных после распылительной сушки.

Результаты. Методами математической статистики удалось установить оптимальные параметры получения порошков для ингаляции: расход сушильного агента составил 37 м³/ч; расход сжатого воздуха, подаваемого на форсунку — 601 л/ч; температура сушильного агента на входе в камеру — 150°C; расход раствора — 45% от мощности встроенного насоса (16.3 г/мин для данного состава композиции); концентрация L-лейцина — 10 мас. %; соотношение компонентов матрицы поливинилпирролидон К-30/маннитол = 1 : 3. При данных условиях, а также при условиях 2-х экспериментов дополнительно выбранных из плана исследований, была проведена наработка композиции с изониазидом в качестве активного вещества и проведен анализ полученных порошков, что позволило подтвердить корректность рекомендованных параметров.

Выводы. Подбор состава композиций и условий распылительной сушки является многокритериальной задачей. Характеристики порошка для ингаляций могут значительно ухудшиться при длительном хранении. Оптимальные параметры были определены с применением статистического анализа и подтверждены экспериментальными данными.

Ключевые слова

распылительная сушка, активный фармацевтический ингредиент, микропорошки, ингаляция, методы планирования эксперимента, оптимизация

Поступила: 30.11.2023

Доработана: 16.02.2024

Принята в печать: 27.06.2024

Для цитирования

Щербакова Л.А., Саитгареева А.И., Гордиенко М.Г., Сафаров Р.Р. Исследование ингаляционных микропорошков, полученных методом распылительной сушки. *Тонкие химические технологии*. 2024;19(4):327–336. <https://doi.org/10.32362/2410-6593-2024-19-4-327-336>

INTRODUCTION

Pulmonary drug delivery is a promising non-invasive method of active pharmaceutical ingredient (API) delivery for the local treatment of lung diseases [1]. This delivery promotes rapid drug absorption and bypasses the first-pass metabolism effect [2].

Studies have shown that for the purposes of targeted drug delivery to the lungs, the particle size should be in the range of 1 to 5 μm [3]. Obtaining particles in the specified size range is possible using spray drying. This technology has such advantages as high product yield (up to 70%), high drying rate, no API overheating, and the ability to obtain a relatively narrow size distribution of powder particles. This factor is especially important in the development of new inhalation drug delivery systems [4, 5].

Drying parameters and the composition of stock solutions have a crucial influence on the release rate, physical characteristics and the stability of powder compositions. Such parameters need to be carefully investigated, in order to ensure the delivery of high doses of drug substance to the lungs. The dispersion composition of the composition also plays an important role in its stability and aerodynamics.

In addition to the aerodynamic diameter requirements, the powder should have a good level of aerosolization, depending on flowability and dispersibility [6]. Flowability (friability) is an important property of inhalation powders, since it determines their behavior when an emitted dose of drug is inhaled from a powder inhaler [7].

The addition of amino acids to powder compositions can improve the solubility of the powder, its aerodynamic characteristics and increase the yield of the product. The introduction of such an amino acid as leucine can reduce the surface tension and reduce the size of droplets formed during atomization [2]. This results in finer particles, preferred for pulmonary drug delivery, and reduces agglomeration of the powder during storage [1].

Due to their non-toxicity, affordability and water solubility, disaccharides such as lactose, trehalose and mannitol are widely used in the manufacture of inhalation powders. The introduction of carbohydrates in inhalation powders should take into account their hygroscopicity, glass transition temperature and possible interaction with other components and APIs. Hygroscopicity affects the ability of the powder to absorb moisture, as well as drug stability and caking. Studies have shown that the addition of non-hygroscopic mannitol to powder composition improves its dispersibility and prevents particle caking [8].

Biocompatible polymers of synthetic and natural origin can be used as carriers in the creation of inhaler compositions [9, 10]. One widely used polymer in the pharmaceutical industry is polyvinylpyrrolidone (PVP). PVP grade K-30 is widely used in pharmaceutical technology as solution stabilizer, filler and binder.

Isoniazid (widely used for the treatment of tuberculosis) which acts on pathogens located extra- and intracellularly [11] was selected as an API. Using a powder composition consisting of isoniazid, mannitol, leucine and PVP, a stable and easy to use dosage form, can be obtained.

Fillers play an important role in dry inhalation powders. They provide the necessary aerodynamic characteristics and stability of physical properties of the composition [12].

Studies on the stability of pharmaceuticals were conducted, in order to study the degradation of drug substances, as well as to preserve the characteristics of the composition under the influence of stress factors (increased values of temperature and humidity) [13]. This is necessary, in order to develop the optimal composition of the drug product, as well as to determine the basic requirements for the creation of primary packaging. Based on the results of studies, specific storage parameters for drug substances were established [14]. In the present work, the stability of powders obtained after spray drying was investigated at temperature $T = 40^{\circ}\text{C}$ and humidity $W = 70\%$.

The aim of the present study was to research the effect of composition and spray drying parameters upon the properties of the obtained powder inhalation composition and its stability during storage.

MATERIALS AND METHODS

Materials. The experimental work for preparation of placebo powders used mannitol, D(-)-mannite E 421 (hereinafter D-mannite) grade (*Merck*, Germany); amino acid L-leucine (*Suzhou Vitajoy Bio-Tech Co.*, China); PVP K-30 grade (*NEO Chemical*, Russia). Mannitol together with PVP K-30 are used as the matrix-forming agents. Isoniazid was used as the API. The pharmaceutical substance was synthesized at the Department of Organic Chemistry, D.I. Mendeleev Chemical University of Russia. The high quality of isoniazid was confirmed by high-performance liquid chromatography.

The experimental design. In order to improve the efficiency of the experiment and obtain reliable results, the experimental design is advisable. Due to the large number of influencing factors and available limitations on the number of experiments, a full factorial experiment combined with two Latin squares was constructed (Table 1).

The most significant controlled parameters were identified: L-leucine concentration (10, 15, 20, and 25%); PVP K-30/D-mannite ratio = 1 : 3 and PVP K-30/D-mannite = 3 : 1. These parameters were varied at four levels. The parameters: drying agent flow rate (32 and 37 m³/h); compressed air flow rate supplied to the nozzle (473 and 601 L/h); drying agent temperature at the chamber inlet (150 and 180°C); liquor flow rate (45 and 55% of the capacity of the built-in pump)—were varied at two levels.

The design of experiment is presented in Table 2. Sixteen experiments were conducted, with experiments No. 8 and No. 9 conducted in three repetitions to assess the homogeneity of variance and reproducibility variance.

Preparation of dry powder compositions. The composition of solutions is presented in Table 3. In order to prepare the solutions, 219.3 g of distilled water were measured into a glass beaker and the required weights of L-leucine, D-mannite, PVP K-30 were added one by one. Then everything was stirred with a magnetic stirrer until the formation of a translucent solution and complete dissolution of these substances. The solutions obtained were dried on a spray dryer Mini Spray Dryer B-290 (*Buchi*, Switzerland). Drying parameters were set according to the planning matrix (Table 2).

Characterization of the obtained dry powder compositions. The yield and the following characteristics were determined for all samples obtained: bulk density, friability, residual moisture content and the angle of repose. The characteristics were measured immediately after filling and after 2 weeks of storage at $T = 40^{\circ}\text{C}$, $W = 70\%$.

The product yield was determined as follows: the ratio of the mass of powder obtained after the spray drying process to the total mass of solid added to prepare the stock solution (1):

Table 1. Variable factors and their acceptable values

No.	Parameter	Values	
		(+)	(-)
X_1	Air flow rate, m ³ /h	37	32
X_2	Compressed air flow rate, L/h	601	473
X_3	Inlet air temperature, °C	180	150
X_4	Power of peristaltic pump, %*	55	45

Factors varying at four levels

X_5	Matrix-forming material	A	B	C	D
		PVP K-30	D-Mannitol	PVP K-30/D-Mannitol = 1 : 3	PVP K-30/D-Mannitol = 3 : 1
X_6	L-Leucine concentration, %	10	15	20	25

*Note: since the compositions of the solutions were different, their density and viscosity varied accordingly, therefore, for each experiment, the flow rate of liquid supplied for drying at a given power was measured individually during the drying process.

Table 2. Design of experiment

No.	X_1	X_2	X_3	X_4	X_5	X_6
1	-	-	-	-	A	10
2	+	-	-	-	B	15
3	-	+	-	-	C	20
4	+	+	-	-	D	25
5	-	-	+	-	B	25
6	+	-	+	-	A	20
7	-	+	+	-	D	15
8	+	+	+	-	C	10
9	-	-	-	+	C	15
10	+	-	-	+	D	10
11	-	+	-	+	A	25
12	+	+	-	+	B	20
13	-	-	+	+	D	20
14	+	-	+	+	C	25
15	-	+	+	+	B	10
16	+	+	+	+	A	15

Table 3. Composition of solutions

No.	PVP, g	D-Mannitol, g	L-Leucine, g	H ₂ O _{dist} , g
1	12.6	0	1.4	219.3
2	0	11.9	2.1	219.3
3	2.8	8.4	2.8	219.3
4	7.9	2.6	3.5	219.3
5	0	10.5	3.5	219.3
6	11.2	0	2.8	219.3
7	8.9	3.0	2.1	219.3
8	3.2	9.5	1.4	219.3
9	3.0	8.9	2.1	219.3
10	9.5	3.2	1.4	219.3
11	10.5	0	3.5	219.3
12	0	11.2	2.8	219.3
13	8.4	2.8	2.8	219.3
14	2.6	7.9	3.5	219.3
15	0	12.6	1.4	219.3
16	11.9	0	2.1	219.3

$$\eta = \frac{m_{\text{after drying}}}{m_{\text{total}}} \times 100\%, \quad (1)$$

wherein η is a product yield.

Determination of particle size distribution. Using Micros MCX-100 Crocus optical microscope (Micros, Austria) with hundredfold magnification, particle sizes were determined. In order to study each powder obtained, a small amount of sample was taken and placed on a Goryaev chamber (Minimed, Russia). The images of micropowders were processed using ImageG software¹. In order to characterize the dispersion composition of the samples, the median diameter as well as the quantile of D_{10} and D_{90} were used. Scanning electron microscopy (JEOL 1610LV scanning electron microscope JEOL 1610LV (JEOL, Japan)) was performed, in order to visualize the diameter, structural and surface morphology of the microparticles.

The residual moisture content of the samples was determined using an Axis AGS500 moisture analyzer (Axis, Sweden) at 40°C in automatic mode.

Bulk density measurement. In order to establish the bulk density values, the powder was placed in a 1-mL microtube (Eppendorf, Germany). The bulk density was determined by the formula as to be the ratio of the mass of the bulk material to the volume occupied by it, including the pores between the particles (2):

$$\rho = \frac{m}{V}, \quad (2)$$

wherein ρ is the bulk density of the powder; m is the mass of the powder; V is the volume of the powder.

The angle of repose is a constant three-dimensional angle relative to the horizontal surface formed by a cone-shaped pyramid of material. The angle of repose value was measured in at least three repetitions using an ADA AngleMeter 40 electronic angle meter (ADA Instruments, China) in three planes and expressed in angular degrees.

Investigation of powder stability under stress conditions. The process of testing powder samples for caking was carried out in the following way. First, sample preparation was carried out. For each sample, two gelatin capsules of 0.25 g of powder were filled. The powder was obtained as a result of the spray drying process. Each pair of capsules was placed in a small filter paper envelope and sent to a Memmert heat-cold-moisture climate chamber HPP110eco, 108 L (Mettler, Germany). Powder caking determination tests were performed at 40°C and 70% humidity. After 14 days of keeping the capsules in the climatic chamber, the powder samples were evaluated, checked for caking or sticking.

Then the following characteristics were determined: residual moisture content, particle size distribution and angle of repose.

Statistical analysis of the results. In order to determine the intensity of the influence of the studied factors on the characteristics of micropowders, statistical analysis of the results was carried out in accordance with [15]. During the analysis, the effects of all factors were calculated and their significance was assessed.

Since multi-criteria problems may not have a local optimum, this case required a transition to a single-criteria problem (convolution of criteria), for example, by the utopian point method [15]. For this purpose, the criteria are normalized in accordance with formula (3):

$$f_j^{\text{norm}} = \frac{f_j}{\text{opt } f_j}, \quad j = 1, 2, \dots, 16, \quad (3)$$

wherein f_j^{norm} is the normalized value of the criterion; $\text{opt } f_j$ is the optimal value of the criterion, j is the ordinal number of the criterion.

The position of the utopian point in the space of vector estimates was determined by equations (4) and (5):

$$F^* = (f_1^*, f_2^*, \dots, f_m^*), \quad m = 1, \dots, 6, \quad (4)$$

$$f_j^* = \text{opt } f_j^{\text{norm}}, \quad (5)$$

wherein F^* are coordinates of the ideal point in the f_m^* criterion space, since no criterion can obtain a higher value; $\text{opt } f_j^{\text{norm}}$ is the optimal value of the normalized criterion, m is the ordinal number of the criterion.

For each experiment, we calculated the distance to the utopian point in space by formula (6):

$$d_j = \sqrt{\sum (f_m^* - f_m^{\text{norm}})^2}, \quad m = 1, \dots, 6, \quad (6)$$

wherein d_j is the distance to the utopian point, m is the ordinal number of the criterion.

The optimal conditions were determined by minimizing the distance to the utopian point.

RESULTS AND DISCUSSION

According to the methodology and experiment plan, 16 experiments were carried out at different values of varying factors. Analytical studies were carried out for each obtained sample, the results of which are presented in Table 4.

Analytical studies of the micropowders obtained showed that the product yields ranged from 29.5 to 73%, with high yields (more than 60%) obtained in experiments Nos. 6, 7, 8, 11, 12, 15, and 16.

¹ <https://imagej.net/>. Accessed May 10, 2023.

Table 4. Analysis of the obtained powders

No.	Product yield, %	Residual moisture content, %	Angle of repose, °	Bulk density, g/cm ³	D_{10} , μm	D_{50} , μm	D_{90} , μm
1	36.6	0.36	43	0.45	2.2	4.0	6.9
2	40.3	0.12	50	0.54	2.5	4.4	7.1
3	31.3	0.25	34	0.50	2.1	2.8	4.9
4	29.5	0.32	36	0.42	2.4	3.1	8.5
5	31.9	0.32	24	0.38	2.0	3.8	6.1
6	66.1	0.65	27	0.39	2.3	3.6	6.4
7	61.4	0.60	36	0.48	3.9	5.1	6.9
8	60.3	0.45	23	0.52	2.7	3.8	4.9
9	47.4	0.18	37	0.61	2.3	3.2	4.6
10	44.4	0.57	37	0.51	2.1	2.8	3.6
11	64.3	0.60	33	0.43	1.3	1.7	2.3
12	73.3	0.19	32	0.50	2.5	3.4	4.5
13	36.8	0.22	33	0.39	6.4	8.8	12.7
14	31.4	0.15	34	0.41	1.6	2.5	3.6
15	72.8	0.12	33	0.59	2.4	3.0	5.1
16	70.9	0.18	38	0.40	5.2	6.2	8.2

The samples studied retain a small percentage of residual moisture content (range from 0.12 to 0.65 wt %).

The angle of repose is in the range of 23–50° (except for powder No. 2). Bulk density for all samples is less than 0.6 g/cm³, indicating a high level of fluidity of the obtained dry powder compositions. The particle sizes in samples Nos. 3, 8–12, 14, and 15 fall within the range of 1–5 μm, which makes them suitable for inhalation application.

Statistical analysis revealed that the residual moisture content in the studied range is not affected by any of the factors. With regard to the remaining criteria, analysis showed the contradictory nature of the influence of the factors. The optimal conditions for spray drying were obtained and established that the distance to the utopian point should be minimal: X_1 is the drying agent flow rate (+) 37 m³/h; X_2 is the compressed air flow rate

supplied to the nozzle (+) 601 L/h; X_3 is the drying agent temperature at the chamber inlet (–) 150°C; X_4 is the solution flow rate (–) 45 (g/min); X_5 is the matrix material (0.621) = C (PVP K-30/D-mannite = 1 : 3), where C is the concentration; X_6 is the L-leucine concentration (0.626 g) = 10%.

Figure shows scanning electron microscope photographs of samples Nos. 2 and 10. The images show that the particles have a regular spherical shape. The particle size of sample No. 2 has greater uniformity.

After storage of pharmaceutical substances under stress conditions, analytical studies were performed (Table 5).

After a two-week storage period of the samples under stress conditions, it was visually determined that powders Nos. 1 and 7 lost their bulkiness (i.e., stuck together). In this way further analysis of these samples became

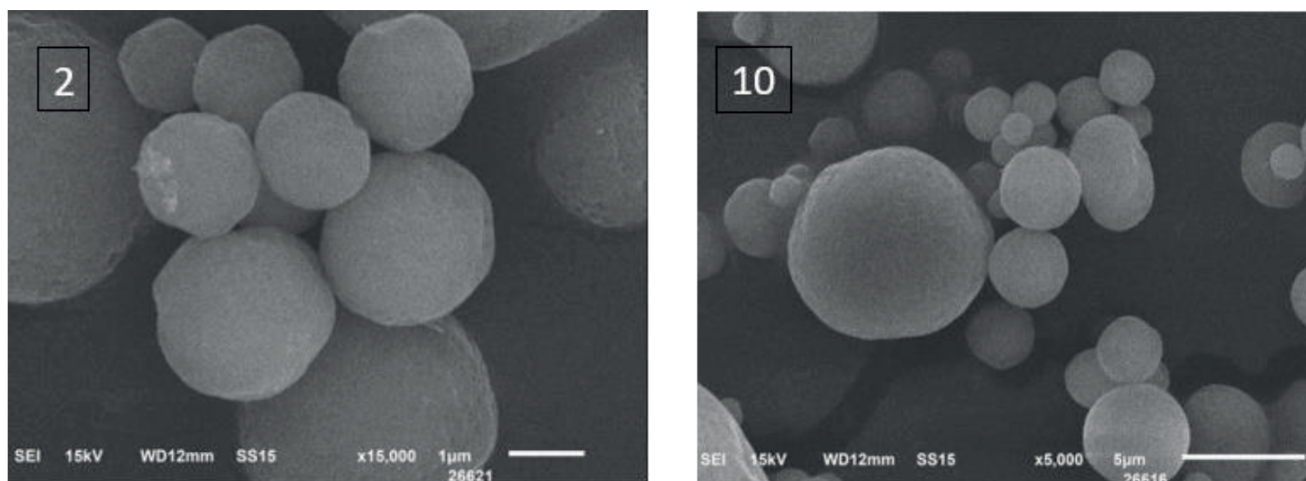


Fig. Scanning electron microscope photographs of samples No. 2 and No. 10. Photographs of the samples were made on the equipment of the Central Research Center of the D.I. Mendeleev University of Chemical Technology of Russia

Table 5. Analysis of powders after storage under stress conditions

No.	Residual moisture content, %	D_{10} , μm	D_{50} , μm	D_{90} , μm	Angle of repose, $^{\circ}$
1	–	–	–	–	–
2	0.41	3.8	5.59	8.1	38
3	0.63	4.3	5.90	8.7	35
4	1.15	2.9	4.90	7.1	23
5	0.28	4.0	5.70	8.5	36
6	2.25	4.1	6.00	8.6	40
7	–	–	–	–	–
8	0.95	3.6	5.80	8.6	27
9	0.81	4.5	6.40	9.2	51
10	2.07	3.6	6.30	8.6	32
11	2.08	4.1	5.90	8.0	30
12	0.30	3.5	5.30	7.8	30
13	1.40	2.4	3.60	5.7	27
14	0.54	3.2	5.00	6.7	41
15	0.12	3.4	4.95	7.6	35
16	2.32	5.0	7.28	10.0	32

impossible. All other samples had a small angle of repose. Comparing the parameters obtained in Tables 4 and 5, we can see that after stress tests the residual moisture content and particle size increased insignificantly.

Based on the above, the conclusion can be drawn that not all powders are suitable for long-term storage under stress conditions. In experiments Nos. 8 and 12, the best parameters were obtained, meeting the requirements for inhalation powders.

Preparation of powder compositions with API. In order to obtain solutions with API (isoniazid), the conditions obtained as a result of criteria convolution (Table 6, sample 3), as well as the parameters of experiments Nos. 8 and 12 (Table 6, samples 1 and 2, respectively) were used. These samples of placebo compositions showed the best characteristics.

Spray drying conditions for these samples are given in Table 7. The results of the study of the samples of compositions are presented in Table 8.

Table 8 shows that in all experiments, a high product yield (more than 60%) was obtained. Since all powders have a small angle of repose and low bulk density, the aerodynamic properties of these samples can be considered good. The particle sizes have narrow particle size distribution, which makes them suitable for inhalation application.

The samples were investigated for stability under stress conditions for a period of two weeks ($T = 40^{\circ}\text{C}$; $W = 70\%$). After this time interval, the characteristics of the samples did not change significantly (Table 9).

Thus, the found optimal conditions ensure the achievement of the stated result.

CONCLUSIONS

The series of studies showed the contradictory influence of composition components and spray drying conditions upon the different characteristics

Table 6. Composition of solutions

No.	PVP, g	D-Mannitol, g	L-Leucine, g	Isoniazid, g	H ₂ O _{dist} , g
1	1.6	4.75	0.7	0.5	109.65
2	0	5.60	1.4	0.5	109.65
3	1.6	4.75	0.7	0.5	109.65

Table 7. Parameters of experiments

No.	X_1	X_2	X_3	X_4	X_5	X_6
1	37	601	180	45	C	10
2	37	601	150	55	B	20
3	37	601	150	45	C	10

Note: X_1 is the flow rate of spray gas, m³/h; X_2 is the flow rate of compressed air per nozzle, L/h; X_3 is the temperature of spray gas at the spray cylinder inlet, °C; X_4 is the power of peristaltic pump, %; X_5 is the matrix material; X_6 is the L-leucine concentration, %; B is D-Mannitol; C stands for PVP K-30/D-Mannitol = 1 : 3.

Table 8. Analysis of the resulting API powders

Sample	Product yield, %	Residual moisture content, %	Angle of repose, °	Bulk density, g/cm ³	D_{10} , μm	D_{50} , μm	D_{90} , μm
1	68.6	3.8	15	0.5	3.5	4.6	6.5
2	66.6	3.8	16	0.3	3.5	4.7	5.8
3	68.6	3.6	21	0.4	2.7	3.7	4.8

Table 9. Analysis of resulting API samples after storage under stress conditions

Sample	Residual moisture content, %	Angle of repose, °	D_{10} , μm	D_{50} , μm	D_{90} , μm
1	4.3	18	3.2	4.5	5.9
2	4.0	17	2.1	3.0	4.3
3	4.6	20	3.1	4.2	6.1

of the dry powder compositions obtained. The utopian point method was used in order to determine the optimal conditions. For the established parameters, a dry powder composition containing isoniazid was produced. This composition included a mixture of PVP K-30/D-mannite = 1 : 3 and L-leucine with a mass loading of 10% as matrix material. Analysis of the characteristics of the product obtained immediately after drying and after two weeks of storage in conditions of high humidity and temperature confirmed that the required values of quality indicators had been achieved: product yield 68.6%; moisture content less than 5%; angle of repose less than 20°; average particle diameter 4.2 μm .

Acknowledgments

The study was supported by the Ministry of Science and Higher Education of the Russian Federation, the state assignment (project FSSM-2022-0004).

Authors' contributions

L.A. Shcherbakova, A.I. Saitgareeva—conducting experiments and analytical research, statistical processing of results, and writing the text of the article.

M.G. Gordienko, R.R. Safarov—formulating the problem and research design, analysis of the obtained results, and revising the article.

The authors declare no conflicts of interest.

REFERENCES

- Ye Y., Ma Y., Zhu J. The future of dry powder inhaled therapy: Promising or discouraging for systemic disorders? *Int. J. Pharm.* 2022;614:121457. <https://doi.org/10.1016/j.ijpharm.2022.121457>
- Alhaji N., O'Reilly N. J., Cathcart H. Leucine as an excipient in spray dried powder for inhalation. *Drug Discov. Today.* 2021;26(10):2384–2396. <https://doi.org/10.1016/j.drudis.2021.04.009>
- AboulFotouh K., Zhang Y., Maniruzzaman M., Williams R.O., Cui Z. Amorphous solid dispersion dry powder for pulmonary drug delivery: Advantages and challenges. *Int. J. Pharm.* 2020;587:119711. <https://doi.org/10.1016/j.ijpharm.2020.119711>
- Stegemann S., Faulhammer E., Pinto J., Paudel A. Focusing on powder processing in dry powder inhalation product development, manufacturing and performance. *Int. J. Pharm.* 2022;614:121445. <https://doi.org/10.1016/j.ijpharm.2021.121445>
- Karimi M., Kamali H., Mohammadi M., Tafaghodi M. Evaluation of various techniques for production of inhalable dry powders for pulmonary delivery of peptide and protein. *J. Drug Deliv. Sci. Technol.* 2022;69(1):103186. <https://doi.org/10.1016/j.jddst.2022.103186>
- Zillen D., Beugeling M., Hinrichs W., Frijlink H., Grasmeyer F. Natural and bioinspired excipients for dry powder inhalation formulations. *Curr. Opin. Colloid Interface Sci.* 2021;56:101497. <https://doi.org/10.1016/j.cocis.2021.101497>
- Weers J.G., Miller D.P. Formulation Design of Dry Powders for Inhalation. *J. Pharm. Sci.* 2015;104(10):3259–3288. <https://doi.org/10.1002/jps.24574>
- Porsio B., Lentini L., Ungaro F., Di Leonardo A., Quaglia F., Giammona G., Cavallaro G. Inhalable nano into micro dry powders for ivacaftor delivery: The role of mannitol and cysteamine as mucus-active agents. *Int. J. Pharm.* 2020;582:119304. <https://doi.org/10.1016/j.ijpharm.2020.119304>
- Allsopp D., Seal K.J., Gaylarde C.C. *Introduction to Biodeterioration*: 2nd ed. Cambridge, UK: Cambridge University Press; 2004. 252 p. ISBN 0-521-82135-5; ISBN 0-521-52887-9
- Miranda M.S., Rodrigues M.T., Domingues R.M.A., Torrado E., Reis R.L., Pedrosa J., Games M.E. Exploring inhalable polymeric dry powders for anti-tuberculosis drug delivery. *Mater. Sci. Eng. C.* 2018;93:1090–1103. <https://doi.org/10.1016/j.msec.2018.09.004>
- Parumasivam T., Chang R.Y.K., Abdelghany S.M., Ye T.T., Britton W.J., Chan H.-K. Dry powder inhalable formulations for anti-tubercular therapy. *Adv. Drug Deliv. Rev.* 2016;102:83–101. <https://doi.org/10.1016/j.addr.2016.05.011>
- Munir M., Jena L., Kett V.L., Dunne N.J., McCarthy H.O. Spray drying: Inhalable powders for pulmonary gene therapy. *Biomater. Adv.* 2022;133:112601. <https://doi.org/10.1016/j.msec.2021.112601>

13. Chang R.Y.K., Chow M.Y.T., Khanal D., Chen D., Chan H.-K. Dry powder pharmaceutical biologics for inhalation therapy. *Adv. Drug Deliv. Rev.* 2021;172:64–79. <https://doi.org/10.1016/j.addr.2021.02.017>
14. Rignall A. ICQ1A(R2) Stability Testing of New Drug Substances and Products and ICHQ1C Stability Testing of New Dosage Forms. In: Teasdale A., Elder D., Nims R.W. (Eds.). *ICH Quality Guidelines: An Implementation Guide*. John Wiley & Sons; 2017. P. 3–44. <https://doi.org/10.1002/9781118971147.ch1>
15. Akhnazarova S.L., Kafarov V.V. *Metody optimizatsii eksperimenta v khimicheskoi tekhnologii (Methods for Optimizing Experiments in Chemical Technology): A textbook for universities*. Moscow: Vysshaya shkola; 1985. 327 p. (in Russ.).

About the authors

Larisa A. Shcherbakova, Postgraduate Student, Department of Chemical and Pharmaceutical Engineering, Mendeleev University of Chemical Technology of Russia (9, Miusskaya pl., Moscow, 125047, Russia). E-mail: shcherbakova.l.a@muctr.ru. <https://orcid.org/0009-0006-4437-2430>

Alsu I. Saitgareeva, Master, Department of Chemical and Pharmaceutical Engineering, Mendeleev University of Chemical Technology of Russia (9, Miusskaya pl., Moscow, 125047, Russia). E-mail: saitgareeva01@bk.ru. <https://orcid.org/0009-0008-4807-7089>

Mariia G. Gordienko, Dr. Sci. (Eng.), Professor, Department of Chemical and Pharmaceutical Engineering, Mendeleev University of Chemical Technology of Russia (9, Miusskaya pl., Moscow, 125047, Russia). E-mail: gordienko.m.g@muctr.ru. Scopus Author ID 8845573700, ResearcherID B-1095-2014, RSCI SPIN-code 7148-5640, <https://orcid.org/0000-0002-8485-9861>

Ruslan R. ogly Safarov, Cand. Sci. (Eng.), Director of the Department of Scientific and Technical Policy, Mendeleev University of Chemical Technology of Russia (9, Miusskaya pl., Moscow, 125047, Russia). E-mail: safarov.r.r@muctr.ru. <https://orcid.org/0000-0002-0342-0049>

Об авторах

Щербакова Лариса Александровна, аспирант кафедры химического и фармацевтического инжиниринга, ФГБОУ ВО «Российский химико-технологический университет им. Д.И. Менделеева» (125047, Россия, Москва, Миусская пл., д. 9). E-mail: shcherbakova.l.a@muctr.ru. <https://orcid.org/0009-0006-4437-2430>

Сайтгареева Алсу Ильдаровна, магистр кафедры химического и фармацевтического инжиниринга, ФГБОУ ВО «Российский химико-технологический университет им. Д.И. Менделеева» (125047, Россия, Москва, Миусская пл., д. 9). E-mail: saitgareeva01@bk.ru. <https://orcid.org/0009-0008-4807-7089>

Гордиенко Мария Геннадьевна, д.т.н., профессор кафедры химического и фармацевтического инжиниринга, ФГБОУ ВО «Российский химико-технологический университет им. Д.И. Менделеева» (125047, Россия, Москва, Миусская пл., д. 9). E-mail: gordienko.m.g@muctr.ru. Scopus Author ID 8845573700, ResearcherID B-1095-2014, SPIN-код РИНЦ 7148-5640, <https://orcid.org/0000-0002-8485-9861>

Сафаров Руслан Рафиг оглы, к.т.н., директор Департамента научно-технической политики, ФГБОУ ВО «Российский химико-технологический университет им. Д.И. Менделеева» (125047, Россия, Москва, Миусская пл., д. 9). E-mail: safarov.r.r@muctr.ru. <https://orcid.org/0000-0002-0342-0049>

Translated from Russian into English by H. Moshkov

Edited for English language and spelling by Dr. David Mossop

UDC 621.315.5

<https://doi.org/10.32362/2410-6593-2024-19-4-337-349>

EDN KPTKXT



RESEARCH ARTICLE

Cold sintering of α - and γ -modifications of aluminum oxohydroxides: A low-temperature route to porous corundum ceramics

Anastasia A. Kholodkova¹✉, Maksim V. Korniyushin¹, Andrey V. Smirnov², Levko A. Arbanas², Arseniy N. Khrustalev², Viktoria E. Bazarova², Aleksey V. Shumyantsev^{3,4}, Stepan Yu. Kupreenko³, Yuriy D. Ivakin^{3,5}

¹ Department of Scientific Research Coordination, State University of Management, Moscow, 109545 Russia

² Laboratory of Ceramic Materials and Technologies, MIREA – Russian Technological University, Moscow, 119454 Russia

³ Chemistry Department, M.V. Lomonosov Moscow State University, Moscow, 119991 Russia

⁴ All-Russian Institute for Scientific and Technical Information, Moscow, 125190 Russia

⁵ Mobile Solutions Engineering Center, MIREA – Russian Technological University, Moscow, 119454 Russia

✉ Corresponding author; e-mail: anastasia.kholodkova@gmail.com

Abstract

Objectives. To obtain porous corundum ceramics using an innovative cold sintering process starting from different phase modifications of aluminum oxohydroxide—boehmite γ -AlOOH and diasporite α -AlOOH; to study the phase and structural properties of the resulting materials; and to assess their permeability to water.

Results. Cold sintering enables the formation of single-phase corundum ceramics with an open porosity of 47.9% directly from the initial boehmite powder with the addition of 5 wt % corundum in the presence of 20 wt % water at a temperature of 450°C, mechanical pressure of 220 MPa, and isothermal exposure for 30 min. Under the same conditions of cold sintering, a mixture of diasporite and boehmite was transformed into α -AlOOH ceramics. This then turned into corundum with an open porosity of 39% when calcined in air at 600°C for 1 h. The resulting materials had permeability for pure water above 5000 L/(m²·h·bar).

Conclusions. Cold sintering is a promising approach to producing porous corundum ceramics which can be used in filtration systems. Compared to traditional ceramic technology, the new approach reduces energy, time, and labor costs in the material manufacturing. It also eliminates the need to use auxiliary substances (binders, pore-forming agents, etc.).

Keywords

cold sintering, aluminum oxide, aluminum oxohydroxide, corundum, boehmite, diasporite, porous permeable ceramics

Submitted: 02.05.2024

Revised: 07.05.2024

Accepted: 01.07.2024

For citation

Kholodkova A.A., Korniyushin M.V., Smirnov A.V., Arbanas L.A., Khrustalev A.N., Bazarova V.E., Shumyantsev A.V., Kupreenko S.Yu., Ivakin Yu.D. Cold sintering of α - and γ -modifications of aluminum oxohydroxides: A low-temperature route to porous corundum ceramics. *Tonk. Khim. Tekhnol. = Fine Chem. Technol.* 2024;19(4):337–349. <https://doi.org/10.32362/2410-6593-2024-19-4-337-349>

НАУЧНАЯ СТАТЬЯ

Холодное спекание α - и γ -модификаций оксогидроксида алюминия: низкотемпературный способ получения пористой корундовой керамики

А.А. Холодкова^{1,✉}, М.В. Корнюшин¹, А.В. Смирнов², Л.А. Арбанас², А.Н. Хрусталеv²,
В.Е. Базарова², А.В. Шумянцев^{3,4}, С.Ю. Купреенко³, Ю.Д. Ивакин^{3,5}

¹ Управление координации научных исследований, Государственный университет управления, Москва, 109542 Россия

² Лаборатория керамических материалов и технологий, МИРЭА – Российский технологический университет, Москва, 119454 Россия

³ Химический факультет, Московский государственный университет им. М.В. Ломоносова, Москва, 119991 Россия

⁴ Всероссийский институт научной и технической информации, Российская академия наук, Москва, 125190 Россия

⁵ Инжиниринговый центр мобильных решений, МИРЭА – Российский технологический университет, Москва, 119454 Россия

✉ Автор для переписки, e-mail: anastasia.kholodkova@gmail.com

Аннотация

Цели. Получить пористую корундовую керамику с помощью инновационного метода холодного спекания с использованием различных фазовых модификаций оксогидроксида алюминия — бемита γ -AlOOH и диаспора α -AlOOH, изучить фазовые и структурные свойства полученных материалов и оценить их проницаемость для воды.

Результаты. С помощью холодного спекания в присутствии 20 мас. % воды при температуре 450°C, механическом давлении 220 МПа и изотермической выдержке 30 мин из исходного порошка бемита с добавлением 5 мас. % корунда была изготовлена однофазная корундовая керамика с открытой пористостью 47.9%. При таких же условиях холодного спекания смесь диаспора и бемита превратилась в керамику α -AlOOH, которая при прокаливании на воздухе при 600°C в течение 1 ч перешла в корунд с открытой пористостью 39%. Полученные материалы обладали проницаемостью для чистой воды более 5000 л/(м²·ч·бар).

Выводы. Холодное спекание является перспективным методом для изготовления пористой корундовой керамики, которая может быть использована в системах фильтрации. По сравнению с традиционной керамической технологией новый подход снижает энергетические, временные и трудозатраты при изготовлении материала, а также исключает необходимость в использовании вспомогательных веществ (связующих, порообразующих агентов и пр.).

Ключевые слова

холодное спекание, оксид алюминия, оксогидроксид алюминия, корунд, бемит, диаспор, пористая проницаемая керамика

Поступила: 02.05.2024

Доработана: 07.05.2024

Принята в печать: 01.07.2024

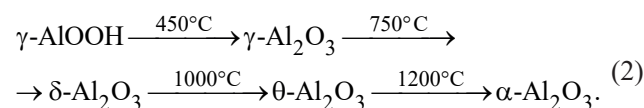
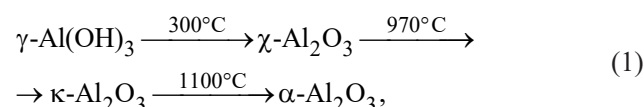
Для цитирования

Холодкова А.А., Корнюшин М.В., Смирнов А.В., Арбанас Л.А., Хрусталеv А.Н., Базарова В.Е., Шумянцев А.В., Купреенко С.Ю., Ивакин Ю.Д. Холодное спекание α - и γ -модификаций оксогидроксида алюминия: низкотемпературный способ получения пористой корундовой керамики. *Тонкие химические технологии*. 2024;19(4):337–349. <https://doi.org/10.32362/2410-6593-2024-19-4-337-349>

1. INTRODUCTION

Ceramics based on aluminum oxide α -Al₂O₃ are widely used in various fields of engineering due to their mechanical characteristics, chemical and temperature resistance, stable dielectric properties and compatibility with biological tissues [1–3]. Aluminum oxide exists in the form of a number of transitional phase modifications which as a result of successive transformations under heating transform into α -Al₂O₃. In practice, the

following chains of transformations [4, 5] are most often realized [4, 5] (formulas 1 and 2):



An important problem of α - Al_2O_3 production is the high temperature of its formation (more than 1100°C), as well as the sintering temperature of corundum ceramics (more than 1500°C). Methods based on the use of aqueous reaction medium for γ - $\text{Al}(\text{OH})_3$ or γ - AlOOH treatment are currently known. They allow for the synthesizing of single-phase α - Al_2O_3 in an autoclave at a temperature of 380 – 450°C [6, 7]. The decisive role in reducing the temperature of corundum formation under such conditions is played by the interaction of solid starting substances with water molecules from the reaction medium. This results in dehydroxylation of γ - $\text{Al}(\text{OH})_3$ with the transition to γ - AlOOH and its transformation into α - Al_2O_3 .

In the field of ceramics technology, a new approach known as the cold sintering process (CSP) has been actively developed during the last decade [8]. Processes similar to those occurring with oxide and hydroxide powders in aqueous medium in a closed reactor (autoclave) are realized, in order to obtain dense or porous ceramic materials. The CSP requires a mold equipped with a heater in which feedstock in the form of powder and the “liquid phase” are placed. The most often used liquids are water, aqueous solutions of acids or alkalis, as well as hydroxides or salts, including their hydrates with a low melting point [9]. CSP is carried out under applied mechanical pressure (usually up to 500 MPa) and isothermal holding at temperatures below 500°C from several minutes to several hours. The lowering of the sintering temperature of ceramics under such conditions when compared to conventional sintering is based on the interaction of the initial powder particles with the liquid phase. The literature considers various possible mechanisms of ceramic microstructure formation during CSP. This includes partial dissolution of solid matter, ion transport through the liquid phase and deposition in energetically more favorable regions (dissolution–precipitation mechanism) [10], as well as mass transfer and coalescence of particles due to increased mobility of the crystal structure under conditions of quasi-equilibrium hydroxylation (in the case of water-based liquid phase) [11, 12]. An important role in the CSP process is attributed to surface diffusion [13]. As of the present time, more than one hundred different ceramic materials fabricated using the CSP method have been reported.

The possibility of lowering the sintering temperature by means of CSP is of particular interest in refractory compositions, including corundum. Given the demand for corundum ceramics in a range of applications, the development of CSP technology for this material will provide significant energy savings in its production. Only a few papers have appeared in literature since 2020 reporting on the successful production of α - Al_2O_3 ceramics using the CSP method. Kang *et al.* [14]

succeeded in producing corundum ceramics in two stages: by CSP of a mixture of α - and γ - Al_2O_3 in glacial acetic acid at 300°C and 300 MPa for 1 h and subsequent calcination of the samples in air at temperatures above 1250°C . In [15], CSP of γ - $\text{Al}(\text{OH})_3$ was realized in a spark plasma sintering unit, in order to obtain γ - AlOOH (boehmite) ceramics in the presence of water (450°C , 70 MPa, 20 min). The calcination of the obtained boehmite in air led to the formation of α - Al_2O_3 ceramics with a porosity of about 60% . This work also shows the transformation of boehmite powder into α - Al_2O_3 under the same conditions, but the obtained corundum sample did not have the satisfactory transport strength.

The fabrication of porous ceramics based on boehmite (porosity of about 38%) from γ - $\text{Al}(\text{OH})_3$ was described by Yamaguchi *et al.* [16]. They performed CSP at 250°C and 270 MPa with the addition of water as a liquid phase. The authors note that the transition of aluminum hydroxide to oxohydroxide is accompanied by a significant increase in the porosity of the material. Based on the data provided in literature on the sequence of transformations of γ - $\text{Al}(\text{OH})_3$ – γ - AlOOH – α - Al_2O_3 in aqueous medium, including at CSP, the possibility of direct production of porous ceramics α - Al_2O_3 with the help of CSP may be assumed. The direct transition of another modification of aluminum oxyhydroxide, α - AlOOH diasporite, into corundum upon heating to a temperature of about 500°C is also known [17]. In the few works concerning the fabrication of alumina ceramics from natural diasporite, a high porosity of the materials obtained is noted [18]. Thus, the diasporite–corundum transition can be considered as a possible basis for the process of obtaining corundum ceramics at reduced temperature, in particular during CSP.

The aim of this work is to obtain porous corundum ceramics by means of CSP of different phase modifications of aluminum oxohydroxide—boehmite γ - AlOOH and diasporite α - AlOOH , as well as to study the phase and structural properties of the obtained materials and to evaluate their water permeability.

2. EXPERIMENTAL

2.1. Synthesis of aluminum oxohydroxide (α - and γ - AlOOH)

The synthesis of α - AlOOH (diasporite) was carried out in two stages: (1) obtaining the precursor—aluminum oxide—by precipitation from aqueous solution and (2) treatment of the precursor in water vapor. Aluminum nitrate octahydrate $\text{Al}(\text{NO}_3)_3 \cdot 9\text{H}_2\text{O}$ (high purity, *Lenreactive*, Russia) and aqueous ammonia solution NH_4OH (particularly high purity, *IREA* experimental plant, Russia) served as starting substances for precursor synthesis. Equal volumes of aqueous solutions of

Table 1. Production conditions of ceramic samples using the CSP method (BCS—boehmite cold sintering, DCS—diaspore cold sintering)

Ceramic sample	Raw material composition (powder)	CSP conditions	Calcination conditions
BCS	γ -AlOOH 95 wt %, α -Al ₂ O ₃ 5 wt %	450°C, 220 MPa, 30 min	–
DCS	α -AlOOH 75.3 wt %, γ -AlOOH 24.7 wt %		–
DCS-600	α -AlOOH 75.3 wt %, γ -AlOOH 24.7 wt %		600°C, 1 h

Al(NO₃)₃ prepared with a concentration of 0.15 M and NH₄OH with a concentration of 0.30 M were added to 400 mL of distilled water under continuous stirring and at a temperature of 75°C. The resulting precipitate was left to age at the same temperature for 3 h. It was then filtered and washed with a large volume of distilled water until the wash water was neutral. The filtered precipitate was air dried at 50°C for 12 h. The resulting powder was calcined in air at 1000°C for 30 min. The precursor synthesized in this way was placed in a container with a lid made of Teflon and placed inside a laboratory autoclave (*Private entrepreneur Vitsukaeva S.N.*, Russia) with a volume of 17 mL. 2 mL of distilled water was poured in advance at the bottom. The hermetically sealed autoclave was heated to a temperature of 200–300°C at a rate of 70°C/h in a SNOL-3.5,3.5,3.5/5-II drying cabinet (*NPF Thermiks*, Russia) and kept at the assigned temperature for up to 260 h. During the treatment, the precursor was separated by container walls from water in the liquid state, while in contact with the vapor phase. The equilibrium vapor pressure of water was 3.97 MPa. The autoclave was then cooled by placing the bottom of the autoclave in cold water outside the desiccator. The synthesized sample was removed from the autoclave and dried in air at 50°C for 5 h.

Aluminum hydroxide (hydrargillite) γ -Al(OH)₃ (MD brand, *Pikalevsky Alumina Plant*, Russia) served as a starting substance for the synthesis of γ -AlOOH (boehmite) in water vapor. When treating γ -Al(OH)₃ in water vapor, equipment and procedures similar to those described above for treating the α -AlOOH precursor were used. The temperature of isothermal soaking in water vapor was 270°C, the equilibrium pressure was 5.50 MPa, and the duration was 14 h. The product obtained was air dried at 50°C for 5 h.

2.2. Ceramics fabrication using the CSP method

The laboratory setup for CSP in aqueous medium consisted of the following: an IP-1250 M-auto hydraulic press

(*Plant of Testing Instruments and Equipment*, Russia); a custom-made steel mold with two composite punches; and a ring heater equipped with a temperature controller Thermodat-17E6 (*NPP Sistemy Kontrolya*, Russia) with two thermocouples. In order to prevent heat dissipation into the press plates and the environment, custom-made heat-insulating bars made of gabbro-dabase were placed under the punches. The unit was placed in a casing made of aluminum foil (*RUSAL – Sayana Foil*, Russia) and refractory kaolin wool MKRV-200 (*Teplopromproekt*, Russia), in order to reduce heat exchange with the environment. Sealing of the working volume of the mold was achieved by using sheets of graphite paper (*NPO Unikhimtek*, Russia) and copper sealing rings (*Metallinvest Corporation*, Russia) at the joints of the mold elements. In order to induce nucleation of the latter at CSP, 5 wt % of aluminum oxide α -Al₂O₃ (corundum) was preliminarily added into γ -AlOOH powder. 1 g of synthesized aluminum oxohydroxide was placed in the working volume of the CSP mold, 0.2 mL distilled water was poured in, and then a mechanical pressure of 220 MPa was applied to the assembled mold. Heating was carried out at a rate of 10°C/min to a temperature of 450°C, and isothermal holding was 30 min. It has previously been shown that the formation of corundum phase from boehmite powder occurs at 450°C under CSP conditions [15]. The mechanical pressure was released, the mold was cooled naturally, and the ceramic sample was removed from the mold. The ceramic sample made from α -AlOOH powder was calcined in air at 600°C for 1 h. The conditions of ceramic sample fabrication are summarized in Table 1.

2.3. Methods of research of synthesized powders and ceramics

The X-ray phase analysis of synthesized powders and fabricated ceramics was carried out using a PowDiX 600 diffractometer (*LINEV ADANI*, Belarus, 2022) by means of monochromatic Cu-K α ₁ radiation with $\lambda = 1.5406 \text{ \AA}$ (0.02-mm Ni filter) on a diffracted beam (30 kV, 10 mA). The θ –2 θ , continuous imaging was carried out in the

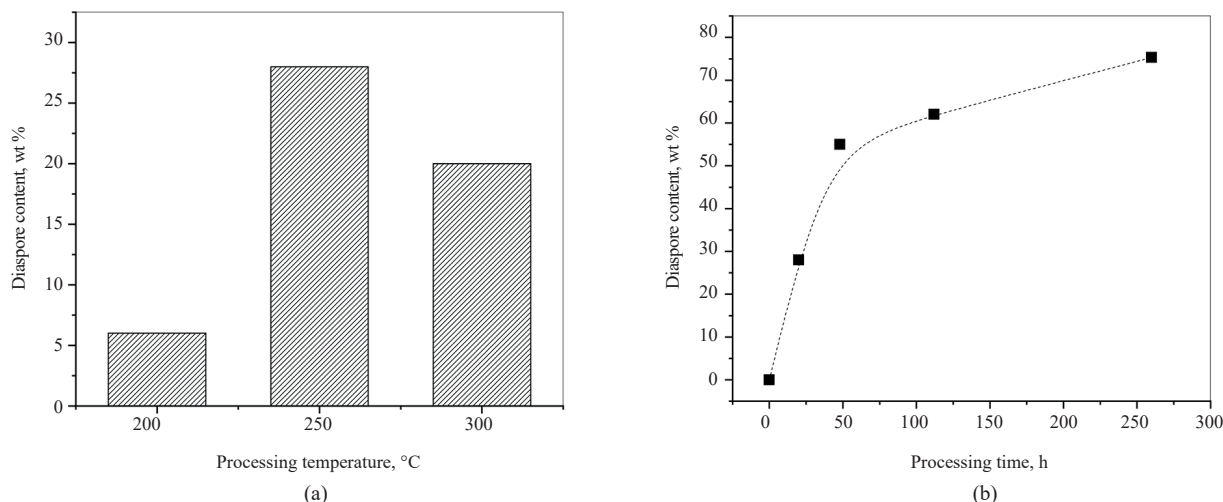


Fig. 2. Diaspore contents after the treatment of alumina in a water vapor atmosphere: (a) 20 h of treatment at different temperatures; (b) different duration of a treatment at 250°C and an autogenous pressure of 3.97 MPa

SEM image (Fig. 1) shows particles of different shapes (rounded, prismatic, irregular) and sizes from 80 nm to 4.6 μm .

As a result of the treatment of the synthesized aluminum oxide powder in a water vapor atmosphere, the formation of a mixture of aluminum oxohydroxides: diaspore α -AlOOH and boehmite γ -AlOOH can be observed. The rate of diaspore accumulation in the system shows sensitivity to the process temperature. As a result of the incubation of aluminum oxide in water vapor at temperatures of 200, 250 and 300°C for 20 h, the formation of the largest amount of diaspore (28.1 wt %) can be observed at 250°C (Fig. 2a). The preparation of boehmite under hydrothermal conditions at temperatures from 150 to 240°C and equilibrium water vapor pressure from amorphous aluminum oxide has been described in the literature [20–22]. The formation of synthetic diaspore was observed under harsher hydrothermal conditions,

at temperatures from 300 to 450°C, and pressures of 6.0 to 34.5 MPa when α -Al₂O₃ powder was treated for more than 72 h [23, 24]. At the same time, the mixture of α - and γ -modifications of Al₂O₃ passes into diaspore through the formation of the boehmite phase [23]. The formation of oxohydroxides from different modifications of aluminum oxide in water vapor most probably occurs with the preservation of the type of close-packing in crystals: hexagonal at the transition of α -Al₂O₃ into diaspore and cubic at the transformation of γ -Al₂O₃ into boehmite. The transition of boehmite into diaspore is associated with a change in the type of close-packing in the crystal. This may explain the slow accumulation of α -AlOOH in the reaction mixture during its prolonged treatment (more than 48 h, Fig. 2b).

After 260 h of treatment of the synthesized aluminum oxide in water vapor at 250°C, the reaction mixture contains 75.3% diaspore and 24.7% boehmite (Fig. 3).

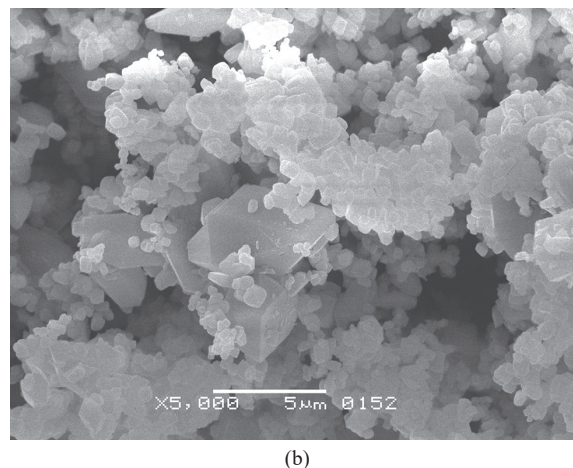
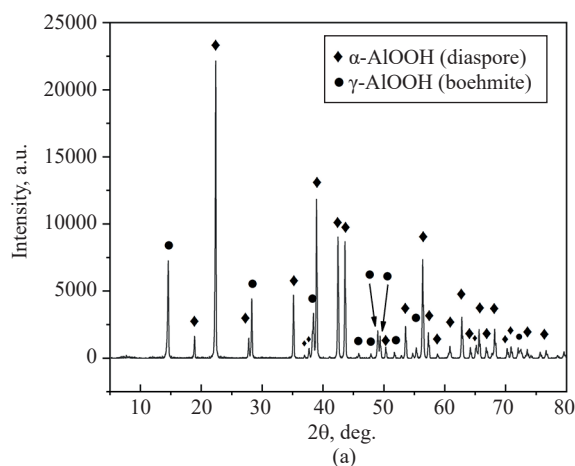


Fig. 3. X-ray diffraction pattern (a) and SEM image (b) of diaspore powder synthesized in a water vapor at 250°C and an autogenous pressure of 3.27 MPa for 260 h

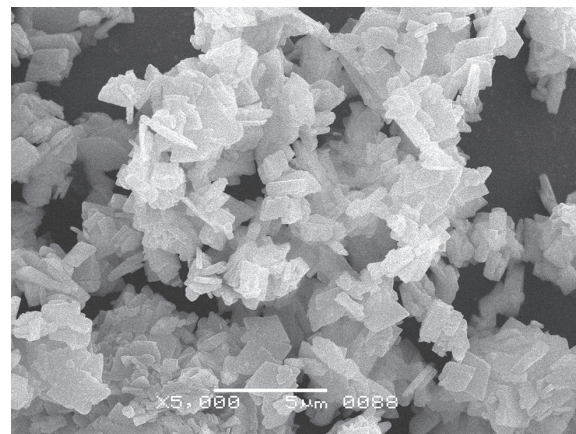
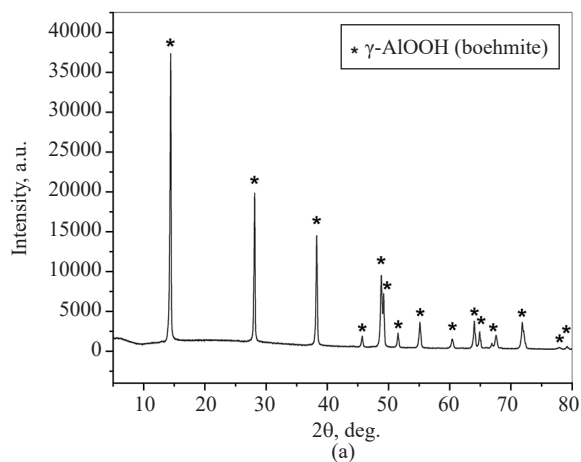


Fig. 4. X-ray diffraction pattern (a) and SEM image (b) of boehmite powder synthesized in a water vapor at 270°C and an autogenous pressure of 5.50 MPa for 14 h

Two types of particles can be distinguished in the obtained powder: strongly agglomerated particles of 0.3–1.4 μm in size, as well as large crystals growing among them, up to 7 μm in size, possessing smooth faces. The appearance of large crystals is a consequence of secondary recrystallization in the system.

As a result of treatment in water vapor of $\gamma\text{-Al}(\text{OH})_3$ hydrargyllite powder at 270°C and equilibrium pressure of 5.50 MPa, a single-phase boehmite with predominantly lamellar particle shape was formed (Fig. 4). The particle size in the sample ranges from 0.5 to 2.9 μm . Such particle shape is also known for boehmite synthesized under classical hydrothermal conditions (in solution) [25, 26].

3.2. Structure and properties of corundum ceramics fabricated using the CSP method

CSP of synthesized powders of α - and γ -oxohydroxides of aluminum, carried out at a temperature of 450°C and applied mechanical pressure of 220 MPa for 30 min, led to the formation of transport-strength ceramic samples. The phase analysis of ceramics made from powder consisting of a mixture of 75.3% diaspore and 24.7% boehmite showed that the phase transition of boehmite to diaspore is completed during the CSP (Fig. 5a). The grains in the material obtained (Fig. 5c) are predominantly close in shape and size to the large crystals formed as a result of secondary recrystallization in the initial powder (Fig. 4). During CSP, single large crystals present in the powder served as nuclei of secondary recrystallization, leading to a significant increase in the average grain size of ceramics when compared to the original particles (from 0.94 to 2.13 μm).

Thermal analysis of the diaspore ceramics revealed an endothermic effect at around 524°C accompanied by a mass loss of 13.97% (Fig. 5b). The data obtained on the decomposition of $\alpha\text{-AlOOH}$ corresponds well with that previously known from the literature for diaspore powder [17]. At the same time, the total mass loss of the diaspore ceramic sample when heated to 700°C was 14.63%, which corresponds to the mass fraction of water released from aluminum oxohydroxide during the transition to Al_2O_3 (15%). Based on these data, the diaspore ceramics were calcined in air at 600°C for 1 h, leading to its complete conversion to $\alpha\text{-Al}_2\text{O}_3$ corundum (Fig. 5a). The microstructure of the corundum ceramics retained the appearance of grains observed in the diaspore ceramics (Fig. 5d), while their average size increased to 2.78 μm .

CSP of boehmite powder in the presence of 5 wt % corundum resulted in the formation of single-phase $\alpha\text{-Al}_2\text{O}_3$ ceramics (Fig. 6). The SEM image of the sample chip shows that the material has a developed pore space, and consists of isometric grains with sizes ranging from 0.42 to 4.23 μm with an average value of 1.42 μm . The grains have a hexagonal shape characteristic of corundum.

Corundum ceramics obtained from aluminum oxohydroxide powders of different phase composition have close values of relative density in the range of 46–48% (Table 2). At the same time, in the sample achieved in one stage CSP from boehmite powder (BCS), there is practically no closed porosity (5.9%), and open pores account for about half of the material volume (47.9%). The DCS-600 sample made from diaspore-containing powder has lower open porosity (39.0%). It should be noted that the DCS sample had only 9.0% open porosity before calcination in air. The calcination

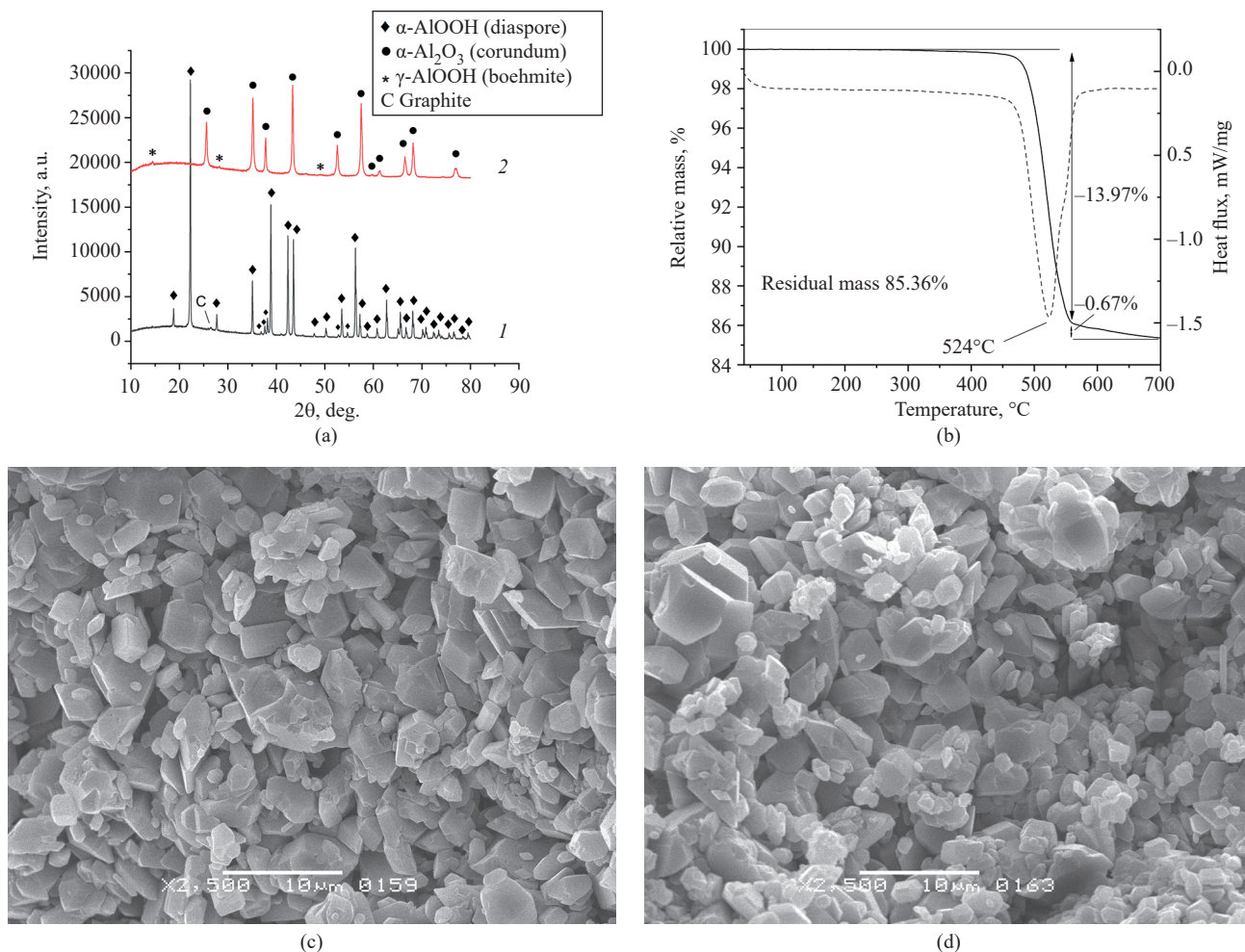


Fig. 5. Study of the ceramics obtained from diaspore powder: (a) X-ray diffraction patterns of the samples manufactured by CSP (1) and CSP with the following calcination at 600°C (2); (b) thermal analysis of the sample after the CSP; (c) SEM image of the sample after CSP; (d) SEM image of the sample after CSP with the following calcination at 600°C

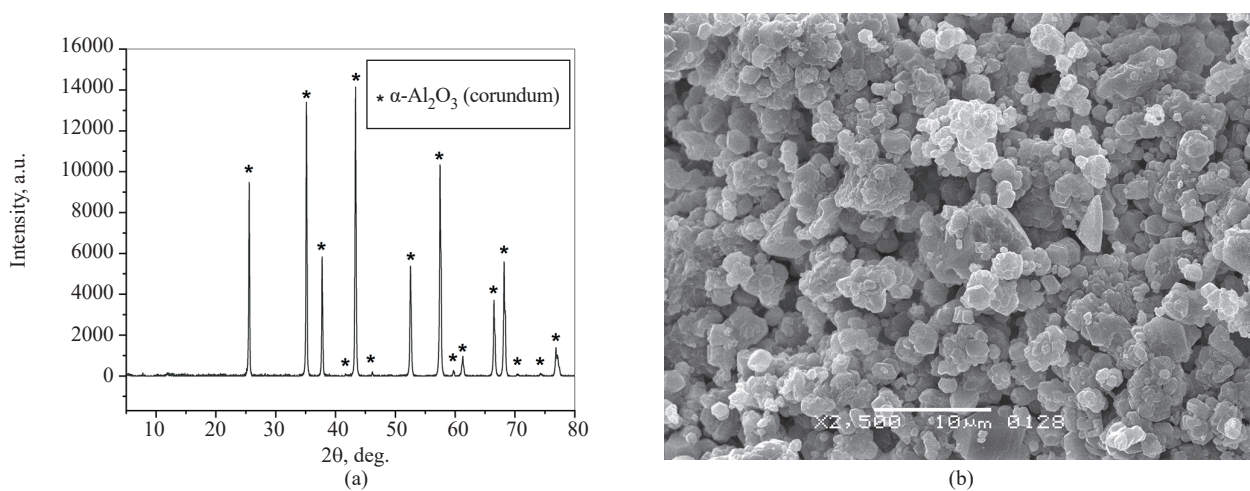


Fig. 6. X-ray diffraction pattern (a) and SEM image (b) of ceramics obtained by a cold sintering processing of a boehmite powder

Table 2. Integral structural characteristics and permeability of corundum ceramics fabricated using the CSP method

Ceramic sample name	Relative density, %	Open porosity, %	Permeability, L/(m ² ·h·bar)
BCS	46.2	47.9	5370
DCS-600	47.2	39.0	5020

had a negligible effect on the closed porosity, an increase from 12.3 to 13.8% was observed. Taking into account the different theoretical density of boehmite and diasporite (3.08 and 3.38 g/cm³, respectively), we can conclude that the decisive role in the formation of open porosity is played by the phase transition of oxohydroxides into α -Al₂O₃, which has a higher theoretical density (3.96 g/cm³).

The values of open porosity observed in the fabricated corundum ceramics are comparable to those reported in the literature for ceramic substrates made of α -Al₂O₃ and intended for the fabrication of filter membranes (30–40% of open porosity) [27, 28]. The permeability of porous materials obtained in the present work for pure water is more than 5000 L/(m²·h·bar) (Table 2). It is consistent with the value of open porosity. Corundum ceramics made of boehmite powder have a higher level of open porosity and permeability than those of diasporite ceramics. Similar permeability values have been reported by a number of authors for α -Al₂O₃ ceramic filter membranes. For example, in [29] corundum substrates with a permeability of 4000 L/(m²·h·bar) were immersed in a suspension of α -Al₂O₃ powder followed by drying and sintering, in order to obtain single-layer membranes with a permeability of about 1000 L/(m²·h·bar). Similarly, Naseer *et al.* [30], using less permeable substrates (614 L/(m²·h·bar)), produced single-layer membranes with a permeability of 388 L/(m²·h·bar) and bilayer membranes with a permeability of 311 L/(m²·h·bar). By filtering a suspension through a substrate with a permeability of 4700 L/(m²·h·bar), a membrane with a permeability of 550 L/(m²·h·bar) was obtained in [31]. In other studies, microfiltration membranes composed entirely of corundum possessed permeabilities for pure water ranging from 2150 to 8000 L/(m²·h·bar) [27, 28, 32]. In comparison with literature data, the permeability of porous ceramic materials obtained in this work allows us to consider the possibility of their use as components of filtration systems. Depending on the purpose of the system (from macro- to nanofiltration), such materials can be promising both for independent application, and as substrates for membranes of finer water purification. A significant advantage of such porous corundum ceramics over the currently known analogues is a high level of energy efficiency, expressiveness and the low labor intensity of the method of its manufacture: CSP of aluminum oxohydroxides, including widely available boehmite powder. The further development of

this technology of porous corundum ceramics involves the study of the structure of its pore space, mechanical properties and the possibility of manufacturing multilayer materials with variable porosity.

4. CONCLUSIONS

The present work shows the possibility of using the CSP method for the fabrication of porous corundum ceramics based on aluminum oxohydroxides and water. The CSP of boehmite γ -AlOOH powder with the addition of α -Al₂O₃ corundum in the presence of 20 wt % water at a temperature of 450°C and an applied mechanical pressure of 220 MPa for 30 min allows single-phase α -Al₂O₃ ceramics with an open porosity of 47.9% to be directly obtained. At CSP of a mixture of α -AlOOH diasporite powders (75.3%) and boehmite (24.3%), single-phase diasporite ceramics are formed. These completely transform into corundum ceramics with an open porosity of 39.0% as a result of calcination in air at 600°C for 1 h. Ceramics made of aluminum oxohydroxides have a permeability level for pure water of more than 5000 L/(m²·h·bar), allowing us to consider them as a material promising for use in filtration systems. The use of CSP provides an increase in the efficiency of porous corundum ceramics production, when compared with the traditional technology due to energy saving and the absence of the need to use auxiliary substances (binders, pore-forming agents, etc.).

Acknowledgments

The research was supported by the Russian Science Foundation, grant No. 22-73-00318.

Authors' contributions

A.A. Kholodkova—general management, scanning electron microscopy, permeability measurements, and writing the text of the article.

A.V. Smirnov—scientific editing, conceptualization.

M.V. Korniyushin, L.A. Arbanas—experiments on the cold sintering.

V.E. Bazarova—density and porosity measurements.

L.A. Arbanas, A.N. Khrustalev—X-ray diffraction analysis.

A.V. Shumyantsev, S.Yu. Kupreenko—thermal analysis.

Yu.D. Ivakin—conceptualization, synthesis of aluminum oxohydroxides.

The authors declare no obvious and potential conflicts of interest related to the publication of this article.

REFERENCES

1. Amrute A.P., Jeske K., Łodziana Z., Prieto G., Schüth F. Hydrothermal Stability of High-Surface-Area α -Al₂O₃ and Its Use as a Support for Hydrothermally Stable Fischer–Tropsch Synthesis Catalysts. *Chem. Mater.* 2020;32(10):4369–4374. <https://doi.org/10.1021/acs.chemmater.0c01587>
2. Huang C.L., Wang J.J., Huang C.Y. Sintering behavior and microwave dielectric properties of nano alpha-alumina. *Mater. Lett.* 2005;59(28):3746–3749. <https://doi.org/10.1016/j.matlet.2005.06.053>
3. Asimakopoulou A., Gkekas I., Kastrinaki G., Prigione A., Zaspalis V.T., Petrakis S. Biocompatibility of α -Al₂O₃ Ceramic Substrates with Human Neural Precursor Cells. *J. Funct. Biomater.* 2020;11(3):65. <https://doi.org/10.3390/jfb11030065>
4. MacKenzie K.J.D., Temuujin J., Okada K. Thermal decomposition of mechanically activated gibbsite. *Thermochim. Acta.* 1999;327(1–2):103–108. [https://doi.org/10.1016/S0040-6031\(98\)00609-1](https://doi.org/10.1016/S0040-6031(98)00609-1)
5. Xie Y., Kocaefe D., Kocaefe Y., Cheng J., Liu W. The Effect of Novel Synthetic Methods and Parameters Control on Morphology of Nano-alumina Particles. *Nanoscale Res. Lett.* 2016;11(1):259. <https://doi.org/10.1186/s11671-016-1472-z>
6. Suchanek W.L. Hydrothermal Synthesis of Alpha Alumina (α -Al₂O₃) Powders: Study of the Processing Variables and Growth Mechanisms. *J. Am. Ceram. Soc.* 2010;93(2):399–412. <https://doi.org/10.1111/j.1551-2916.2009.03399.x>
7. Ivakin Yu.D., Danchevskaya M.N., Muravieva G.P. Induced formation of corundum crystals in supercritical water fluid. *Russ. J. Phys. Chem. B.* 2015;9(7):1082–1094. <https://doi.org/10.1134/S1990793115070088> [Original Russian Text: Ivakin Yu.D., Danchevskaya M.N., Muravieva G.P. Induced formation of corundum crystals in supercritical water fluid. *Sverkhkritischeskie Flyuidy: Teoriya i Praktika.* 2014;9(3):36–54 (in Russ.).]
8. Galotta A., Sglavo V.M. The cold sintering process: A review on processing features, densification mechanisms and perspectives. *J. Eur. Ceram. Soc.* 2021;41(16):1–17. <https://doi.org/10.1016/j.jeurceramsoc.2021.09.024>
9. Ndayishimiye A., Sengul M.Y., Sada T., Dursun S., Bang S.H., Grady Z.A., *et al.* Roadmap for densification in cold sintering: Chemical pathways. *Open Ceram.* 2020;2:100019. <https://doi.org/10.1016/j.oceram.2020.100019>
10. Huang Y., Huang K., Zhou S., Lin C., Wu X., Gao M., *et al.* Influence of incongruent dissolution-precipitation on 8YSZ ceramics during cold sintering process. *J. Eur. Ceram. Soc.* 2022;42(5):2362–2369. <https://doi.org/10.1016/j.jeurceramsoc.2021.12.072>
11. Ndayishimiye A., Fan Z., Mena-Garcia J., Anderson J.M., Randall C.A. Coalescence in cold sintering: A study on sodium molybdate. *Open Ceram.* 2022;11:100293. <https://doi.org/10.1016/j.oceram.2022.100293>
12. Ivakin Yu.D., Smirnov A.V., Kormilitsin M.N., Kholodkova A.A., *et al.* Effect of Mechanical Pressure on the Recrystallization of Zinc Oxide in a Water Fluid Medium under Cold Sintering. *Russ. J. Phys. Chem. B.* 2021;15(8):1228–1250. <https://doi.org/10.1134/S1990793121080054> [Original Russian Text: Ivakin Yu.D., Smirnov A.V., Kormilitsin M.N., Kholodkova A.A., Vasin A.A., Korniyushin M.V., Tarasovskii V.P., Rybal'chenko V.V. Effect of Mechanical Pressure on the Recrystallization of Zinc Oxide in a Water Fluid Medium under Cold Sintering. *Sverkhkritischeskie Flyuidy: Teoriya i Praktika.* 2021;16(1):17–51 (in Russ.). <https://doi.org/10.34984/SCFTP.2021.16.1.002>]
13. Sengul M.Y., Guo J., Randall C.A., van Duin A.C.T. Water-Mediated Surface Diffusion Mechanism Enables the Cold Sintering Process: A Combined Computational and Experimental Study. *Angew. Chem. Int. Ed.* 2019;58(36):12420–12424. <https://doi.org/10.1002/anie.201904738>
14. Kang S., Zhao X., Guo J., Liang J., Sun J., Yang Y., *et al.* Thermal-assisted cold sintering study of Al₂O₃ ceramics: Enabled with a soluble γ -Al₂O₃ intermediate phase. *J. Eur. Ceram. Soc.* 2023;43(2):478–485. <https://doi.org/10.1016/j.jeurceramsoc.2022.10.039>
15. Kholodkova A.A., Korniyushin M.V., Pakhomov M.A., Smirnov A.V., Ivakin Y.D. Water-Assisted Cold Sintering of Alumina Ceramics in SPS Conditions. *Ceramics.* 2023;6(2):1113–1128. <https://doi.org/10.3390/ceramics6020066>
16. Yamaguchi K., Hashimoto S. Effect of phase transformation in cold sintering of aluminum hydroxide. *J. Eur. Ceram. Soc.* 2024;44(5):2754–2761. <https://doi.org/10.1016/j.jeurceramsoc.2023.12.054>
17. Kloprogge J.T., Ruan H.D., Frost R.L. Thermal decomposition of bauxite minerals: infrared emission spectroscopy of gibbsite, boehmite and diaspor. *J. Mater. Sci.* 2002;37(6):1121–1129. <https://doi.org/10.1023/A:1014303119055>
18. Banerjee J.C., De S.K., Nandi D.N. Diaspore as a Refractory Raw Material. *Trans. Indian Ceram. Soc.* 1966;25(1):80–84. <https://doi.org/10.1080/0371750X.1966.10855557>
19. Parida K.M., Pradhan A.C., Das J., Sahu N. Synthesis and characterization of nano-sized porous gamma-alumina by control precipitation method. *Mater. Chem. Phys.* 2009;113(1):244–248. <https://doi.org/10.1016/j.matchemphys.2008.07.076>
20. He F., Li W., Pang T., Zhou L., Wang C., Liu H., *et al.* Hydrothermal synthesis of boehmite nanorods from alumina sols. *Ceram. Int.* 2022;48(13):18035–18047. <https://doi.org/10.1016/j.ceramint.2022.02.212>
21. Kozerozhets I.V., Panasyuk G.P., Semenov E.A., Avdeeva V.V., Danchevskaya M.N., Simonenko N.P., *et al.* Recrystallization of nanosized boehmite in an aqueous medium. *Powder Technol.* 2023;413:118030. <https://doi.org/10.1016/j.powtec.2022.118030>
22. Egorova S.R., Muhamedyarova A.N., Zhang Yu., Lamberov A.A. Effect of hydrothermal treatment of γ -Al₂O₃ on boehmite properties. *Butlerov Commun.* 2017;51(7):102–114 (in Russ.). <https://doi.org/10.37952/ROI-jbc-01/17-51-7-102>
23. Torkar K. Untersuchungen über Aluminiumhydroxyde und -oxyde. 5. Mitt.: Darstellung von reinstem α -Aluminiumoxyd und Diaspor. *Monatshfte für Chemie.* 1960;91(5):757–763. <https://doi.org/10.1007/BF00929547>
24. Carim A.H., Rohrer G.S., Dando N.R., Tzeng S., Rohrer C.L., Perrotta A.J. Conversion of Diaspore to Corundum: A New α -Alumina Transformation Sequence. *J. Am. Ceram. Soc.* 1997;80(10):2677–2680. <https://doi.org/10.1111/j.1151-2916.1997.tb03171.x>
25. Oh C.J., Yi Y.K., Kim S.J., Tran T., Kim M.J. Production of micro-crystalline boehmite from hydrothermal processing of Bayer plant alumina tri-hydrate. *Powder Technol.* 2013;235:556–562. <https://doi.org/10.1016/j.powtec.2012.10.041>
26. Santos P.D.S., Coelho A.C.V., Santos H.D.S., Kiyohara P.K. Hydrothermal synthesis of well-crystallised boehmite crystals of various shapes. *Mater. Res.* 2009;12(4):437–445. <http://doi.org/10.1590/S1516-14392009000400012>
27. Liu Y., Zhu W., Guan K., Peng C., Wu J. Preparation of high permeable alumina ceramic membrane with good separation performance via UV curing technique. *RSC Adv.* 2018;8(24):13567–13577. <https://doi.org/10.1039/C7RA13195J>

28. Zhu J., Fan Y., Xu N. Modified dip-coating method for preparation of pinhole-free ceramic membranes. *J. Membr. Sci.* 2011;367(1–2):14–20. <https://doi.org/10.1016/j.memsci.2010.10.024>
29. Ha J.H., Abbas Bukhari S.Z., Lee J., Song I.H., Park C. Preparation processes and characterizations of alumina-coated alumina support layers and alumina-coated natural material-based support layers for microfiltration. *Ceram. Int.* 2016;42(12):13796–13804. <https://doi.org/10.1016/j.ceramint.2016.05.181>
30. Naseer D., Ha J.H., Lee J., Song I.H. Preparation of Al_2O_3 Multichannel Cylindrical-Tube-Type Microfiltration Membrane with Surface Modification. *Appl. Sci.* 2022;12(16):7993. <https://doi.org/10.3390/app12167993>
31. Song I.H., Bae B.S., Ha J.H., Lee J. Effect of hydraulic pressure on alumina coating on pore characteristics of flat-sheet ceramic membrane. *Ceram. Int.* 2017;43(13):10502–10507. <https://doi.org/10.1016/j.ceramint.2017.05.098>
32. Feng J., Fan Y., Qi H., Xu N. Co-sintering synthesis of tubular bilayer α -alumina membrane. *J. Membr. Sci.* 2007;288(1–2):20–27. <https://doi.org/10.1016/j.memsci.2006.09.034>

About the authors

Anastasia A. Kholodkova, Cand. Sci. (Chem.), Senior Researcher, Department of Scientific Research Coordination, State University of Management (99, Ryazansky pr., Moscow, 109545, Russia). E-mail: anastasia.kholodkova@gmail.com. Scopus Author ID 56530861400, Researcher ID M-2169-2016, RSCI SPIN-code 7256-7784, <https://orcid.org/0000-0002-9627-2355>

Maksim V. Korniyushin, Junior Researcher, Department of Scientific Research Coordination, State University of Management (99, Ryazansky pr., Moscow, 109545, Russia). E-mail: maksim.korn0312@yandex.ru. Scopus Author ID 57219230569, RSCI SPIN-code 7995-3408, <https://orcid.org/0000-0001-6104-7716>

Andrey V. Smirnov, Cand. Sci. (Eng.), Head of the Laboratory of Ceramic Materials and Technologies, MIREA – Russian Technological University (86, Vernadskogo pr., Moscow, 119571, Russia). E-mail: smirnov_av@mirea.ru. ResearcherID J-2763-2017, Scopus Author ID 56970389000, RSCI SPIN-code 2919-9250, <https://orcid.org/0000-0002-4415-5747>

Levko A. Arbanas, Research Intern, Laboratory of Ceramic Materials and Technologies, MIREA – Russian Technological University (86, Vernadskogo pr., Moscow, 119571, Russia). E-mail: levko.147@icloud.com. Scopus Author ID 58523360800, <https://orcid.org/0009-0005-9813-8829>

Arseniy N. Khrustalev, Engineer, Laboratory of Ceramic Materials and Technologies, MIREA – Russian Technological University (86, Vernadskogo pr., Moscow, 119571, Russia). E-mail: lywn@yandex.ru. RSCI SPIN-code 6804-4093, <https://orcid.org/0000-0002-5386-7850>

Viktoriya E. Bazarova, Engineer, Laboratory of Ceramic Materials and Technologies, MIREA – Russian Technological University (86, Vernadskogo pr., Moscow, 119571, Russia). E-mail: bazarovave@yandex.ru. <https://orcid.org/0009-0000-8865-2828>

Aleksey V. Shumyantsev, Cand. Sci. (Chem.), Researcher, Laboratory of Catalysis and Gas Electrochemistry, Chemistry Department, Lomonosov Moscow State University (1-9, Leninskie Gory, Moscow, 119991, Russia); Chief Specialist of the Department, Russian Institute for Scientific and Technical Information (20, Usievicha ul., Moscow, 125190, Russia). E-mail: alex-chim@mail.ru. Scopus Author ID 57193644084, <https://orcid.org/0000-0002-0166-4912>

Stepan Yu. Kupreenko, Cand. Sci. (Phys.-Math.), Senior Researcher, Laboratory of Catalysis and Gas Electrochemistry, Chemistry Department, Lomonosov Moscow State University (1-9, Leninskie Gory, Moscow, 119991, Russia). E-mail: kupreenko@physics.msu.ru. Scopus Author ID 54784525900, RSCI SPIN-code 4587-9183, <https://orcid.org/0000-0003-3469-9406>

Yurii D. Ivakin, Cand. Sci. (Chem.), Senior Researcher, Laboratory of Catalysis and Gas Electrochemistry, Chemistry Department, Lomonosov Moscow State University (1-9, Leninskie Gory, Moscow, 119991, Russia); Senior Researcher, Mobile Solutions Engineering Center, MIREA – Russian Technological University (86, Vernadskogo pr., Moscow, 119571, Russia). E-mail: ivakin@kge.msu.ru. Scopus Author ID 6603058433, RSCI SPIN-code 7337-4173, <https://orcid.org/0000-0002-8416-3071>

Об авторах

Холодкова Анастасия Андреевна, к.х.н., старший научный сотрудник Управления координации научных исследований, ФГБОУ ВО «Государственный университет управления» (109542, Россия, Москва, Рязанский пр-т, д. 99). E-mail: anastasia.kholodkova@gmail.com. Scopus Author ID 56530861400, Researcher ID M-2169-2016, SPIN-код РИНЦ 7256-7784, <https://orcid.org/0000-0002-9627-2355>

Корнюшин Максим Витальевич, младший научный сотрудник, Управление координации научных исследований, ФГБОУ ВО «Государственный университет управления» (109542, Россия, Москва, Рязанский пр-т, д. 99). E-mail: maksim.korn0312@yandex.ru. Scopus Author ID 57219230569, SPIN-код РИНЦ 7995-3408, <https://orcid.org/0000-0001-6104-7716>

Смирнов Андрей Владимирович, к.т.н., заведующий Лабораторией керамических материалов и технологий, ФГБОУ ВО «МИРЭА – Российский технологический университет» (119571, Россия, Москва, пр-т Вернадского, д. 86). E-mail: smirnov_av@mirea.ru. ResearcherID J-2763-2017, Scopus Author ID 56970389000, SPIN-код РИНЦ 2919-9250, <https://orcid.org/0000-0002-4415-5747>

Арбанас Левко Андреевич, стажер-исследователь, Лаборатория керамических материалов и технологий, ФГБОУ ВО «МИРЭА – Российский технологический университет» (119571, Россия, Москва, пр-т Вернадского, д. 86). E-mail: levko.147@icloud.com. Scopus Author ID 58523360800, <https://orcid.org/0009-0005-9813-8829>

Хрусталеv Арсений Николаевич, инженер, Лаборатория керамических материалов и технологий, ФГБОУ ВО «МИРЭА – Российский технологический университет» (119571, Россия, Москва, пр-т Вернадского, д. 86). E-mail: lywn@yandex.ru. SPIN-код РИНЦ 6804-4093, <https://orcid.org/0000-0002-5386-7850>

Базарова Виктория Евгеньевна, инженер, Лаборатория керамических материалов и технологий, ФГБОУ ВО «МИРЭА – Российский технологический университет» (119571, Россия, Москва, пр-т Вернадского, д. 86). E-mail: bazarovave@yandex.ru. <https://orcid.org/0009-0000-8865-2828>

Шумянец Алексей Викторович, к.х.н., научный сотрудник, Лаборатория катализа и газовой электрохимии кафедры физической химии, Химический факультет, ФГБОУ ВО «Московский государственный университет имени М.В. Ломоносова» (119991, Россия, Москва, Ленинские Горы, д. 1, стр. 9); главный специалист подразделения, ФГБУН «Всероссийский институт научной и технической информации Российской академии наук» (125190, Россия, Москва, ул. Усиевича, д. 20). E-mail: alex-chim@mail.ru. Scopus Author ID 57193644084, <https://orcid.org/0000-0002-0166-4912>

Купреенко Степан Юрьевич, к.ф.-м.н., старший научный сотрудник, Лаборатория катализа и газовой электрохимии кафедры физической химии, Химический факультет, ФГБОУ ВО «Московский государственный университет имени М.В. Ломоносова» (119991, Россия, Москва, Ленинские Горы, д. 1, стр. 9). E-mail: kupreenko@physics.msu.ru. Scopus Author ID 54784525900, SPIN-код РИНЦ 4587-9183, <https://orcid.org/0000-0003-3469-9406>

Ивакин Юрий Дмитриевич, к.х.н., старший научный сотрудник, Лаборатория катализа и газовой электрохимии кафедры физической химии, Химический факультет, ФГБОУ ВО «Московский государственный университет имени М.В. Ломоносова» (119991, Россия, Москва, Ленинские Горы, д. 1, стр. 9); старший научный сотрудник, Инжиниринговый центр мобильных решений, ФГБОУ ВО «МИРЭА – Российский технологический университет» (119571, Россия, Москва, пр-т Вернадского, д. 86). E-mail: ivakin@kge.msu.ru. Scopus Author ID 6603058433, SPIN-код РИНЦ 7337-4173, <https://orcid.org/0000-0002-8416-3071>

Translated from Russian into English by H. Moshkov

Edited for English language and spelling by Dr. David Mossop

Synthesis and processing of polymers and polymeric composites
Синтез и переработка полимеров и композитов на их основе

UDC 655.026

<https://doi.org/10.32362/2410-6593-2024-19-4-350-359>

EDN EZTLUE



RESEARCH ARTICLE

Application of interlayer perforation and installation of transparent elements in the technology of duplicated decorative polymer films

Alexander A. Nikolaev✉, Alexander P. Kondratov

Moscow Polytechnic University, Moscow, 127008 Russia

✉ Corresponding author, e-mail: nikolaevaleksandr1992@gmail.com

Abstract

Objectives. To develop technologies for producing multilayer films of transparent thermoplastic polymers; to study methods of modifying their supramolecular structure; and to determine their optical properties by means of optical-polarization methods for the use of modified films as decorative and design materials in modern architecture.

Methods. Industrial samples of polystyrene, low-density polyethylene, polypropylene, and polyvinyl chloride films from various manufacturers (*Don Polimer*, *Vektor*, and *Sibur*) were the objects of the study. The optical properties of the films were studied by means polarized-light spectrophotometry. In order to modify the supramolecular structure of the polymers, the surfaces of the films were treated under isometric conditions with volatile solvents or their aqueous solutions. Parts of the layers of multilayer films were removed by cutting with a punching knife using a press or with a manual device for perforating printing materials.

Results. The spectral characteristics of multilayer films of several transparent thermoplastic polymers in polarized light were determined. The study showed that a wide palette of colors and contrasting images can be obtained by mechanically removing part of the layers of multilayer films. The phenomenon of pseudo-disappearance of the outermost layer was discovered after treatment of a stack of films under isometric conditions with volatile solvents or their aqueous solutions.

Conclusions. Based on the example of large-scale production thermoplastics, it was shown that a combination of technological methods of stacking, perforation, and local plasticization of films of transparent thermoplastic polymers can produce pleochroic multicolor materials for a range of human activities. The possibility of hidden coding of information on multilayer packaging materials, and its visualization and instrumental reading in polarized light was confirmed by color differential and contrast of 150 and 60 units, respectively. It was also shown that several monochrome tones of different lightness and brightness can be obtained by varying the number of layers or perforating the films in multilayer materials.

Keywords

birefringence, interference image, modification, shrink films, internal stresses, supramolecular structure

Submitted: 28.02.2023

Revised: 27.12.2023

Accepted: 21.06.2024

For citation

Nikolaev A.A., Kondratov A.P. Application of interlayer perforation and installation of transparent elements in the technology of duplicated decorative polymer films. *Tonk. Khim. Tekhnol. = Fine Chem. Technol.* 2024;19(4):350–359. <https://doi.org/10.32362/2410-6593-2024-19-4-350-359>

НАУЧНАЯ СТАТЬЯ

Применение межслойной перфорации и закладки прозрачных элементов в технологии дублированных декоративных полимерных пленок

А.А. Николаев✉, А.П. Кондратов

Московский политехнический университет, Москва, 127008 Россия

✉ Автор для переписки, e-mail: nikolaevaleksandr1992@gmail.com

Аннотация

Цель. Исследовать технологии многослойных пленок из прозрачных термопластичных полимеров, способы модификации их надмолекулярной структуры, а также изучить их оптические свойства с помощью оптико-поляризационных методов для использования модифицированных пленок в качестве декоративных и дизайнерских материалов в современной архитектуре.

Методы. Объектами исследования являлись промышленные образцы пленок полистирола, полиэтилена низкой плотности, полипропилена и поливинилхлорида различных производителей («Дон Полимер», «Вектор» и «Сибур»). Оптические свойства пленок исследовали с помощью спектрофотометрии в поляризованном потоке света. Для модификации надмолекулярной структуры полимеров поверхности пленок обрабатывали в изометрических условиях летучими растворителями или их водными растворами. Части слоев многослойных пленок удаляли высечкой штанцевым ножом с помощью пресса или ручным устройством для перфорации полиграфических материалов.

Результаты. Получены спектральные характеристики многослойных пленок из нескольких прозрачных термопластичных полимеров в поляризованном потоке света. Показаны возможности получения широкой палитры цветов и контрастных изображений механическим удалением части слоев многослойных пленок. Обнаружен эффект «псевдоисчезновения» внешнего слоя при обработке пакета пленок в изометрических условиях летучими растворителями или их водными растворами.

Выводы. На примере крупнотоннажных термопластов показано, что сочетанием технологических приемов сборки, перфорирования и локальной пластификации пленок из прозрачных термопластичных полимеров можно решать задачи создания многоцветных материалов с эффектом плеохроизма для различных сфер деятельности человека. Возможность скрытого кодирования информации на многослойных упаковочных материалах, ее визуализации и инструментального считывания в поляризованном свете подтверждена достаточным цветовым отличием и контрастом в 150 и 60 единиц соответственно. Показана возможность получения нескольких монохромных тонов различной светлоты и яркости варьированием числа слоев или перфорацией пленок в многослойных материалах.

Ключевые слова

двойное лучепреломление, интерференционное изображение, модификация, термоусадочные пленки, внутренние напряжения, надмолекулярная структура

Поступила: 28.02.2023

Доработана: 27.12.2023

Принята в печать: 21.06.2024

Для цитирования

Николаев А.А., Кондратов А.П. Применение межслойной перфорации и закладки прозрачных элементов в технологии дублированных декоративных полимерных пленок. *Тонкие химические технологии*. 2024;19(4):350–359. <https://doi.org/10.32362/2410-6593-2024-19-4-350-359>

INTRODUCTION

Established optical phenomena in polarized light in the form of a bright color of alternating stripes in transparent polymer bodies when under mechanical stresses enable their destruction to be predicted. They also enable the permissible level of load during operation to be monitored [1–2]. This practically important and effective method of non-destructive testing and mechanical testing of models constructed from transparent materials is used in the design of complex machine parts and building structures. Another

important application of optical color effects in polarized light in transparent polymers is hidden packaging marking technology [3]. The creation of colored labels, multilayer labels, and other elements of original polymer products can also provide protection from counterfeiting. The advantages of such technologies include the creation of eye-catching color effects on products and packaging without the use of toxic dyes and pigments, the possibility of recycling used products and packaging made of thermoplastic polymer materials, as well as the production of feedstock (large-scale production polymers) [4].

Colors resulting from the interaction of light with spatially ordered or quasi-amorphous nanostructures or microstructures are called structural colors [5]. Such colors are widely found in nature in a range of insects, plants, and animals [6, 7]. Structural colors with a wide range of shades also appear in transparent polymer films with a high level of internal stress when polarized light passes through them. The heat sensitivity of the structural color of films of large-scale production thermoplastics is very specific. It depends on the presence of low-molecular ingredients in them and the features of the film formation technology. This may slightly increase their cost, but significantly expands the scope of application [8].

Internal stresses in polymer products and films are a natural consequence of their production technology [9]. Thin polymer films are produced by the extrusion and jet drawing of a melt. This is followed by the orientation of an elastic preform, during which internal stresses in the film are frozen. This procedure creates one-dimensional anisotropic shrink labels and biaxially oriented films of thermoplastics: polypropylene, polyethylene, polyvinyl chloride, and polyamides [10, 11]. The combination and duplication of these materials opens up new possibilities for their practical application in a range of industries and construction. A further factor is the variety of optical phenomena [12] caused by refraction, reflection, polarization, and interference of natural daylight and artificial light, as a combination of multiphase electromagnetic radiation [13].

The intensity of white light after passing through the polarizer–stressed structures–polarizer transparent system can be determined by the following expression:

$$I = \sin^2 2\alpha \sum I_\lambda \sin^2 \frac{\Phi_\lambda}{2},$$

where I is the light intensity, α is the angle between the polarization axis and the vector of the incident light, I_λ is the light intensity of the wavelength from the spectrum, and Φ_λ is the difference in the wavelength path from the radiation spectrum [1].

The phase difference of light-emitting and light-reflecting objects at the point of observation through the film depends on internal stresses and causes the phenomenon of pleochroism, i.e., the dependence of their color on their relative position relative to the radiation source and the observer. The use of pleochroism was proposed, in order to create new methods for protecting products made of transparent polymers from counterfeiting and for identifying original products by packaging, as well as to produce decorative light panels and transparent interior design elements [14, 15].

The purpose of this work was to investigate methods for controlling pleochroism in multilayer polymer materials made of thermoplastic polymers by varying the polymer used and treatment method and to justify the possibility of using them for the hidden recording of information by bar coding.

EXPERIMENTAL

Industrial samples of colorless transparent shrink films made of thermoplastic carbon-chain polymers produced in Russia were the objects of the study. They are low-density polyethylene with a thickness of $50 \pm 2 \mu\text{m}$, Biaxplen HGPL polypropylene $30 \pm 1.5 \mu\text{m}$ thick (*Sibur-Biaksplen*, Russia), polyvinyl chloride $50 \pm 2 \mu\text{m}$ thick (*Don-Polimer*, Russia), and polystyrene $60 \pm 2 \mu\text{m}$ thick (*Vektor*, Russia).

Birefringence experiments were carried out on a laboratory setup (Fig. 1) designed for photography and optical measurements in transmitted polarized light. The radiation source was a light-emitting diode (LED) strip with a color temperature of the transmitted light flux (6500 K) and a nonlinear spectral characteristic (Fig. 2). The LED strip was mounted around the perimeter of a sealed box with a transparent window made of silicate glass, on which a film linear polarizer (*Nitto Denko*, Japan) was placed. After passing through the polarizer and the analyzer in a crossed position, the radiation spectrum can be considered to be either monotonic or linear [1, 13] (Fig. 2).

The spectral characteristics of the radiation source, polarizing films, and stacks of shrink films before and after external influences were determined using an X-Rite i1Pro spectrophotometer (*X-Rite Inc.*, USA). The spotread command line tool from the ArgylCMS software¹, version 2.3.0, was used. The measurements were made in the “high-resolution” mode (measurement step 3.333 nm). The radiation characteristics and the color of the transmitted light were recorded in units of spectral radiance: watt per steradian per square meter per nanometer ($\text{mW}/(\text{sr}\cdot\text{m}^2\cdot\text{nm})$). The spectrophotometer was also used to evaluate the contrast of images visible in polarized light and to determine the CIE Lab² color coordinates used to calculate the color difference ΔE_{ab} :

$$\Delta E_{ab} = \sqrt{(L_2^* - L_1^*)^2 + (a_2^* - a_1^*)^2 + (b_2^* - b_1^*)^2},$$

where L^* is lightness, a^* are red–green coordinates, and b^* are yellow–blue coordinates.

Based on the spectral transmittances of different areas of the multilayer films, color coordinates were calculated

¹ <https://www.argyllcms.com/>. Accessed February 8, 2023.

² CIE Lab is a color space defined by the International Commission on Illumination (CIE) in 1976.

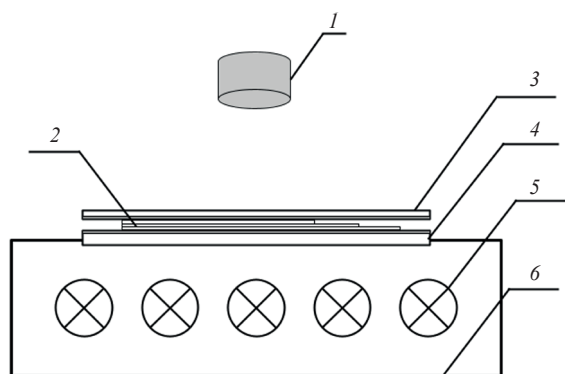


Fig. 1. Schematic of a setup for measuring the spectral characteristics of film samples: (1) spectrophotometer, (2) a film sample or a stack of films (Stoletov's stack), (3) movable polarizer, (4) fixed polarizer, (5) LED strip around the perimeter of the camera, and (6) sealed chamber

in the XYZ space, where Y is the luminance component. Then, from one Y_1 value, the Y_2 value for the adjacent area was subtracted, in order to give the symbol contrast.

The internal stresses in samples of polymer films were altered by plasticization through local treatment with active solvents and their aqueous solutions (tetrahydrofuran, acetone, methylformamide, Russia). Heat treatment was performed in laboratory-scale apparatuses for welding polymer films of various designs [16].

The color effects were visually recorded using a Nikon D7000 camera (*Nikon*, Japan).

From the selected polymer materials, films were arranged in Stoletov's stacks. This also involved the cutting of part of the layers or the addition of flat transparent elements using both monopolymer films or a combination of films of different thermoplastics.

RESULTS AND DISCUSSION

In order to obtain and quantify pleochroism, film samples were cut into strips of various lengths and 30 mm wide along (or across) the winding direction of the roll and stacked on top of each other in Stoletov stacks. From 2 to 14 layers were used, in order to prepare a stack of films. The stacking of more layers of film significantly reduces the intensity of transmitted light and the accuracy of measurements [12].

The maximum rainbow effect was seen on films of amorphous glassy polymers: polyvinyl chloride and polystyrene. Films of elastic crystallizable polymers produced color palettes with were less bright and less multicolor. The lower level of brightness of the colors in polyethylene stacks is apparently due to decreasing the level of internal stress in the materials because of relaxation during storage. Table 1 indicates the original

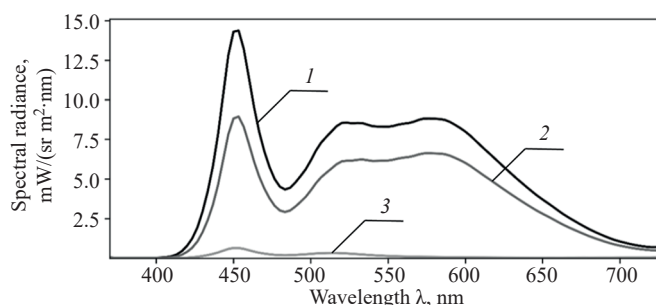


Fig. 2. Spectral radiances of the LED strip: (1) light spectrum of the radiation source, (2) light spectrum through two linear polarizers with mutually parallel polarization axes, and (3) light spectrum through two linear polarizers with mutually perpendicular polarization axes

color when observed at a right angle, the order of color changes and changes in the lightness of shades, the frequency of occurrence and alternation of the color gamut for each polymer and film stack. For polyvinyl chloride and polystyrene films, color and lightness are repeated every 2–3 layers. In low-density polyethylene and polypropylene film stacks, color is repeated in every other layer.

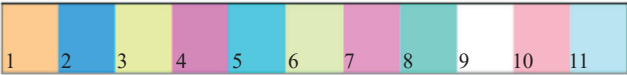
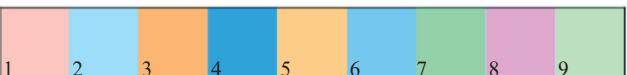
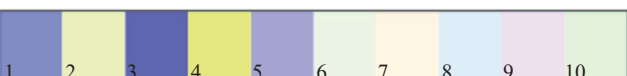
For the purposes of the practical application of the results of the spectrophotometry of multilayer films of all the polymers studied, Fig. 3 indicates points with color coordinates in the color diagram (Fig. 3).

Active solvents which cause plasticization of polymers and a decrease in internal stresses in films affect the color palette of a stack of films of amorphous glassy polymers: polyvinyl chloride and polystyrene. The reason for the change in color of the film stack in polarized light is due to a change in the internal stresses of these polymers due to plasticization [17]. Even short-term (several minutes) exposure of the film surface to a solvent led to a noticeable local change in the color of the film stack (Fig. 4). In the case of multilayer samples, in the areas of contact between the film and the liquid, the colors of adjacent internal layers appear under the outermost layer which absorbs a certain amount of solvent. This phenomenon can be called pseudo-disappearance of the outermost layer of the multilayer film. After the solvent evaporates, this local optical effect persists for a long time, indicating an irreversible decrease in internal stresses.

The effect of solvents on the film color can be used in the technology of special liquid-sensitive materials for security printing. One of the methods of operational visual control is wetting the surface of prints on special water and fluid-sensitive materials with test liquids or solutions. This can be used to verify the authenticity of banknotes and documents [18].

It is reasonable to assume that the transillumination of a film stack causes no changes in the outermost layer

Table 1. Film colors when observed at a right angle

Polymer	Color palette
Polyvinyl chloride	
Polystyrene	
Low-density polyethylene	
Polypropylene	

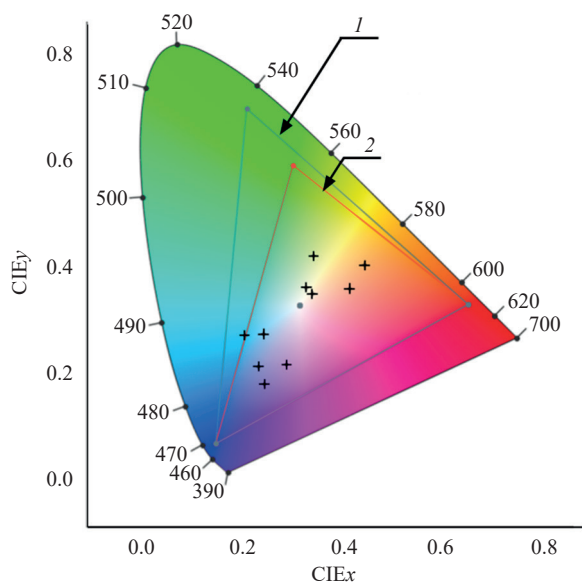


Fig. 3. Positions of colors of a polyvinyl chloride film stack on the CIE_{xy} chromaticity diagram: (1) Adobe RGB (1998) color gamut and (2) sRGB color gamut

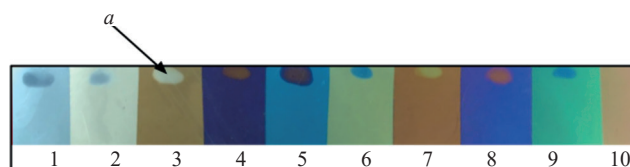


Fig. 4. Exposure of a PVC film to the solvent in areas *a*. The numbers 1–10 show the number of layers in ascending order

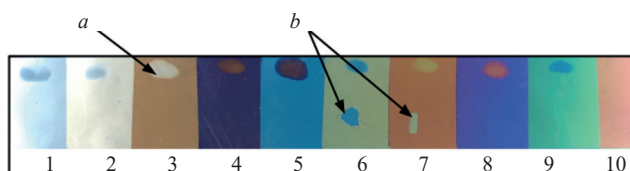


Fig. 5. Short-term local exposure of a film to solvent in areas *a* and cutting of one layer of film in areas *b*

of the film in the direction and phases of the light beam. This is due to the absence of film in this place. This phenomenon is known as pseudo-disappearance of the outermost layer from the stack of transparent films. Since the transmission of polarized light through a medium with internal stresses gives rise to an interference pattern, after contact with the solvent, there are either no internal stresses in the film, or their level is significantly reduced to such an extent that it is insufficient to change the characteristics of the transmitted light. In order to confirm this assumption about the physical essence of

the phenomenon of pseudo-disappearance, fragments of films inside and on the surface in different layers were specially cut out in a multilayer stack near the place where a drop of plasticizing liquid was applied. Transmitted polarized light from the film stack with perforated layers led to the same effect as exposure of the film to a volatile solvent (plasticizer).

The perforation of films has an important technological and operational advantage over treatment with solvent. It is not only the outer layers of films of multilayer materials that can be perforated (or not to any significant

Table 2. Color difference between adjacent layers

Material of polymer film	Color difference _{max}	Layers
Polystyrene	150	Between layer 10 and layer 5
Polyvinyl chloride	126	Between layer 8 and layer 6 Between layer 10 and layer 8
Polypropylene	125	Between layer 4 and layer 3
Low-density polyethylene	117	Between layer 9 and layer 8

Table 3. Contrasts of gradient color areas of a polyethylene film

Compared areas of multilayer stack	1–3	1–5	3–5	2–4	2–6	4–6	7–9
Contrast	44	48	12	29	23	9	11

extent), but also any inner ones. When the inner layers are perforated, the multilayer material with an image or text hidden from the naked eye will have a higher degree of strength and a higher resistance to external influences when used, e.g., as commercial packaging.

For the practical application of this effect, it is necessary to determine between which layers part of the film should be removed, in order to obtain the maximum color difference between adjacent areas. For quantitative assessment, the CIE76 color difference formula was used [3]. For each of the films, the maximum values of color difference and the number of layers at which it occurs were identified (Table 2).

Such indicators of color difference are many times greater than the threshold value distinguishable by the human eye: $\Delta E \approx 2-3$ [12]. These quantitative estimates are confirmed visually, since the lightness or brightness curves of these colors are different. In order to resolve the problems of hidden marking of multilayer films intended for packaging and protection against counterfeiting of expensive original products [12, 18], the most important factor is to compare the color indicators between shades of the same color. For example, in the case of low-density polyethylene films with repeating colors, a table of contrasts of areas of a multilayer film of the same spectral color, but different tones (gradient color), was compiled (Table 3).

The colors of such areas of the film appear identical, but their color difference ΔE is many times greater than the resolution of the human eye. This color difference

was determined for all polymer materials studied in this work. The presence of several shades of the same color in materials made of one polymer, but with a different number of layers, expands the artistic possibilities for creating a tone image.

Another important characteristic of multilayer films intended for marking is the contrast of adjacent areas of the film with different numbers of layers or cut locations. Image contrast is a quantity different from the color difference which shows the difference between two parameters [19].

For the film stacks under consideration and collected in Stoletov's stack (Fig. 3), the contrast was calculated (Table 4).

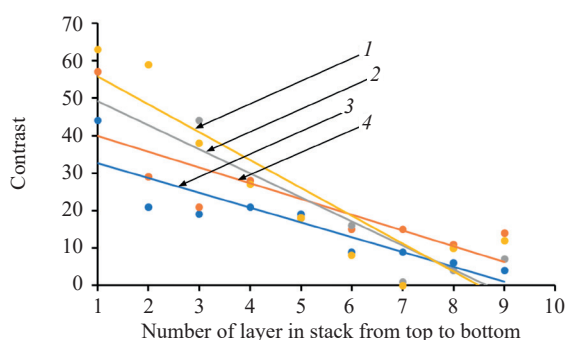
It can be noted (Fig. 6) that for the majority of the studied polymer films, maximum contrast occurs in the stack between layer 1 and layer 2. This is very important for use in the production of two-layer materials with high-contrast protective elements. It can be seen that the contrast of adjacent areas in multilayer films decreases as the number of layers increases (Fig. 6). Among the films studied, the level of contrast is maximum in Biaxplen HGPL polypropylene film (Biaxplen, Russia) intended for packaging food and dietary products for children.

CONCLUSIONS

Based on the example of large-scale production thermoplastics, the study showed that a combination

Table 4. Maximum contrast values of adjacent areas

Material of polymer film	Contrast _{max}	Layers
Low-density polyethylene	44	Between layer 1 and layer 2
Polystyrene	46	Between layer 10 and layer 3
Polyvinyl chloride	57	Between layer 1 and layer 2
Polypropylene	63	Between layer 1 and layer 2

**Fig. 6.** Color contrast of adjacent layers in films of thermoplastic polymers: (1) polypropylene, (2) polystyrene, (3) polyvinyl chloride, and (4) polyethylene

of technological methods of stacking, perforating, and plasticizing films of transparent thermoplastic polymers can produce colored materials for use in various human activities: architecture and construction for creating stained glass and multicolor theatrical scenery; in the production of multilayer light filters; and in retail trade for the coding and protection of product packaging from counterfeiting. Multilayer polymer materials which change color in polarized light depending on the location of the polarizers, the direction of the transmitted light, and the position of the observer (pleochroism) are structured from films of glassy amorphous and amorphous–crystalline polymers with a high level of internal stress. Changing the level of internal stresses in films without changing their overall dimensions can be achieved by treating the outer layers of polymer films

with volatile liquid solvents or plasticizers. The decrease in the level of internal stresses in the outer layers of duplicated polymer materials comprising N films after exposure to plasticizers, thus causing a change in the color of the film stack in polarized light to the color of materials comprising $N - 1$ layers of films, is referred to as pseudo-disappearance of the outermost layer. It forms the basis of a new technological method in production of decorative polymer materials and artistic works.

The pseudo-disappearance of the outermost layer and the perforation of the inner layers cause a significant color difference and contrast of adjacent areas of the film stack, reaching 150 and 60 units respectively. These contrast values are sufficient for the hidden barcoding of transparent product packaging, identifiable in polarized light.

Acknowledgments

This work was financially supported by the Moscow Polytechnic University within the framework of the Vladimir Fortov grant.

Authors' contributions

A.A. Nikolaev — planning the experiment, carrying out the study, collection and provision of the material, writing the article.

A.P. Kondratov — writing the article, scientific editing.

The authors declare no conflicts of interest.

REFERENCES

1. Aleksandrov A.Ya., Akhmetzyanov M.Kh. *Polyarizatsionno-opticheskie metody mekhaniki deformiruemogo tela (Polarization-Optical Methods of Mechanics of Deformable Body)*. Moscow: Nauka; 1973. 576 p. (in Russ.).
2. Markov A.V., Lobanov V.A. Study of the stress state of polycarbonate monolithic sheets using optical-polarization methods. *Tonk. Khim. Tekhnol. = Fine Chem. Technol.* 2022;17(1):65–75 (Russ., Eng.). <https://doi.org/10.32362/2410-6593-2022-17-1-65-75>
3. Nikolaev A.A., Ermakova I.N., Kondratov A.P. Variation range of color multilayer protective packaging elements made of polymers identified in polarized light. *Izvestiya TulGU. Tekhnicheskie nauki = Proceedings of the TSU. Technical Sciences.* 2017;(12–2):78–88 (in Russ.).
4. Ivanova N.G., Ivanchev S.S., Domareva N.M. Effect of conditions of synthesis on the composition and composition heterogeneity of poly-(styrene-block-methyl methacrylates), obtained by radical polymerization initiated by polyfunctional peroxides. *Polymer Sci. U.S.S.R.* 1976;18(12):3190–3196. [https://doi.org/10.1016/0032-3950\(76\)90434-2](https://doi.org/10.1016/0032-3950(76)90434-2) [Original Russian Text: Ivanova N.G., Ivanchev S.S., Domareva N.M. Effect of conditions of synthesis on the composition and composition heterogeneity of poly-(styrene-block-methyl methacrylates), obtained by radical polymerization initiated by polyfunctional peroxides. *Vysokomolekulyarnye Soedineniya. Seriya A.* 1976;18(12):2788–2792 (in Russ.). URL: http://polymsci.ru/static/Archive/1976/VMS_1976_T18_12/VMS_1976_T18_12_2788-2792.pdf]
5. Lim Y.-S., Kim J.S., Choi J.H., Kim J.M., Shim T.S. Solvatochromic discrimination of alcoholic solvents by structural colors of polydopamine nanoparticle thin films. *Colloid Interface Sci. Commun.* 2022;48:100624. <https://doi.org/10.1016/j.colcom.2022.100624>
6. Hsiung B.-K., Siddique R.H., Stavenga D.G., Otto J.C., Allen M.C., Liu Y., Lu Y.-F., Deheyn D.D., Shawkey M.D., Blackledge T.A. Rainbow peacock spiders inspire miniature super-iridescent optics. *Nat. Commun.* 2017;8(1):2278. <https://doi.org/10.1038/s41467-017-02451-x>
7. Teyssier J., Saenko S.V., van der Marel D., Milinkovitch M.C. Photonic crystals cause active colour change in chameleons. *Nat. Commun.* 2015;6:6368. <https://doi.org/10.1038/ncomms7368>
8. Wen X., Lu X., Li J., Wei C., Qin H., Liu Y., Yang S. Multi-responsive, flexible, and structurally colored film based on a 1D diffraction grating structure. *iScience.* 2022;25(4):104157. <https://doi.org/10.1016/j.isci.2022.104157>
9. Kondratov A.P., Cherkasov E.P., Paley V., Volinsky A.A. Recording, storage, and reproduction of information on polyvinylchloride films using shape memory effects. *Polymer.* 2021;13(11):1802. <https://doi.org/10.3390/polym13111802>
10. Vlasov S.V., Kuleznev V.N., Markov A.V., Lapin G.F., Markov N.G., Dontsova E.P., Blinov F.V., Zimin Yu.V. Biaxial orientation of polyamide films. *Plasticheskie Massy.* 1983;(2):41–43 (in Russ.).
11. Vlasov S.V., Markov A.V., Shcherbakova E.A., Chimed E. Highly oriented films from polypropylene and polypropylene compositions. *Konstruktsii iz kompozitsionnykh materialov = Composite Materials Constructions.* 2000;(3):21–25 (in Russ.).
12. Kondratov A.P., Yakubov V., Volinsky A.A. Recording digital color information on transparent polyethylene films by thermal treatment. *Appl. Opt.* 2019;58(1):172–176. <https://doi.org/10.1364/AO.58.000172>
13. Shurkliff W.A. *Polarized Light. Production and Use.* Cambridge, Massachusetts: Harvard University Press; 1962. 207 p.
14. Kondratov A.P. New materials for light strain-optical panels. *Light & Engineering.* 2014;22(3):74–77.
15. Kondratov A.P., Nazarov V.G., Nikolaev A.A. *Method for Recording and Reading Information on Colorless Transparent Polymer Films*: RF Pat. 2776598. Publ. 07.22.2022. (in Russ.).
16. Kondratov A.P., Volinsky A.A., Zhang Yi., Nikulchev E.V. Polyvinylchloride film local isometric heat treatment for hidden 3D printing on polymer packaging. *J. Appl. Polym.* 2016;133(8):43046. <http://doi.org/10.1002/app.43046>
17. Shibaev V.P., Petrukhin B.S., Zubov V.A., Kargin V.A., Plate N.A. Effect of branching length on crystallization and structure formation of polymers with different microstructures. In: *Elektronnaya mikroskopiya tverdykh tel i biologicheskikh ob'ektov.* Moscow: Nauka; 1969. P. 150. (in Russ.).
18. Maresin V.M. *Zashchishchennaya poligrafija: spravochnik (Security Printing: Reference Book)*. Moscow: Flinta; 2019. 640 p. (in Russ.).
19. Peli E. Contrast in complex images. *J. Opt. Soc. Am. A.* 1990;7(10):2032–2040. <https://doi.org/10.1364/JOSAA.7.002032>

СПИСОК ЛИТЕРАТУРЫ

1. Александров А.Я., Ахметзянов М.Х. Поляризационно-оптические методы механики деформируемого тела. Москва: Наука; 1973. 576 с.
2. Марков А.В., Лобанов В.Н. Синтез и переработка полимеров и композитов на их основе. *Тонкие химические технологии.* 2022;17(1): 65–75. <https://doi.org/10.32362/2410-6593-2022-17-1-65-75>
3. Николаев А.А., Ермакова И.Н., Кондратов А.П. Диапазон варьирования цвета многослойных защитных элементов упаковки из полимеров идентифицируемой в поляризованном свете. *Известия ТулГУ. Технические науки.* 2017;(12-2):78–88.
4. Иванова Н.Г., Иванчев С.С., Домарева Н.М. Влияние условий синтеза на состав и композиционную неоднородность поли-(стирол-блок-метилметакрилатов), получаемых радикальной полимеризацией, инициированной полифункциональными перекисными инициаторами. *Высокомолекулярные соединения. Серия А.* 1976;18(12): 2788–2792. URL: http://polymsci.ru/static/Archive/1976/VMS_1976_T18_12/VMS_1976_T18_12_2788-2792.pdf
5. Lim Y.-S., Kim J.S., Choi J.H., Kim J.M., Shim T.S. Solvatochromic discrimination of alcoholic solvents by structural colors of polydopamine nanoparticle thin films. *Colloid Interface Sci. Commun.* 2022;48:100624. <https://doi.org/10.1016/j.colcom.2022.100624>

6. Hsiung B.-K., Siddique R.H., Stavenga D.G., Otto J.C., Allen M.C., Liu Y., Lu Y.-F., Deheyn D.D., Shawkey M.D., Blackledge T.A. Rainbow peacock spiders inspire miniature super-iridescent optics. *Nat. Commun.* 2017;8(1):2278. <https://doi.org/10.1038/s41467-017-02451-x>
7. Teyssier J., Saenko S.V., van der Marel D., Milinkovitch M.C. Photonic crystals cause active colour change in chameleons. *Nat. Commun.* 2015;6:6368. <https://doi.org/10.1038/ncomms7368>
8. Wen X., Lu X., Li J., Wei C., Qin H., Liu Y., Yang S. Multi-responsive, flexible, and structurally colored film based on a 1D diffraction grating structure. *iScience.* 2022;25(4):104157. <https://doi.org/10.1016/j.isci.2022.104157>
9. Kondratov A.P., Cherkasov E.P., Paley V., Volinsky A.A. Recording, storage, and reproduction of information on polyvinylchloride films using shape memory effects. *Polymer.* 2021;13(11):1802. <https://doi.org/10.3390/polym13111802>
10. Власов С.В., Кулезнёв В.Н., Марков А.В., Лапин Г.Ф., Марков Н.Г., Донцова Э.П., Блинов Ф.В., Зимин Ю.В. Двухосная ориентация полиамидных пленок. *Пласт. массы.* 1983;(2):41–43.
11. Власов С.В., Марков А.В., Щербакова Е.А., Чимед Э. Высокоориентированные пленки из полипропилена и полипропиленовых композиций. *Конструкции из композиционных материалов.* 2000;(3):21–25.
12. Kondratov A.P., Yakubov V., Volinsky A.A. Recording digital color information on transparent polyethylene films by thermal treatment. *Appl. Opt.* 2019;58(1):172–176. <https://doi.org/10.1364/AO.58.000172>
13. Shurkliff W.A. *Polarized Light. Production and Use.* Cambridge, Massachusetts: Harvard University Press; 1962. 207 p.
14. Kondratov A.P. New materials for light strain-optical panels. *Light & Engineering.* 2014;22(3):74–77.
15. Кондратов А.П., Назаров В.Г., Николаев А.А. Способ записи и считывания информации на бесцветных прозрачных полимерных пленках: пат. 2776598 РФ. Заявка № 2021130867; заявл. 22.10.2021; опубл. 22.07.2022. Бюл. № 21.
16. Kondratov A.P., Volinsky A.A., Zhang Yi., Nikulchev E.V. Polyvinylchloride film local isometric heat treatment for hidden 3D printing on polymer packaging. *J. Appl. Polym.* 2016;133(8):43046. <http://doi.org/10.1002/app.43046>
17. Шибаев В.П., Петрухин Б.С., Зубов В.А., Каргин В.А., Платэ Н.А. Влияние длины разветвлений на кристаллизацию и структурообразование полимеров различной микроструктуры. В сб.: *Электронная микроскопия твердых тел и биологических объектов.* М.: Наука; 1969. С. 150.
18. Маресин В.М. *Защищенная полиграфия: справочник.* М.: Флинта; 2019. 640 с.
19. Peli E. Contrast in complex images. *J. Opt. Soc. Am. A.* 1990;7(10):2032–2040. <https://doi.org/10.1364/JOSAA.7.002032>

About the authors

Alexander A. Nikolaev, Lecturer, Department of Innovative Materials of the Print Media Industry, Moscow Polytechnic University (38, Bolshaya Semenovskaya ul., Moscow, 127008, Russia). E-mail: nikolaevaleksandr1992@gmail.com. Scopus Author ID 57224628186, ResearcherID AHB-3757-2022, RSCI SPIN-code 8146-7143, <https://orcid.org/0000-0003-3232-6753>

Alexander P. Kondratov, Dr. Sci. (Eng.), Professor, Head of the Department of Innovative Materials of the Print Media Industry, Moscow Polytechnic University (38, Bolshaya Semenovskaya ul., Moscow, 127008, Russia). E-mail: apkrezerw@mail.ru. Scopus Author ID 6603924314, RSCI SPIN-code 8689-3888, <https://orcid.org/0000-0001-6118-0808>

Об авторах

Николаев Александр Африканович, преподаватель кафедры «Инновационные материалы принтмедиаиндустрии», Полиграфический институт, ФГАОУ ВО «Московский политехнический университет» (127008, Россия, Москва, ул. Большая Семеновская, д. 38). E-mail: nikolaevaleksandr1992@gmail.com. Scopus Author ID 57224628186, ResearcherID АНВ-3757-2022, SPIN-код РИНЦ 8146-7143, <https://orcid.org/0000-0003-3232-6753>

Кондратов Александр Петрович, д.т.н., профессор, заведующий кафедрой «Инновационные материалы принтмедиаиндустрии», Полиграфический институт, ФГАОУ ВО «Московский политехнический университет» (127008, Россия, Москва, ул. Большая Семеновская, д. 38). E-mail: apkrezerv@mail.ru. Scopus Author ID 6603924314, SPIN-код РИНЦ 8689-3888, <https://orcid.org/0000-0001-6118-0808>

Translated from Russian into English by H. Moshkov

Edited for English language and spelling by Dr. David Mossop

Synthesis and processing of polymers and polymeric composites
Синтез и переработка полимеров и композитов на их основе

UDC 678.7

<https://doi.org/10.32362/2410-6593-2024-19-4-360-371>

EDN FGQTQY



RESEARCH ARTICLE

N-[(1*RS*)-Camphan-2-ylidene]-4-ethoxyaniline and its reduction product as stabilizers of nitrile butadiene rubbers

Dmitry A. Nilidin¹, Marat A. Vaniev¹,✉, Andrey A. Vernigora¹, Andrey V. Davidenko¹, Nikita A. Salykin¹, Thuy Dang Minh², Sergey G. Gubin², Ivan A. Novakov¹

¹ Volgograd State Technical University, Volgograd, 400005 Russia

² Institute of Tropical Materials Science, Joint Vietnam-Russia Tropical Science and Technology Research Center, Hanoi, Vietnam

✉ Corresponding author, e-mail: vaniev@vstu.ru

Abstract

Objectives. To investigate the protective efficacy of unreduced and reduced forms of the condensation product of D,L-camphor and *p*-ethoxyaniline in nitrile butadiene rubber formulations when compared with the conventional stabilizer *N*-isopropyl-*N'*-phenyl-*p*-phenylenediamine aged under laboratory and *in situ* climatic conditions in the tropics.

Methods. The thermostabilizing effect of the condensation product of D,L-camphor and *p*-ethoxyaniline was evaluated by means of infrared spectroscopy using the dynamics of changes in the absorption bands of carbonyl and hydroxyl groups. The features of rubber vulcanization were studied by means of rotorless rheometry. Changes in the physical and mechanical properties of rubbers and degree of cross-linking were evaluated after thermo-oxidative aging in laboratory conditions. They also took into account the results of long-term exposure of samples in undeformed and deformed state in a tropical climate, taking into account meteorological data of the Can Gio climatic testing station.

Results. It was found for the first time that condensation products of D,L-camphor and *p*-ethoxyaniline exhibit a stabilizing effect in formulations of rubbers based on polar nitrile butadiene rubber.

Conclusions. According to the results of laboratory and *in situ* tests, the study established that the use of *N*-[(1*RS*,2*RS*)-camphan-2-yl]-4-ethoxyaniline (reduced form) as an antifatigue agent is preferable. This is due to the presence of a mobile hydrogen atom at the nitrogen atom. The protective effect is manifested in terms of the better preservation of elastic-strength properties of rubbers with less change in hardness.

Keywords

condensation product of D,L-camphor and *p*-ethoxyaniline, nitrile butadiene rubber, antifatigue agent, exposure in tropical climate

Submitted: 27.11.2023

Revised: 01.02.2024

Accepted: 25.06.2024

For citation

Nilidin D.A., Vaniev M.A., Vernigora, A.A. Davidenko A.V., Salykin N.A., Thuy Dang Minh, Gubin S.G., Novakov I.A. *N*-[(1*RS*)-Camphan-2-ylidene]-4-ethoxyaniline and its reduction product as stabilizers of nitrile butadiene rubbers. *Tonk. Khim. Tekhnol. = Fine Chem. Technol.* 2024;19(4):360–371. <https://doi.org/10.32362/2410-6593-2024-19-4-360-371>

НАУЧНАЯ СТАТЬЯ

N-[(1*RS*)-Камфан-2-илиден]-4-этоксианилин и продукт его восстановления как стабилизаторы бутадиен-нитрильных резин

Д.А. Нилидин¹, М.А. Ваниев¹✉, А.А. Вернигора¹, А.В. Давиденко¹, Н.А. Салыкин¹, Данг Минь Тхуи², С.Г. Губин², И.А. Новаков¹

¹ Волгоградский государственный технический университет, Волгоград, 400005 Россия

² Институт тропического материаловедения, Совместный Российско-Вьетнамский Тропический научно-исследовательский и технологический центр, Ханой, Вьетнам

✉ Автор для переписки, e-mail: vaniev@vstu.ru

Аннотация

Цели. Исследовать эффективность защитного действия невосстановленной и восстановленной форм продукта конденсации D,L-камфоры и *n*-этоксианилина в рецептурах резин на основе бутадиен-нитрильных каучуков в сравнении с традиционным стабилизатором *N*-изопропил-*N'*-фенил-*n*-фенилендиамином, состаренных в лабораторных и натуральных климатических условиях тропиков.

Методы. Оценку термостабилизирующего влияния продукта конденсации D,L-камфоры и *n*-этоксианилина проводили методом инфракрасной спектроскопии по динамике изменения полос поглощения карбонильных и гидроксильных групп. Особенности вулканизации резин изучали методом безроторной реометрии. Изменение физико-механических свойств резин и степени поперечного сшивания оценивали после термоокислительного старения в лабораторных условиях, а также по результатам длительной экспозиции образцов в недеформированном и деформированном состояниях в тропическом климате с учетом метеоданных климатической испытательной станции Кон Зо.

Результаты. Впервые установлено, что продукты конденсации D,L-камфоры и *n*-этоксианилина проявляют стабилизирующее действие в рецептурах резин на основе полярного бутадиен-нитрильного каучука.

Выводы. По результатам лабораторных и натуральных испытаний выявлено, что в качестве противостарителя наиболее предпочтительно использование *N*-[(1*RS*,2*RS*)-камфан-2-ил]-4-этоксианилина (восстановленная форма), что связано с наличием подвижного атома водорода при атоме азота. Защитный эффект проявляется в лучшем сохранении упруго-прочностных свойств резин при меньшем изменении твердости.

Ключевые слова

продукт конденсации D,L-камфоры и *n*-этоксианилина, бутадиен-нитрильный каучук, противостаритель, экспозиция в тропическом климате

Поступила: 27.11.2023

Доработана: 01.02.2024

Принята в печать: 25.06.2024

Для цитирования

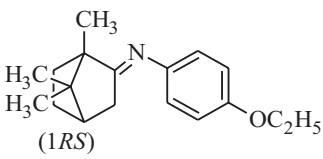
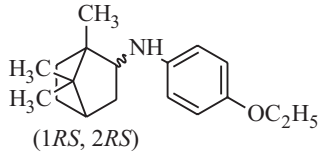
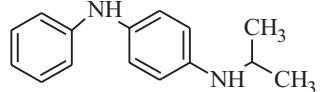
Нилидин Д.А., Ваниев М.А., Вернигора А.А., Давиденко А.В., Салыкин Н.А., Тхуи Данг Минь, Губин С.Г., Новаков И.А. *N*-[(1*RS*)-Камфан-2-илиден]-4-этоксианилин и продукт его восстановления как стабилизаторы бутадиен-нитрильных резин. *Тонкие химические технологии*. 2024;19(4):360–371. <https://doi.org/10.32362/2410-6593-2024-19-4-360-371>

INTRODUCTION

Rubbers based on nitrile butadiene rubber (NBR) are most common in the manufacture of oil and gas resistant rubber products. However, NBR-based rubbers are prone to structuring under conditions of high temperatures due to the presence of acrylonitrile links in macromolecules. Due to the relatively high unsaturated nature of macromolecules, the materials possess insufficient resistance to various types of aging [1]. Altogether, this leads to an increase in hardness, loss of elasticity and deterioration of rubber properties in general [2].

In order to resolve this problem, stabilizers of different nature are used. The most widely used as thermostabilizers are spatially hindered amines, for example, *N*-phenyl-*N'*-isopropyl-*n*-phenylenediamine (Diafen FP, IPPD); oligomer of 2,2,4-trimethyl-1,2-dihydroquinoline (Acetonanil P); *N*-phenyl-2-naphthalenamine (Naftam-2); *N,N'*-diphenyl-*n*-phenylenediamine (Diafen FF), etc. [3]. At the same time, the above-listed amines do not fully meet modern sanitary and hygienic standards. It should also be noted that the protective effect of their use is insufficient, especially under conditions of complex influence of climatic factors on rubber.

Table 1. Structural formulas and codes of substances used in rubber formulations

Structural formula	Name of substance	Code of substance
	<i>N</i> -[(1 <i>RS</i>)-Camphan-2-ylidene]-4-ethoxyaniline	Product I
	<i>N</i> -[(1 <i>RS</i> ,2 <i>RS</i>)-Camphan-2-yl]-4-ethoxyaniline	Product II
	<i>N</i> -Isopropyl- <i>N'</i> -phenyl- <i>p</i> -phenylene diamine (IPPD)	IPPD (comparison sample)

This determines the need to search for new effective and low-toxic stabilizers. The condensation products of camphor and aniline and their reduction products are of considerable interest in this respect. The first information on the use of substances obtained by the interaction of camphor with aromatic amines in the formulation of natural rubber-based rubbers is provided in US patent No. 2211629 [4]. The synthesis of new compounds of this type is described in [5–8]. Furthermore, there is data on the possibility of using camphor anilines and their reduction products as antimicrobial [9] and antiviral medical preparations [10].

Earlier in [11], we investigated the effect of *N*-[(1*RS*)-camphan-2-ylidene]-2-methylaniline, *N*-[(1*RS*)-camphan-2-ylidene]-2-ethylaniline and *N*-[(1*RS*)-camphan-2-ylidene]aniline on the properties of NBR-based rubbers, including the evaluation of their efficiency as thermal stabilizers. At the same time, a pronounced stabilizing protective effect was not revealed, due to the absence of a hydrogen atom at the nitrogen atom in the unreduced form of camphor anilines [12]. Taking this circumstance into account, the reduced form of *N*-[(1*RS*)-camphan-2-ylidene]-4-ethoxyaniline was synthesized.

The aim of this study was to evaluate the protective effect of the unreduced and reduced form of the condensation product of D,L-camphor and *n*-ethoxyaniline in BPA-based rubber formulations, when compared to the conventional stabilizer *N*-isopropyl-*N'*-phenyl-*n*-phenylenediamine aged

under laboratory and *in situ* climatic conditions in the tropics.

MATERIALS AND METHODS

NBR vulcanizates of BNKS-40 AMS grade with mass fraction of bound acrylic acid nitrile 36–40% (TU 38.30313-2006) were used as objects of the study. An effective vulcanizing system including sulfur donors thiuram D and dithiomorpholine (China) was used for vulcanization. Table 1 presents the structural formulas of the D,L-camphor aniline used and its reduction product synthesized by the authors of this paper. The other ingredients of rubber compounds are given in Table 2.

The following compounds were used as antifatigue agents of rubber mixtures: *N*-[(1*RS*)-camphan-2-ylidene]-4-ethoxyaniline (I), *N*-[(1*RS*,2*RS*)-camphan-2-yl]-4-ethoxyaniline (II), obtained according to known methods [6, 7]. Diafen FP (Russia) was also used as a substance of comparison. The content of basic substances was ≥98.5%. The synthesis of functionalized D,L-camphor derivatives was carried out according to Scheme 1.

Laboratory rollers Lb 320/160/160 (POLYMERMASH, Russia) were used to produce the blends. Rubber without a stabilizing agent is hereinafter referred to as base rubber.

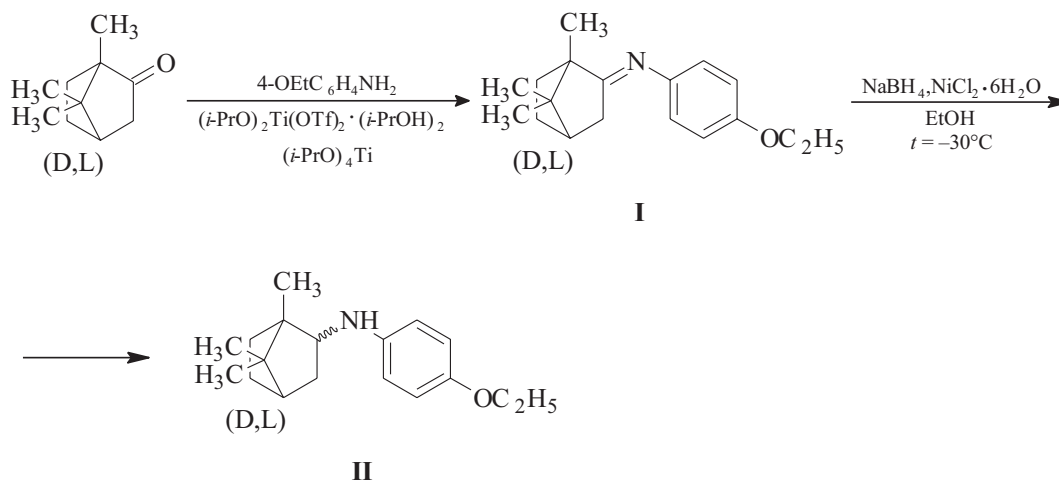
Vulcanization characteristics were studied using an MDR 3000 Professional rotorless rheometer (MonTech, Germany) in accordance with GOST 34751-2021¹.

¹ GOST 34751-2021. Interstate Standard. Rubber mixtures. Determination of vulcanization characteristics using rotorless rheometers. Moscow: Russian Institute of Standardization; 2021. <https://docs.cntd.ru/document/1200181424?ysclid=lteg4izk40725865149>. Accessed November 06, 2023.

Table 2. Rubber formulations

Component	Formulation code			
	0*	I	II	IPPD
	Ingredient content, parts by wt			
Nitrile butadiene rubber BNKS-40 AMN	100	100	100	100
Carbon black P-234	40	40	40	40
Carbon black P-803	20	20	20	20
Tetramethylthiuram disulfide	2.5	2.5	2.5	2.5
Dithiodimorpholine	1.5	1.5	1.5	1.5
Sulfenamide C (<i>N</i> -cyclohexyl-2-benzothiazole-sulfenamide, CBS)	1.5	1.5	1.5	1.5
Product I	–	2	–	–
Product II	–	–	2	–
IPPD	–	–	–	2
ZnO	5	5	5	5
Stearic acid	1.5	1.5	1.5	1.5

*0—rubber compound without anti-fatigue agent.



Scheme 1. Synthesis of functionalized D,L-camphor derivatives

In situ tests of rubber samples at the Can Gio testing station (Ho Chi Minh City, Vietnam) were carried out according to GOST 9.066² on deformed

samples in the form of strips with the help of clamps, as well as standard plates in their regular state.

² GOST 9.066. State Standard of the USSR. Unified system of corrosion and ageing protection. Vulcanized rubbers. Method of ageing resistance testing under weather conditions. Moscow: Izdatel'stvo standartov; 1994. <https://docs.cntd.ru/document/1200015036?ysclid=lteg68jel7692111363>. Accessed November 06, 2023.

The physical and mechanical properties of the samples were determined in accordance with GOST 270-75³ on a 5.0 kN Zwicki-line testing machine (*Zwick/Roell*, Germany). The hardness of rubbers was measured according to GOST 263-75⁴. The assessment of the resistance of rubbers to thermal aging in air environment was carried out in accordance with GOST 9.024-74⁵. Cross-linking density was determined according to the equilibrium swelling method [13].

The study of spectral characteristics in the infrared (IR) range was carried out using an FT-801 Simex IR Fourier spectrometer with a universal attachment of frustrated total internal reflection (FTIR) (*Simex*, Russia), equipped with a diamond element. The spectra obtained were processed in ZaIR 3.5 software⁶.

RESULTS AND DISCUSSION

The features of thermo-oxidative aging of NBR films were preliminarily studied by means of IR spectroscopy in the range of 800–4000 cm⁻¹. The rubber was purified from the anti-fatigue agent by re-precipitation using 3% toluene solution with methyl alcohol with further drying until the solvent was completely removed. Products **I**, **II**, and IPPD were added to a 10% solution of rubber in toluene in an amount of 0.25 wt % per rubber. After removing the solvent and drying to constant weight, film samples of about 100 μm thickness were subjected to aging in a thermal

cabinet at 100°C. After a certain time, the IR spectrum was determined using an FTIR attachment with a diamond crystal. The process was monitored by the change in the absorption bands at 1720 and 3615 cm⁻¹ corresponding to carbonyl (–C=O) and hydroxyl (–OH) groups. The results are presented in Figs. 1 and 2.

The dependencies presented in Figs. 1 and 2 show the dynamics of carbonyl and hydroxyl group accumulation, indicating that in the presence of product **II** and IPPD, the oxidative process develops more slowly. Thus, their effectiveness as anti-fatigue agents were tentatively established.

Figure 3 and Table 3 present the results of rheometric studies characterizing the features of rubber vulcanization depending on the type of the used substance.

As can be seen from the results of evaluating the vulcanization characteristics of rubbers, the addition of IPPD has almost no effect on the sub-vulcanization time (τ_s). In turn, the addition of *N*-[(1*RS*)-camphan-2-ylidene]-4-ethoxyaniline and *N*-[(1*RS*,2*RS*)-camphan-2-yl]-4-ethoxyaniline leads to an increase in the sub-vulcanization time from 2.2 min to 3.2 and 3.7 min, respectively. It can be concluded from the slope angle of the rheometric curves that the process rate in the presence of IPPD and products **I** and **II** slightly decreases due to the inhibition of radical reactions occurring during vulcanization. It can also be observed that in the presence of these substances the values of maximum

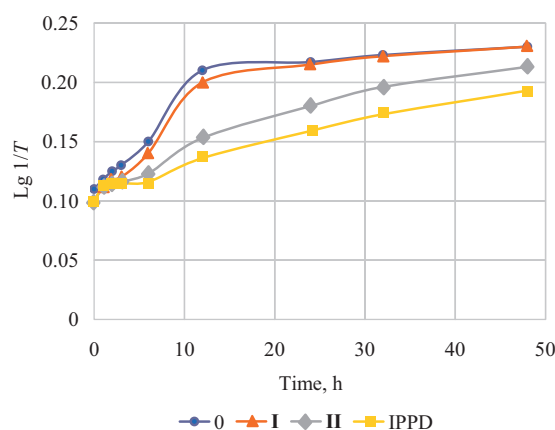


Fig. 1. Dynamics of change of intensity of absorption band 1720 cm⁻¹(–C=O)

³ GOST 270-75. Interstate Standard. Rubber. Method for determining elastic-strength properties under tension. Moscow: IPK Izdatel'stvo standartov; 2008. <https://docs.cntd.ru/document/1200018619?ysclid=ltegg818rc7736832141>. Accessed October 12, 2023.

⁴ GOST 263-75. State Standard of the USSR. Rubber. Method for determination of Shore A hardness. Moscow: Izdatel'stvo standartov; 1989. <https://docs.cntd.ru/document/1200018610?ysclid=ltegg99zuyum336475224>. Accessed October 12, 2023.

⁵ GOST 9.024-74. State Standard of the USSR. Unified system of corrosion and ageing protection. Rubbers. Methods of heat ageing stability determination. Moscow: IPK Izdatel'stvo standartov; 1994. <https://docs.cntd.ru/document/1200015022?ysclid=ltegg6r6kl786947653>. Accessed September 07, 2023.

⁶ https://old.simex-ftir.ru/product_5.html. Accessed September 07, 2023.

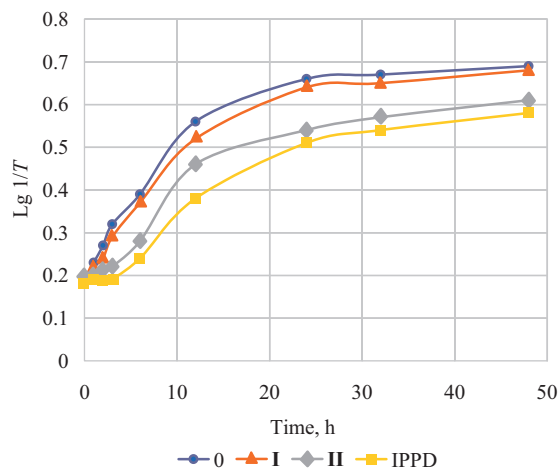


Fig. 2. Dynamics of change of intensity of absorption band $3615\text{ cm}^{-1}(-\text{OH})$

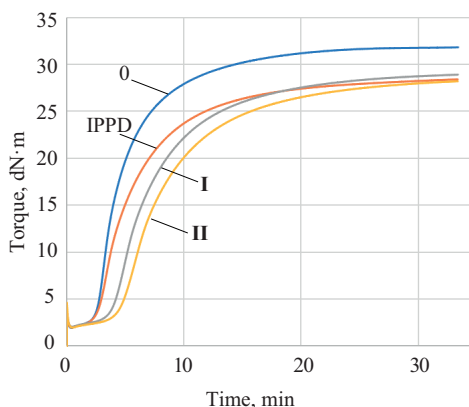


Fig. 3. Rheometric curves of vulcanization ($T = 150^\circ\text{C}$) of BNKS-40AMN based rubbers

torque are about 3 torque units lower when compared to the base formulation. This indicates a slightly lower degree of crosslinking of these rubbers. Based on these studies, and taking into account the τ_{90} index (time required to reach 90% of full vulcanization), rubber samples were produced for further laboratory and climatic tests under tropical conditions.

Table 4 shows the results of evaluating the physical and mechanical properties of the rubbers, as well as the level of change in the parameters after laboratory aging at 125°C for 72 h.

Table 5 presents meteorological data for 8 months of natural exposure in the territory of the Can Gio test climatic station.

Table 3. Rheometric data of rubber compounds ($T = 150^\circ\text{C}$)

Code	τ_s , min	τ_{90} , min	Minimum torque, dN·m	Maximum torque, dN·m
0	2.2	11.4	1.9	31.8
IPPD	2.3	14.5	2.0	28.9
I	3.3	17.4	2.0	28.9
II	3.7	18.0	2.0	28.1

Note: τ_s is the sub-vulcanization time; τ_{90} is the time required to reach 90% vulcanization.

Table 4. Comparative data on the initial properties of rubbers and aged rubbers under laboratory and *in situ* climatic conditions in the tropics

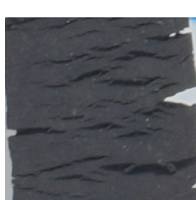
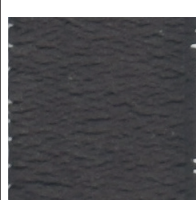
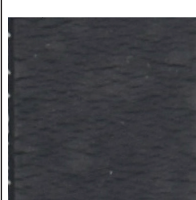
Rubber code	0	I	II	IPPD
Conditional tensile strength, MPa	26.3	25.4	26.2	26.1
Relative elongation at break, %	373	352	364	369
Hardness, Shore A units	74	74	74	74
Degree of cross-linking $\nu \times 10^{-4}$, mol/cm ³	8.2	8.1	7.8	8.1
Change of properties of rubbers after aging at 125°C, 72 h				
Change in conditional tensile strength, %	-37	-15	-5	-3
Change in relative elongation at break, %	-51	-43	-31	-28
Change in hardness, Shore A units	+8	+4	+4	+4
Degree of cross-linking $\nu \times 10^{-4}$, mol/cm ³	10.3	9.6	9.3	9.2
Changes in properties after 8 months of exposure in tropical climates				
Change in conditional tensile strength, %	-29	-18	-6	-11
Change in relative elongation at break, %	-29	-26	-11	-19
Change in hardness, Shore A units	+6	+4	+3	+3
Degree of cross-linking $\nu \times 10^{-4}$, mol/cm ³	9.5	9.4	9.1	9.0

Table 5. Meteorological data at the Can Gio climatic testing station for 2022*

Month	Air temperature, °C			Air humidity, %			Precipitation, mm	Total solar radiation, MJ/m ²
	Average monthly	Minimum absolute	Maximum absolute	Average monthly	Minimum absolute	Maximum absolute		
March	30.3	26.1	35.7	69.6	37.3	85.7	–	680
April	31.6	25.7	36.7	72.7	43.6	96.0	173.7	624
May	32.0	27.0	37.8	72.1	48.0	85.8	87.4	362
June	30.1	24.0	38.7	76.3	49.0	94.5	136.2	513
July	29.6	22.0	38.7	76.0	50.0	92.0	210.1	438
August	30.3	24.0	37.6	77.1	43.0	94.1	96.8	306
September	30.1	24.0	36.7	76.6	53.0	91.0	287.0	391
October	29.3	24.0	36.9	79.9	57.6	90.0	246.5	392
Cumulative*	–	–	–	–	–	–	633.3	3706

* 8 months of exposure data.

Table 6. Results of climatic tests of rubber samples in deformed state (tensile)

Rubber code		0	I	II	IPPD
Time of appearance of the first cracks on the surface, days	Deformation 10%	2	5	7	8
	Deformation 20%	1	4	2	4
Surface photos of rubber strips after 8 months of exposure in a tropical climate	Deformation 10%				
	Deformation 20%				

The data shown in Table 4 shows that the presence of a mobile hydrogen atom at nitrogen significantly affects the activity of the substance as an anti-fatigue agent. In particular, if we compare the effectiveness of the unreduced and reduced forms of *N*-[(1*RS*)-camphan-2-ylidene]-4-ethoxyaniline (products **I** and **II**), the best protective effect is observed for samples containing the reduced form. This is manifested in the better preservation of elastic-strength properties, a lower level of change in the hardness and cross-linking degree index both after laboratory and *in situ* tests of samples subjected to the combined influence of tropical atmospheric factors (Table 5). The properties of the base rubber without an anti-fatigue agent change more significantly, as expected. The comparison shows that the protective effect due to the introduction of product **II** is commensurate with the traditional IPPD stabilizer. This, in turn, is consistent with the known theory on the mechanism of action of amine-type anti-fatigue agents [14].

Table 6 shows the results of tropical tests of rubber samples in the deformed state.

As predicted, under test conditions, the first cracks on specimens without anti-fatigue agent were seen in a shorter period of time. When such specimens are stretched in clamps by 10 and 20%, the first cracks form after two and one day, respectively. Rubbers filled with products **I** and **II**, as well as IPPD, show first cracks after 2 to 8 days depending on the degree of deformation. At a relatively low tensile strain (10%), a commensurate

protective effect is observed in the cases of product **II** and IPPD.

The photographs presented in Table 6 demonstrate the condition of samples exposed for 8 months in tropical climates under 10 and 20% stretching conditions. The base rubbers (without anti-fatigue agent) are characterized by the presence of larger and deeper cracks regardless of the degree of deformation. A visually different picture can be seen in rubber samples where *N*-[(1*RS*)-camphan-2-ylidene]-4-ethoxyaniline and its reduction product were used. In these cases, the development of the destructive process is much less pronounced, if judged by the number and size of cracks.

CONCLUSIONS

According to the results of testing of NBR-based rubbers in laboratory conditions and in full-scale climatic tests, it was established for the first time that condensation products of D,L-camphor and *n*-ethoxyaniline exhibit a noticeable stabilizing effect. The use of the reduced form of *N*-[(1*RS*)-camphan-2-ylidene]-4-ethoxyaniline is preferable as an anti-fatigue agent in formulations of NBR-based rubbers, determined by the presence of a mobile hydrogen atom at the nitrogen atom. The protective effect is manifested as the better degree of preservation of elastic-strength properties of rubbers with less change in hardness. In particular, after 8 months of exposure in tropical climate the rubbers display a loss of tensile strength and relative elongation at break by 6 and 11%

respectively. The level of hardness of the materials increases insignificantly, namely by 3 Shore A units. The comparison samples containing *N*-isopropyl-*N'*-phenyl-*n*-phenylenediamine display a loss of tensile strength by 11% and relative elongation at break by 19%.

Acknowledgments

The study was funded by the Russian Science Foundation grant No. 22-13-20062, <https://rscf.ru/project/22-13-20062/>, and the Volgograd Oblast Administration grant under Agreement No. 2 dated June 10, 2022. The authors thank the staff of the “Creation of elastomeric materials providing a multiplicative effect in the field of increasing the efficiency of equipment and machinery operated in tropical climate conditions” (Ecolan T-1.5) project and the staff of the Can Gio climatic testing station at the Joint Vietnam–Russia Tropical Science and Technology Research Center in Ho Chi Minh City.

Authors' contributions

D.A. Nilidin—conducting experiments in laboratory conditions, analyzing and interpreting the obtained data.

M.A. Vaniev—planning and controlling the experiment, data analysis, preparing and editing the text, and approval of the final version of the article.

A.A. Vernigora—synthesis of *N*-[(1*RS*)-camphan-2-ylidene]-4-ethoxyaniline and *N*-[(1*RS*,2*RS*)-camphan-2-yl]-4-ethoxyaniline.

N.A. Salykin—purification of *N*-[(1*RS*)-camphan-2-ylidene]-4-ethoxyaniline and *N*-[(1*RS*,2*RS*)-camphan-2-yl]-4-ethoxyaniline and sample preparation.

A.V. Davidenko—identification of the structure of *N*-[(1*RS*)-camphan-2-ylidene]-4-ethoxyaniline and *N*-[(1*RS*,2*RS*)-camphan-2-yl]-4-ethoxyaniline by physicochemical methods.

Dang Minh Thuy—collection, analysis, and statistical processing of meteorological data in the territory of the climate test station, development of methodology of climate tests.

S.G. Gubin—designing and conducting the experiment in tropical climate conditions, data analysis.

I.A. Novakov—scientific guidance, idea formation, formulation of the aims and objectives of the research.

The authors declare no conflicts of interest.

REFERENCES

1. Piotrovskii K.B., Tarasova Z.N. *Starenie i stabilizatsiya sinteticheskikh kauchukov i vulkanizatorov (Aging and Stabilization of Synthetic Rubbers and Vulcanizers)*. Moscow: Khimiya; 1980. 264 p. (in Russ.).
2. Reznichenko S.V., Morozov Yu.L. (Eds.) *Bol'shoi spravochnik rezinshchika (Large Rubber Manufacturer's Reference Book): in 2 v. V. 1. Kauchuki i ingredienty. (Caoutchoucs and Ingredients)*. Moscow: Tehinform MAI; 2012. 774 p. (in Russ.).
3. Zweifel H., Maier R.D., Schiller M. *Dobavki k polimeram. Spravochnik (Plastics Additives. Handbook)*. 6th ed. Uzdenskii V.B., Grigorov A.O. (Eds.): transl. from Engl. St. Petersburg: Professiya; 2016. 1088 p. ISBN 978-5-91884-008-5 (in Russ.). [Zweifel H., Maier R.D., Schiller M. *Plastics Additives. Handbook*: 6th ed. Hanser; 1248 p.]
4. Winfield S. *Age Resistor*: US Pat. 2211629, Int. Cl. C08K5/29; Appl. 09.07.1936; Publ. 13.08.1940. https://worldwide.espacenet.com/publicationDetails/biblio?II=0&ND=3&adjacent=true&locale=en_EP&FT=D&date=19400813&CC=US&NR=2211629A&KC=A
5. Love B.E., Ren J. Synthesis of Sterically Hindered Imines. *J. Org. Chem.* 1993;58(20):5556–5557. <https://doi.org/10.1021/jo00072a051>
6. Vernigora A.A., Brunilin R.V., Burmistrov V.V., Davidenko A.V., Navrotskij M.B., Salykin N.A., Chernyshov V.V., Novakov I.A. New Efficient Approach to the Preparation of (+)-Camphor and (–)-Fenchone Anils under Homogeneous Catalysis Conditions. *Dokl. Chem.* 2023;512(1):260–265. <https://doi.org/10.1134/S0012500823600700> [Original Russian Text: Vernigora A.A., Brunilin R.V., Burmistrov V.V., Davidenko A.V., Navrotskij M.B., Salykin N.A., Chernyshov V.V., Novakov I.A. New Efficient Approach to the Preparation of (+)-Camphor and (–)-Fenchone Anils under Homogeneous Catalysis Conditions. *Doklady Rossiiskoi Akademii Nauk. Khimiya, Nauki o Materialakh.* 2023;512(1):52–58 (in Russ.).]
7. Brunilin R.V., Vernigora A.A., Vostrikova O.V., Davidenko A.V., Nawrozskij M.B., Salykin N.A., Novakov I.A. Development and competitive evaluation of methods for the reduction of (het)arylimines of cage-structured monoterpenoid ketones. *Russ. Chem. Bull.* 2022;71(8):1662–1669. <https://doi.org/10.1007/s11172-022-3576-1> [Original Russian Text: Brunilin R.V., Vernigora A.A., Vostrikova O.V., Davidenko A.V., Nawrozskij M.B., Salykin N.A., Novakov I.A. Development and competitive evaluation of methods for the reduction of (het)arylimines of cage-structured monoterpenoid ketones. *Izvestiya Akademii Nauk. Seriya Khimicheskaya.* 2022;71(8):1662–1669 (in Russ.).]
8. Vernigora A.A., Davidenko A.V., Salykin N.A., Brunilina L.L., Nebykov D.N., Lavrenov S.N., Isakova E.B., Trenin A.S., Nefedov A.A., Krasnov V.I., Polovyanenko D.N., Novakov I.A. Aniline derivatives containing a cage monoterpenoid fragment at the nitrogen atom: synthesis and study of antibacterial properties. *Russ. Chem. Bull.* 2024;73(1):168–178. <https://doi.org/10.1007/s11172-024-4129-6> [Original Russian Text: Vernigora A.A., Davidenko A.V., Salykin N.A., Brunilina L.L., Nebykov D.N., Lavrenov S.N., Isakova E.B., Trenin A.S., Nefedov A.A., Krasnov V.I., Polovyanenko D.N., Novakov I.A. Aniline derivatives containing a cage monoterpenoid fragment at the nitrogen atom: synthesis and study of antibacterial properties. *Izvestiya Akademii Nauk. Seriya Khimicheskaya.* 2024;73(1):168 (in Russ.).]
9. Da Silva E.T., Araújo A.da S., Moraes A.M., de Souza L.A., Lourenço M.C.S., de Souza M.V.N., Wardell J.L., Wardell S.M.S.V. Synthesis and Biological Activities of Camphor Hydrazone and Imine Derivatives. *Sci. Pharm.* 2016;84(3):467–483. <https://doi.org/10.3390/scipharm84030467>
10. Yarovaya O.I., Salakhutdinov N.F. Mono- and sesquiterpenes as a starting platform for the development of antiviral drugs. *Russ. Chem. Rev.* 2021;90(4):488–510. <https://doi.org/10.1070/RCR4969> [Original Russian Text: Yarovaya O.I., Salakhutdinov N.F. Mono- and sesquiterpenes as a starting platform for the development of antiviral drugs. *Uspekhi Khimii.* 2021;90(4):488–510 (in Russ.). <https://doi.org/10.1070/RCR4969>]
11. Vernigora A.A., Nilidin D.A., Davidenko A.V., Fan Ngok Tu, Gubin S.G., Gubina E.V., Vaniev M.A., Novakov I.A. Influence of anyles D,L-camphora on thermal oxidating stability of butadiene rubber based elastomer. *Izvestiya VolgGTU = Izvestia VSTU.* 2021;252(5):47–52 (in Russ.). <https://doi.org/10.35211/1990-5297-2021-5-252-47-52>
12. Kuleznev V.N., Shershnev V.A. *Khimiya i fizika polimerov (Chemistry and Physics of Polymers)*. Moscow: Lan; 2014. 368 p. (in Russ.). ISBN 978-5-8114-1779-7
13. Averko-Antonovich I.Yu., Bikmullin R.T. *Metody issledovaniya struktury i svoistv polimerov (Methods of Research of Structure and Properties of Polymers)*. Kazan: KGTU; 2002. 604 p. (in Russ.). ISBN 5-7882-0221-3
14. Kuzminskii A.S. (Ed.). *Starenie i stabilizatsiya polimerov (Aging and Stabilization of Polymers)*. Moscow: Khimiya; 1966. 212 p. (in Russ.).

СПИСОК ЛИТЕРАТУРЫ

1. Пиотровский К.Б., Тарасова З.Н. *Старение и стабилизация синтетических каучуков и вулканизаторов*. М.: Химия; 1980. 264 с.
2. Резниченко С.В., Морозов Ю.Л. (ред.). *Большой справочник резинщика*; в 2-х ч. Ч. 1. *Каучуки и ингредиенты*. М.: ООО «Издательский центр «Техинформ» МАИ; 2012. 774 с.
3. Цвайфель Х., Маер Р.Д., Шиллер М. *Добавки к полимерам. Справочник*: пер. с англ. 6-го изд. Узденский В.Б., Григоров А.О. (ред.). СПб.: ЦОП «Профессия»; 2016. 1088 с. ISBN 978-5-91884-008-5
4. Winfield S. *Age Resistor*: Пат. US 2211629, МПК C08K5/29; Заяв. 09.07.1936; Опубл. 13.08.1940. https://worldwide.espacenet.com/publicationDetails/biblio?II=0&ND=3&adjacent=true&locale=en_EP&FT=D&date=19400813&CC=US&NR=2211629A&KC=A
5. Love B.E., Ren J. Synthesis of Sterically Hindered Imines. *J. Org. Chem.* 1993;58(20):5556–5557. <https://doi.org/10.1021/jo00072a051>
6. Вернигора А.А., Брунилин Р.В., Бурмистров В.В., Давиденко А.В., Навроцкий М.Б., Салыкин Н.А., Чернышов В.В., Новаков И.А. Новый эффективный подход к получению анилов камфоры и фенхона в условиях гомогенного катализа. *Доклады Российской академии наук. Химия, науки о материалах*. 2023;512(1):52–58. <https://doi.org/10.31857/S2686953522600775>
7. Брунилин Р.В., Вернигора А.А., Вострикова О.В., Давиденко А.В., Навроцкий М.Б., Салыкин Н.А., Новаков И.А. Исследование и сравнительная оценка методов восстановления (гет)арилиминов монотерпеноидных кетонов каркасного строения. *Известия Академии Наук. Серия химическая*. 2022;71(8):1662–1669.
8. Вернигора А.А., Давиденко А.В., Салыкин Н.А., Брунилина Л.Л., Небыков Д.Н., Лавренов С.Н., Исакова Е.Б., Тренин А.С., Нефедов А.А., Краснов В.И., Половяненко Д.Н., Новаков И.А. Производные анилина, содержащие каркасный монотерпеноидный фрагмент при атоме азота: синтез и исследование антибактериальных свойств. *Известия Академии Наук. Серия химическая*. 2024;73(1):168–178. <https://doi.org/10.1007/s11172-024-4129-6>
9. Da Silva E.T., Araújo A.da S., Moraes A.M., de Souza L.A., Lourenço M.C.S., de Souza M.V.N., Wardell J.L., Wardell S.M.S.V. Synthesis and Biological Activities of Camphor Hydrazone and Imine Derivatives. *Sci. Pharm.* 2016;84(3):467–483. <https://doi.org/10.3390/scipharm84030467>
10. Яровая О.И., Салахутдинов Н.Ф. Моно- и сесквитерпены в качестве стартовой платформы для создания противовирусных средств. *Успехи химии*. 2021;90(4):488–510. <https://doi.org/10.1070/RCR4969>
11. Вернигора А.А., Нилюдин Д.А., Давиденко А.В., Фан Нгок Ту, Губин С.Г., Губина Е.В., Ваниев М.А., Новаков И.А. Влияние анилов D,L-камфоры на термоокислительную стойкость резины на основе бутадиеннитрильного каучука. *Известия ВолгГТУ*. 2021;252(5):47–52. <https://doi.org/10.35211/1990-5297-2021-5-252-47-52>
12. Кулезнев В.Н., Шершнева В.А. *Химия и физика полимеров*. М.: Лань; 2014. 368 с. ISBN 978-5-8114-1779-7
13. Аверко-Антонович И.Ю., Бикмуллин Р.Т. *Методы исследования структуры и свойств полимеров*. Казань: Изд-во КГТУ; 2002. 604 с. ISBN 5-7882-0221-3
14. Кузьминский А.С. (ред.). *Старение и стабилизация полимеров*. М.: Химия; 1966. 212 с.

About the authors

Dmitry A. Nilidin, Assistant, Chemistry and Technology of Elastomer Processing Department, Volgograd State Technical University (28, pr. im. Lenina, Volgograd, 400005, Russia). E-mail: dmitry.nilidin@gmail.com. Scopus Author ID 57210897476, RSCI SPIN-code 5156-4095, <https://orcid.org/0009-0002-6088-2132>

Marat A. Vaniev, Dr. Sci. (Eng.), Head of the Department of Chemistry and Technology of Elastomer Processing, Volgograd State Technical University (28, pr. im. Lenina, Volgograd, 400005, Russia). E-mail: vaniev@vstu.ru. Scopus Author ID 14063995400, RSCI SPIN-code 9260-2745, <https://orcid.org/0000-0001-6511-5835>

Andrey A. Vernigora, Postgraduate Student, Organic Chemistry Department, Volgograd State Technical University (28, pr. im. Lenina, Volgograd, 400005, Russia). E-mail: vernigora.andrey@gmail.com. Scopus Author ID 57191338560, RSCI SPIN-code 8776-4755, <https://orcid.org/0000-0001-6456-0910>

Andrey V. Davidenko, Student, Volgograd State Technical University (28, pr. im. Lenina, Volgograd, 400005, Russia). E-mail: davidenko.andrey2017@yandex.ru. Scopus Author ID 57604966600, <https://orcid.org/0000-0002-4205-0810>

Nikita A. Salykin, Student, Volgograd State Technical University (28, pr. im. Lenina, Volgograd, 400005, Russia). E-mail: behefun@gmail.com. Scopus Author ID 57415508300, RSCI SPIN-code 7262-9636, <https://orcid.org/0000-0003-3380-0568>

Thuy Dang Minh, Researcher, Institute for Tropical Materials Science, Joint Vietnam-Russia Tropical Science and Technology Research Center (63, Nguyen Van Huyen St., Cau Giay, Hanoi, Vietnam). E-mail: thuybsu@gmail.com. <https://orcid.org/0000-0003-3428-4059>

Sergey G. Gubin, Head of the Can Gio climate testing station, Institute for Tropical Materials Science, Russian-Vietnamese Tropical Center (119071, Moscow, Leninsky prospekt, 33). E-mail: sgubin@yandex.ru

Ivan A. Novakov, Academician of the Russian Academy of Sciences, Dr. Sci. (Chem.), President of the Volgograd State Technical University (28, pr. im. Lenina, Volgograd, 400005, Russia). E-mail: president@vstu.ru. Scopus Author ID 7003436556, ResearcherID I-4668-2015, RSCI SPIN-code 2075-5298, <https://orcid.org/0000-0002-0980-6591>

Об авторах

Нилидин Дмитрий Андреевич, ассистент, кафедра «Химия и технология переработки эластомеров», ФГБОУ ВО «Волгоградский государственный технический университет» (400005, Россия, Волгоград, пр-т им. В.И. Ленина, д. 28). E-mail: dmitriy.nilidin@gmail.com. Scopus Author ID 57210897476, SPIN-код РИНЦ 5156-4095, <https://orcid.org/0009-0002-6088-2132>

Ваниев Марат Абдурахманович, д.т.н., доцент, заведующий кафедрой «Химия и технология переработки эластомеров», ФГБОУ ВО «Волгоградский государственный технический университет» (400005, Россия, Волгоград, пр-т им. В.И. Ленина, д. 28). E-mail: vaniev@vstu.ru. Scopus Author ID 14063995400, SPIN-код РИНЦ 9260-2745, <https://orcid.org/0000-0001-6511-5835>

Вернигора Андрей Александрович, аспирант, кафедра «Органическая химия», ФГБОУ ВО «Волгоградский государственный технический университет» (400005, Россия, Волгоград, пр-т им. В.И. Ленина, д. 28). E-mail: vernigora.andreyu@gmail.com. Scopus Author ID 57191338560, SPIN-код РИНЦ 8776-4755, <https://orcid.org/0000-0001-6456-0910>

Давиденко Андрей Владимирович, студент, ФГБОУ ВО «Волгоградский государственный технический университет» (400005, Россия, Волгоград, пр-т им. В.И. Ленина, д. 28). E-mail: davidenko.andrey2017@yandex.ru. Scopus Author ID 57604966600, <https://orcid.org/0000-0002-4205-0810>

Салькин Никита Андреевич, студент, ФГБОУ ВО «Волгоградский государственный технический университет» (400005, Россия, Волгоград, пр-т им. В.И. Ленина, д. 28). E-mail: behefun@gmail.com. Scopus Author ID 57415508300, SPIN-код РИНЦ 7262-9636, <https://orcid.org/0000-0003-3380-0568>

Тхун Данг Минь, научный сотрудник, Институт тропического материаловедения, Совместный Российско-Вьетнамский Тропический научно-исследовательский и технологический центр (63, Nguyen Van Huyen St., Cau Giay, Hanoi, Vietnam). E-mail: thuybsu@gmail.com. <https://orcid.org/0000-0003-3428-4059>

Губин Сергей Геннадиевич, начальник климатической испытательной станции Кон Зо, Институт тропического материаловедения, Совместный Российско-Вьетнамский Тропический научно-исследовательский и технологический центр (119071, Москва, Ленинский проспект, д. 33) E-mail: sgubin@yandex.ru.

Новаков Иван Александрович, академик РАН, д.х.н., профессор, президент, ФГБОУ ВО «Волгоградский государственный технический университет» (400005, Россия, Волгоград, пр-т им. В.И. Ленина, д. 28). E-mail: president@vstu.ru. Scopus Author ID 7003436556, ResearcherID I-4668-2015, SPIN-код РИНЦ 2075-5298, <https://orcid.org/0000-0002-0980-6591>

Translated from Russian into English by H. Moshkov

Edited for English language and spelling by Dr. David Mossop

UDC 543.552.054.1:615.322:621.3.035.221.43:661.472:661.474

<https://doi.org/10.32362/2410-6593-2024-19-4-372-383>

EDN CNMDML



RESEARCH ARTICLE

Development of a new inversion-voltammetric technique in determining inorganic iodine in *Laminariae thalli* L. for the quality control of raw materials in factory laboratories

Alexander V. Nikulin, Leonid Yu. Martynov, Ramnat S. Gabaeva, Mikhail A. Lazov✉

MIREA — Russian Technological University (M.V. Lomonosov Institute of Fine Chemical Technologies), Moscow, 119571 Russia

✉ Corresponding author, e-mail: lazov@mirea.ru

Abstract

Objectives. To develop and validate a methodology for determining inorganic iodine in *Laminariae thalli* L., corresponding to the norms of the State Pharmacopoeia of the Russian Federation, 15th edition (SPh 15). The methodology needs to be valid and suitable for the quality control of pharmaceutical raw materials in factory laboratories.

Methods. Cathode inversion voltammetry was used as an instrumental method for determining inorganic iodine using a graphite electrode capable of sorbing electroactive ion associates of surfactant–iodine.

Results. When compared with the titrimetric technique recommended by SPh 15, the proposed technique is more selective, sensitive and less time-consuming. The efficiency and metrological characteristics of the technique were confirmed by validation in accordance with the requirements of SPh 15.

Conclusion. The paper presents a new method for determining the gross content of inorganic iodine in *Laminariae thalli* L. This technique can be used not only in scientific research, but also in the routine quality control of medicinal plant raw materials in control and analytical laboratories engaged in pharmaceutical quality control.

Keywords

Laminariae thalli L., gross iodine content, inversion voltammetry

Submitted: 18.04.2024

Revised: 03.05.2024

Accepted: 27.06.2024

For citation

Nikulin A.V., Martynov L.Yu., Gabaeva R.S., Lazov M.A. Development of a new inversion-voltammetric technique in determining inorganic iodine in *Laminariae thalli* L. for the quality control of raw materials in factory laboratories. *Tonk. Khim. Tekhnol. = Fine Chem. Technol.* 2024;19(4):372–383. <https://doi.org/10.32362/2410-6593-2024-19-4-372-383>

НАУЧНАЯ СТАТЬЯ

Разработка новой инверсионно-вольтамперометрической методики определения неорганического йода в слоевищах ламинарии (*Laminariae thalli* L.) для контроля качества сырья в условиях заводских лабораторий

А.В. Никулин, Л.Ю. Мартынов, Р.С. Габаева, М.А. Лазов✉

МИРЭА — Российский технологический университет (Институт тонких химических технологий им. М.В. Ломоносова), Москва, 119571 Россия

✉ Автор для переписки, e-mail: lazov@mirea.ru

Аннотация

Цели. Разработка и валидация методики определения неорганического йода в талломе ламинарии (*Laminariae thalli* L.), соответствующей нормам Государственной Фармакопеи Российской Федерации XV издания (ГФ РФ XV). Методика должна быть валидной и пригодной для контроля качества фармацевтического сырья в условиях заводских лабораторий.

Методы. В качестве инструментального метода определения неорганического йода была применена катодная инверсионная вольтамперометрия с использованием графитового электрода, способного сорбировать электроактивные ионные ассоциаты поверхностно-активного вещества (ПАВ)–йода.

Результаты. По сравнению с титриметрической методикой, рекомендуемой ГФ РФ XV, предлагаемая методика более селективна, чувствительна и менее трудоемка. Работоспособность и метрологические характеристики методики были подтверждены валидацией согласно требованиям ГФ РФ XV.

Выводы. В работе представлена новая методика определения валового содержания неорганического йода в слоевищах ламинарии (*Laminariae thalli* L.). Данная методика может быть использована не только в научных исследованиях, но и в рутинном контроле качества лекарственного растительного сырья в контрольно-аналитических лабораториях, занимающихся фармацевтическим контролем качества.

Ключевые слова

слоевища ламинарии, валовое содержание йода, инверсионная вольтамперометрия

Поступила: 18.04.2024

Доработана: 03.05.2024

Принята в печать: 27.06.2024

Для цитирования

Никулин А.В., Мартынов Л.Ю., Габаева Р.С., Лазов М.А. Разработка новой инверсионно-вольтамперометрической методики определения неорганического йода в слоевищах ламинарии (*Laminariae thalli* L.) для контроля качества сырья в условиях заводских лабораторий. *Тонкие химические технологии*. 2024;19(4):372–383. <https://doi.org/10.32362/2410-6593-2024-19-4-372-383>

INTRODUCTION

Iodine is a trace element essential for human health [1–2]. In particular, iodine is necessary for the synthesis of thyroid hormones—thyroxine and triiodothyronine which play a major role in ensuring normal metabolism [3–4]. Insufficient iodine intake has significant effects on the functioning of muscles, heart, liver, kidneys and brain [5]. It can also cause a wide range of endocrine and neurological diseases [3, 6–10]. To this day, iodine deficiency remains a

persistent medical problem, despite international efforts to eliminate it.

Herbal medicines deserve special attention in the treatment of iodine deficiency conditions due to their low toxicity and mild action [11]. The highest concentration of iodine is known to be found in seaweed [12]. Iodine content and its chemical form in these plants vary among species, but the largest amount of this element is to be found in brown algae, in particular in various types of laminaria [13]. For this reason, *Laminariae thalli* L. is

considered one of the best sources of iodine. This type of medicinal plant raw materials is included in the State Pharmacopoeia of the Russian Federation, 15th edition (SPh 15)¹, the European² and British³ Pharmacopoeia. The most bioavailable are believed to be inorganic forms of iodine, which, according to literature, are represented by iodides and iodates [14–15], which account for approximately 80 to 90% of the total iodine content [16].

Various chemical and physicochemical methods were used, in order to determine iodine in *Laminariae thalli* L. Thus, for the purpose of quality control of medicinal plant raw materials according to the Iodine indicator, SPh 15 and foreign pharmacopoeias recommend the use of insufficiently selective iodometric titration. At the same time, sample preparation used for the purposes of determination (burning in an open flame or using the Schöniger method) is time-consuming and can lead to significant losses of the analyte.

For the purposes of scientific research, iodine determination is most often performed by inductively coupled plasma mass spectrometry (ICP-MS) [17–20], and the fairly sensitive Sandell–Kolthoff kinetic method [21–26]. The ICP-MS method is expensive, extremely sensitive to the presence of organic components in the analyzed solutions, and insufficiently selective due to significant isobaric influences from the matrix components [27]. The isobaric influences are most often corrected by introducing an isotopic tracer—a radioactive isotope of iodine, ¹²⁹I, which is hazardous to health [19–20, 28–29]. The kinetic method is labor-intensive and not selective enough [25–26], requiring the use of special sample preparation procedures. The listed disadvantages of the Sandell–Kolthoff and ICP-MS methods prevent their use in routine quality control of medicinal plant raw materials in pharmaceutical

enterprises. A more accessible and simpler alternative is to use electrochemical methods. The most modern version, in particular, is inverse voltammetry (IVA)⁴ [30]. This method is characterized by a high level of sensitivity and does not require the use of expensive equipment.

For the purposes of the routine determination of iodine (most often in the form of iodates) by means of the IVA method⁵, silver or mercury film electrodes (MFE's) are predominantly used (GOST 31660-2012⁶) [31, 32]. Despite the fact that RPEs make it possible to obtain a stable signal, their use in flow analysis is severely limited by the toxicity of mercury salts used to obtain a mercury film on the electrode surface. Silver electrodes are safe to use, make it easier to provide a renewed surface and have a higher detection sensitivity when compared to MFE's. However, they are not sufficiently resistant to complex matrices of natural samples. There are works in which electrodes covalently modified with commercially difficult to obtain organic reagents were used to increase the determination selectivity and sensitivity⁷ [33, 34]. The process of obtaining this type of electrodes is labor-intensive and multi-stage. This significantly limits their use in flow analysis in factory quality control laboratories. Standardized commercially available graphite electrodes are more promising from this point of view. They are capable of sorbing organic reagent–analyte element complexes on their surface. Surfactants can be proposed as available organic reagents. In the work by D.M. Fedulov⁸ research was conducted on the influence of the nature and structure of surfactants on the deposition of surfactant–iodine complexes on the surface of a graphite electrode. Based on the research conducted, the authors have proposed methodological guidelines for the determination of iodine in food products, food raw materials, food

¹ State Pharmacopoeia of the Russian Federation. 15th ed. Moscow: Ministry of Health of the Russian Federation, 2018;4:6181–6187. <https://pharmacopoeia.regmed.ru/pharmacopoeia/izdanie-15/>. Accessed May 11, 2024.

² European Pharmacopoeia. 6th ed. Strasburg: EDQM, 2008;2:2213–2214. <https://archive.org/details/europeanpharmaco2008unse>. Accessed May 11, 2024.

³ British Pharmacopoeia. Herbal drugs and herbal drug preparations. Kelp. London: Medicines and healthcare products regulatory agency, 2009(3):1–2. <https://archive.org/details/britishpharmacop0003unse>. Accessed May 11, 2024.

⁴ *Opredelenie massovoi kontsentratsii ioda v pishchevykh produktakh, prodovol'stvennom syr'e, pishchevykh i biologicheskii aktivnykh dobavkakh vol'tamperometriceskim metodom: Metodicheskie ukazaniya (Determination of the Mass Concentration of Iodine in Food Products, Food Raw Materials, Food and Biologically Active Additives by Voltamperometric Method: Guidelines)*. Moscow: Federal'nyi tsentr gossanepidnadzora Minzdrava Rossii; 2003.42 p. (in Russ.).

⁵ Noskova G.N. *Determination of various forms of iodine-containing compounds in waters by voltammetric methods*. Diss. Cand. Sci. (Chem.). Tomsk: 2004. 177 p.

⁶ GOST 31660-2012. Interstate Standard. Foods. Anodic stripping voltammetric method of iodine mass concentration determination. Moscow: Standartinform; 2012. <https://docs.cntd.ru/document/1200095486?ysclid=lvxs4018b2463460075>. Accessed May 11, 2024.

⁷ Pham K.N. *Voltammetric behavior of iodine, selenium and nickel on organo-modified electrodes*. Diss. Cand. Sci. (Chem.). Tomsk: 2012. 160 p.

⁸ Fedulov D.M. *Determination of iodine, lead and selenium in environmental objects in the presence of organic compounds by inversion voltammetry*. Diss. Cand. Sci. (Chem.). Moscow: 2004. 162 p.

additives and biologically active additives. This approach is convenient in that it does not require the complex preparation of the electrode for measurements (there is no impregnation stage). However, the authors consider this procedure to have two significant drawbacks. The first drawback is the influence of matrix components, which they propose to be removed by “dry” mineralization of samples (analyte loss). The second drawback is the need to select conditions for converting all forms of iodine into the iodide form. This form provides the highest level of sensitivity in determining the element. Unfortunately, the authors do not prescribe methods for sample preparation and transfer of the element into an analyzed form. Moreover, metrological certification of the method using water as an example show that, despite the ease of performing measurements using the additive method⁹, it is not possible to obtain validation characteristics which meet the requirements of the SPh 15, even for such a simple object. Accordingly, the procedure described in the guidelines is not applicable for complex natural samples. Therefore, in order to determine the gross content of inorganic iodine in a pharmaceutical sample—the *Laminariae thalli* L.—it is necessary not only to reproduce the determination conditions, but to develop and validate a new method compliant with the standards of the SPh 15. In this case, the technique should include labor-intensive sample preparation, which to the maximum extent possible eliminates the loss of the element being determined. It should also include a simple method of converting the element into a single analyzed form, as well as an effective combination of the above stages with the stage of IVA determination using a surfactant.

Thus, the purpose of this work is to develop and validate a simple, reproducible, selective, highly sensitive, combined IVA method for determining the total iodine content in a new type of pharmaceutical object for IVA analysis—*Laminariae thalli* L. containing inorganic iodine mainly in the form of iodides and iodates easily soluble in water¹⁰ [35, 36]. At the same time, the methodology must comply with the capabilities of the control and analytical laboratories of pharmaceutical enterprises and the requirements of the SPh 15.

MATERIALS AND METHODS

Sample preparation was carried out using a WiseVen drying cabinet (*Wisd*, South Korea) and a laboratory

centrifuge SM-6M (*Elmi*, Latvia). Inorganic iodine determination was performed using a voltammetric analyzer Ekotest-VA (*Ekoniks-Expert*, Russia) by means of a three-electrode cell consisting of a working impregnated graphite electrode (IGE) (*Ekoniks-Expert*, Russia), a silver-silver chloride reference electrode ESr-10107 (*Izmeritel'naya Tekhnika (Measuring Equipment)*, Russia), a platinum auxiliary electrode EPL-02 (*Gomel Plant of Measuring Equipment*, Belarus), and a magnetic stirrer (*Elmi*, Latvia).

The following reagents were used in the work: purified water (conductivity <4.3 μS/cm at 20°C), concentrated sulfuric acid (chemically pure, *Lenreaktiv*, Russia), potassium iodide (chemically pure, *Chemical Line*, Russia), potassium bromide (reagent grade, *Lenreaktiv*, Russia), cetyltrimethylammonium bromide (*Sisco Research Laboratories*, India), and zinc dust 95% (*Clearysynth*, India).

Solutions of 1 M H₂SO₄ and 10% potassium bromide were prepared in accordance with SPh 15. Samples of *Laminariae thalli* L. which meet the requirements of SPh 15 were purchased from a pharmacy chain in Moscow.

0.1 M solution of potassium bromide

12.0 mL of 10% potassium bromide solution were placed into a 100-mL volumetric flask. The volume of the solution was brought to the mark with water, and the mixture was stirred.

Cetyltrimethylammonium bromide solution

An exactly weighed portion of cetyltrimethylammonium bromide weighing 0.1850 g was placed into a 250-mL volumetric flask. The volume of the solution was adjusted to the mark with water, and the mixture was stirred.

Standard solution

An exactly weighed portion of 1.3081 g of potassium iodide was placed in a 1000-mL volumetric flask. 700 mL of water was added, and the mixture was stirred until the sample was completely dissolved. The solution volume was adjusted to the mark with the same solvent, and the mixture was stirred (iodine concentration 1.0 mg/mL, solution A).

Solution A of 5.0 mL was added to a 50-mL volumetric flask. The volume of the solution was adjusted to the mark with water, and the mixture was stirred (iodine concentration 100.0 μg/mL, solution B).

⁹ The additive method is one of the standard quantitative methods in analytical chemistry, in which a precisely known amount of the substance being determined is introduced into the test sample, and the content of this substance in the sample (test sample) is calculated from the change in the analytical signal.

¹⁰ Savchuk I.A. *Investigation of pharmacological properties and chemical composition of dry Japanese kelp extract*. Diss. Cand. Sci. (Biol.). Smolensk: 2012. 122 p.

Solution B of 10.0 mL was placed into a 100-mL volumetric flask, the volume of the solution was adjusted to the mark with water, and the mixture was stirred (iodine concentration 10.0 µg/mL, solution C).

Solutions for studying the method linearity (calibration solutions)

Solution C of 0.05–0.75 mL, 0.50 mL of the cetyltrimethylammonium bromide solution, 2.5 mL of 1 M H₂SO₄, and 1.0 mL of 0.1 M potassium bromide solution were added to a 25-mL volumetric flask. The volume of the solution was adjusted to the mark with water, and the mixture was stirred (iodine concentration was 20–300 µg/L).

Test solution

A sample of the raw material passed through a sieve with a hole size of 2 mm, weighing 0.5 g (exactly weighed), was placed into a 100-mL conical flask, and 40 mL of water were added. The mixture was kept at 90°C for 15 min and centrifuged for 15 min at a speed of 2000 rpm. The supernatant was transferred to a 250-mL volumetric flask. The precipitate was filtered off, and the filtrate was transferred into the same volumetric flask through cheesecloth. The solution volume was adjusted to the mark with water, and the mixture was stirred.

The resulting solution of 5.0 mL, 10.0 mL of 1 M H₂SO₄, and 0.5 g of zinc dust were placed into a 100-mL volumetric flask. The mixture was kept at 80°C for 30 min and cooled. The solution volume was brought to the mark with water. The mixture was stirred and filtered through a paper filter from the *Sinyaya Lenta* (*Blue Ribbon*) brand (Russia).

Reference solution

Cetyltrimethylammonium bromide solution of 0.5 mL, 2.5 mL of 1 M H₂SO₄, and 1.0 mL of 0.1 M potassium bromide solution were placed into to a 25.0 mL volumetric flask. The solution volume was adjusted to the mark with water, and the mixture was stirred.

Procedure

The test solution of 4.0 mL was placed in a 25-mL volumetric flask, then 0.5 mL of cetyltrimethylammonium bromide solution, 2.5 mL of 1 M H₂SO₄, and 1.0 mL of 0.1 M potassium bromide solution were added. The solution volume was adjusted to the mark with water, and the mixture was stirred. The determination was carried out using the calibration curve method.

The voltammograms of the test solution and of the reference solution were recorded in the potential range from –200 to 800 mV.

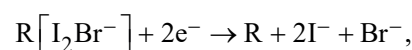
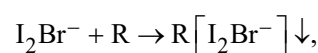
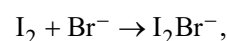
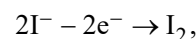
The amount of inorganic iodine (X , %) in the raw material was calculated using the following formula:

$$X = \frac{(C - C_0) \times 250 \times 100 \times 25 \times 100 \times 10^{-9} \times P}{4 \times 5 \times a \times 100 \times (100 - W)} \times 100 = \frac{(C - C_0) \times 3.12 \times 10^{-3} \times P}{a \times (100 - W)},$$

where a is the mass of a sample of plant raw materials, g; C is the concentration of inorganic iodine in the test solution determined from the calibration curve, µg/L; C_0 is iodine concentration in the reference solution, µg/L; P is the main substance content in the standard sample of potassium iodide, %; W is raw material moisture, %.

RESULTS AND DISCUSSION

The IVA determination of iodine was based on the electrochemical oxidation of iodide ions to molecular iodine [34]. At the accumulation step, in the presence of bromide ions and a quaternary ammonium base (cetyltrimethylammonium bromide), the resulting iodine is adsorbed onto the surface of the working IGE in the form of a poorly soluble ionic associate. When the potential is deployed to the cathode region, electrochemical dissolution of the precipitate occurs, and a peak of electrochemical reduction of iodine appears on the voltammogram. This process can be roughly represented as follows:

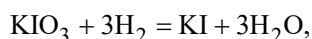
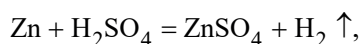


wherein R is the quaternary ammonium base. The precipitate dissolution is accompanied by the flow of a cathodic current, the magnitude of which is an analytical signal.

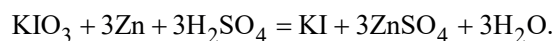
At the first stage of the study, we succeeded in showing that the greatest recovery of inorganic forms of iodine is achieved when extracting analytes with water under the following conditions: raw material particle size—less than 2 mm; extractant volume—40 mL; extraction temperature—90°C; extraction time—15 min; and extraction multiplicity is 1. It was also found that the simplest version of the method described in [34] is not suitable for the bulk determination of iodine inorganic form. This is due to the extreme complexity of the matrix composition of the natural analyzed sample, as well as the simultaneous presence of the analyte in several forms. For this reason, the work explored the possibility

of converting various inorganic forms of iodine (iodides and iodates) into a single form (iodides).

Iodates can be converted to iodides under the action of hydrogen, easily obtained by the reaction of zinc dust with acid. Therefore, mixing sulfuric acid and zinc dust with the resulting extract and additional heating to speed up the reaction allowed us to obtain the required result. The reactions carried out can be roughly represented as follows:



or in general:



The influence of temperature, reaction time, mass of zinc dust, and concentration of sulfuric acid solution on the completeness of the reaction was studied using a model solution of potassium iodate (iodine concentration was 202 µg/L). The assessment was carried out on the basis of the resulting iodides content using ionometry. As a result of the complete reaction, the concentration of iodide ions should be about 202 ng/mL, corresponding to the most complete transition of iodate to iodide. The results of the experiments are presented in Table 1.

Table 1. Influence of different parameters on the completeness of iodates to iodides conversion (the volume of the test solution is 5 mL, the volume of sulfuric acid is 10 mL)

Reaction temperature, °C	Sulfuric acid concentration, M	Zinc powder mass, g	Reaction time, min	Mass concentration C(I), mcg/L
Reaction temperature				
25	0.1	0.5	30	196.2
40	0.1	0.5	30	198.5
80	0.1	0.5	30	207.1
100	0.1	0.5	30	200.2
Sulfuric acid concentration				
80	0.1	0.5	30	205.2
80	0.5	0.5	30	199.1
80	1.0	0.5	30	195.0
80	2.0	0.5	30	184.7
Zinc mass				
80	0.1	0.5	30	205.2
80	0.1	0.75	30	178.4
80	0.1	1.0	30	179.4
80	0.1	2.0	30	182.4
Reaction time				
80	0.1	0.5	10	181.7
80	0.1	0.5	20	175.7
80	0.1	0.5	30	201.9
80	0.1	0.5	60	172.0

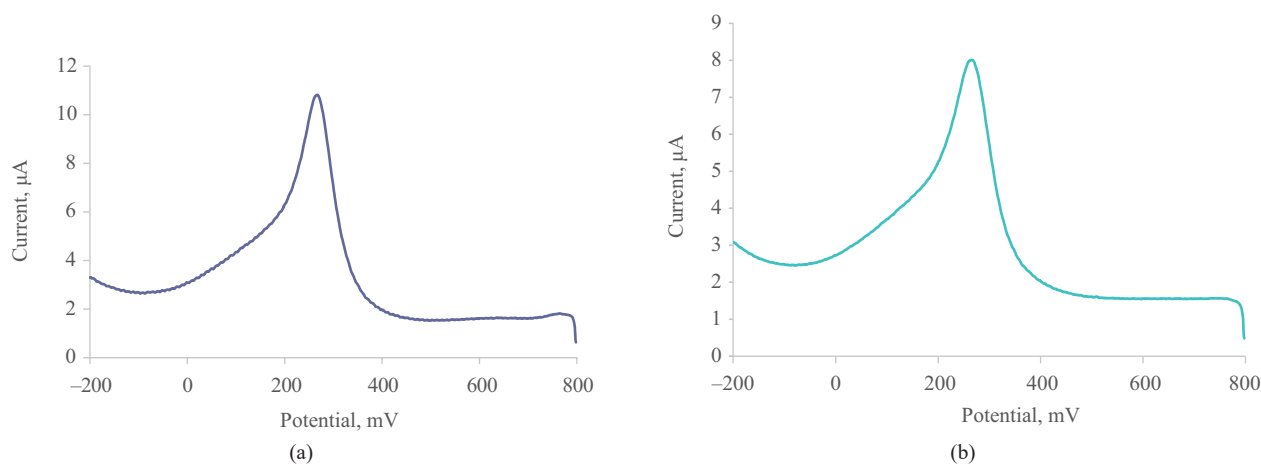


Fig. 1. Voltammograms of: (a) the standard solution with the iodine concentration of 200 µg/L, (b) the test solution

The data presented in Table 1 indicates that the most complete conversion of iodates into iodides is achieved at a temperature of 80°C, a reaction time of 30 min, a concentration of sulfuric acid of 0.1 M, and a mass of zinc dust of 0.5 g. The results obtained are quite easy to explain. Thus, as the temperature increases, the reaction rate increases. The increase in the concentration of the sulfuric acid solution leads to a decrease in the content of the element being determined in the solution due to the formation of volatile iodine (reaction between KIO_3 and KI). Iodine leaves the reaction sphere during the reaction mixture heating. An increase in the mass of zinc dust prevents hydrogen bubbles from moving freely in the solution, also complicating the reaction of iodides formation.

Since laminaria is a typical representative of the brown seaweed family, it tends to accumulate elements contained in seawater in the largest quantities. These elements include sodium, potassium, calcium, and magnesium. Therefore, we studied the matrix influence of these elements upon the analytical signal of the element being determined. As a result of the experiments, it was found that sodium, potassium, calcium and magnesium with a thousandfold excess in the test solution do not interfere with the analytical signal. Thus, as a result of the research, a new voltammetric method was proposed for the quantitative determination of the gross content of inorganic iodine in the *Laminariae thalli* L. The study of metrological characteristics was carried out in accordance with the requirements of the SPh 15.

Figure 1 shows voltammograms of one of the standard solutions used to plot the calibration curve (Fig. 1a) and of the test solution (Fig. 1b) recorded in the range from -200 to 800 mV.

Figure 1 indicates that the local maximum is achieved at a potential of 233 ± 10 mV both in the voltammogram of the standard and in the voltammogram of the test

solutions. No maxima were found in the reference solution voltammogram. The results obtained indicate a fairly high specificity of the proposed method in relation to the analyte.

Figure 2 shows the effect of iodine concentration on the analytical signal of the element being determined.

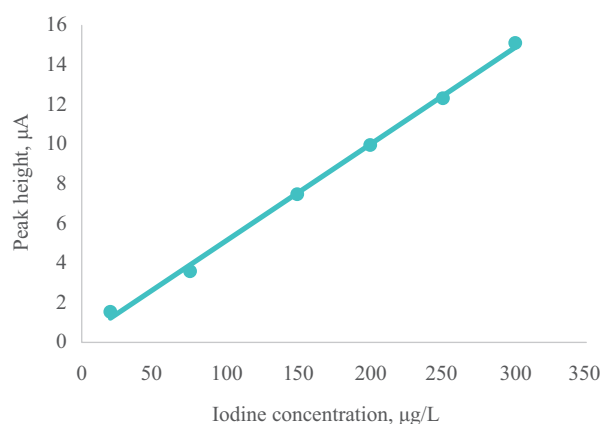


Fig. 2. Dependence of the cathode current value on the iodine concentration

Analysis of the graph presented in Fig. 2 showed that the relationship between the iodine content in the analyzed solution and the cathode current is linear in the concentration range of the element being determined from 20 to 300 µg/L ($R^2 = 0.9993$).

The addition method was used to study the correctness. It consisted in adding the exact amount of a standard sample of potassium iodide (in terms of iodine) to extracts diluted to a half concentration (for working in the linear region of the technique). Discoverability was calculated as the ratio of the experimentally found amount of an element to its theoretical content. The results are shown in Table 2.

Table 2. Evaluation of the discoverability of the iodine content in the sample ($h^* = 3.26 \mu\text{g}$, $m_{\text{test}}^{**} = 2.21 \mu\text{g}$)

Added (m), μg	h_{add}	$m + m_{\text{test}}$, μg	h_{theor}	Found, μg	h_{exp}	Discoverability, %
0.60	1.07	2.81	4.33	2.91	4.23	103.5
0.60	1.02	2.81	4.28	2.91	4.23	103.5
0.60	1.04	2.81	4.30	2.90	4.22	103.3
1.50	2.31	3.71	5.57	3.82	5.49	103.1
1.50	2.27	3.71	5.53	3.83	5.50	103.3
1.50	2.28	3.71	5.54	3.82	5.49	103.1
2.70	3.91	4.91	7.17	5.07	7.20	103.2
2.70	3.93	4.91	7.19	5.07	7.21	103.3
2.70	3.88	4.91	7.14	5.08	7.22	103.5

* h is an analytical signal (peak height) of the solution diluted to half concentration.

** m_{test} is the content of the determined component in the test solution diluted to half concentration.

On the basis of the data obtained, it was concluded that the method enables correct determination of the analyte in the analyzed solution obtained at sample preparation stage. The accuracy ranges from 100 to 105%, and the coefficient of variation (with the number of parallel measurements $n = 9$) was 0.2%.

The study of repeatability consisted in calculating the variability index and confidence interval on the basis of the results of quantitative determination of inorganic iodine gross content in *Laminariae thalli* L. in several replicates. The results are presented in Table 3.

Table 3. Evaluation of the reproducibility of the technique of inorganic iodine determination (the number of parallel measurements $n = 6$, confidence level $p = 0.95$), the content of the main substance in the standard sample of potassium iodide $P = 99.9\%$, raw material humidity $W = 8.80\%$

Parameter	Measurements					
	1	2	3	4	5	6
h_1	6.11	6.10	6.06	6.12	6.18	6.22
h_2	6.12	6.16	6.09	6.13	6.16	6.25
h_3	6.15	6.14	6.10	6.17	6.15	6.20
Average h	6.13	6.13	6.08	6.14	6.16	6.20
X , %	1.15	1.15	1.14	1.15	1.16	1.16
X_{ave} , %	1.15					
Standard deviation, S	0.01					
Standard deviation of the average result, S_0	0.003					
Coefficient of variation, S_0 , %	0.90					
Confidence interval, %	1.14–1.16					
Analysis result, %	1.15 ± 0.01					

Table 4. Assessment of intralaboratory precision of the IVA method for determining the gross content of inorganic iodine ($n = 6$, $p = 0.95$), $P = 99.9\%$, $W = 8.80\%$

Parameter	Measurements					
	1	2	3	4	5	6
h_1	5.98	6.02	6.10	6.06	6.20	6.17
h_2	5.97	5.98	6.12	6.10	6.15	6.15
h_3	6.00	5.97	6.16	6.09	6.19	6.11
Average h	5.98	5.99	6.13	6.08	6.18	6.14
X , %	1.12	1.12	1.15	1.14	1.16	1.15
X_{ave} , %	1.14					
Standard deviation, S	0.02					
Standard deviation of the average result, S_0	0.007					
Coefficient of variation, S_0 , %	1.80					
Confidence interval, %	1.12–1.16					
Analysis result, %	1.14 ± 0.02					

The results presented in Table 3 show that the coefficient of variation of the results of inorganic iodine quantitative determination ($n = 6$) was 0.9%, and the confidence interval was in the range of $\pm 0.01\%$.

Intralaboratory precision was studied by means of quantifying the element in six replicates on a different day by a different analytical chemist. The data is shown in Table 4.

The data shown in Tables 3 and 4 allows a comparison of the variances of the average results of the two samples using the Fisher and Student tests. The calculated values of Fisher $F_{\text{exp}} = 4.700$ and Student $t_{\text{exp}} = 0.141$ criteria were lower than the tabulated ones ($F_{\text{table}} = 5.050$; $t_{\text{table}} = 2.571$). This confirms that the two samples belong to the general population. The results of inorganic iodine quantitative determination using the method developed herein are reproducible and showed satisfactory intralaboratory precision.

CONCLUSIONS

As a result of the study, a new highly sensitive, selective, combined IVA method for determining inorganic iodine in *Laminariae thalli* L. was developed. Unlike the most commonly used pharmacopoeial methods, the proposed method involves extremely simple sample preparation.

This method consists of extraction of the inorganic analyte with water and subsequent conversion of the iodate and iodide forms of iodine (the most common in the *Laminariae thalli* L.) into a single analytical form by processing the extract with zinc dust in acidic environment. The validation results demonstrated that the new method provides a satisfactory level of metrological characteristics (specificity, linearity, discoverability, repeatability, intralaboratory precision). The method also complies with the requirements of the SPH 15 and can be recommended for use in control and analytical laboratories involved in pharmaceutical quality control.

Authors' contributions

A.V. Nikulin—planning and conducting the experiments, writing and editing the main section of the article, data processing, and discussion of the results.

L.Yu. Martynov—planning and conducting the experiments related to inversion voltammetry, data processing, and discussion of the results.

R.S. Gabaeva—writing the main section of the article, conducting the experiments, preparing figures and tables, and discussion of the results.

M.A. Lazov—conducting the experimental work related to obtaining the total amount of iodine, and editing and formatting the article.

The authors declare no conflicts of interest.

REFERENCES

1. Ahad F., Ganie S.A. Iodine, Iodine metabolism and Iodine deficiency disorders revisited. *Indian J. Endocrinol. Metab.* 2010;14(1):13–17. <https://pubmed.ncbi.nlm.nih.gov/21448409>
2. Swanson C.A., Pearce E.N. Iodine insufficiency: a global health problem? *Adv. Nutr.* 2013;4(5):533–535. <https://doi.org/10.3945/an.113.004192>
3. Haldimann M., Alt A., Blanc A., Blondeau K. Iodine content of food groups. *J. Food Compos. Anal.* 2005;18(6):461–471. <https://doi.org/10.1016/j.jfca.2004.06.003>
4. Eftychia G.K., Roupas N.D., Markou K.B. Effect of excess iodine intake on thyroid on human health. *Minerva Med.* 2017;108(2):136–146. <https://doi.org/10.23736/s0026-4806.17.04923-0>
5. Kapil U. Health consequences of iodine deficiency. *Sultan Qaboos Univ. Med. J.* 2007;7(3):267–272. <https://pubmed.ncbi.nlm.nih.gov/21748117/>
6. Thilly C.H., Vanderpas J.B., Bebe N., Ntambue K., Contempre B., Swennen B., Moreno-Reyes R., Bourdoux P., Delange F. Iodine deficiency, other trace elements, and goitrogenic factors in the etiopathogeny of iodine deficiency disorders (IDD). *Biol. Trace Elem. Res.* 1992;32:229–243. <https://doi.org/10.1007/bf02784606>
7. Delange F. The role of iodine in brain development. *Proc. Nutr. Soc.* 2000;59(1):75–79. <https://doi.org/10.1017/s0029665100000094>
8. Morreale de Escobar G., Obregón M.J., Escobar del Rey F. Role of thyroid hormone during early brain development. *Eur. J. Endocrinol.* 2004;151(3):U25–U37. <https://doi.org/10.1530/eje.0.151u025>
9. Zimmermann M.B. Iodine deficiency. *Endocrin. Rev.* 2009;30(4):376–408. <https://doi.org/10.1210/er.2009-0011>
10. Lazarus J.H. The importance of iodine in public health. *Environ. Geochem. Health.* 2015;37:605–618. <https://doi.org/10.1007/s10653-015-9681-4>
11. Nerhus I., Odland M., Kjellevold M., Midtbø L.K., Markhus M.W., Graff I.E., Lie Ø., Kvestad I., Frøyland L., Dahl L., Øyen J. Iodine status in Norwegian preschool children and associations with dietary iodine sources: the FINS-KIDS study. *Eur. J. Nutr.* 2019;58:2219–2227. <https://doi.org/10.1007/s00394-018-1768-0>
12. Müssig K. Iodine-induced toxic effects due to seaweed consumption. *Comprehensive handbook of iodine.* 2009:897–908. <https://doi.org/10.1016/B978-0-12-374135-6.00093-5>
13. Smyth P.P.A. Iodine, seaweed, and the thyroid. *Eur. Thyroid J.* 2021;10(2):101–108. <https://doi.org/10.1159/000512971>
14. Martinelango P.K., Tian K., Dasgupta P.K. Perchlorate in seawater: bioconcentration of iodide and perchlorate by various seaweed species. *Anal. Chim. Acta.* 2006;567(1):100–107. <https://doi.org/10.1016/j.aca.2006.02.015>
15. Yang M., Her N., Ryu J., Yoon Y. Determination of perchlorate and iodide concentrations in edible seaweeds. *Int. J. Environ. Sci. Technol.* 2014;11:565–570. <https://doi.org/10.1007/s13762-013-0263-7>
16. Leblanc C., Colin C., Cosse A., Delage L., La Barre S., Morin P., Fiévet B., Voiseux C., Ambroise Y., Verhaeghe E., Amouroux D., Donard O., Tessier E., Potine P. Iodine transfers in the coastal marine environment: the key role of brown algae and of their vanadium-dependent haloperoxidases. *Biochimie.* 2006;88(11):1773–1785. <https://doi.org/10.1016/j.biochi.2006.09.001>
17. Tinggi U., Schoendorfer N., Davies P.S., Scheelings P., Olszowy H. Determination of iodine in selected foods and diets by inductively coupled plasma-mass spectrometry. *Pure Appl. Chem.* 2011;84(2):291–299. <https://doi.org/10.1351/PAC-CON-11-08-03>
18. Pröfrock D., Prange A. Inductively coupled plasma–mass spectrometry (ICP-MS) for quantitative analysis in environmental and life sciences: a review of challenges, solutions, and trends. *Appl. Spectrosc.* 2012;66(8):843–868. <https://doi.org/10.1366/12-06681>
19. Dyke J.V., Dasgupta P.K., Kirk A.B. Trace iodine quantitation in biological samples by mass spectrometric methods: the optimum internal standard. *Talanta.* 2009;79(2):235–242. <https://doi.org/10.1016/j.talanta.2009.03.038>
20. Haldimann M., Zimmerli B., Als C., Gerber H. Direct determination of urinary iodine by inductively coupled plasma mass spectrometry using isotope dilution with iodine-129. *Clin. Chem.* 1998;44(4):817–824. <https://doi.org/10.1093/clinchem/44.4.817>
21. Shelor C.P., Dasgupta P.K. Review of analytical methods for the quantification of iodine in complex matrices. *Anal. Chim. Acta.* 2011;702(1):16–36. <https://doi.org/10.1016/j.aca.2011.05.039>
22. Bellanger J.R., Tressol J.C., Piel H.P. A semi-automated method for the determination of iodine in plants. *Ann. Rech. Vet.* 1979;10(1):113–118. <https://pubmed.ncbi.nlm.nih.gov/539772/>
23. Fischer P.W., L'abbé M.R. Acid digestion determination of iodine in foods. *J. Assoc. Off. Anal. Chem.* 1981;64(1):71–74. <https://doi.org/10.1093/jaoac/64.1.71>
24. Fischer P.W., L'Abbé M.R., Giroux A. Colorimetric determination of total iodine in foods by iodide-catalyzed reduction of Ce⁴⁺. *J. Assoc. Off. Anal. Chem.* 1986;69(4):687–689. <https://doi.org/10.1093/jaoac/69.4.687>
25. Sandell E.B., Kolthoff I.M. Micro determination of iodine by a catalytic method. *Microchim. Acta.* 1937;1:9–25. <https://doi.org/10.1007/BF01476194>
26. May W., Wu D., Eastman C., Bourdoux P., Maberly G. Evaluation of automated urinary iodine methods: problems of interfering substances identified. *Clin. Chem.* 1990;36(6):865–869. <https://doi.org/10.1093/clinchem/36.6.865>
27. Pupyshv A.A., Surikov V.T. *Mass-spektrometriya s indukativno svyazannoi plazmoi. Obrazovanie ionov (Inductively Coupled Plasma Mass Spectrometry: Formation of Ions)*. Yekaterinburg: Ural Otd. Ross. Akad. Nauk; 2006. 237 p. (in Russ.).
28. Poluzzi V., Cavalchi B., Mazzoli A., Alberini G., Lutman A., Coan P., Ciani I., Trentini P., Ascanelli M., Davoli V. Comparison of two different inductively coupled plasma mass spectrometric procedures and high-performance liquid chromatography with electrochemical detection in the determination of iodine in urine. *J. Anal. At. Spectrom.* 1996;11(9):731–734. <https://doi.org/10.1039/JA9961100731>
29. Santamaria-Fernandez R., Evans P., Wolff-Briche C.S., Hearn R. A high accuracy primary ratio method for the determination of iodine in complex matrices by double isotope dilution using MC-ICPMS and ¹²⁹I spike. *J. Anal. At. Spectrom.* 2006;21(4):413–421. <https://doi.org/10.1039/B516767A>
30. Vydra F., Shtulik K., Yulakova E. *Inversionnaya vol'tamperometriya (Inversion Voltammetry)*. Moscow: Mir; 1980. 278 p. (in Russ.).

31. Deryabina V.I., Slepchenko G.B., Fam K.N., Kirillova M.E. *Method for quantitative determination of iodine through stripping voltammetry*: RF Pat. 2459199. Publ. 20.08.2012 (in Russ.).
32. Espada-Bellido E., Bi Z., Salaün P., van den Berg C.M.G. Determination of iodide and total iodine in estuarine waters by cathodic stripping voltammetry using a vibrating silver amalgam microwire electrode. *Talanta*. 2017;174:165–170. <https://doi.org/10.1016/j.talanta.2017.06.004>
33. Bibi S., Zaman M.I., Niaz A., Tariq M., Khan S.Z., Zulfiqar A., Rahim A., Jan S. Electrocatalytic response of chitosan modified multiwall carbon nanotube paste electrode toward iodide: A facile voltammetric method for determination of iodide in biological sample. *Mater. Chem. Phys.* 2023;294:126984. <https://doi.org/10.1016/j.matchemphys.2022.126984>
34. Cunha-Silva H., Arcos-Martinez M.J. Cathodic stripping voltammetric determination of iodide using disposable sensors. *Talanta*. 2019;199:262–269. <https://doi.org/10.1016/j.talanta.2019.02.061>
35. Elupov V.Yu., Denisov V.L. *Method for production of laminaria extract with increased iodine content*: RF Pat. 2311043. Publ. 27.11.2007 (in Russ.).
36. Podkorytova A.V. *Marine algae – macrophytes and herbs*. Moscow: VNIRO; 2005. 174 p. (in Russ.).

About the authors

Alexander V. Nikulin, Dr. Sci.(Pharm.) Associate Professor, I.P. Alimarin Department of Analytical Chemistry, M.V. Lomonosov Institute of Fine Chemical Technologies, MIREA – Russian Technological University (86, Vernadskogo pr., Moscow, 119571, Russia). E-mail: alexander_sinus@mail.ru. Scopus Author ID 57194137763, RSCI SPIN-code 8611-5567, <https://orcid.org/0009-0004-2755-2734>

Leonid Yu. Martynov, Cand. Sci.(Chem.), Associate Professor, I.P. Alimarin Department of Analytical Chemistry, M.V. Lomonosov Institute of Fine Chemical Technologies, MIREA – Russian Technological University (86, Vernadskogo pr., Moscow, 119571, Russia). E-mail: martynov_leonid@mail.ru. Scopus Author ID 56084953700, RSCI SPIN-code 7339-1203, <https://orcid.org/0000-0001-9861-7890>

Ramnat S. Gabaeva, Master Student, M.V. Lomonosov Institute of Fine Chemical Technologies, MIREA – Russian Technological University (86, Vernadskogo pr., Moscow, 119571, Russia). E-mail: radima.gabaeva@yandex.ru. <https://orcid.org/0009-0002-7095-1453>

Mikhail A. Lazov, Cand. Sci. (Chem.), Assistant Professor, I.P. Alimarin Department of Analytical Chemistry, M.V. Lomonosov Institute of Fine Chemical Technologies, MIREA – Russian Technological University (86, Vernadskogo pr., Moscow, 119571, Russia). E-mail: lazov@mirea.ru, lazovm@gmail.com. Scopus Author ID 56466030700, RSCI SPIN-code 9661-9280, <https://orcid.org/0000-0001-8578-1683>

Об авторах

Никулин Александр Владимирович, д.фарм.н., доцент кафедры аналитической химии им. И.П. Алимарина, Институт тонких химических технологий им. М.В. Ломоносова, ФГБОУ ВО «МИРЭА – Российский технологический университет» (119571, Россия, Москва, пр-т Вернадского, д. 86). E-mail: alexander_sinus@mail.ru. Scopus Author ID 57194137763, SPIN-код РИНЦ 8611-5567, <https://orcid.org/0009-0004-2755-2734>

Мартынов Леонид Юрьевич, к.х.н., доцент кафедры аналитической химии им. И.П. Алимарина, Институт тонких химических технологий им. М.В. Ломоносова, ФГБОУ ВО «МИРЭА – Российский технологический университет» (119571, Россия, Москва, пр-т Вернадского, д. 86). E-mail: martynov_leonid@mail.ru. Scopus Author ID 56084953700, SPIN-код РИНЦ 7339-1203, <https://orcid.org/0000-0001-9861-7890>

Габаева Рамнат Султановна, магистрант, Институт тонких химических технологий им. М.В. Ломоносова, ФГБОУ ВО «МИРЭА – Российский технологический университет» (119571, Россия, Москва, пр-т Вернадского, д. 86). E-mail: radima.gabaeva@yandex.ru. <https://orcid.org/0009-0002-7095-1453>

Лазов Михаил Александрович, к.х.н., доцент кафедры аналитической химии им. И.П. Алимарина, Институт тонких химических технологий им. М.В. Ломоносова, ФГБОУ ВО «МИРЭА – Российский технологический университет» (119571, Россия, Москва, пр-т Вернадского, д. 86). E-mail: lazov@mirea.ru, lazovm@gmail.com. Scopus Author ID 56466030700, SPIN-код РИНЦ 9661-9280, <https://orcid.org/0000-0001-8578-1683>

Translated from Russian into English by M. Povorin

Edited for English language and spelling by Dr. David Mossop

Erratum
Исправления

<https://doi.org/10.32362/2410-6593-2024-19-4-384-385>



Erratum to the article “Development of technology for culturing a cell line producing a single-domain antibody fused with the Fc fragment of human IgG1”

D.S. Polyansky, E.I. Ryabova, A.A. Derkaev, N.S. Starkov, I.S. Kashapova, D.V. Shcheblyakov, A.P. Karpov, I.B. Esmagambetov

Tonkie Khimicheskie Tekhnologii = Fine Chemical Technologies. 2024;19(3):240–257

Исправления к статье «Разработка технологии культивирования клеточной линии, продуцирующей однодоменное антитело, слитое с Fc-фрагментом IgG1 человека»

Д.С. Полянский, Е.И. Рябова, А.А. Деркаев, Н.С. Старков, И.С. Кашапова, Д.В. Щебляков, А.П. Карпов, И.Б. Есмагамбетов

Тонкие химические технологии = Fine Chemical Technologies. 2024;19(3):240–257

FOR ENGLISH VERSION OF THE ARTICLE

Page 241, after the title of the article instead of:

Д.М. Полянский

should read:

Д.С. Полянский

Page 241, instead of:

Для цитирования

Полянский Д.М., Рябова Е.И., Деркаев А.А., Старков Н.С., Кашапова И.С., Щебляков Д.В., Карпов А.П., Есмагамбетов И.Б. Разработка технологии культивирования клеточной линии, продуцирующей однодоменное антитело, слитое с Fc-фрагментом IgG1 человека. *Тонкие химические технологии.* 2024;19(3):240–257. <https://doi.org/10.32362/2410-6593-2024-19-3-240-257>

should read:

Для цитирования

Полянский Д.С., Рябова Е.И., Деркаев А.А., Старков Н.С., Кашапова И.С., Щебляков Д.В., Карпов А.П., Есмагамбетов И.Б. Разработка технологии культивирования клеточной линии, продуцирующей однодоменное антитело, слитое с Fc-фрагментом IgG1 человека. *Тонкие химические технологии*. 2024;19(3):240–257. <https://doi.org/10.32362/2410-6593-2024-19-3-240-257>

The original article can be found under <https://doi.org/10.32362/2410-6593-2024-19-3-240-257>

ДЛЯ РУССКОЯЗЫЧНОЙ ВЕРСИИ СТАТЬИ

На странице 240 после названия статьи вместо:

Д.М. Полянский

следует читать:

Д.С. Полянский

В нижнем колонтитуле вместо:

Д.М. Полянский

следует читать:

Д.С. Полянский

На странице 241 вместо:

Для цитирования

Полянский Д.М., Рябова Е.И., Деркаев А.А., Старков Н.С., Кашапова И.С., Щебляков Д.В., Карпов А.П., Есмагамбетов И.Б. Разработка технологии культивирования клеточной линии, продуцирующей однодоменное антитело, слитое с Fc-фрагментом IgG1 человека. *Тонкие химические технологии*. 2024;19(3):240–257. <https://doi.org/10.32362/2410-6593-2024-19-3-240-257>

следует читать:

Для цитирования

Полянский Д.С., Рябова Е.И., Деркаев А.А., Старков Н.С., Кашапова И.С., Щебляков Д.В., Карпов А.П., Есмагамбетов И.Б. Разработка технологии культивирования клеточной линии, продуцирующей однодоменное антитело, слитое с Fc-фрагментом IgG1 человека. *Тонкие химические технологии*. 2024;19(3):240–257. <https://doi.org/10.32362/2410-6593-2024-19-3-240-257>

На страницах 241, 243, 245, 247, 249, 251, 255, 257 в верхних колонтитулах вместо:

Д.М. Полянский и др.

следует читать:

Д.С. Полянский и др.

Оригинальная статья может быть найдена: <https://doi.org/10.32362/2410-6593-2024-19-3-240-257>

MIREA – Russian Technological University
78, Vernadskogo pr., Moscow, 119454, Russian Federation.
Publication date *August 29, 2024*.
Not for sale

МИРЭА – Российский технологический университет
119454, РФ, Москва, пр-т Вернадского, д. 78.
Дата опубликования *29.08.2024*.
Не для продажи

www.finechem-mirea.ru

